1-1-2004

Solid phase synthesis of graft copolymers of poly(thiophene)s and peptides containing 3-thienylalanine.

David W. Flanagan
University of Massachusetts Amherst

SOLID PHASE SYNTHESIS OF GRAFT COPOLYMERS OF POLY(THIOPHENE)S AND PEPTIDES CONTAINING 3-THIENYLALANINE

A Dissertation Presented

by

DAVID W. FLANAGAN

Submitted to the Graduate School of the
University of Massachusetts Amherst in partial fulfillment
of the requirements for the degree of

DOCTOR OF PHILOSOPHY

September 2004

Polymer Science and Engineering

SOLID PHASE SYNTHESIS OF GRAFT COPOLYMERS OF POLY(THIOPHENE)S AND PEPTIDES CONTAINING 3-THIENYLALANINE

A Dissertation Presented

by

DAVID W. FLANAGAN

Approved as to style and content by:

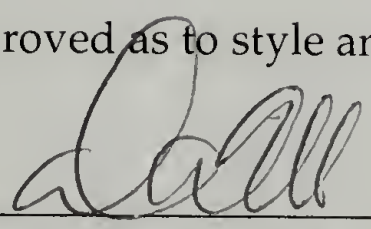

David A. Tirrell, Chair

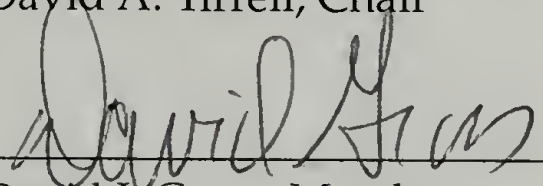

David J. Gross, Member

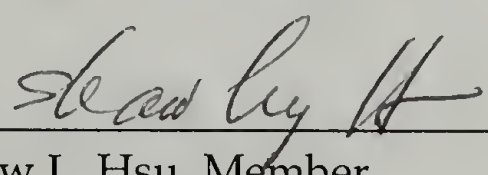

Shaw L. Hsu, Member

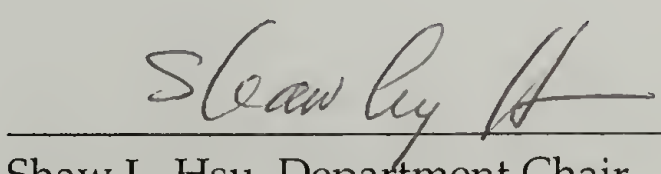

Shaw L. Hsu, Department Chair
Polymer Science and Engineering

for

gabi

I am in blood

Stepp'd in so far that, should I wade no more,

Returning were as tedious as go o'er.

MACBETH (III.iv.136–138)

Acknowledgments

Distilling the work of a graduate career into about 100 cubic inches of paper requires one to reflect upon the experiments performed, the data collected, and the conclusions reached. This process also brings forth memories of the people whose lives intersected mine, professionally and personally, in the years when these experiments were performed. I now have an opportunity to thank them for their contributions, individually and collectively.

First, I would like to express my gratitude to my advisor, Prof. David Tirrell, and my committee, Profs. Shaw Ling Hsu and David Gross, for their patience and guidance during a graduate career spanning eight years and two coasts. Prof. Tirrell maintains high standards, both in his research program and his conduct in the scientific community, and so I aspire to match his standards in my career. I am also thankful that he granted me the freedom to design and execute my own research project. In hindsight, this freedom has allowed me to complete a body of work which I can truly consider my own. Finally, from observing his everyday dealings with diverse personalities in his research group, I learned that injection of a little levity into a potentially awkward student-advisor relationship could go a long way towards lessening that tension.

For example, I had agreed to drive Dave's green Ford Ranger pickup across the country, from Amherst to Pasadena. I thought it would be a great adventure; for some reason, he didn't seem to want to drive it himself. My belongings were packed and my prospectus and proposal were complete, and Dave drove me from campus to his house so that I could take possession of the truck for the next two weeks. When we arrived, he gave me a brief rundown of the controls, the radio, where the spare tire was stowed. "Great," I said, "How about the air conditioning?" We would be driving through the Badlands of Montana and the deserts of

the Southwest in July. He looked at me, and gave me his sort-of half-cocked smile. "What air conditioning?"

❦

Working in a large research group means that I have interacted with a great number of students, postdoctoral associates, and visiting scientists during my graduate career, whose suggestions and ideas I greatly appreciate. However, there are certain colleagues who I would especially like to thank for their contributions, roughly in order of appearance: Howard Bowman, Wendy Naimark, Jan van Hest, Ralf Weberskirsch, Takatoshi Kinoshita, Jinsang Kim, Alex Kros, Marissa Mock, Sarah Heilshorn, Isaac Carrico, Andy Spakowitz, and Paul Nowatzki.

To Jeffrey Linhardt and his wife, Dawn, I offer my special thanks for their companionship in Amherst and in Pasadena. Although they moved on to greener pastures nearly three years ago, I still consider them two of my closest friends.

The support staff in Amherst and in Pasadena are excellent, and their skill and dedication to students made many of the experiments in this thesis possible. In particular, I would like to thank Greg Dabkowski for performing elemental analyses, and Mona Shahgholi for performing mass spectroscopy. Charlie Dickinson at UMass, and Scott Ross and the late Robert Lee at Caltech, maintained excellent NMR facilities during my graduate career. The PSE graduate secretaries, Eileen Besse and Joann Chauvin, were excellent guides for navigating the UMass bureaucracy. I would also like to thank Polymer Laboratories, for supplying samples of their solid phase synthesis resins, and Pat Whitcomb of Stat-Ease, Inc., for his responses to my questions about statistics and DoE.

❦

Next, I turn to my family to offer them my heart-felt thanks. My parents made sacrifices for me when I was young, guided me when I was older, and provided

encouragement when I needed it most in graduate school. Their unwavering commitment to my education will, I hope, be validated by this completed dissertation. I can only hope that someday I will be able to match their efforts.

Finally, it is difficult to express in words my gratitude to my wife. Spouses usually provide encouragement and support to their husbands or wives as they work towards their doctorate, but I doubt that many contribute scientifically to the dissertation itself as much as she has. Through her suggestions for experiments and analysis of results, production of figures and critical reading of this manuscript, she has shepherded me to the completion of this thesis. Thank you, Gabi.

DAVE FLANAGAN

Pasadena, California
July 2004

ABSTRACT

SOLID PHASE SYNTHESIS OF GRAFT COPOLYMERS OF POLY(THIOPHENE)S AND PEPTIDES CONTAINING 3-THIENYLALANINE

SEPTEMBER 2004

DAVID W. FLANAGAN

B.S., RENSSELAER POLYTECHNIC INSTITUTE

M.S., UNIVERSITY OF MASSACHUSETTS AMHERST

Ph.D., UNIVERSITY OF MASSACHUSETTS AMHERST

Directed by: Professor David A. Tirrell

Graft copolymers of conjugated poly(3-hexylthiophene) and polypeptides containing an artificial amino acid, 3-thienylalanine (3TA), were synthesized and purified using solid phase synthesis techniques. The structures of the graft copolymers were characterized by NMR, and binding of biotinylated graft copolymers to avidin and streptavidin was studied using fluorescence spectroscopy.

The hydroxmethylbenzoic acid (HMBA) solid phase resin linker was stable in the presence of an oxidative polymerization catalyst, ferric chloride, for up to five hours as shown by infrared spectroscopy and elemental analysis. A two-level factorial design was used to identify three factors which had statistically significant effects on the solution fluorescence emission maxima of the copolymers: catalyst to monomer ratio, monomer addition rate, and addition of bithiophene. Additionally, two two-factor interactions had significant effects: the interactions of

monomer ratio and monomer concentration, and of monomer ratio and addition of Proton-Sponge.

A peptide containing 3TA and biocytin, separated by a triglycine spacer, was synthesized on HMBA resin and characterized by mass spectroscopy fragmentation and by two-dimensional correlational NMR spectroscopy. The peptide, and an analog substituting biocytin with an acetylated lysine, were produced in 84 to 89% purity. The integrity of the peptide backbone and the successful copolymerization were confirmed by 2D NMR after polymerization. Number average molecular weights of 7300 g/mol for the acetylated lysine copolymer, and 10 850 g/mol for the biocytin copolymer could be estimated from the NMR spectra. Strong fluorescence emission maxima at long wavelengths were observed for the copolymers, indicating high conjugation lengths. This system is not limited to peptides and 3-hexylthiophene, and should be generally applicable to synthesis of copolymers of conjugated polymers and biomolecules that can be immbolilized on a solid support.

TABLE OF CONTENTS

LIST OF TABLES

LIST OF FIGURES

CHAPTER 1

INTRODUCTION

1.1 Artificial amino acids and engineered peptides

In the last century, polymer scientists have excelled at creating new materials of immense benefit to society with a great variety of properties – toughness, transparency, flexibility, lightness, chemical resistance, adhesiveness – conferred by the diversity of available monomers. Similarly, nature has evolved a staggering variety of proteins responsible for nearly all the processes of life – photosynthesis, signal transduction, and metabolism – where a function is determined by precise sequence control of amino acids. However, while the polymer chemist can choose from thousands of monomers to make a material, nature is mostly limited to the twenty naturally-occurring, canonical amino acids. Conversely, polymer chemists cannot hope to accomplish the sequence-, length-, and stereospecificity of proteins using purely synthetic tools, even with recent advances in controlled polymerization techniques, on the scale that nature produces every day. As a result, the last decade has witnessed a number of efforts to combine the *precision* of peptide synthesis with the *variety* of polymer chemistry.

1.1.1 Precision: sequence and length control

In 1994, Krejchi et al. synthesized a family of regular, periodic polypeptides by bacterial expression.[1] The peptide sequence,

$$\texttt{-[(AlaGly)}_x\texttt{GluGly]}_n\texttt{-}$$

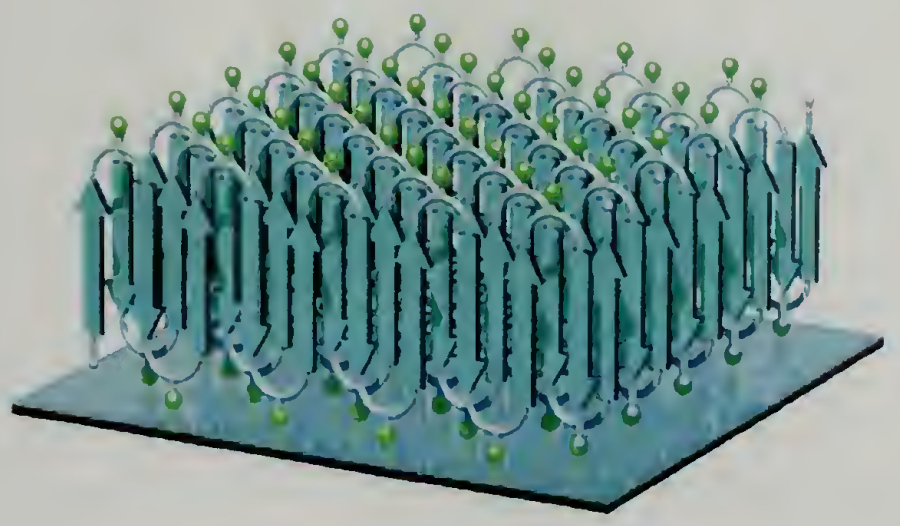

Figure 1.1. Single lamellar thickness crystal constructed from regular, periodic peptide. Reprinted with permission from van Hest, J. C. M.; Tirrell, D. A. *Chem. Commun.*, **2001,** 1897–1904. Copyright 2001 The Royal Society of Chemistry.

was designed so that the chains would fold into a regular lamellar structure with controllable thickness, surface structure, and unit cell structure (figure 1.1).[2] These properties were confirmed by vibrational spectroscopy, solid-state NMR, and wide-angle X-ray diffraction. Yu et al. complemented this result in 1997, by benzylating monodisperse poly(α,L-glutamic acid) prepared by bacterial expression.[3] Poly(γ-benzyl-α,L-glutamate) (PBLG) synthesized by conventional polymerization processes has a distribution of chain lengths around the target molecular weight, resulting in nematic liquid crystals with orientational, but not positional, molecular order. The biosynthesized PBLG, with a degree of polymerization of exactly 76 monomer units, formed a smectic liquid crystal with both orientational and positional order, as predicted by Flory in 1956.[4]

1.1.2 Variety: artificial amino acids

Examples of substitutions of amino acid analogs into proteins have been known for more than fifty years.[5] Microbiologists noted that bacterial growth was slowed

in the presence of certain amino acid analogs, and found that the analogs had partially replaced their natural counterparts in bacterial protein extracts. This occurs because the enzyme responsible for linking the correct amino acid to the corresponding tRNA, aminoacyl-tRNA synthetase, cannot always distinguish between the natural amino acid and its analog. Using this technique, a number of amino acid analogs, including selenomethionine (an analog of methionine),[6] *p*-fluorophenylalanine and 3-thienylalanine (analogs of phenylalanine),[7,8] and homoallylglycine and homopropargylglycine (analogs of methionine)[9] have been incorporated into engineered proteins.

In cases where the aminoacyl-tRNA synthetase is able to distinguish between the natural amino acid and its non-natural analog, so that it is not normally incorporated, the synthetase can be engineered to lower its specificity. Kirshenbaum et al., using an *Escheria coli* strain with a mutant phenylalanyl-tRNA synthetase (PheRS) with an enlarged amino acid binding pocket produced by a single point mutation, incorporated eight different phenylalanine analogs into a test protein. In comparison, five of the eight analogs were not incorporated into the test protein in an *E. coli* strain lacking the mutated PheRS.[10] Computational redesign of the PheRS binding pocket suggested two mutations which would permit binding of one of the analogs not incorporated in the earlier study, *p*-acetylphenylalanine. After the two mutations were made, 80% of the phenylalanine residues in the test protein were replaced by *p*-acetylphenylalanine.[11]

The preceding methods result in multisite incorporation of an amino acid analog – that is, all of the sites corresponding to a given amino acid can potentially be replaced in the protein. (The overall percentage of replacement will depend on the analog; incorporation is often less than 100%.) The next level of complexity, and the subject of much current research, is the replacement of an amino acid with its analog at a single site in the protein, leaving the natural analog intact in every other

site. In 1998, Furter demonstrated a technique for site-directed incorporation of a "twenty-first" amino acid into a protein.[12] A yeast aminoacyl-tRNA synthetase, and its counterpart yeast tRNA, were incorporated into *E. coli*. The anticodon of the yeast tRNA was modified to pair with an amber suppression codon (one of the three nonsense codons in the genetic code), so that the amino acid attached to the yeast tRNA would be incorporated exclusively at an amber codon in the peptide sequence. By using the yeast synthetase and tRNA, one can incorporate an amino acid at a specific site, while being completely orthogonal to the native *E. coli* synthetases and tRNAs.

In practice, the effectiveness of the amber suppression system is limited by modest suppression efficiencies. Recently, Kwon et al. have reengineered *E. coli* protein synthesis by introducing an orthogonal yeast aminoacyl-tRNA synthetase and a novel cognate tRNA. In *E. coli*, two codons encode phenylalanine, UUC and UUU, that can pair with the one tRNA that carries phenylalanine. The UUC codon forms a Watson-Crick pair with the tRNA GAA anticodon, while UUU forms a less stable "wobble" pair with GAA. A yeast PheRS with an enlarged phenylalanine binding pocket resulting from a single mutation and a yeast phenylalanyl-tRNA with the UUC anticodon were introduced into *E. coli*. A test protein with nine phenylalanine sites, four encoded by UUC and five encoded by UUU, was then expressed in the engineered *E. coli* in the presence of the phenylalanine analog L-3-(2-naphthyl)alanine. Matrix assisted laser desorption/ionization (MALDI) mass spectra of tryptic digests of the test protein demonstrated that five phenylalanine residues and four analog residues were incorporated at the predicted sites.[13]

With further developments of techniques like these, in the near future it may be possible to overcome the limitations of natural proteins routinely, producing biomaterials with engineered structures and containing chemical functionalities found both in nature and in the laboratory.

1.2 Conducting polymers

The study of conducting polymers, and especially poly(thiophene)s (PTs), has intensified during the last three decades. The maturation of the field of conducting polymers was confirmed by the awarding of the 2000 Nobel Prize in Chemistry to Alan Heeger, Alan MacDiarmid, and Hideki Shirakawa "for the discovery and development of conductive polymers." The most notable property of these materials, electrical conductivity, results from the delocalization of electrons along the polymer backbone – hence the term, "synthetic metals". But, conductivity is not the only interesting property resulting from electron delocalization. The optical properties of these materials respond to environmental stimuli, with dramatic color shifts in response to changes in solvent, temperature, applied potential, and binding to other molecules. Both color changes and conductivity changes are induced by the same mechanism – twisting of the polymer backbone, disrupting conjugation – making conjugated polymers attractive as sensors that can provide a range of optical and electronic responses.

A number of comprehensive reviews have been published on PTs, the earliest dating from 1981.[14] Schopf and Koßmehl published a comprehensive review of the literature published between 1990 and 1994.[15] Roncali surveyed electrochemical synthesis in 1992,[16] and the electronic properties of substituted PTs in 1997.[17] McCullough's 1998 review focussed on chemical synthesis of conducting PTs.[18] A general review of conjugated polymers from the 1990s was conducted by Reddinger and Reynolds in 1999.[19] Finally, Swager et al. examined conjugated polymer-based chemical sensors in 2000.[20] These reviews are an excellent guide to the highlights of the primary PT literature from the last two decades.

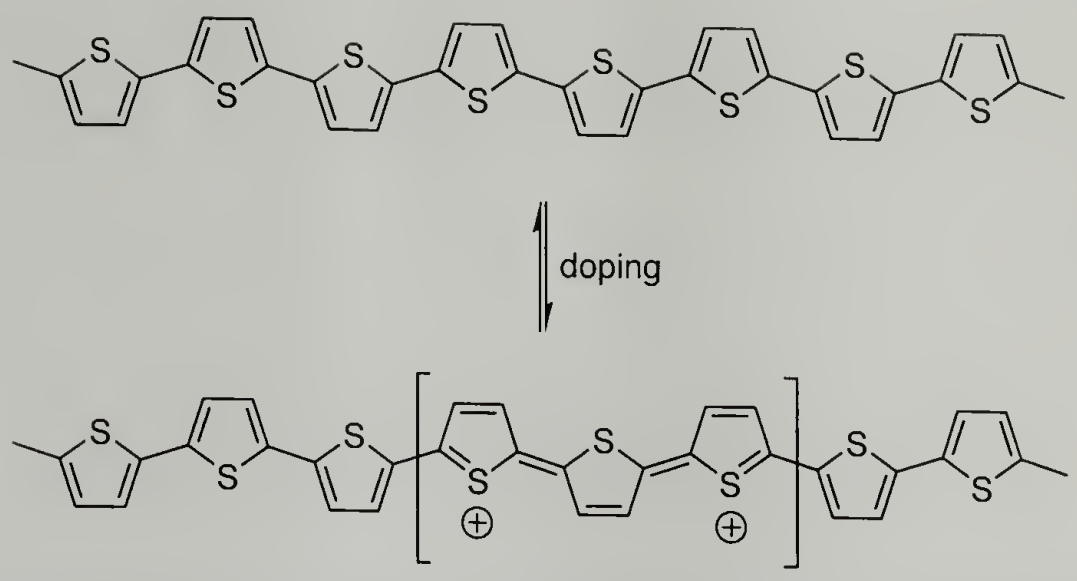

Figure 1.2. Removal of two electrons (p-doping) from a PT chain produces a bipolaron.

1.2.1 Mechanism of conductivity and doping

Electrons are delocalized along the conjugated backbones of conducting polymers, usually through overlap of π-orbitals, resulting in an extended π-system with a filled valence band. By removing electrons from the π-system ("p-doping"), or adding electrons into the π-system ("n-doping"), a charged unit called a bipolaron is formed (figure 1.2). Doping is performed at much higher levels (20–40%) in conducting polymers than in semiconductors (<1%). The bipolaron moves as a unit up and down the polymer chain, and is responsible for the macroscopically observed conductivity of the polymer. For some samples of poly(3-dodecylthiophene) doped with iodine, the conductivity can approach 1000 S/cm.[21] (In comparison, the conductivity of copper is approximately 5×10^5 S/cm.) Generally, the conductivity of PTs is lower than 1×10^3 S/cm, but high conductivity is not necessary for many applications of conducting polymers (see section 1.2.4 for examples).

Simultaneous oxidation of the conducting polymer and introduction of counter ions, p-doping, can be accomplished electrochemically or chemically. During the electrochemical synthesis of a PT, counter ions dissolved in the solvent can asso-

ciate with the polymer as it is deposited onto the electrode in its oxidized form. By doping the polymer as it is synthesized, a thick film can build up on an electrode – the polymer conducts electrons from the substrate to the surface of the film. Alternatively, a neutral conducting polymer film or solution can be doped post-synthesis.

Reduction of the conducting polymer, n-doping, is much less common than p-doping. An early study of electrochemical n-doping of poly(bithiophene) found that the n-doping levels are less than those of p-doping, the n-doping cycles were less efficient, the number of cycles required to reach maximum doping was higher, and the n-doping process appeared to be kinetically limited, possibly due to counter ion diffusion in the polymer.[22]

A variety of reagents have been used to dope PTs. Iodine and bromine produce high conductivities,[21] but are unstable and slowly evaporate from the material.[23] Organic acids, including trifluoroacetic acid, propionic acid, and sulfonic acids produce PTs with lower conductivities than iodine, but with higher environmental stabilities.[23,24] Oxidative polymerization with ferric chloride can result in doping by residual catalyst,[25] although MALDI-MS studies have shown that poly(3-hexylthiophene)s are also partially halogenated by the residual oxidizing agent.[26] Poly(3-octylthiophene) dissolved in toluene can be doped by solutions of ferric chloride hexahydrate dissolved in acetonitrile, and can be cast into films with conductivities reaching 1 S/cm.[27] Other, less common p-dopants include gold trichloride[28] and trifluoromethanesulfonic acid.[29]

1.2.2 Structure and optical properties

1.2.2.1 Conjugation length and chromisms

The extended π-systems of conjugated PTs produce some of the most interesting properties of these materials – their optical properties. As an approxima-

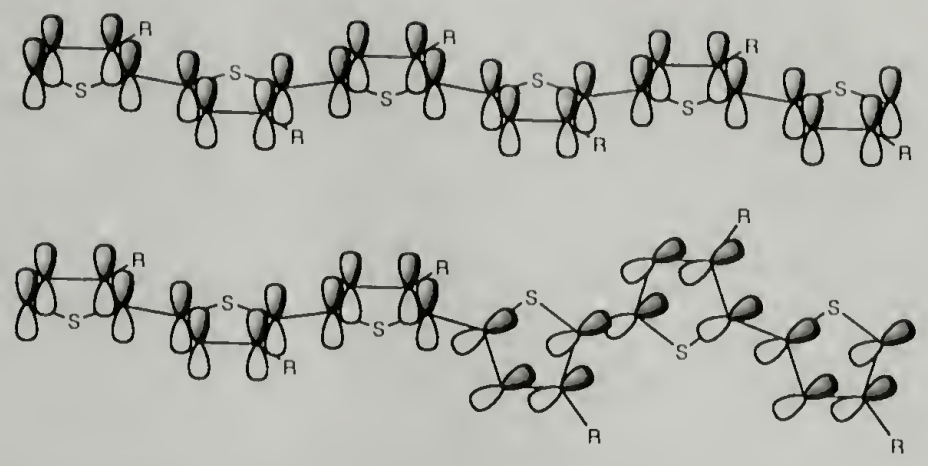

Figure 1.3. Conjugated π-orbitals of a coplanar and a twisted substituted PT.

tion, the conjugated backbone can be considered as a real-world example of the "electron-in-a-box" solution to the Schrödinger equation; however, the development of refined models to accurately predict absorption and fluorescence spectra of well-defined oligo(thiophene) systems is ongoing.[30] Conjugation relies upon overlap of the π-orbitals of the aromatic rings, which, in turn, requires the thiophene rings to be coplanar (figure 1.3, top). The number of coplanar rings determines the conjugation length – the longer the conjugation length, the lower the separation between adjacent energy levels, and the longer the absorption wavelength. Deviation from coplanarity may be permanent, resulting from mislinkages during synthesis or especially bulky side chains; or temporary, resulting from changes in the environment or binding. This twist in the backbone reduces the conjugation length (figure 1.3, bottom), and the separation between energy levels is increased. This results in a shorter absorption wavelength.

Determining the maximum effective conjugation length requires the synthesis of regioregular PTs of defined length. The absorption band in the visible region is increasingly red-shifted as the conjugation length increases, and the maximum effective conjugation length is calculated as the saturation point of the red shift. Early studies by ten Hoeve et al. estimated that the effective conjugation extended over 11 repeat units,[31] while later studies increased this estimate to 20 units.[32] More

recently, Otsubo et al. synthesized 48-[33] and 96-mer[34] oligo(thiophene)s, and found that the red shift, while small (a difference of 0.1 nm between the 72- and the 96-mer), does not saturate, meaning that the effective conjugation length may be even longer than 96 units.[34]

A variety of environmental factors can cause the conjugated backbone to twist, reducing the conjugation length and causing an absorption band shift, including solvent, temperature, application of an electric field, and dissolved ions. The absorption band of poly(3-thiophene acetic acid) in aqueous solutions of poly(vinyl alcohol) (PVA) shifts from 480 nm at pH 7 to 415 nm at pH 4. This is attributed to formation of a compact coil structure which can form hydrogen bonds with PVA upon partial deprotonation of the acetic acid group.[35] Chiral PTs showed no induced circular dichroism (ICD) in chloroform, but displayed intense, but opposite, ICDs in chloroform-acetonitrile mixtures versus chloroform-acetone mixtures.[36] Also, a PT with a chiral amino acid side chain[37] displayed moderate absorption band shifts and ICDs, depending upon the pH and the concentration of buffer.[38]

Shifts in PT absorption bands due to changes in temperature result from a conformational transition from a coplanar, rodlike structure at lower temperatures to a nonplanar, coiled structure at elevated temperatures. For example, poly(3-(octyloxy)-4-methylthiophene) undergoes a color change from red-violet at 25 °C to pale yellow at 150 °C. An isosbestic point (a point where the absorbance curves at all temperatures overlap) indicates coexistence between two phases, which may exist on the same chain or on different chains.[39] Not all thermochromic PTs exhibit an isosbestic point: highly regioregular poly(3-alkylthiophene)s show a continuous blue shift with increasing temperature if the side chains are short enough so that they do not melt and interconvert between crystalline and disordered phases at low temperatures.[40]

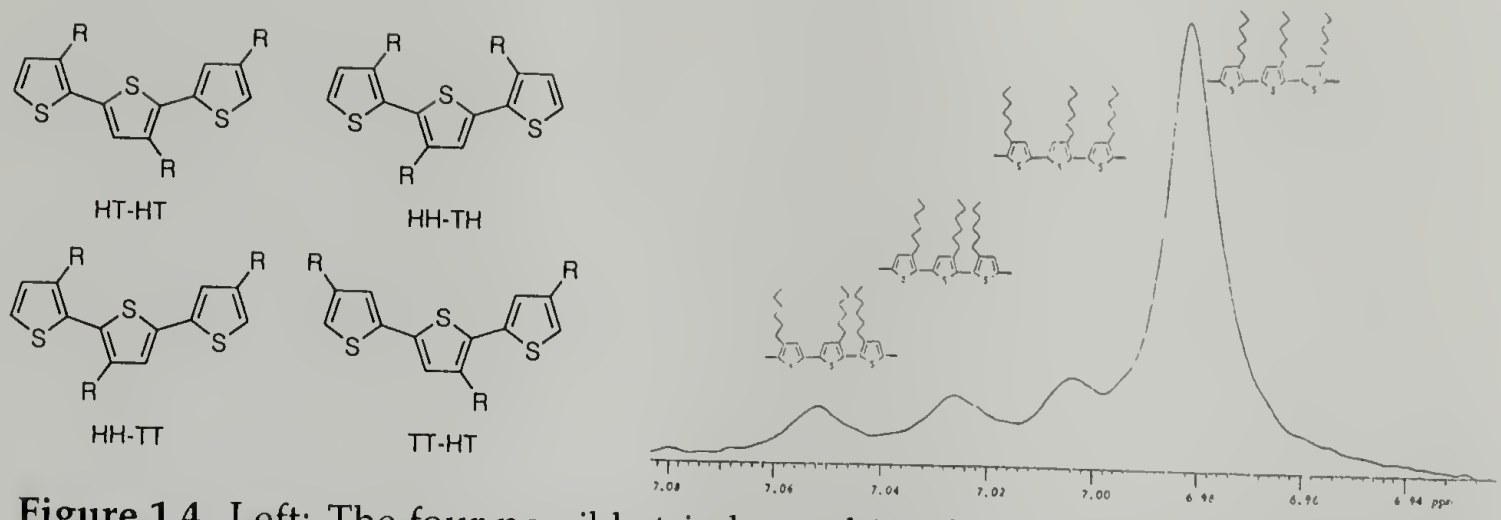

Figure 1.4. Left: The four possible triads resulting from coupling of 3-substituted thiophenes. Right: ^{1}H NMR spectrum of a sample of poly(3-hexylthiophene) obtained by ferric chloride oxidative polymerization, showing the resonances corresponding to the 4-position proton. Reprinted with permission from Barbarella, G.; Bongini, A.; Zambianchi, M. *Macromolecules* **1994,** 27, 3039–3045. Copyright 1994 American Chemical Society.

Finally, PTs can exhibit absorption shifts due to application of electric potentials (electrochromism),[41] or to introduction of alkali ions (ionochromism).[42] These effects will be discussed in the context of applications of PTs in section 1.2.4.

1.2.2.2 Regioregularity

The asymmetry of 3-substituted thiophenes results in three possible couplings when two monomers are linked between the 2- and the 5-positions. These couplings are:

- 2,5′, or head-tail (HT), coupling
- 2,2′, or head-head (HH), coupling
- 5,5′, or tail-tail (TT), coupling

These three diads can be combined into four distinct triads, shown in figure 1.4 (left). The triads are distinguishable by NMR spectroscopy (figure 1.4, right), and the degree of regioregularity can be estimated by integration.[43,44]

Elsenbaumer et al. first noticed the effect of regioregularity on the properties of PTs. A regiorandom copolymer of 3-methylthiophene and 3-butylthiophene possessed a conductivity of 50 S/cm, while a more regioregular copolymer with a 2:1 ratio of HT to HH couplings had a higher conductivity of 140 S/cm.[45] Films of regioregular poly(3-(4-octylphenyl)thiophene) (POPT) with greater than 94% HT content possessed conductivities of 4 S/cm, compared with 0.4 S/cm for regioirregular POPT.[46] Poly(alkylthiophenes) prepared using Rieke zinc formed "crystalline, flexible, and bronze-colored films with a metallic luster." On the other hand, the corresponding regiorandom polymers produced "amorphous and orange-colored films."[47] Comparison of the thermochromic properties of the Rieke poly(alkylthiophene)s showed that, while the regioregular polymers showed strong thermochromic effects, the absorbance spectra of the regioirregular polymers did not change significantly at elevated temperatures. This was likely due to the formation of only weak and localized conformational defects.[48] Finally, Xu and Holdcroft demonstrated that the fluorescence absorption and emission maxima of poly(3-hexylthiophene)s occur at increasingly lower wavelength (higher energy) with increasing HH dyad content. The difference between absorption and emission maxima, the Stokes shift, also increases with HH dyad content, which they attributed to greater relief from conformational strain in the first excited state.[49]

1.2.2.3 Solubility

Unsubstituted PTs are conductive after doping, and have excellent environmental stability compared with some other conducting polymers such as poly(acetylene), but are intractable and soluble only in solutions like mixtures of arsenic trifluoride and arsenic pentafluoride.[50] However, in 1987 examples of organic-soluble PTs were reported. Elsenbaumer et al., using a nickel-catalyzed Grignard cross-coupling, synthesized two soluble PTs, poly(3-butylthiophene) and poly(3-

methylthiophene-*co*-3′-octylthiophene), which could be cast into films and doped with iodine to reach conductivities of 4 to 6 S/cm.[51] Hotta et al. synthesized poly(3-butylthiophene) and poly(3-hexylthiophene) electrochemically[52] (and later chemically[53]), and characterized the polymers in solution[54] and cast into films.[55] The soluble poly(alkylthiophene)s (PATs) demonstrated both thermochromism and solvatochromism (section 1.2.2.1) in chloroform and 2,5-dimethyltetrahydrofuran.[56]

Also in 1987, Wudl et al. reported the syntheses of water-soluble sodium poly(3-thiophenealkanesulfonate)s.[57] In addition to conferring water solubility, the pendant sulfonate groups act as counterions, producing self-doped conducting polymers. Substituted PTs with tethered carboxylic acids,[58] acetic acids,[59] amino acids,[37] and urethanes[60] are also water-soluble.

More recently, poly(3-(perfluorooctyl)thiophene)s soluble in supercritical carbon dioxide[61] were electrochemically and chemically synthesized by Collard et al.[62] Finally, unsubstituted oligo(thiophene)s capped at both ends with thermally-labile alkyl esters were cast as films from solution, and then heated to remove the solublizing end groups. AFM images showed a significant increase in long-range order after heating.[63]

1.2.3 Synthesis

PTs can be synthesized electrochemically, by applying a potential across a solution of the monomer to be polymerized, or chemically, using oxidants or cross-coupling catalysts. Both methods have their advantages and disadvantages.

1.2.3.1 Electrochemical synthesis

In an electrochemical polymerization, a potential is applied across a solution containing thiophene and an electrolyte, producing a conductive PT film on the anode.[64] Electrochemical polymerization is convenient, since the polymer does not need to be isolated and purified, but it produces structures with varying de-

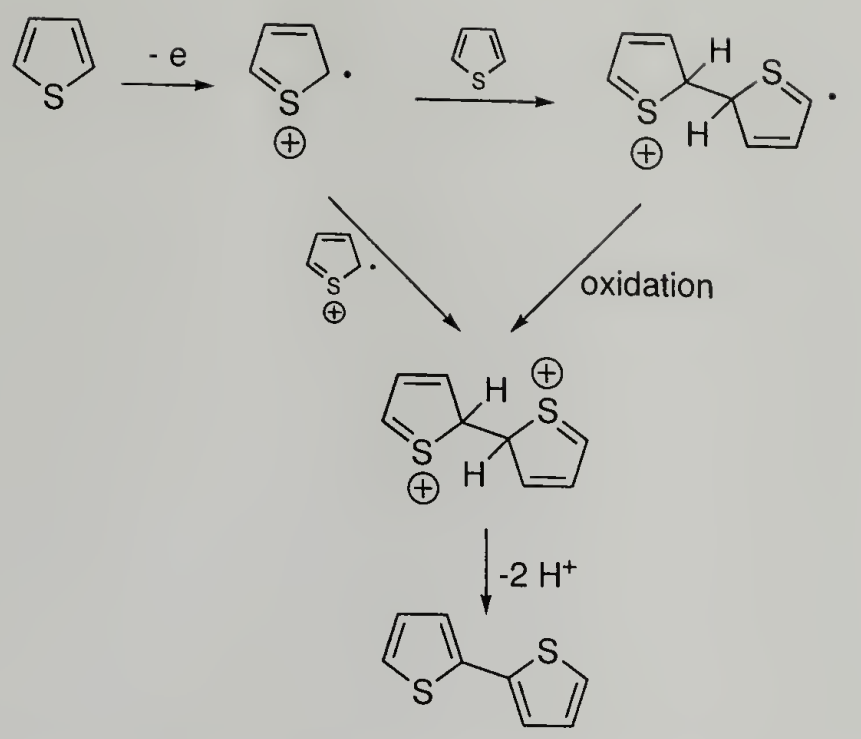

Figure 1.5. Initial steps in the electropolymerization of thiophenes.

grees of structural irregularities, such as crosslinking. As shown in figure 1.5, oxidation of a monomer produces a radical cation, which can then couple with a second radical cation to form a dication dimer, or with another monomer to produce a radical cation dimer. A number of techniques, including in situ video microscopy,[65] cyclic spectrovoltammetry,[66] photocurrent spectroscopy,[67] and electrochemical quartz crystal microbalance measurements,[68] have been used to elucidate the nucleation and growth mechanism leading to deposition of polymer onto the anode. Deposition of long, well-ordered chains onto the electrode surface is followed by growth of either long, flexible chains, or shorter, more crosslinked chains, depending upon the polymerization conditions.

The quality of an electrochemically prepared PT film is affected by a number of factors. These include the electrode material, current density, temperature, solvent, electrolyte, presence of water, and monomer concentration.[15] Two other important but interrelated factors are the structure of the monomer and the applied potential. The potential required to oxidize the monomer depends upon the electron density in the thiophene ring π-system. Electron-donating groups lower the oxidation po-

tential, while electron-withdrawing groups increase the oxidation potential. Thus, 3-methylthiophene polymerizes in acetonitrile and tetrabutylammonium tetrafluoroborate at a potential of about 1.5 V vs. SCE (standard calomel electrode), while unsubstituted thiophene polymerizes at about 1.7 V vs. SCE. Steric hindrance resulting from branching at the α-carbon of a 3-substituted thiophene inhibits polymerization.[69] This observation leads to the so-called "poly(thiophene) paradox": the oxidation potential of many thiophene monomers is higher than the oxidation potential of the resulting polymer. In other words, the polymer can be irreversibly oxidized and decompose at a rate comparable to the polymerization of the corresponding monomer.[70] This remains one of the major disadvantages of electrochemical polymerization, and limits its application for many thiophene monomers with complex side groups.

1.2.3.2 Chemical synthesis

Chemical synthesis offers two advantages compared with electrochemical synthesis of PTs: a greater selection of monomers, and, using the proper catalysts, the ability to synthesize perfectly regioregular substituted PTs. While PTs may have been chemically synthesized by accident more than a century ago,[71] the first planned chemical syntheses using metal-catalyzed polymerization of 2,5-dibromothiophene were reported by two groups independently in 1980. Yamamoto et al. used magnesium in THF and nickel(bipyridine) dichloride, analogous to the Kumada coupling of Grignard reagents to aryl halides.[72] Lin and Dudek also used magnesium in THF, but with a series of acetylacetonate catalysts ($Pd(acac)_2$, $Ni(acac)_2$, $Co(acac)_2$, and $Fe(acac)_3$).[73]

Later developments produced higher molecular weight PTs than those initial efforts, and can be grouped into two categories based on their structure. Regioregular PTs can be synthesized by catalytic cross-coupling reactions of bromothio-

phenes, while polymers with varying degrees of regioregularity can be simply synthesized by oxidative polymerization.

The first synthesis of perfectly regioregular PATs was described by McCullough et al. in 1992.[74] As shown in figure 1.6 (top), selective bromination produces 2-bromo-3-alkylthiophene, which is followed by metallation and then Kumada cross-coupling in the presence of a nickel catalyst. This method produces approximately 100% HT-HT couplings, according to NMR spectroscopy analysis of the diads. In the method subsequently described by Rieke et al. in 1993,[75] 2,5-dibromo-3-alkylthiophene is treated with highly reactive "Rieke zinc"[76] to form a mixture of organometallic isomers (figure 1.6, bottom). Addition of a catalytic amount of $Pd(PPh_3)_4$ produces a regiorandom polymer, but treatment with $Ni(dppe)Cl_2$ yields regioregular poly(3-alkylthiophene) in quantitative yield.[77]

While the McCullough and Rieke methods produce structurally homogenous PATs, they require low temperatures, the careful exclusion of water and oxygen, and brominated monomers. In contrast, the oxidative polymerization of thiophenes using ferric chloride described by Sugimoto in 1986 can be performed at room temperature under less demanding conditions.[78] This method has proven to be extremely popular; the antistatic coating Baytron P is prepared on a commercial scale using ferric chloride (see section 1.2.4).[79]

A number of studies have been conducted in attempts to improve the yield and quality of the product obtained using the oxidative polymerization technique. In addition to ferric chloride, other oxidizing agents, including ferric chloride hydrate, copper perchlorate, and iron perchlorate have also been used successfully to polymerize 2,2′-bithiophene.[80] Slow addition of ferric chloride to the monomer solution produced poly(3-(4-octylphenyl)thiophene)s with approximately 94% head-to-tail content.[46] Precipitation of ferric chloride in situ (in order to maximize the surface area of the catalyst) produced significantly higher yields and monomer

McCullough method:

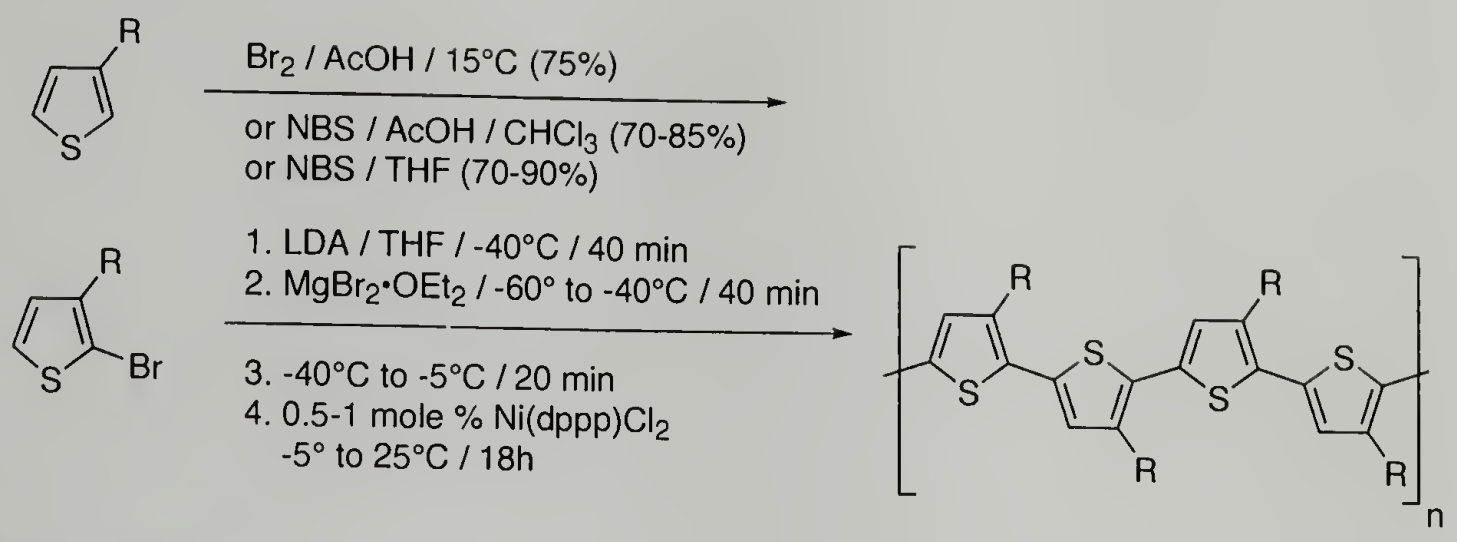

Rieke method:

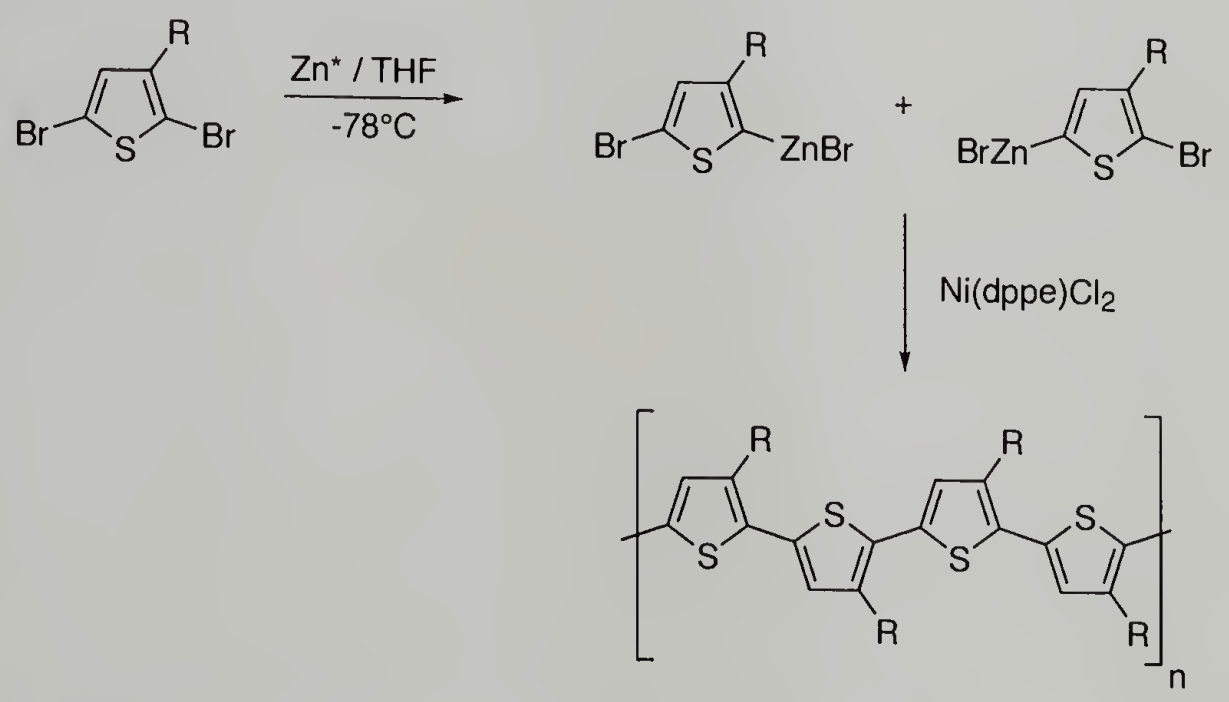

Figure 1.6. Crosscoupling methods for preparing regioregular poly(3-alkylthiophenes).

conversions than adding monomer directly to crystalline catalyst.[81,82] Higher molecular weights were reported when dry air was bubbled through the reaction mixture during polymerization.[83] Exhaustive Soxhlet extraction after polymerization with polar solvents was found to effectively fractionate the polymer and remove residual catalyst before NMR spectroscopy.[43] Using a lower ratio of catalyst to monomer (2:1, rather than 4:1) may increase the regioregularity of poly(3-dodecylthiophene)s.[84] Andreani et al. reported higher yields of soluble poly(dialkylterthiophene)s in carbon tetrachloride rather than chloroform, which they attributed to the stability of the radical species in carbon tetrachloride.[85] Higher quality catalyst, added at a slower rate and at reduced temperature, was shown to produce high molecular weight PATs with no insoluble polymer residue.[86] Laakso et al. used a factorial design to determine that increasing the ratio of catalyst to monomer increased the yield of poly(3-octylthiophene), and claimed* that a longer polymerization time also increased the yield.[87]

The mechanism of the oxidative polymerization using ferric chloride has been controversial. Sugimoto et al. did not speculate on a mechanism in their 1986 report.[78] In 1992, Niemi et al. proposed a radical mechanism, shown in figure 1.7 (top). They based their mechanism on two assumptions. First, since they observed polymerization only in solvents where the catalyst was either partially or completely insoluble (chloroform, toluene, carbon tetrachloride, pentane, and hexane, and not diethyl ether, xylene, acetone, or formic acid), they concluded that the active sites of the polymerization must be at the surface of solid ferric chloride. Therefore, they discounted the possibilities of either two radical cations reacting with each other, or two radicals reacting with each other, "because the chloride ions at the surface of the crystal would prevent the radical cations or radicals from

*Our own analysis of their factorial design indicates that the increase in yield observed when they used a longer polymerization time is, in fact, insignificant (see section 3.1.1).

Radical:

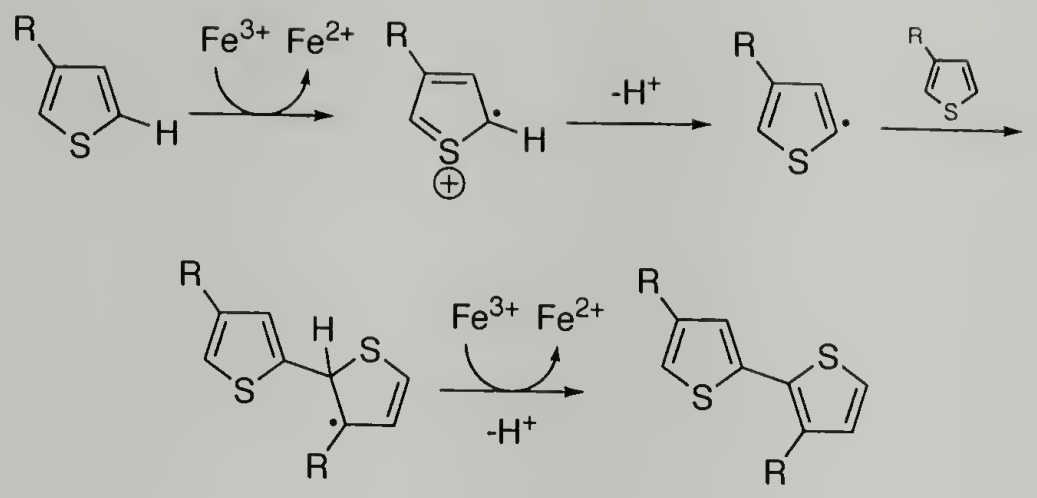

Carbocation:

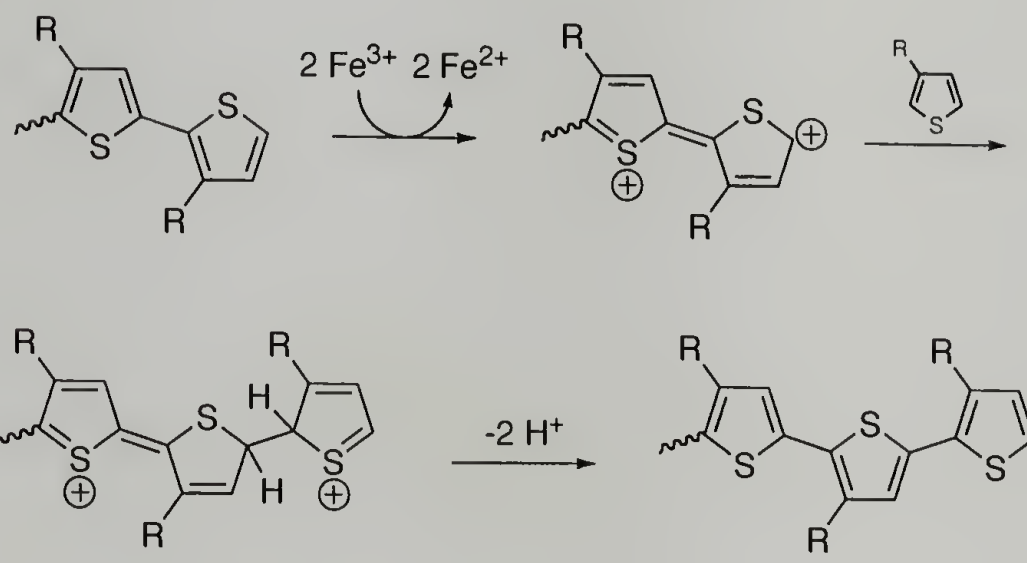

Radical cation:

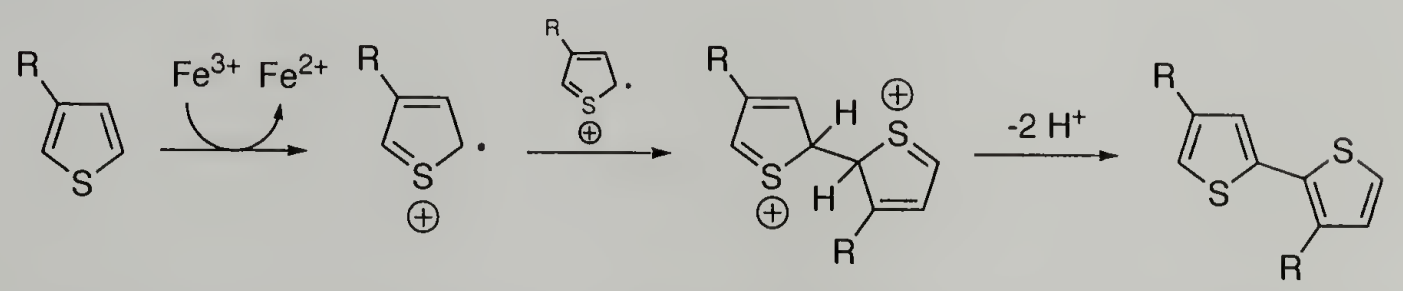

Figure 1.7. Proposed mechanisms for ferric chloride oxidative polymerizations of thiophenes.

assuming positions suitable for dimerization."[88] Second, using 3-methylthiophene as a prototypical monomer, they performed quantum mechanical calculations to determine the energies and the total atomic charges on the carbon atoms of the four possible polymerization species (neutral 3-methylthiophene, the radical cation, the radical on carbon 2, and the radical on carbon 5).

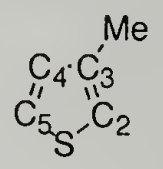

Since the most negative carbon of the neutral 3-methylthiophene is also carbon 2, and the carbon with the highest odd electron population of the radical cation is carbon 2, they concluded that a radical cation mechanism would lead to mostly 2–2, head-to-head links.† They then calculated the total energies of the species with the radicals at the 2 and the 5 carbons, and found that the latter was more stable by 1.5 kJ mol^{-1}. Therefore, the more stable radical could react with the neutral species, forming head-to-tail couplings as shown in figure 1.7 (top).

Andersson et al. offered an alternative mechanism in the course of their studies of the polymerization of 3-(4-octylphenyl)thiophene with ferric chloride, where they found a high degree of regioregularity when the catalyst was added to the monomer mixture slowly. They concluded that, given the selectivity of the couplings, and the strong oxidizing conditions, the reaction could proceed via a carbocation mechanism (figure 1.7, middle).[46]

The radical mechanism was directly challenged in a short communication in 1995, when Olinga and François noted that thiophene could be polymerized by ferric chloride in acetonitrile, a solvent in which the catalyst is completely soluble. Their analysis of the kinetics of thiophene polymerization also seemed to contradict the predictions of the radical polymerization mechanism.[89] Barbarella

---

†Niemi et al. describe the linkage between carbon 2 and carbon 2 as "tail-to-tail", and not "head-to-head" as is the convention in current poly(3-alkylthiophene) literature.

et al. studied the oligomerization of 3-(alkylsulfanyl)thiophenes, and concluded from their quantum mechanical calculations, and considerations of the enhanced stability of the radical cation when delocalized over a planar conjugated oligomer, that a radical cation mechanism analogous to that generally accepted for electrochemical polymerization was more likely (figure 1.7, bottom).[90] Given the difficulties of studying a system with a heterogeneous, strongly oxidizing catalyst that produces difficult to characterize rigid-rod polymers, the mechanism of oxidative polymerization is by no means decided. However, the radical cation mechanism shown in figure 1.7 is generally accepted as the most likely route for PT synthesis.

1.2.4 Applications

A number of applications have been proposed for conducting PTs, including field-effect transistors,[91] electroluminescent devices, solar cells, photochemical resists, nonlinear optic devices,[92] batteries, and diodes. In general, there are two categories of applications for conducting polymers. Static applications rely upon the intrinsic conductivity of the materials, combined with their ease of processing and material properties common to polymeric materials. Dynamic applications utilize changes in the conductive and optical properties, resulting either from application of electric potentials or from environmental stimuli.

As an example of a static application, Bayer AG's poly(ethyldioxythiophene)-poly(styrene sulfonate) (PEDOT-PSS) product Baytron P (figure 1.8) has been extensively used as an antistatic coating (as packaging materials for electronic components, for example). AGFA coats 200×10^6 m^2 of photographic film per year with Baytron because of its antistatic properties. The thin layer of Baytron is virtually transparent and colorless, prevents electrostatic discharges during film rewinding, and reduces dust buildup on the negatives after processing.

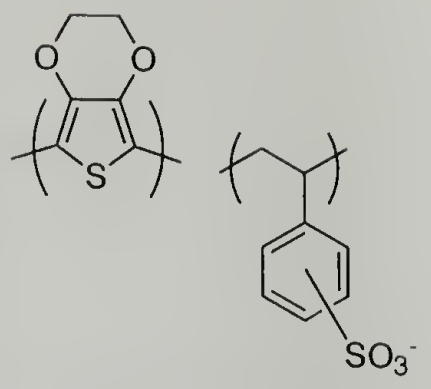

Figure 1.8. PEDOT-PSS (Baytron P).

PEDOT can also be used in dynamic applications where a potential is applied to a polymer film. The electrochromic properties of PEDOT are used to manufacture windows and mirrors which can become opaque or reflective upon the application of an electric potential.[41] Widespread adoption of electrochromic windows could save billions of dollars per year in air conditioning costs.[93] Finally, Phillips has commercialized a cellular telephone with an electrically switchable PEDOT mirror.

The use of PTs as sensors responding to an analyte has also been the subject of intense research. Biosensor applications will be discussed in Chapter 3, but PTs can also be functionalized with synthetic receptors for detecting metal ions or chiral molecules as well. PTs with pendant[94] and main-chain[42] crown ether functionalities were reported in 1993 by the research groups of Bäuerle and Swager, respectively (figure 1.9). Electrochemically polymerized thin films of the Bäuerle pendant crown ether PT were exposed to millimolar concentrations of alkali cations (Li^+, Na^+, and K^+). The current which passed through the film at a fixed potential dropped dramatically in lithium ion solutions, less so for sodium ion solutions, and only slightly for potassium ion solutions. The Swager main chain crown ether PTs were prepared by chemical coupling and characterized by absorbance spectroscopy. Addition of the same alkali cations resulted in absorbance shifts of 46 nm (Li^+), 91 nm (Na^+), and 22 nm (K^+). The size of the shifts corresponds to the

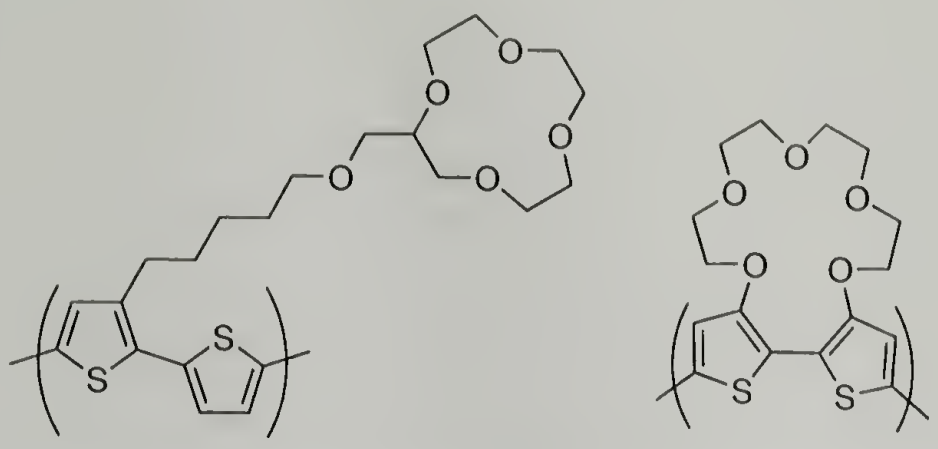

Figure 1.9. Ionoselective PTs reported by Bäuerle[94] (left) and Swager[42] (right).

ion binding preferences of the corresponding crown ether, resulting from a twist in the conjugated polymer backbone induced by ion binding.

In the course of their studies of the optical properties of chiral PTs,[95–98] Yashima and Goto found that a PT with a chiral primary amine (figure 1.10, left) was sensitive to chiral amino alcohols, producing mirror image split ICD responses in the π–π^* transition region (figure 1.10, right).[99] This was the first example of chiral recognition by PTs using a chiral detection method (CD spectroscopy). This distinguished it from earlier work by Lemaire et al. who used an achiral detection method (cyclic voltammetry) to detect incorporation of chiral dopant anions into an electrochemically polymerized chiral PT.[100]

1.3 Project overview

The genesis of the project described herein was the incorporation of 3-thienylalanine (3TA) into a periodic protein by Kothakota et al.[8]

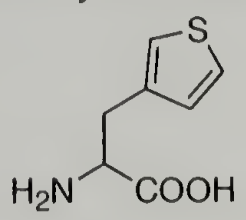

This artificial amino acid could provide a link between the precision of engineered proteins with the unique electronic properties of conducting polymers. Biosensor

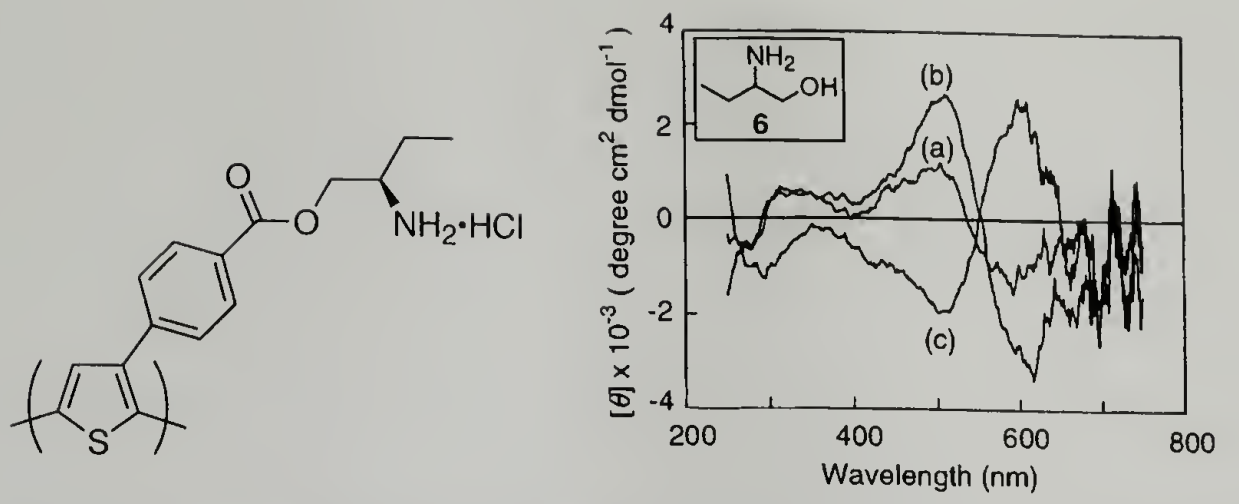

Figure 1.10. CD spectra of chiral PT (left) in DMSO (a), and in mixtures of DMSO and *(R)*-2-amino-1-butanol (b) and *(S)*-2-amino-1-butanol (c). Reprinted with permission from Yashima, E.; Goto, H.; Okamoto, Y. *Macromolecules* **1997**, *32*, 7942–7945. Copyright 1997 American Chemical Society.

devices made with enzymes attached through covalent bonds could have longer lifetimes than sensors with entrapped enzymes that can diffuse out of the device. And, since the covalent bonds would be located at specific sites on the protein (instead of random lysine residues, for example), the devices would have higher enzyme activities than sensors with indiscriminate bonds between the conducting polymer and the enzyme which could interfere with enzyme activity. Cell-binding sequences could be used to create conductive films which would cause adhesion of specific cell types. For example, a conducting polymer film with a neuron cell-binding domain could be used to build an interface between an electric circuit and a nerve.

By dissolving a protein containing 3TA in an appropriate solvent and applying an electric field, it was hoped that a conductive film of the protein would be electrochemically deposited on the anode. However, early experiments showed that this scenario was unlikely. The steric constraints imposed by a large peptide, even a periodic peptide with 3TA localized at the folds (figure 1.1), would preclude attaining a degree of polymerization greater than two or three. Introduction of a comonomer could alleviate these steric constraints by forming conjugated poly-

mer bridges between thiophene groups anchored to the protein. Electrochemical techniques were developed to create conditions for such a copolymerization, but two obstacles remained. First, copolymerization would require oxidation of both the monomer and the protein-anchored thiophene. But, the oxidation potentials, the electric potentials required to remove electrons from the rings, were different for comonomer thiophenes and the peptide thiophenes. Second, even if both the comonomer and the peptide-anchored thiophene could be oxidized and coupled successfully, the polymerization would result in a large excess of homopolymer that did not include the protein (since the oxidation potential of the comonomer is lower than that of the peptide). An unwanted excess of homopolymer would dilute any expected observable effects resulting from protein incorporation into the conducting film.

These two problems were solved by switching from electrochemical to chemical polymerization, and by adopting the methodology of solid phase synthesis. By using a chemical oxidant, both the peptide-anchored thiophene and the comonomer could be oxidized simultaneously. And, by mounting the peptide on a solid phase resin, the desired copolymer could be isolated, purified, and characterized. This framework for synthesis of conducting graft copolymers is flexible and expandable. Diverse sets of peptides or conducting polymers could be synthesized by varying amino acid sequence or thiophene monomer structure. The ability to purify just the copolymer might someday make it possible to isolate detectable amounts of copolymer obtained by electrochemical polymerization. And, since the resin beads are macroscopic, some characterization methods might be performed more conveniently while the copolymers were still mounted on the bead (such as fluorescence spectroscopy[101]).

The choice of a linker between the bead and a peptide is described in Chapter 2. The linker needed to be stable under oxidative polymerization conditions,

but cleavable under orthogonal conditions in order to isolate the intact copolymer. Conditions for loading protected 3TA onto resins with greater than 90% efficiency were determined by measuring the concentration of the protecting groups and by elemental analysis. Loaded resins with three different linkers were then exposed to ferric chloride for five hours, and the hydroxymethylbenzoic acid (HMBA) linker was found to be the most stable. This was determined by measuring the concentration of retained protecting groups and by elemental analysis.

Chapter 3 details determination of conditions for oxidative copolymerization of the 3TA-loaded HMBA beads with 3-hexylthiophene. Eight different factors that could affect the copolymerization were identified. A two-level Resolution IV factorial design was used, reducing the number of required experiments from 64 to 24. The fluorescence emission maxima, dependent upon conjugation length, were measured for the 24 different copolymers. (The conjugation length, in turn, depends on degree of polymerization and on regioregularity.) Five of the eight factors were found to have statistically significant effects on the fluorescence emission.

The solid phase synthesis of two peptides containing 3TA, a glycine spacer, and a biotinylated residue (or a nonbiotinylated control residue) are described in Chapter 4. The peptides were characterized by electrospray ionization mass spectroscopy, and their structures confirmed by their fragmentation patterns. The factors found to be significant in Chapter 3 were used to determine copolymerization conditions for the peptides and 3-hexylthiophene. After purification and cleavage, the structures and molecular weights of the copolymers were determined by two-dimensional NMR spectroscopy. Fluorescence emission spectra of the copolymers confirmed their high degrees of polymerization.

Finally, a summary of the data and some thoughts on future directions for this system are presented in Chapter 5. As mentioned above, this method enables the

synthesis and, especially, the purification of these exciting materials, and is not necessarily limited to the peptide sequences or thiophene monomers presented in this work.

1.4 References

(1) Krejchi, M. T.; Atkins, E. D. T.; Waddon, A. J.; Fournier, M. J.; Mason, T. L.; Tirrell, D. A. *Science* **1994,** *265,* 1427-1432.

(2) van Hest, J. C. M.; Tirrell, D. A. *Chem. Commun.* **2001,** 1897-1904.

(3) Yu, S. J. M.; Conticello, V. P.; Zhang, G. H.; Kayser, C.; Fournier, M. J.; Mason, T. L.; Tirrell, D. A. *Nature* **1997,** *389,* 167-170.

(4) Flory, P. J. *Proc. R. Soc. London, Ser. A* **1956,** *234,* 73-89.

(5) Richmond, M. H. *Bacteriological Rev.* **1962,** *26,* 398-420.

(6) Dougherty, M. J.; Kothakota, S.; Mason, T. L.; Tirrell, D. A.; Fournier, M. J. *Macromolecules* **1993,** *26,* 1779-1781.

(7) Yoshikawa, E.; Fournier, M. J.; Mason, T. L.; Tirrell, D. A. *Macromolecules* **1994,** *27,* 5471-5475.

(8) Kothakota, S.; Mason, T. L.; Tirrell, D. A.; Fournier, M. J. *J. Am. Chem. Soc.* **1995,** *117,* 536-537.

(9) van Hest, J. C. M.; Kiick, K. L.; Tirrell, D. A. *J. Am. Chem. Soc.* **2000,** *122,* 1282-1288.

(10) Kirshenbaum, K.; Carrico, I. S.; Tirrell, D. A. *ChemBioChem* **2002,** *3,* 235-237.

(11) Datta, D.; Wang, P.; Carrico, I. S.; Mayo, S. L.; Tirrell, D. A. *J. Am. Chem. Soc.* **2002,** *124,* 5652-5653.

(12) Furter, R. *Protein Sci.* **1998,** *7,* 419-426.

(13) Kwon, I.; Kirshenbaum, K.; Tirrell, D. A. *J. Am. Chem. Soc.* **2003,** *125,* 7512-7513.

(14) Street, G. B.; Clarke, T. C. *IBM J. Res. Dev.* **1981,** *25,* 51-57.

(15) Schopf, G.; Koßmehl, G. *Adv. Polym. Sci.* **1997,** *129,* 1-166.

(16) Roncali, J. *Chem. Rev.* **1992,** *92,* 711-738.

(17) Roncali, J. *Chem. Rev.* **1997,** *97,* 173-205.

(18) McCullough, R. D. *Adv. Mater.* **1998,** *10,* 93-116.

(19) Reddinger, J. L.; Reynolds, J. R. *Adv. Polym. Sci.* **1999,** *145,* 57-122.

(20) McQuade, D. T.; Pullen, A. E.; Swager, T. M. *Chem. Rev.* **2000,** *100,* 2537-2574.

(21) McCullough, R. D.; Tristramnagle, S.; Williams, S. P.; Lowe, R. D.; Jayaraman, M. *J. Am. Chem. Soc.* **1993,** *115,* 4910-4911.

(22) Mastragostino, M.; Soddu, L. *Electrochim. Acta* **1990,** *35,* 463-466.

(23) Loponen, M. T.; Taka, T.; Laakso, J.; Väkiparta, K.; Suuronen, K.; Valkeinen, P.; Österholm, J. E. *Synth. Met.* **1991,** *41,* 479-484.

(24) Bartus, J. *J. Macromol. Sci., Chem.* **1991,** *A28,* 917-924.

(25) Qiao, X. Y.; Wang, X. H.; Mo, Z. S. *Synth. Met.* **2001,** *122,* 449-454.

(26) McCarley, T. D.; Noble, C. O.; DuBois, C. J.; McCarley, R. L. *Macromolecules* **2001,** *34,* 7999-8004.

(27) Heffner, G. W.; Pearson, D. S. *Synth. Met.* **1991,** *44,* 341-347.

(28) Abdou, M. S. A.; Holdcroft, S. *Synth. Met.* **1993,** *60,* 93-96.

(29) Rudge, A.; Raistrick, I.; Gottesfeld, S.; Ferraris, J. P. *Electrochim. Acta* **1994,** *39,* 273-287.

(30) Bässler, H. Electronic Excitation. In *Electronic Materials: The Oligomer Approach*; Müllen, K.; Wegner, G., Eds.; Wiley-VCH: Weinheim, 1998.

(31) ten Hoeve, W.; Wynberg, H.; Havinga, E. E.; Meijer, E. W. *J. Am. Chem. Soc.* **1991,** *113,* 5887-5889.

(32) Meier, H.; Stalmach, U.; Kolshorn, H. *Acta Polym.* **1997,** *48,* 379-384.

(33) Nakanishi, H.; Sumi, N.; Aso, Y.; Otsubo, T. *J. Org. Chem.* **1998,** *63,* 8632-8633.

(34) Izumi, T.; Kobashi, S.; Takimiya, K.; Aso, Y.; Otsubo, T. *J. Am. Chem. Soc.* **2003,** *125,* 5286-5287.

(35) de Souza, J. M.; Pereira, E. C. *Synth. Met.* **2001,** *118,* 167-170.

(36) Goto, H.; Yashima, E.; Okamoto, Y. *Chirality* **2000,** *12,* 396-399.

(37) Andersson, M.; Ekeblad, P. O.; Hjertberg, T.; Wennerström, O.; Inganäs, O. *Polym. Commun.* **1991,** *32,* 546-548.

(38) Nilsson, K. P. R.; Andersson, M. R.; Inganäs, O. *J. Phys.: Condes. Matter* **2002,** *14,* 10011-10020.

(39) Roux, C.; Leclerc, M. *Macromolecules* **1992,** *25,* 2141-2144.

(40) Yang, C.; Orfino, F. P.; Holdcroft, S. *Macromolecules* **1996,** *29,* 6510-6517.

(41) Heuer, H. W.; Wehrmann, R.; Kirchmeyer, S. *Adv. Funct. Mater.* **2002,** *12,* 89-94.

(42) Marsella, M. J.; Swager, T. M. *J. Am. Chem. Soc.* **1993,** *115,* 12214-12215.

(43) Barbarella, G.; Bongini, A.; Zambianchi, M. *Macromolecules* **1994,** *27,* 3039-3045.

(44) Diaz-Quijada, G. A.; Pinto, B. M.; Holdcroft, S. *Macromolecules* **1996,** *29,* 5416-5421.

(45) Elsenbaumer, R. L.; Jen, K.-Y.; Miller, G. G.; Eckhardt, H.; Shacklette, L. W.; Jow, R. Poly(alkyl thiophenes) and Poly(substituted heteroaromatic vinylenes): Versatile, Highly Conductive, Processible Polymers with Tunable Properties. In *Electronic Properties of Conjugated Polymers;* Kuzmany, H.; Mehring, M.; Roth, S., Eds.; Springer: Berlin, 1987.

(46) Andersson, M. R.; Selse, D.; Berggren, M.; Järvinen, H.; Hjertberg, T.; Inganäs, O.; Wennerström, O.; Österholm, J. E. *Macromolecules* **1994,** *27,* 6503-6506.

(47) Chen, T. A.; Wu, X.; Rieke, R. D. *J. Am. Chem. Soc.* **1995,** *117,* 233-244.

(48) Faïd, K.; Fréchette, M.; Ranger, M.; Mazerolle, L.; Lévesque, I.; Leclerc, M.; Chen, T. A.; Rieke, R. D. *Chem. Mat.* **1995,** *7,* 1390-1396.

(49) Xu, B.; Holdcroft, S. *Macromolecules* **1993,** *26,* 4457-4460.

(50) Frommer, J. E. *Acc. Chem. Res.* **1986,** *19,* 2-9.

(51) Elsenbaumer, R. L.; Jen, K. Y.; Oboodi, R. *Synth. Met.* **1986,** *15,* 169-174.

(52) Hotta, S.; Rughooputh, S. D. D. V.; Heeger, A. J.; Wudl, F. *Macromolecules* **1987,** *20,* 212-215.

(53) Hotta, S.; Soga, M.; Sonoda, N. *Synth. Met.* **1988,** *26,* 267-279.

(54) Hotta, S. *Synth. Met.* **1987,** *22,* 103-113.

(55) Hotta, S.; Rughooputh, S. D. D. V.; Heeger, A. J. *Synth. Met.* **1987,** *22,* 79-87.

(56) Rughooputh, S. D. D. V.; Hotta, S.; Heeger, A. J.; Wudl, F. *J. Polym. Sci., Polym. Phys. Ed.* **1987,** *25,* 1071-1078.

(57) Patil, A. O.; Ikenoue, Y.; Wudl, F.; Heeger, A. J. *J. Am. Chem. Soc.* **1987,** *109,* 1858-1859.

(58) Englebienne, P.; Weiland, M. *Chem. Commun.* **1996,** 1651-1652.

(59) Kim, B. S.; Chen, L.; Gong, J. P.; Osada, Y. *Macromolecules* **1999,** *32,* 3964-3969.

(60) Jung, S. D.; Hwang, D. H.; Zyung, T.; Kim, W. H.; Chittibabu, K. G.; Tripathy, S. K. *Synth. Met.* **1998,** *98,* 107-111.

(61) DeSimone, J. M.; Guan, Z.; Elsbernd, C. S. *Science* **1992,** *257,* 945-947.

(62) Li, L.; Counts, K. E.; Kurosawa, S.; Teja, A. S.; Collard, D. M. *Adv. Mater.* **2004,** *16,* 180-183.

(63) Murphy, A. R.; Fréchet, J. M. J.; Chang, P.; Lee, J.; Subramanian, V. *J. Am. Chem. Soc.* **2004,** *126,* 1596-1597.

(64) Tourillon, G.; Garnier, F. *J. Electroanal. Chem.* **1982,** *135,* 173-178.

(65) Lukkari, J.; Tuomala, R.; Ristimaki, S.; Kankare, J. *Synth. Met.* **1992,** *47,* 217-231.

(66) Lukkari, J.; Kankare, J.; Visy, C. *Synth. Met.* **1992,** *48,* 181-192.

(67) Lukkari, J.; Alanko, M.; Pitkänen, V.; Kleemola, K.; Kankare, J. *J. Phys. Chem.* **1994,** *98,* 8525-8535.

(68) Visy, C.; Lukkari, J.; Kankare, J. *Synth. Met.* **1997,** *87,* 81-87.

(69) Roncali, J.; Garreau, R.; Yassar, A.; Marque, P.; Garnier, F.; Lemaire, M. *J. Phys. Chem.* **1987,** *91,* 6706-6714.

(70) Krische, B.; Zagorska, M. *Synth. Met.* **1989,** *28,* C263-C268.

(71) Meyer, V. *Ber. Deutsch. Chem. Ges.* **1883,** *16,* 1465-1478.

(72) Yamamoto, T.; Sanechika, K.; Yamamoto, A. *J. Polym. Sci., Polym. Lett. Ed.* **1980,** *18,* 9-12.

(73) Lin, J. W. P.; Dudek, L. P. *J. Polym. Sci., Polym. Chem. Ed.* **1980,** *18,* 2869-2873.

(74) McCullough, R. D.; Lowe, R. D. *J. Chem. Soc., Chem. Commun.* **1992,** 70-72.

(75) Chen, T. A.; O'Brien, R. A.; Rieke, R. D. *Macromolecules* **1993,** *26,* 3462-3463.

(76) Zhu, L.; Wehmeyer, R. M.; Rieke, R. D. *J. Org. Chem.* **1991,** *56,* 1445-1453.

(77) Chen, T. A.; Rieke, R. D. *J. Am. Chem. Soc.* **1992,** *114,* 10087-10088.

(78) Sugimoto, R.; Taketa, S.; Gu, H. B.; Yoshino, K. *Chem. Express* **1986,** *1,* 635-638.

(79) Jonas, F.; Heywang, G.; Schmidtberg, W.; Heinze, J.; Dietrich, M. US Patent 5 035 926, 1991.

(80) Ruckenstein, E.; Park, J. S. *Synth. Met.* **1991,** *44,* 293-306.

(81) Bizzarri, P. C.; Andreani, F.; Della Casa, C.; Lanzi, M.; Salatelli, E. *Synth. Met.* **1995,** *75,* 141-147.

(82) Fraleoni-Morgera, A.; Della Casa, C.; Lanzi, M.; Bizzarri, P. C. *Macromolecules* **2003,** *36,* 8617-8620.

(83) Pomerantz, M.; Tseng, J. J.; Zhu, H.; Sproull, S. J.; Reynolds, J. R.; Uitz, R.; Arnott, H. J.; Haider, M. I. *Synth. Met.* **1991,** *41,* 825-830.

(84) Qiao, X. Y.; Wang, X. H.; Zhao, X. J.; Liu, J.; Mo, Z. S. *Synth. Met.* **2000,** *114,* 261-265.

(85) Andreani, F.; Salatelli, E.; Lanzi, M. *Polymer* **1996,** *37,* 661-665.

(86) Gallazzi, M. C.; Bertarelli, C.; Montoneri, E. *Synth. Met.* **2002,** *128,* 91-95.

(87) Laakso, J.; Järvinen, H.; Skagerberg, B. *Synth. Met.* **1993,** *55,* 1204-1208.

(88) Niemi, V. M.; Knuuttila, P.; Österholm, J. E.; Korvola, J. *Polymer* **1992,** *33,* 1559-1562.

(89) Olinga, T.; François, B. *Synth. Met.* **1995,** *69,* 297-298.

(90) Barbarella, G.; Zambianchi, M.; DiToro, R.; Colonna, M.; Iarossi, D.; Goldoni, F.; Bongini, A. *J. Org. Chem.* **1996,** *61,* 8285-8292.

(91) Garnier, F. Field-Effect Transistors Based on Conjugated Materials. In *Electronic Materials: The Oligomer Approach*; Müllen, K.; Wegner, G., Eds.; Wiley-VCH: Weinheim, 1998.

(92) Harrison, M. G.; Friend, R. H. Optical Applications. In *Electronic Materials: The Oligomer Approach*; Müllen, K.; Wegner, G., Eds.; Wiley-VCH: Weinheim, 1998.

(93) Rosseinsky, D. R.; Mortimer, R. J. *Adv. Mater.* **2001,** *13,* 783-793.

(94) Bäuerle, P.; Scheib, S. *Adv. Mater.* **1993,** *5,* 848-853.

(95) Goto, H.; Okamoto, Y.; Yashima, E. *Chem. Eur. J.* **2002,** *8,* 4027-4036.

(96) Goto, H.; Okamoto, Y.; Yashima, E. *Macromolecules* **2002,** *35,* 4590-4601.

(97) Goto, H.; Yashima, E. *J. Am. Chem. Soc.* **2002,** *124,* 7943-7949.

(98) Sakurai, S.; Goto, H.; Yashima, E. *Org. Lett.* **2001,** *3,* 2379-2382.

(99) Yashima, E.; Goto, H.; Okamoto, Y. *Macromolecules* **1999,** *32,* 7942-7945.

(100) Lemaire, M.; Delabouglise, D.; Garreau, R.; Guy, A.; Roncali, J. *J. Chem. Soc., Chem. Commun.* **1988,** 658-661.

(101) Pina-Luis, G.; Badía, R.; Díaz-García, M. E.; Rivero, I. A. *J. Comb. Chem.* **2004,** *6,* 391-397.

CHAPTER 2

SELECTION OF A SOLID PHASE SYNTHESIS RESIN FOR OXIDATIVE COPOLYMERIZATION

2.1 Introduction

In 1963, Merrifield described a method for peptide synthesis using a polystyrene support that would overcome "the technical difficulties with solubility and purification" involved in stepwise synthesis, thus enabling the chemical synthesis of polypeptides.[1] The general applicability of solid phase synthesis (SPS), for which he received the 1984 Nobel Prize in Chemistry,* provides the foundation for DNA and peptide synthesis, and combinatorial chemistry.[2,3]

There are six major advantages of performing chemistry on solid supports, compared with traditional, solution-phase chemistry:[2]

1. Purification and isolation of the product is simplified because it is covalently linked to the support.

2. An excess of reagents can be used to drive the reaction to completion, increasing yield.

3. The support can be regenerated and reused if appropriate cleavage conditions and linker groups are used.

4. Individual molecules can be isolated on low loading supports, reducing the frequency of undesired side reactions such as crosslinking.

---

*Awarded "for his development of methodology for chemical synthesis on a solid matrix."

5. Stability of certain reagents may be enhanced when attached to a solid support.

6. Appropriate choices of supports, linkers, and reaction schemes can enable automation, necessary for the efficient synthesis of large libraries of compounds.

In the mid-1990s, it was recognized that regioregular oligo(thiophene)s were useful not only as well-defined model compounds of poly(thiophene)s (PTs), but also that they have interesting optical and electronic properties in their own right.[4–6] However, the Stille or Suzuki cross-coupling reactions used for the stepwise synthesis of oligo(thiophene)s typically result in low yields. Additionally, purification is complicated by the appearance of homocoupling products. Researchers recognized the applicability of solid phase synthesis to this problem, and in 1998 Malenfant and Fréchet reported the synthesis of an octylthiophene pentamer using a chloromethylated styrene support (figure 2.1).[7] After coupling 2,2′-bithiophene-5-carboxylic acid to 1.03 mmol/g Argopore resin, the terminal thiophene ring was brominated at the 2 position using NBS, followed by Stille coupling with 2-(trimethylstannyl)-4-octylthiophene catalyzed by $Pd(PPh_3)_2Cl_2$. This cycle was repeated to produce the dimer, trimer, tetramer, and pentamer, in yields decreasing from 98 to 90%.

Bäuerle and coworkers pursued the solid phase synthesis of oligo(thiophene)s, using Suzuki couplings to produce dodeca(3-hexylthiophene) in 15% yield over eight steps.[8,9] By using a traceless silyl linker rather than chloromethylated polystyrene, they were able to synthesize a quater(3-arylthiophene) without decarboxylating the first thiophene at the 5-position.[10] More recently, they utilized their traceless linker method to produce a 256-member library of regioregular substituted quater(3-arylthiophene)s.[11,12] By automating the synthesis and electrochemical characterization of the library, they were able to explore the influence of four

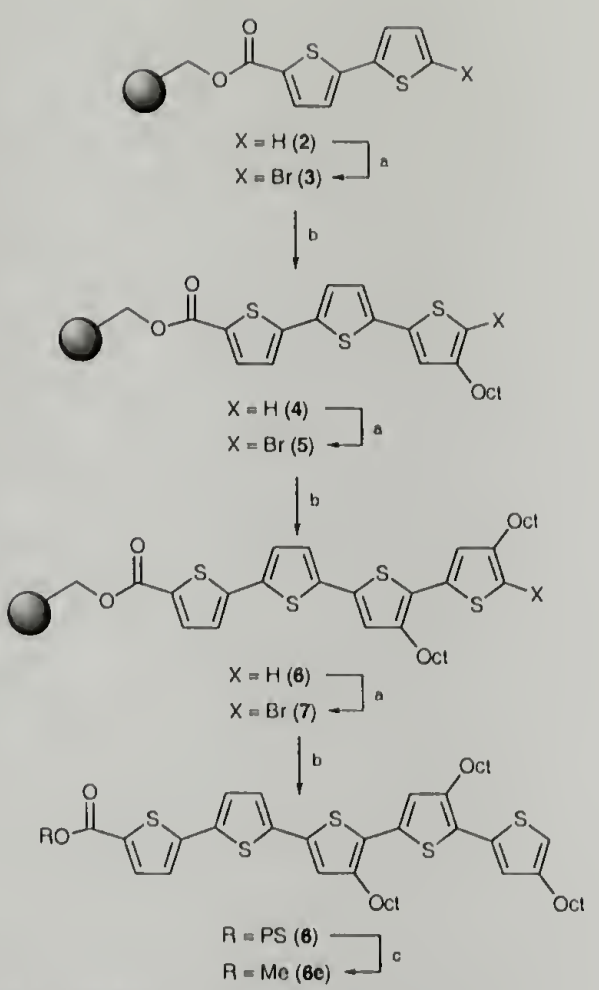

Scheme 1 *Reagents and conditions*: a, NBS, DMF, room temp.; b, 2-(trimethylstannyl)-4-octylthiophene, $Pd(PPh_3)_2Cl_2$, DMF, 80 °C; c, NaOMe, THF, reflux, 1 h, then MeI, 18-C-6, reflux, 3 h.

Figure 2.1. The first solid phase synthesis of an oligothiophene. Reprinted with permission from Malenfant, P. R. L.; Fréchet, J. M. J. *Chem. Commun.*, **1998**, 2657–2658. Copyright 1998 The Royal Society of Chemistry.

different electron-donating substituents on the first and second oxidation potentials (E_1^0 and E_2^0), and found a correlation with the sum of the Hammett constants[13] ($\Sigma\sigma_p^+$) of the individual substituents (figure 2.2).

To our knowledge, ferric chloride-catalyzed oxidative polymerization of alkylthiophenes using a solid support has not been reported. Using a solid support offers two advantages over oxidative polymerization in solution. First, purification is greatly simplified for substituted PTs that do not precipitate easily. For example, NMR-quality samples of poly(3-hexylthiophene) can be prepared by oxidative polymerization in chloroform, followed by precipitation in methanol and Soxhlet extraction of the precipitate. Our targeted copolymers have both aqueous- and

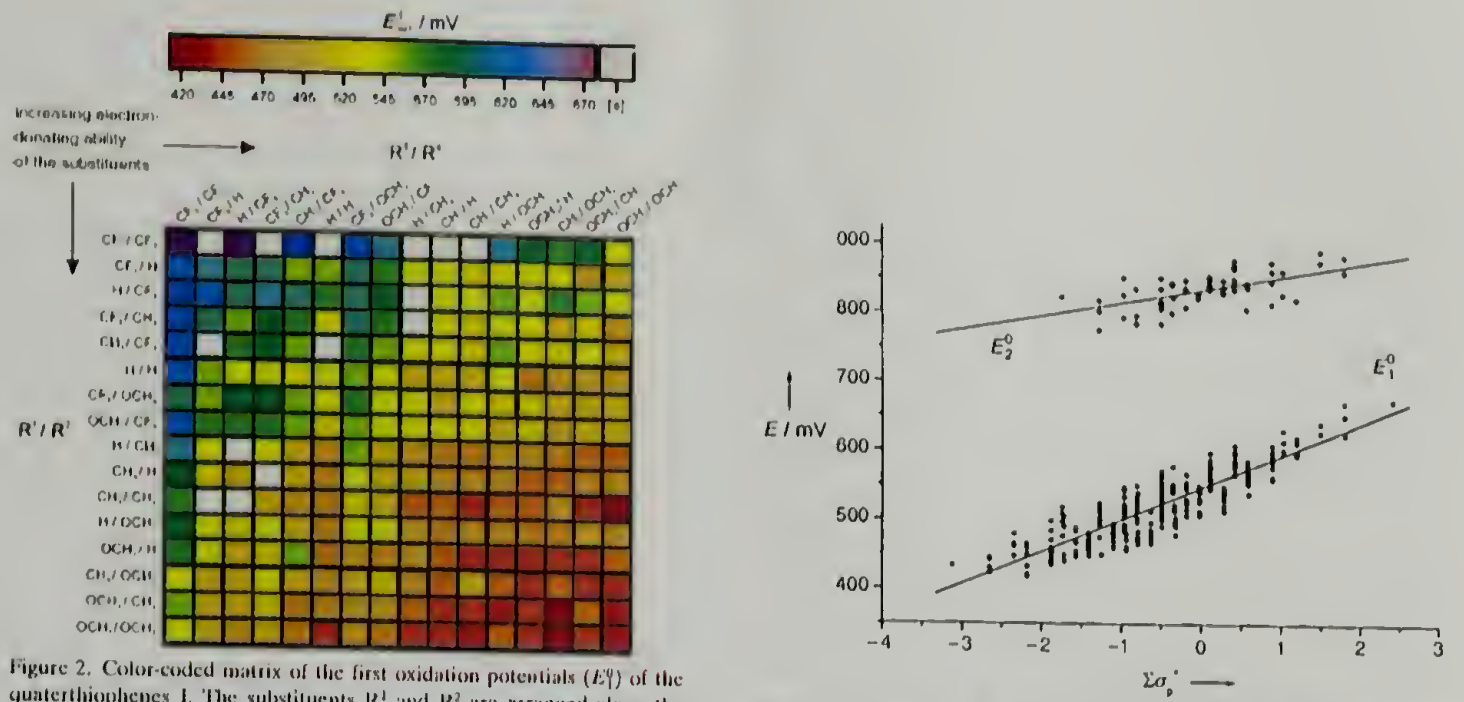

Figure 2. Color-coded matrix of the first oxidation potentials (E^0_1) of the quaterthiophenes 1. The substituents R^1 and R^2 are arranged along the ordinate, the substituents R^3 and R^4 along the abscissa. [a] Not determined because of sample impurity.

Figure 3. Correlation between the first and second oxidation potentials E^0_1 and E^0_2 of the quaterthiophenes 1 and the substituent descriptor $\Sigma\sigma_p^+$.

Figure 2.2. First oxidation potentials E_1^0 (left), and correlation between first and second oxidation potentials E_1^0 and E_2^0 and the sum of the Hammett substituent constants $\Sigma\sigma_p^+$ (right), for a library of 256 quater(arylthiophene)s. Reprinted with permission from Briehn, C. A.; Schiedel, M. S.; Bonsen, E. M.; Schuhmann, W.; Bauerle, P. *Angew. Chem. Int. Ed.*, **2001**, *40*, 4680–4683. Copyright 2001 Wiley-VCH.

organic-soluble blocks, and so do not precipitate in either polar or nonpolar solvents. By attaching the copolymer to an insoluble crosslinked poly(styrene) resin bead, samples can be purified by Soxhlet extraction as if they had been precipitated.

The second advantage of using a solid support is the ability to separate copolymer, consisting of 3-thienylalanine (3TA) and a comonomer, from homopolymer consisting only of the comonomer. Since the copolymer is bound to the bead via 3TA, Soxhlet extraction with an appropriate solvent can remove all the contaminating homopolymer, leaving only the desired product. In the case of a copolymerization with 3-hexylthiophene (3HT), Soxhlet extraction with THF would remove the unwanted poly(3-hexylthiophene).

Solid phase synthesis has two other potential advantages. First, working with 100 μm beads enables the use of many techniques developed for SPS, especially

parallel processes. Depending upon how many processes can be run in parallel, the time and material required to make a variety of polymers can be significantly less than that required by traditional solution phase chemistry. Second, by choosing appropriate supports, linkers, and protecting groups, compatibility with other SPS systems, such as peptide synthesis, can be achieved. We have chosen to develop a system where manual solid-phase peptide synthesis (SPPS) is followed by oxidative polymerization, producing graft copolymers of polypeptides and PTs. However, other combinations with SPS of oligosaccharides,[14] oligonucleotides,[15] or dendrimers[16] could also be imagined.

This chapter will describe construction of a ten-unit parallel synthesizer; optimization of first amino acid loading conditions; characterization of the loading density using colorimetric assays, FT-IR, and elemental analysis; and selection of an appropriate linker that is stable under oxidative polymerization conditions.

2.2 Experimental

2.2.1 Materials and characterization

2.2.1.1 Materials

PL-Wang resin (1.7 mmol/g), PL-HMS resin (2.0 mmol/g), and PL-HMBA resin (0.96 mmol/g) were obtained from Polymer Laboratories (Amherst, MA). Fmoc-L-3-thienylalanine (Fmoc-3TA) was obtained from PepTech (Cambridge, MA) and used as received. Tetraethylammonium chloride hydrate, phenol (99.99+%), potassium cyanide (97%, A.C.S. reagent), 1-hydroxybenzotriazole (HOBt, less than 5% water), 4-(dimethylamino)pyridine (DMAP, 99+%), potassium bromide (99+%, FT-IR grade), ninhydrin (A.C.S. reagent) and 1,3-diisopropylcarbodiimide (DIC, 99%) were obtained from Aldrich (Milwaukee, WI) and used as received. Acetic anhydride (*puriss. p.a.*, $\geq$99.5%) was obtained from Fluka (Milwaukee, WI). Pyridine, dichloromethane (DCM), and *N*,*N*-dimethylformamide (DMF) were obtained from

EM Science (Gibbstown, NJ). Absolute ethanol was obtained from Aaper Alcohol (Shelbyville, KY). Mixed Bed Resin TMD-8 was obtained from Sigma (St. Louis, MO).

2.2.1.2 Characterization

Infrared spectra were recorded using a Perkin-Elmer 1600 FT-IR using 1% w/w KBr pellets, and are reported in wavenumbers (cm^{-1}). Elemental analyses for nitrogen and sulfur were performed by the Microanalytical Laboratory at the University of Massachusetts, Amherst.

2.2.2 Resin loading

Loading a solid support resin with Fmoc-3TA using DIC/HOBt typically proceeded as follows:[17]

In a 6 dram (24 ml) vial equipped with a Teflon-lined septum cap, 500 mg (0.85 mmol) Wang resin was suspended in 10 ml 9:1 (v/v) DCM:DMF. In a 2 dram (8 ml) vial, 668.3 mg (1.70 mmol) Fmoc-3TA was dissolved in about 2 ml DMF to produce a viscous yellow liquid. To this solution, 229.7 mg (1.70 mmol) HOBt was added and dissolved. This solution was then added to the resin suspension.

In a 1/2 dram (2 ml) vial, 10.5 mg (0.09 mmol) DMAP was dissolved in about 0.25 ml DMF. Approximately 216 mg (1.70 mmol) DIC was added to the resin suspension (*Caution!* DIC has been known to cause blindness! Avoid eye contact!), followed by the DMAP solution. The resin suspension was then shaken under an argon blanket at room temperature for three hours.

Approximately 174 mg (1.70 mmol) acetic anhydride and 134 mg (1.70 mmol) pyridine was added to the resin suspension to end-cap unreacted linker, and the suspension shaken for an additional 30 minutes. The resin was then filtered and washed with three 15 ml volumes each of DMF, then DCM, then methanol. The

air-dried resin was then dried overnight under vacuum over anhydrous calcium sulfate to yield 830.3 mg resin, a mass increase of 330.3 mg.

2.2.3 Monitoring

2.2.3.1 Fulvene-piperidine adduct

Quantification of resin loading density by spectrophotometric measurement of the formation of the fulvene-piperidine chromophore proceeded as follows:[18]

First, 2 mg samples of resin (approximately 1 μmole with respect to resin) were weighed into 10×75 mm test tubes, and 2 ml of 20% (v/v) piperidine/DMF added. The suspensions were shaken for 30 minutes at room temperature, and diluted to 50 ml with DMF in a volumetric flask. The absorbance at 301 nm was recorded in a 1 cm quartz cuvette, and the loading density D_λ calculated by

$$D_\lambda = \frac{A_\lambda \cdot V_{ml}}{\epsilon' \cdot W_{mg} \cdot c} \cdot 10^3 \tag{2.1}$$

where A_λ is the absorbance at the wavelength λ, V_{ml} is the diluted volume, in this case 50 ml, ϵ' is the effective molar absorptivity at the given wavelength, W_{mg} is the mass of the resin, and c is the path length in centimeters. The extinction coefficient of the fulvene-piperidine adduct is $\epsilon'_{301} = 7\,000\ \mathrm{M}^{-1}\ \mathrm{cm}^{-1}$.

2.2.3.2 Kaiser test

Reagents for the Kaiser test, used to detect free terminal amino groups, were prepared as described by Merrifield et al.:[19,20]

Reagent a. Solution 1. With gentle heating, 40 g phenol was dissolved in 10 ml of absolute ethanol. The solution was stirred with 4 g of Mixed Bed Resin TMD-8 for 45 minutes, and filtered.

Solution 2. Potassium cyanide (65 mg) was dissolved in 100 ml distilled, deionized water (*Caution!* Potassium cyanide reacts with trace amounts of acid to form

toxic HCN gas! Treat excess KCN with a 20% solution of bleach in 1 M sodium hydroxide, then neutralize before disposal.) Of this stock solution, 2 ml was diluted to 100 ml with pyridine. The diluted solution was stirred with 4 g of TMD-8 for 45 minutes, and filtered. Solutions 1 and 2 were then combined to produce Reagent a.

Reagent b. Ninhydrin (2.5 g) was dissolved in 50 ml of absolute ethanol. The bottle was tightly stoppered and stored in the dark.

A typical quantification of free amines by the Kaiser test proceeded as follows:

The Fmoc protecting group was removed by suspending 5 mg of resin in 5 ml 20% (v/v) piperidine/DMF solution, followed by shaking for 30 minutes at room temperature. The resin was filtered, washed three times with DMF, then three times with DCM, and dried overnight under vacuum over calcium sulfate.

A 2 to 5 mg sample of the resin was weighed into a 10×75 mm test tube, followed by addition of 200 μl of Reagent a and 50 μl of Reagent b. As a negative control, only Reagents a and b were added to another tube. After mixing, the tubes were placed in a sand bath preheated to 100 °C. After 10 minutes, the tubes were cooled on ice, and 2 ml of 60% (v/v) ethanol/water was added. After mixing thoroughly, the solution was filtered through a glass wool plug in a Pasteur pipet. The resin was extracted twice with 0.5 ml of 0.5 M Et_4NCl in DCM. The combined solutions were diluted to 50 ml with 60% ethanol, and the absorbance of the sample filtrate at 570 nm was measured against that of the negative control.

The molar absorptivity of the Ruhemann's purple formed by the reaction of ninhydrin with the free amines used is ϵ'_{570}=15 000 $M^{-1}cm^{-1}$, and can be substituted into equation 2.1 to quantify the amount of free amine.

2.3 Results and discussion

2.3.1 Design of parallel synthesizer

In section 2.1, it was noted that SPS lends itself to parallelization – running many different reactions simultaneously – so that libraries of compounds can be synthesized more efficiently than by traditional solution phase synthesis. While our initial SPS trials were conducted using standard laboratory glassware, a ten unit parallel synthesizer was eventually built (figure 2.3). A solid block of nylon, chosen for its excellent chemical resistance, was machined to hold ten 6 dram (24 ml) vials, and bolted to a vortexer. A second block of nylon could be bolted to the vortexer if a second size vial was needed. The tolerance on the wells is high enough so that the vials are held in place even at high shaking frequencies. There are also windows allowing visual monitoring of the reactions. The vials are equipped with Teflon-lined septa caps, so that monomer solutions can be added by syringe. The vials are connected by flexible thick-wall needle-terminated Teflon tubing to a Firestone valve. This valve permits the vials to be alternately purged with inert gas and evacuated, in order to remove moisture and oxygen. The Firestone valve also allows a blanket of inert gas to be maintained over the vials without requiring a high gas flow rate, minimizing evaporation of solvent. The parallel synthesizer has operated flawlessly under constant use for hundreds of hours.

2.3.2 Optimization of first amino acid loading

Formation of the ester linkage between the first amino acid and the resin hydroxyl group is more difficult than formation of amide linkages, and thus more care is needed to ensure high loading levels. A higher concentration of Fmoc-protected amino acid is used for loading than for subsequent coupling, and a transesterification catalyst, DMAP, is added to promote reaction. DMAP catalyzes hydrolysis of the activated amino acid as well as transesterification, so anhydrous

Figure 2.3. Ten unit parallel synthesizer. Top: synthesizer, Teflon gas distribution lines, and Firestone valve. Bottom left: windows allow visual monitoring of reactions run in 24 ml disposable vials. Bottom right: Inert gas and monomer solutions can be introduced via syringe through resealing Teflon-lined septa.

Table 2.1. Three Fmoc-3TA to linker hydroxyl group ratios for resins with different linker densities.

Run	Ratio Fmoc-3TA: resin —OH	linker type	linker density (mmol/g)	mass resin (g)	mmol —OH
1	2.0	Wang	1.7	0.505	0.86
2	3.0	HMS	2.0	0.503	1.01
3	3.5	HMBA	1.0	0.501	0.48

conditions are required for high loading. After loading, unreacted linker hydroxyl groups can be blocked by acetylation, although growth of truncated peptide chains from unblocked sites under amide bond-forming reaction conditions is uncommon.[21]

During the course of the experiments described in this chapter, three different resins were loaded with Fmoc-3TA. The linking groups, and their concentrations, were different for the three resins, but the conditions required for forming ester bonds between Fmoc-3TA and the linking groups are comparable. (The structures of the linking groups will be discussed in section 2.3.3 in the context of their stability.) A different ratio of amino acid to resin hydroxyl group was used to load each resin in an attempt to determine which would produce the highest loading level. The ratios of Fmoc-3TA to available resin hydroxyl groups, and the mmoles of available hydroxyl groups in each sample, are shown in table 2.1.

After loading, the degree of Fmoc-3TA coverage for each loading ratio was determined by two methods. First, as shown in figure 2.4, an Fmoc-amino acid can be deprotected with piperidine, forming a stable chromophore. Using equation 2.1, the amount of Fmoc-3TA per gram of resin can be calculated from the absorptivity of the fulvene-piperidine chromophore. Second, elemental analysis can be used to determine the degree of coverage. Sulfur elemental analysis provides a direct measurement of 3TA per gram of sample. These measurements for the three loading ratios are summarized in table 2.2. The percent loading coverages can then be calculated, taking into account the mass increase resulting from resin loading. As

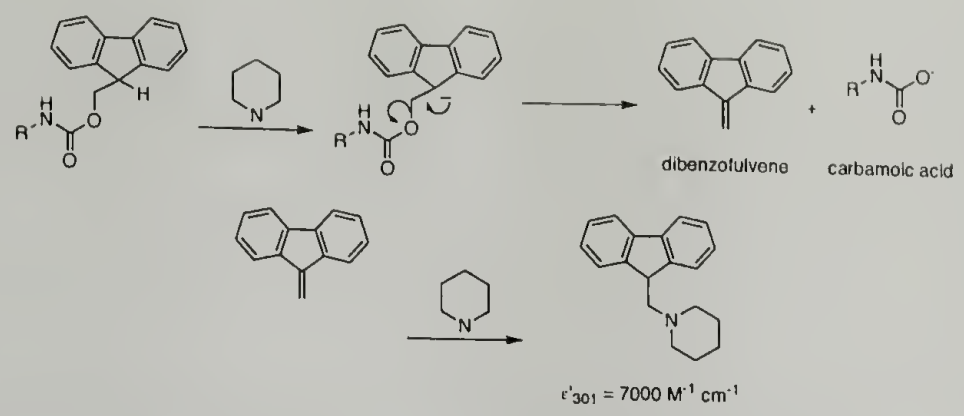

Figure 2.4. Deprotection of Fmoc-protected amino acids with piperidine, resulting in a stable chromophore.

Table 2.2. Spectrophotometric measurement of Fmoc concentration and elemental analysis of sulfur to determine loading density of Fmoc-3TA.

Run	Ratio Fmoc-3TA: resin —OH	Fmoc (mmol/g)	sulfur (mmol/g)	average (mmol/g)
1	2.0	0.97 ± 0.01	0.89	0.93
2	3.0	1.06 ± 0.06	0.95	1.01
3	3.5	0.67 ± 0.09	0.66	0.67

Table 2.3. Calculation of Fmoc-3TA loading coverages.

Run	Ratio Fmoc-3TA: resin —OH	mmol —OH	final wt. (g)	loaded Fmoc-3TA (mmol)	loading coverage (%)
1	2.0	0.86	0.830	0.77	89.5
2	3.0	1.01	0.808	0.82	81.2
3	3.5	0.48	0.667	0.45	93.8

shown in table 2.3, Run 3 (a 3.5:1 ratio of Fmoc-3TA to available resin hydroxyl groups) provided the highest degree of coverage, 93.8%. This ratio was used for first amino acid loading in subsequent experiments.

2.3.3 Choice of linker

The three loaded resins described in table 2.1 were synthesized in order to determine the effects of the oxidative polymerization conditions on the linker. Specifically, since oxidative polymerization requires a Lewis acid catalyst, and produces HCl as a byproduct (figure 1.7), the stability of the linker under those conditions was not guaranteed.

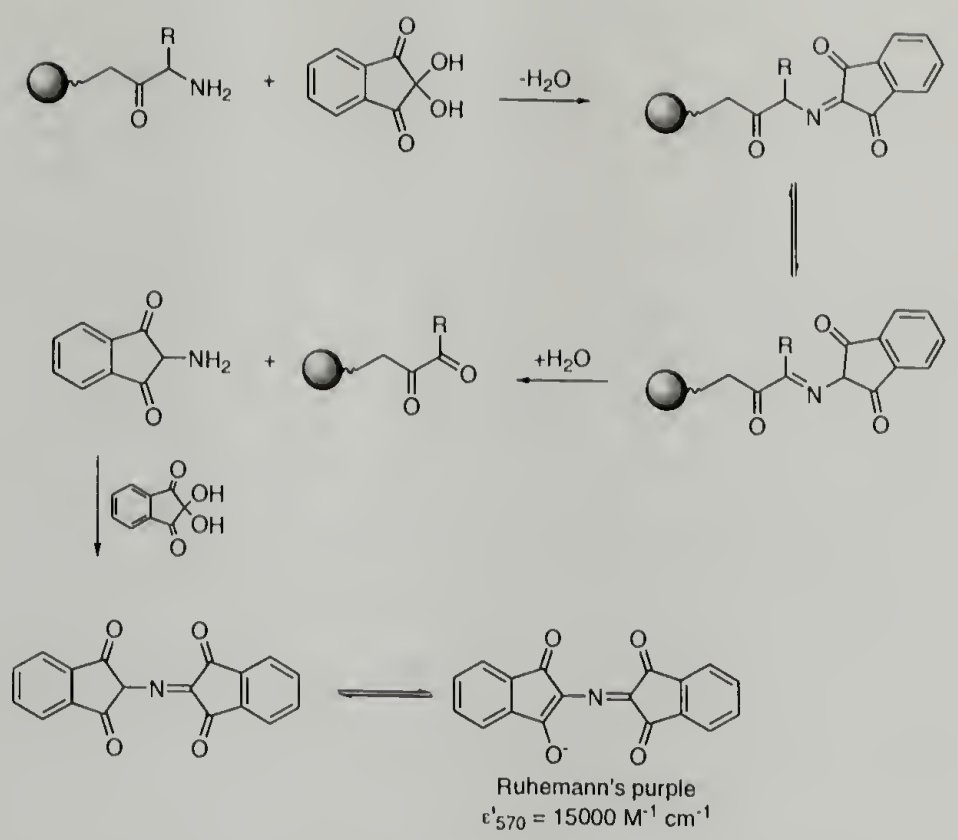

Figure 2.5. Kaiser test: Ninhydrin reacts with a primary amine to produce an intensely colored chromophore.[20]

The linker stabilities were monitored by four techniques. FT-IR was used to observe any structural changes in the resin during the reaction. The amino acid loading was determined using the fulvene-piperidine assay and by elemental analysis. Finally, the concentration of free amine after deprotection was measured by the Kaiser test (figure 2.5).[19,20]

Before the infrared spectra of these resins could be analyzed, it was useful to assign the peaks that correspond to the crosslinked polystyrene before addition of the amino acid. Of the three resins studied in this chapter, HMS resin has the simplest structure. The structure and FT-IR spectrum of HMS resin are shown in figure 2.6. Nearly all the peaks can be assigned (table 2.4) based on the polystyrene literature,[22] despite the 1% crosslinking. The vibrational modes listed are illustrated in figure 2.7.

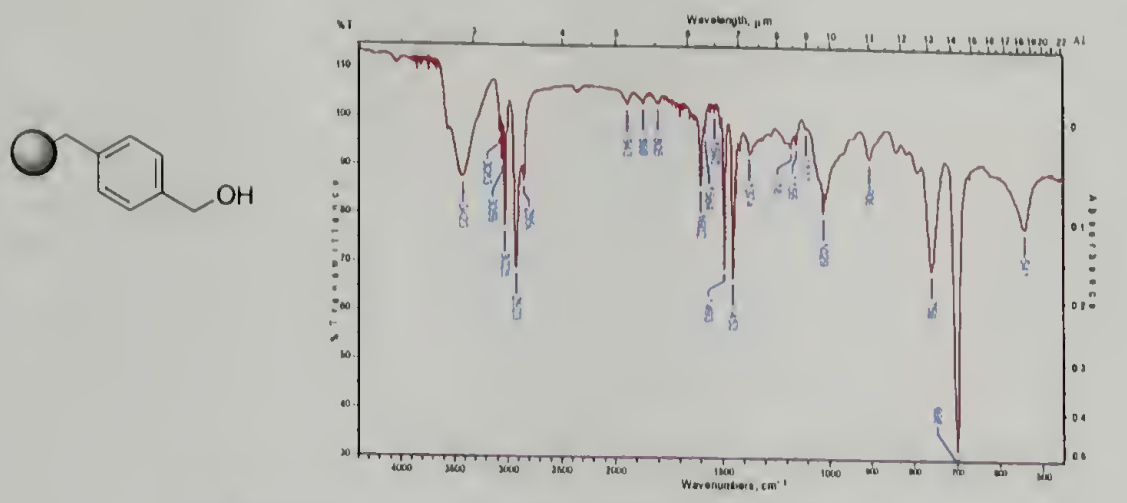

Figure 2.6. FT-IR spectrum of HMS resin.

Table 2.4. FT-IR assignments for HMS resin (figure 2.6).

Measured	Literature[22]	Assignment
3423	–	O—H stretch
3083	3083	$\nu_{20B}(B_1)$
3059	3061	$\nu'_2(A_1)$
3025	3029	$\nu'_{20A}(A_1)$
2923	2923	$\nu_a(\mathrm{CH_2})$
2850	2851	$\nu_s(\mathrm{CH_2})$
1943	1945	$\nu_{17A} + \nu_5 = 1945$
1869	1875	$\nu_{17B} + \nu_5 = 1875$
1805	1800	$\nu_{10A} + \nu_{17A} = 1807$
1602	1602	$\nu_{9B}(B_1)$
1584	1585	$\nu_{9A}(A_1)$
1540	1543	$\nu_{11} + \nu_{10A} = 1542$
1493	1493	$\nu_{19A}(A_1)$
1453	1450	$\delta(\mathrm{CH_2}), \nu_{19}(B_1)$
1374	1376	$\delta(\mathrm{CH})$
1181	1180	$\nu_5 + \nu_{16B} = 1197$
1155	1154	$\nu'_{15}(B_1)$
1111	1110	$\nu_{11} + \nu_{16A} = 1110$
1029	1027	$\nu_{18A}(A_1)$
906	906	$\nu_{17B}(B_2)$
759	760	$\nu_{10B}(B_2)$
698	700	$\nu 11(B_2)$
541	540	$\nu_4(B_2)$

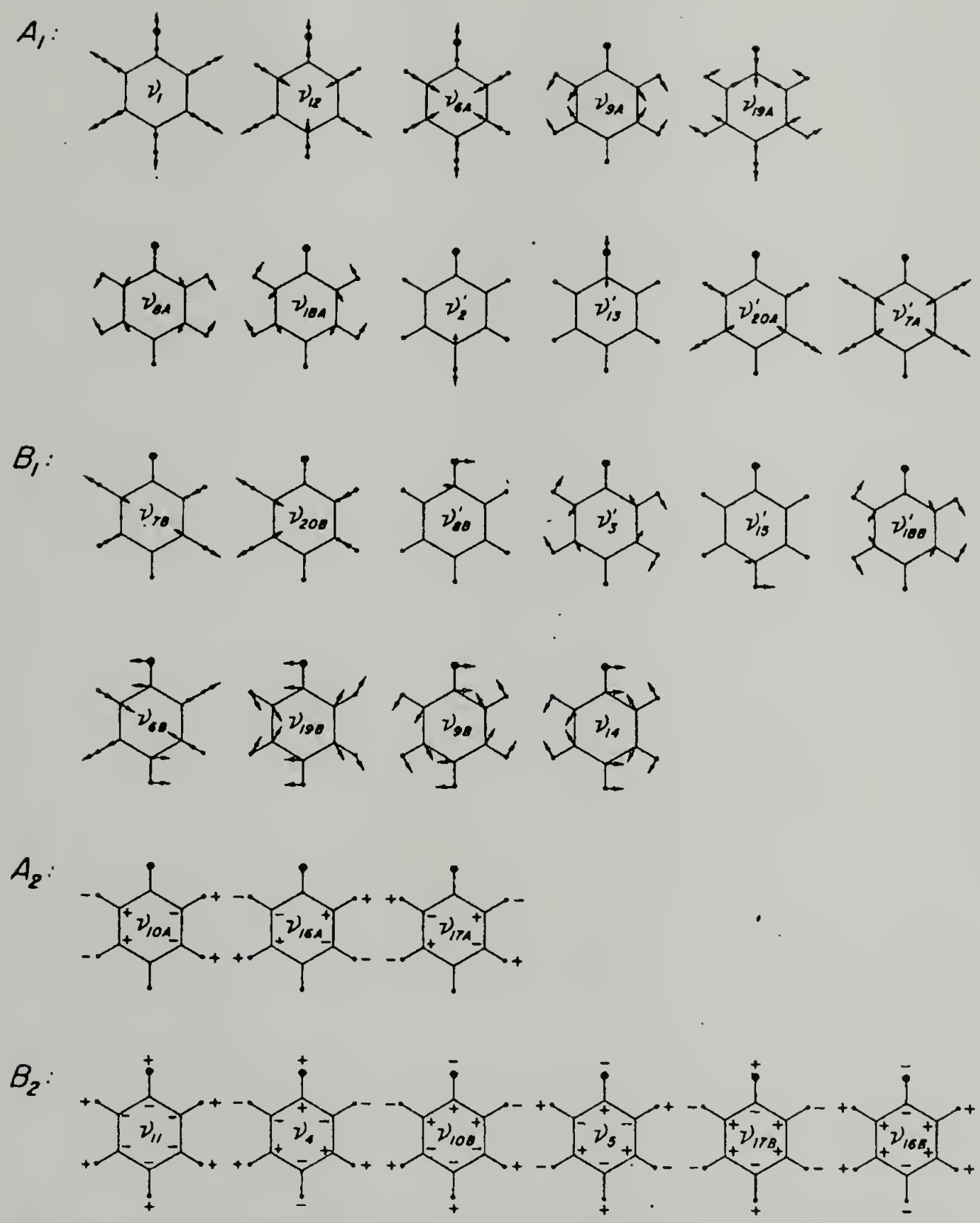

Fig. 2. Approximate normal modes of monosubstituted benzene (see discussion in text).

Figure 2.7. Normal modes of monosubstituted benzene, which approximate those observed for polystyrene listed in table 2.4. Reprinted with permission from Liang, C. Y.; Krimm, S. *J. Polym. Sci.* **1958,** *27*, 241-254. Copyright 1958 John Wiley & Sons, Inc.

2.3.3.1 Wang resin

The first resin tested for stability was Wang resin,[23] because it is the resin of choice for Fmoc-protected SPPS.[3]

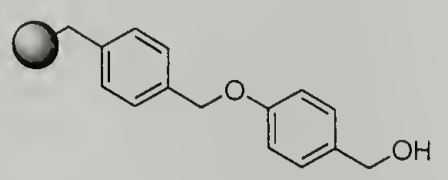

The loaded resin was swollen in chloroform for 30 minutes, and then ferric chloride was added to produce an 0.2 M solution. While this experiment does not take into account the HCl that is formed during polymerization, the ferric chloride was not anhydrous, so some HCl may be produced. The resin beads turned red after ten minutes, and the color intensified over the next five hours.

The FT-IR spectra of the resin beads over 300 minutes are shown in figure 2.8, with assignments provided in table 2.5. Three changes in the FT-IR spectra can be noted after exposure to ferric chloride for ten minutes. First, the broad absorbance of the hydroxyl O—H stretch at around 3400 cm^{-1} becomes relatively more intense. Second, the maximum absorbance of the peak in the carbonyl region corresponding to the ester C=O stretch shifts from 1727 to 1719 cm^{-1}. Finally, the absorbance corresponding to the ester O—C—O stretch at 1173 cm^{-1} disappears. These observations indicate that the ester linkage between the resin and the amino acid is being broken, and the benzyl alcohol is being regenerated.

This conclusion is confirmed by the concentration measurements of the Fmoc protecting group and free amines after deprotection, shown in figure 2.9. There is a significant decrease in the Fmoc concentration after 10 minutes exposure to ferric chloride.† The Fmoc group was selected because of its stability under strongly acidic conditions, as demonstrated by Carpino and Han.[24,25] Therefore, it is likely

---

†The error bars correspond to the least significant difference (LSD) among the five levels of the factor time, with a 95% confidence level, based on analysis of variance (ANOVA) for the three replicates (the red circles) at each time point.

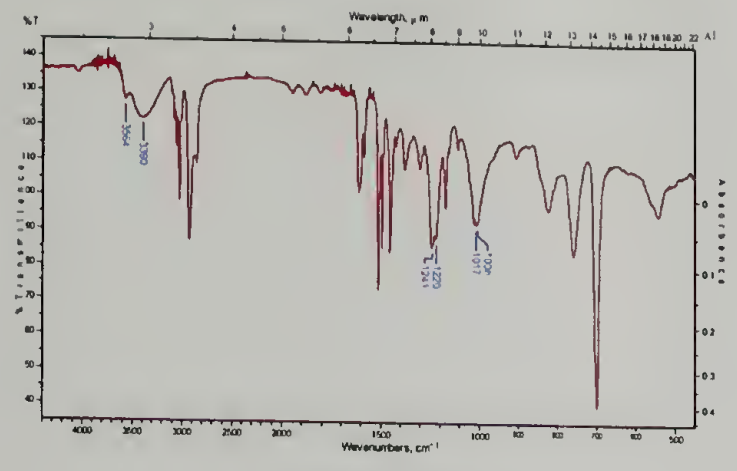

Wang resin

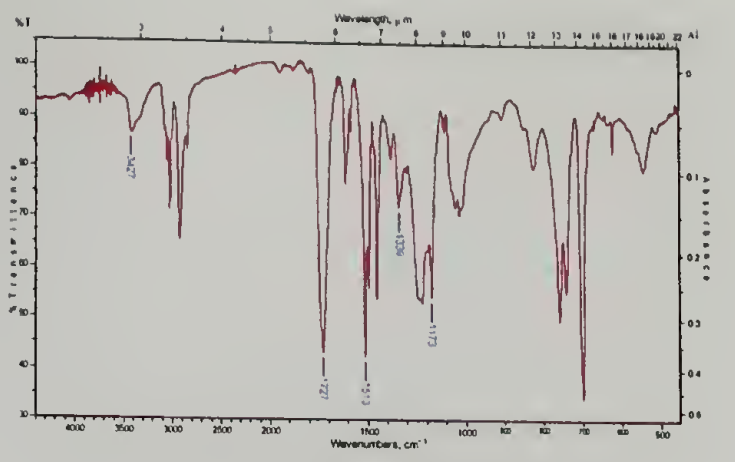

Fmoc-3TA loaded Wang resin

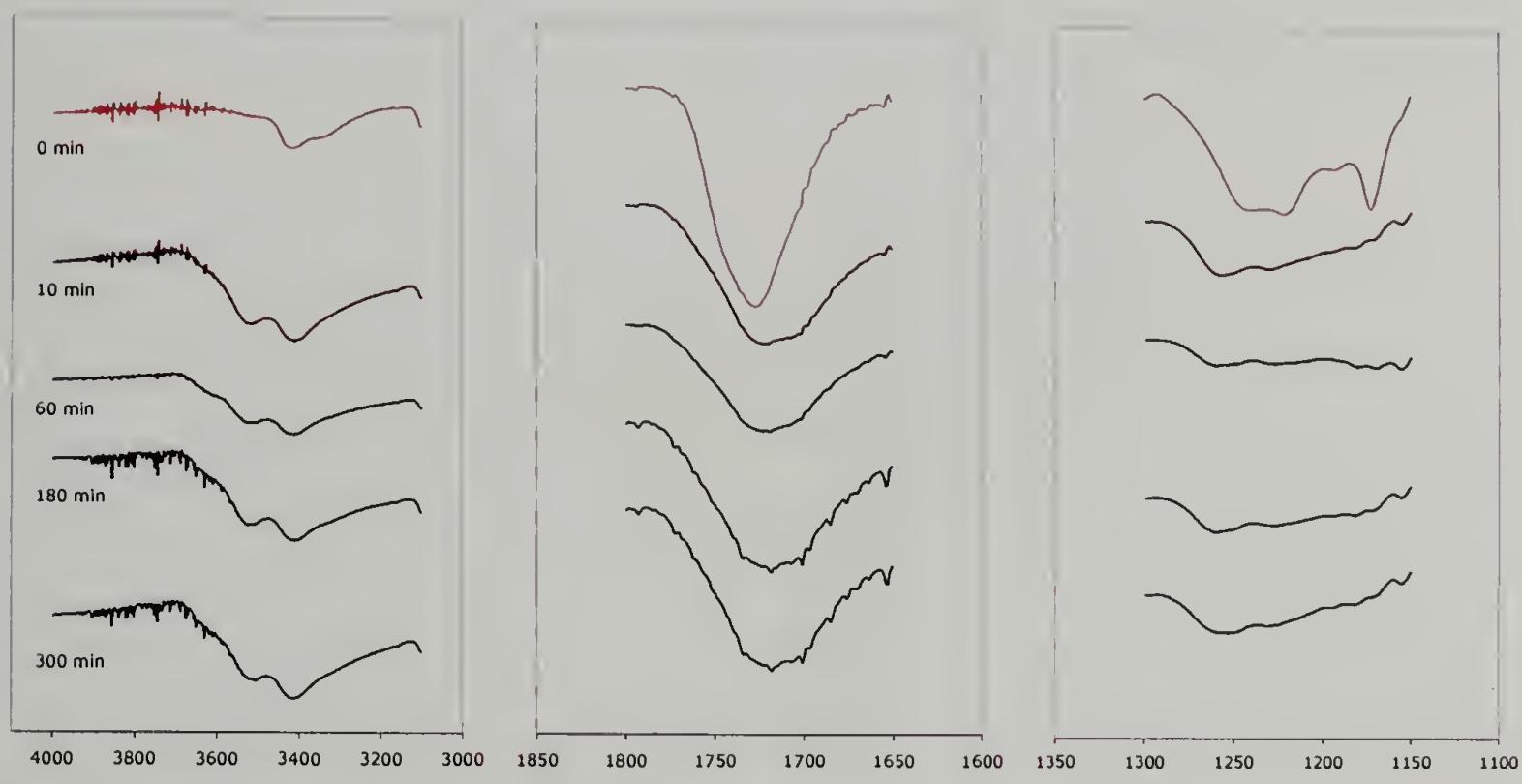

hydroxyl
O—H stretch

ester
C=O stretch

ester
O—C—O stretch

Figure 2.8. FT-IR of unloaded Wang resin (top left) and loaded resin (top right) treated with $FeCl_3$ for up to five hours (bottom).

Table 2.5. FT-IR assignments for unloaded and loaded Wang resins.

	Wavenumber (cm^{-1})	Assignment	
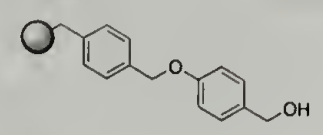	3564, 3390	O—H stretch	alcohol
	1241, 1220	C—O—C asym. stretch	ether
	1017, 1008	C—O—C sym. stretch	ether
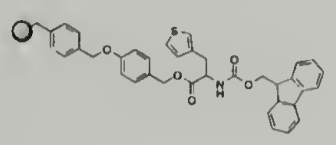	3427	N—H stretch	carbamate
	3390	O—H stretch	alcohol
	1727	C=O stretch	ester and carbamate
	1513	N—H bend	carbamate
	1339	C—C(=O)—O stretch	ester
	1241, 1220	C—O—C asym. stretch	ether
	1173	O—C—C stretch	ester
	1017, 1008	C—O—C sym. stretch	ether

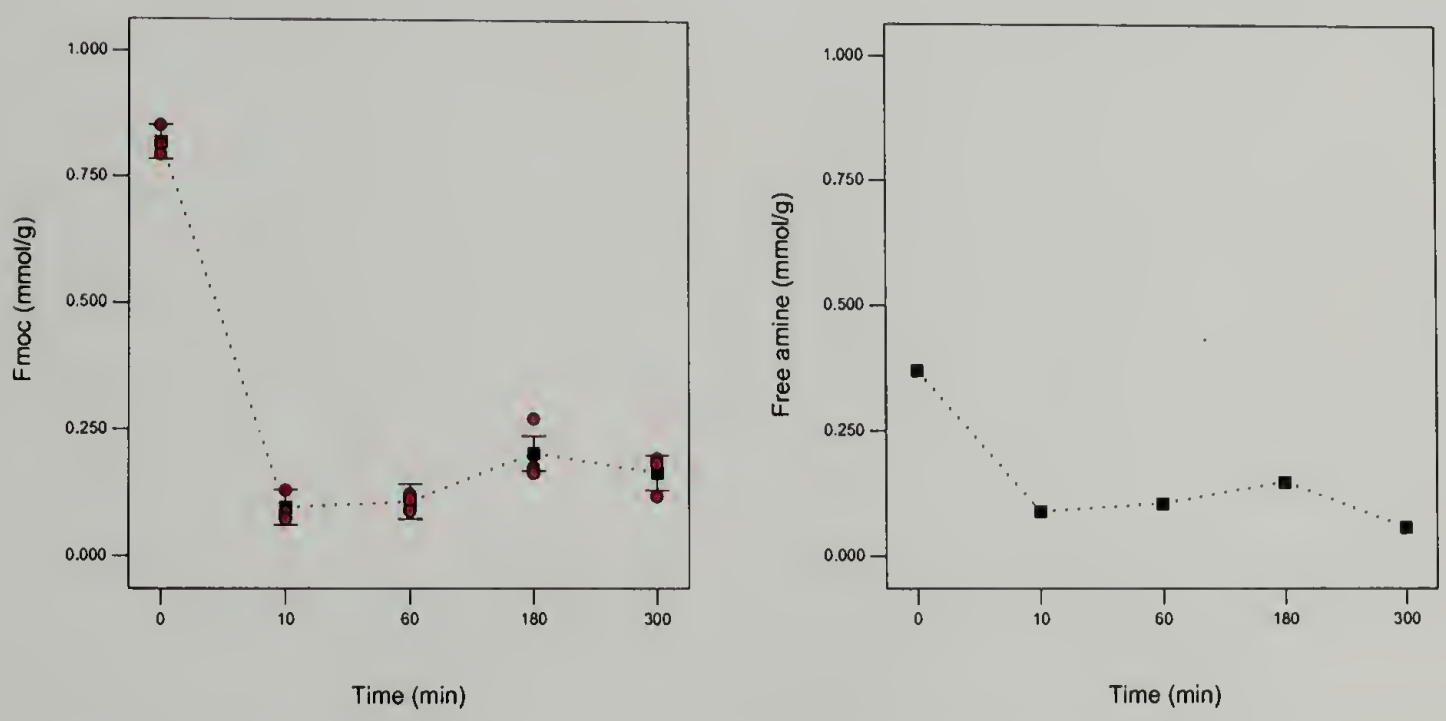

Figure 2.9. Concentration of Fmoc protecting groups (left) and free amine concentration after deprotection (right) of loaded Wang resin during treatment with ferric chloride.

that the Wang ester linkage, rather than the carbamate, is being cleaved. A similar result is observed when the concentration of free amine is measured using the Kaiser test. The level of measured free amine for the deprotected loaded resin, without any exposure to $FeCl_3$, is 0.370 mmol/g. This is less than half that measured by the fulvene-piperidine assay and by elemental analysis. The Ruhemann's purple is tightly retained by the beads despite thorough washing, resulting in lower than expected readings. This proved to be true for the other two resins we studied as well.

2.3.3.2 HMS resin

Typically, polypeptides are cleaved from Wang resin by shaking in a 1:1 solution of TFA:DCM at room temperature for 30 minutes. Since the Wang resin did not provide sufficient stability under our oxidative polymerization conditions, we reasoned that a resin which required harsher cleavage conditions would have improved stability. Typically, highly ionizing acids like hydrogen fluoride or trifluoromethanesulfonic (triflic) acid are used to cleave amino acids from hydroxymethylstyrene (HMS) resin.[26]

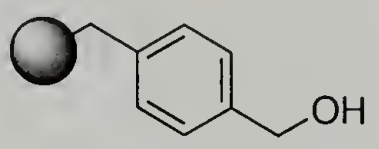

After exposure to $FeCl_3$ for ten minutes, the HMS resin turned red, as did the Wang resin. The FT-IR spectra of the resin are shown in figure 2.10, with the assignments provided in table 2.6. In this case, the carbonyl absorption band at 1727 cm^{-1} does not shift to a lower wavenumber, as in the case of the Wang resin, but it does appear to decrease in intensity. Intensity decreases are also observed for the ester-related absorptions at 1339 and 1191 cm^{-1}. Again, it appears that the amino acid is cleaved from the linker under the polymerization conditions. This conclu-

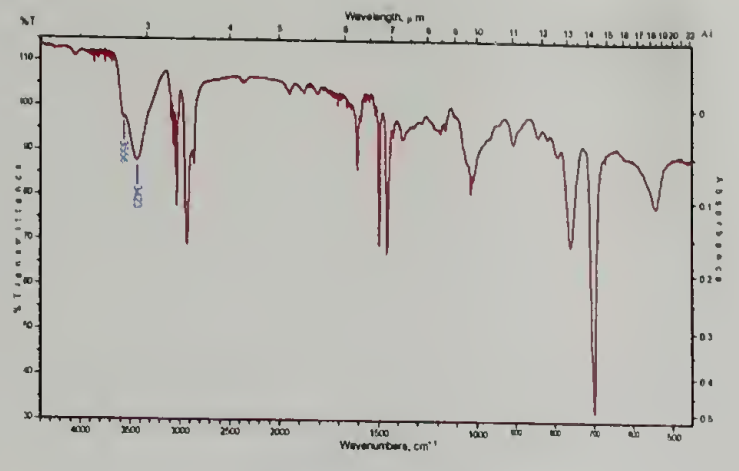

HMS resin

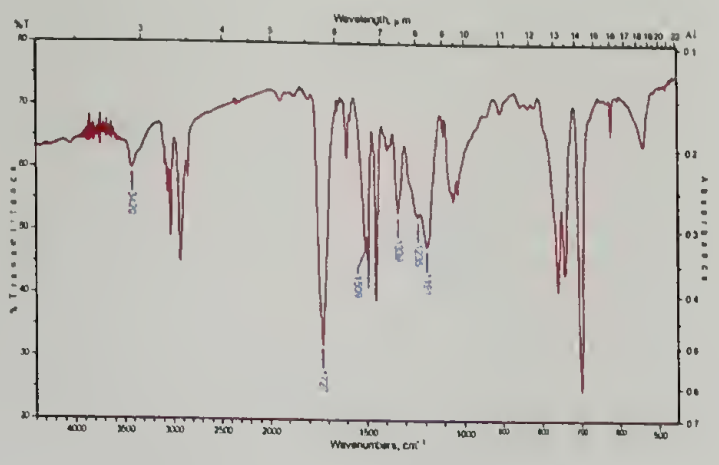

Fmoc-3TA loaded HMS resin

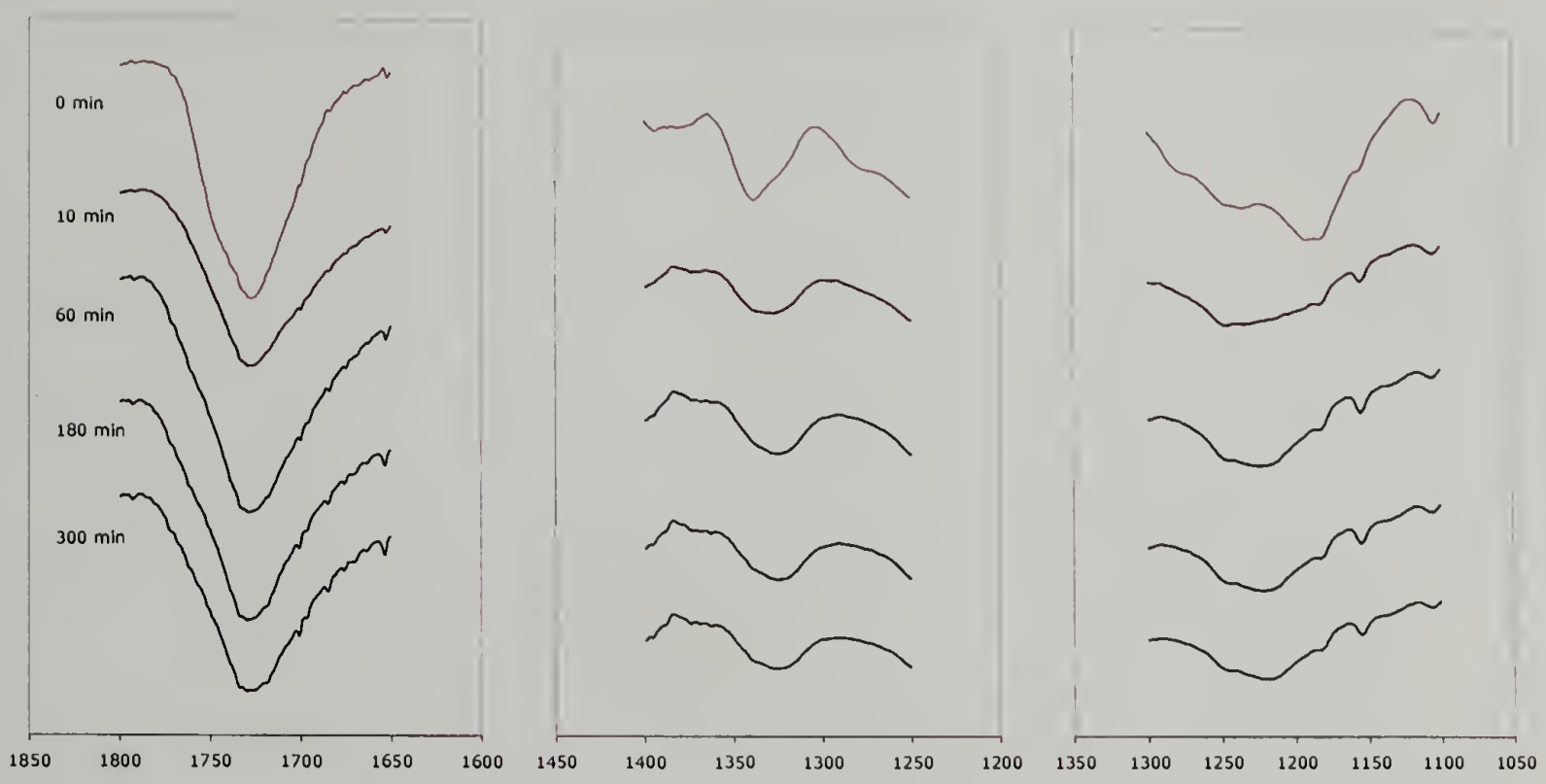

ester
C=O stretch

ester
C—C(=O)—O stretch

ester
O—C—C stretch

Figure 2.10. FT-IR of unloaded HMS resin (top left) and loaded resin (top right) treated with $FeCl_3$ for up to five hours (bottom).

sion is confirmed by the fulvene-piperidine and free amine assays, shown in figure 2.11, which show a significant decrease in attached amino acid after 10 minutes.

Table 2.6. FT-IR assignments for unloaded and loaded HMS resin.

	Wavenumber (cm^{-1})	Assignment	
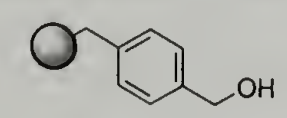	3556, 3423	O—H stretch	alcohol
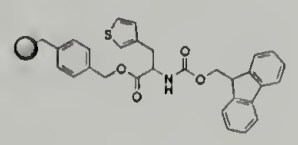	3423	O—H stretch	alcohol
	3420	N—H stretch	carbamate
	1727	C=O stretch	ester and carbamate
	1509	N—H bend	carbamate
	1339	C—C(=O)—O stretch	ester
	1235	N—H bend and C—N stretch	carbamate
	1191	O—C—C stretch	ester

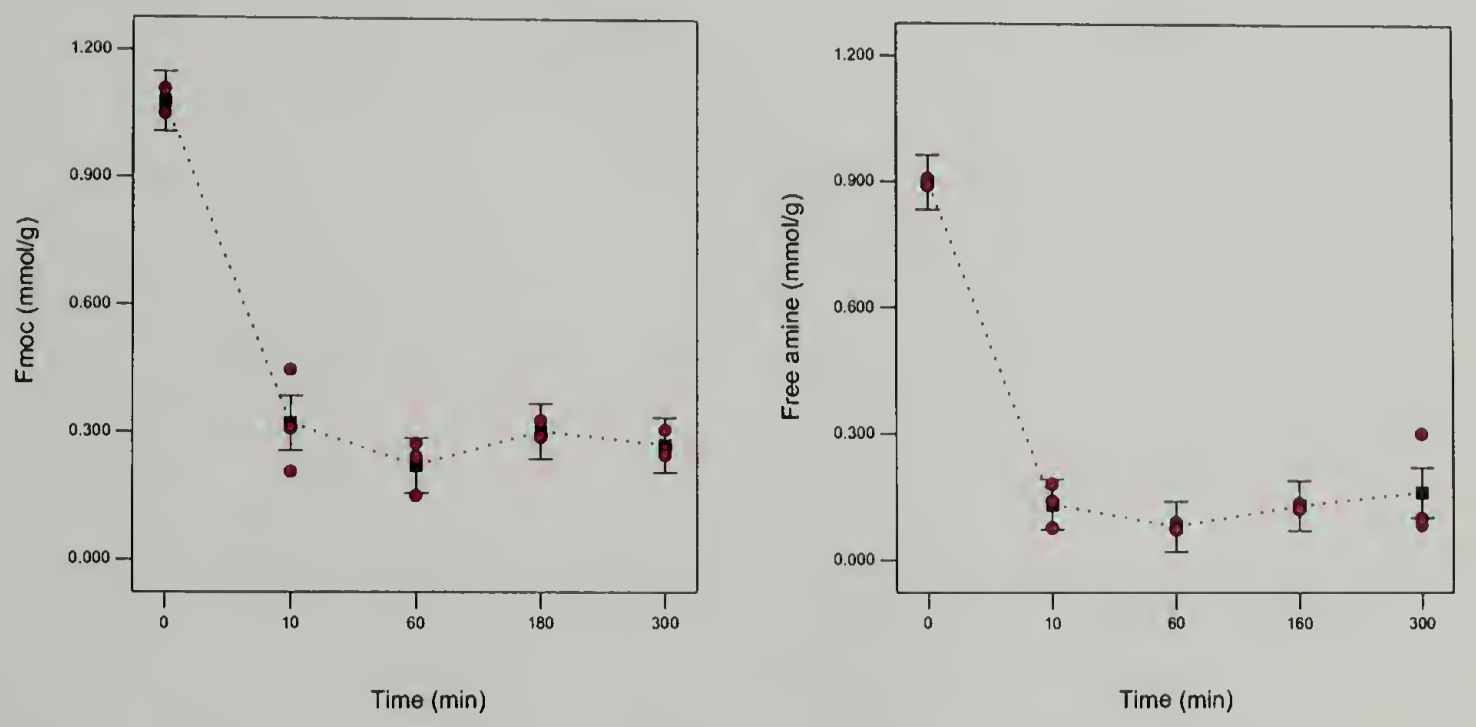

Figure 2.11. Concentration (mmol/g) of Fmoc protecting groups (left) and free amine concentration after deprotection (right) of loaded HMS resin during treatment with ferric chloride.

Table 2.7. FT-IR assignments for unloaded and loaded HMBA resin.

	Wavenumber (cm^{-1})	Assignment	
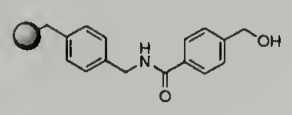	3564, 3428	O—H and N—H stretches	alcohol and amide
	1663	C=O stretch	amide I
	1654	N—H bend	amide II
	1526	N—H bend and C—N stretch	amide
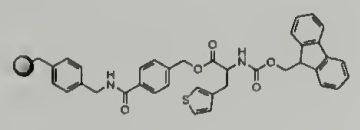	3564, 3420	O—H and N—H stretches	alcohol and amide
	3420	N—H stretch	carbamate
	1728	C=O stretch	ester and carbamate
	1668	C=O stretch	amide I
	1654	N—H bend	amide II
	1526	N—H bend and C—N stretch	amide
	1520	N—H bend	carbamate
	1339	C—C(=O)—O stretch	ester
	1183	O—C—C stretch	ester

2.3.3.3 HMBA resin

Because of the acid-sensitivity of the linkers described above, it was necessary to look beyond the Fmoc-protected SPPS literature to find a linker which would be stable under our polymerization conditions. One possibility was an acid-stable linker susceptible to nucleophilic cleavage such as hydroxymethylbenzoic acid (HMBA) resin.[27–29]

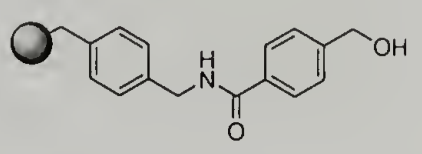

The HMBA resin did not immediately turn red, as in the previous two cases, when exposed to ferric chloride for ten minutes. However, it did turn red after five hours. The FT-IR spectra are shown in figure 2.12, with the assignments provided in table 2.7. In this case, the absorption bands corresponding to the ester linkage at 1728, 1339, and 1183 cm^{-1} do not shift over the 300 minutes, and do not appear to change in relative intensity compared to the polystyrene absorption bands. This indicates that the linker is stable under the polymerization conditions.

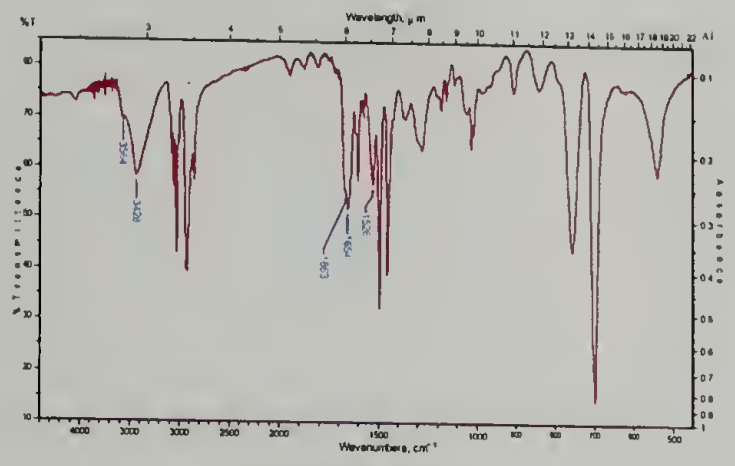

HMBA resin

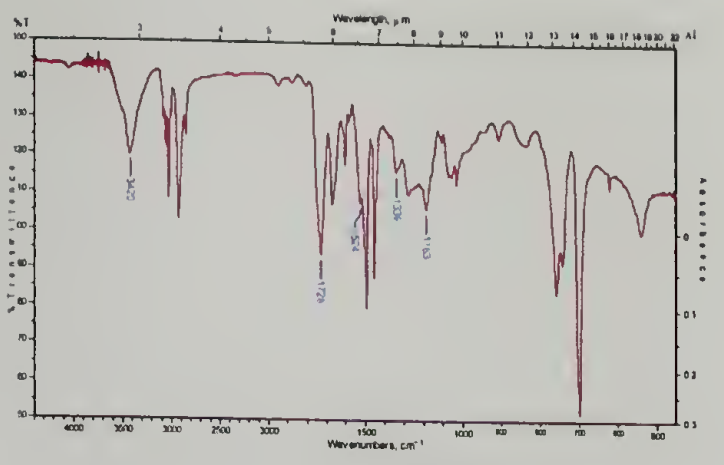

Fmoc-3TA loaded HMBA resin

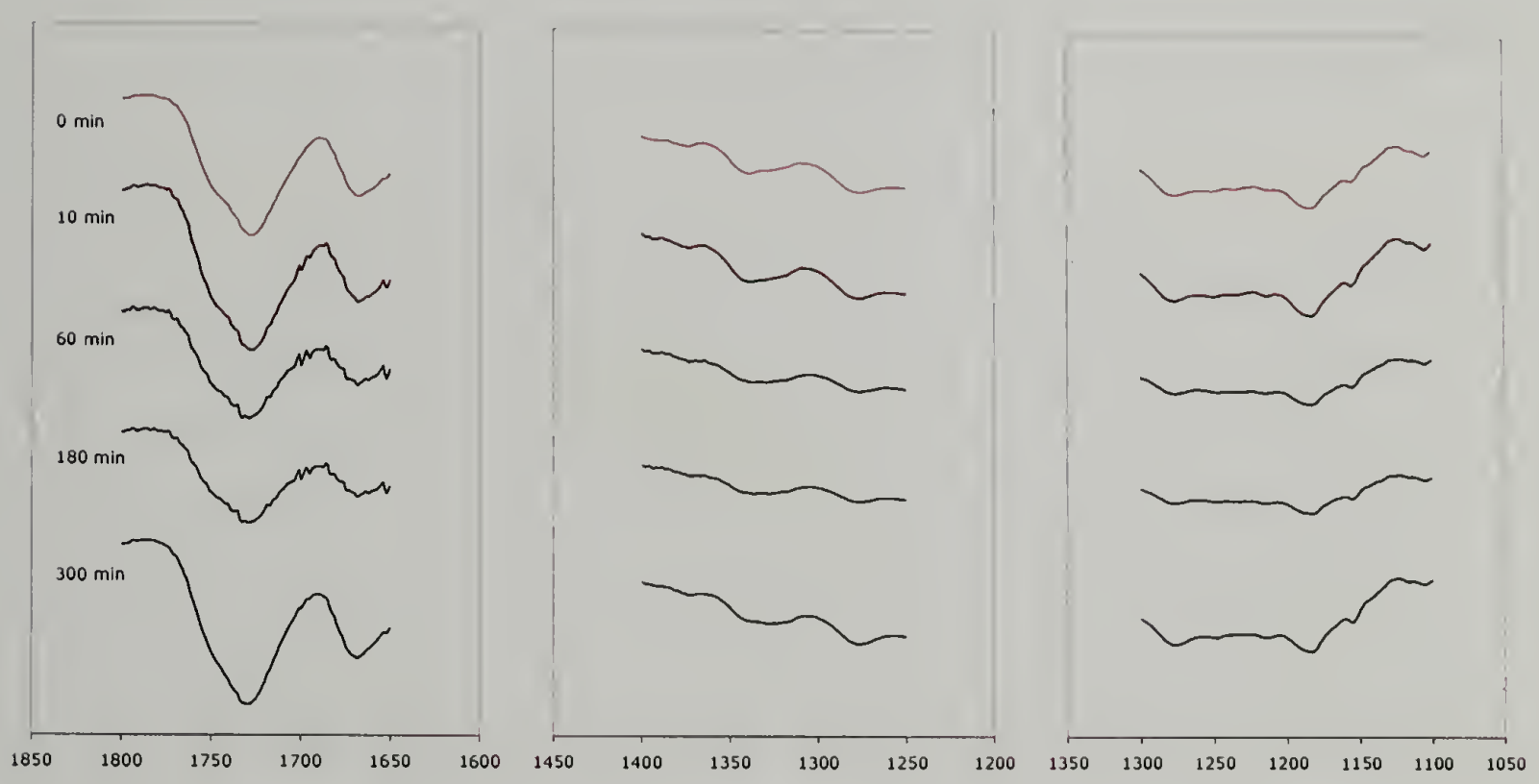

ester
C=O stretch

ester
C—C(=O)—O stretch

ester
O—C—C stretch

Figure 2.12. FT-IR of unloaded HMBA resin (top left) and loaded resin (top right) treated with $FeCl_3$ for up to five hours (bottom).

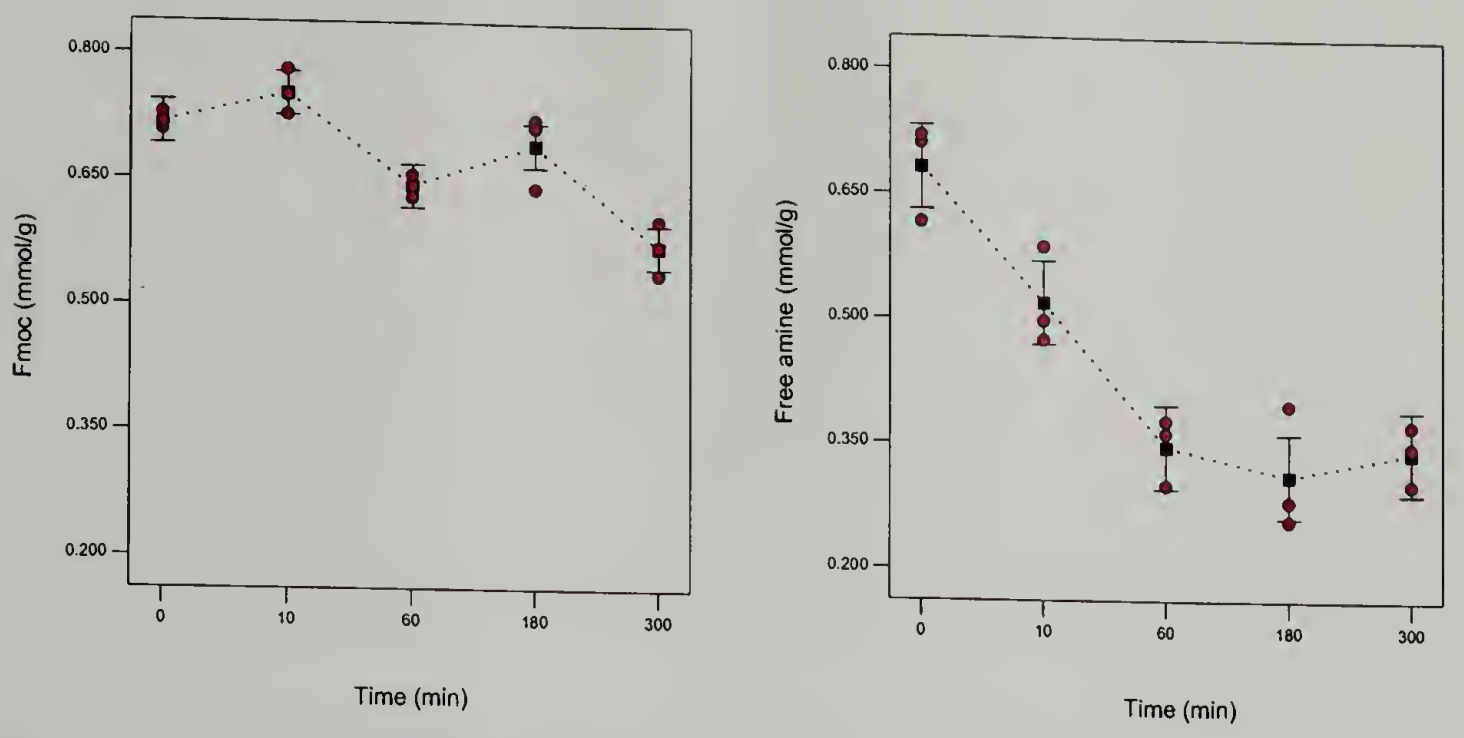

Figure 2.13. Concentration (mmol/g) of Fmoc protecting groups (left) and free amine concentration after deprotection (right) of loaded HMBA resin before and after treatment with ferric chloride.

This result is confirmed by the fulvene-piperidine assay (figure 2.13, left), where a significant but small decrease in the Fmoc concentration is observed up to 300 minutes. This decrease may be due to loss of amino acid due to linker cleavage, or to an increase of the mass of the beads due to irreversible complexation with ferric chloride (the observed red color which develops over time), resulting in a lower Fmoc concentration per gram of beads, or both. However, the free amine concentration (figure 2.13, right) contradicts this result, showing a significant decrease over 300 minutes to about half of the original concentration.

Because of the disagreement between the two spectroscopic assays, elemental analysis was performed to measure the amino acid loading at each time during exposure (table 2.8). From the resin loading assay (table 2.3), the concentration of linker hydroxyl groups per gram of loaded resin can be calculated as

$$\frac{0.48 \text{ mmol linker}}{0.66 \text{ g loaded resin}} = 0.72 \text{ mmol linker/g loaded resin} \tag{2.2}$$

Table 2.8. Elemental analyses of HMBA resins loaded with Fmoc-3TA and exposed to $FeCl_3$.

$FeCl_3$ exposure time (min)	% N	mmol N (total)/ g loaded resin	mmol N (a.a.)/ g loaded resin	% loading
0	1.89	1.35	0.63	88
10	1.78	1.27	0.55	77
60	1.70	1.21	0.49	69
180	1.69	1.21	0.49	69
300	1.76	1.26	0.54	75

$FeCl_3$ exposure time (min)	% S	mmol S/ g loaded resin	% loading
0	2.03	0.63	88
10	2.01	0.63	88
60	2.13	0.66	93
180	2.17	0.68	94
300	2.26	0.70	98

Then, we can calculate the number of moles of nitrogen and sulfur per gram loaded resin using the elemental analyses. In the case of nitrogen, the number of moles of nitrogen in the linker is subtracted from the total to yield the number of moles corresponding to the amino acid. There is no sulfur in the linker, so that correction is not necessary. Finally, the percent loading can be calculated by dividing the concentration of the element by the concentration of the linker:

$$\% \text{ loading} = \frac{\text{mmol element/g loaded resin}}{0.72 \text{ mmol linker/g loaded resin}} \times 100 \tag{2.3}$$

Some of the resin was lost during the deprotection, so corrections cannot be made for increasing mass due to irreversible complexation of ferric chloride. The nitrogen elemental analysis shows that about 15% of the amino acid is lost after five hours under the reaction conditions, without correction for any mass increases. On the other hand, it appears from the sulfur elemental analysis that the loading densities *increase* by 11% over five hours. However, this is probably one of two artifacts from the analysis: either the crosslinked polystyrene resin beads fail to combust

completely, or the presence of iron interferes with the measurement. Overall, the elemental analysis agrees with the fulvene-piperidine assay shown in figure 2.13 (left), indicating that the linker is stable to the oxidative polymerization conditions. The reasons for the inconsistent result produced by the Kaiser test are not known. One possibility is interference with the formation of the chromophore by residual ferric chloride binding to free amines.

2.4 Conclusions

Using an activated ester, SPS resins could be loaded with greater than 90% efficiency, as confirmed by measuring the concentration of the fulvene-piperidine adduct and by elemental analysis. Two resins commonly used in SPPS, Wang and HMS, were found to be unsuitable for oxidative polymerization because the linkers were unstable in the presence of ferric chloride. Conversely, HMBA resin was found to be stable, based on measuring the concentration of retained Fmoc protecting groups and elemental analysis.

In the next chapter, conditions for copolymerizing thiophenes with 3TA immobilized on HMBA resin will be optimized using a factorial design. Designing a method of extracting residual catalyst and unwanted homopolymer from the immobilized copolymer will produce a complete solution for running parallel experiments, from polymerization to purification.

2.5 References

(1) Merrifield, R. B. *J. Am. Chem. Soc.* **1963,** *85,* 2149-2154.

(2) Früchtel, J. S.; Jung, G. *Angew. Chem. Int. Ed.* **1996,** *35,* 17-42.

(3) Dörwald, F. Z. *Organic Synthesis on Solid Phase;* Wiley-VCH: Weinheim, 2000.

(4) Tour, J. M. *Chem. Rev.* **1996,** *96,* 537-553.

(5) Roncali, J. *Chem. Rev.* **1997,** *97,* 173-205.

(6) McCullough, R. D. *Adv. Mater.* **1998,** *10,* 93-116.

(7) Malenfant, P. R. L.; Fréchet, J. M. J. *Chem. Commun.* **1998,** 2657-2658.

(8) Kirschbaum, T.; Briehn, C. A.; Bäuerle, P. *J. Chem. Soc., Perkin Trans. 1* **2000,** *8,* 1211-1216.

(9) Kirschbaum, T.; Bäuerle, P. *Synth. Met.* **2001,** *119,* 127-128.

(10) Briehn, C. A.; Kirschbaum, T.; Bäuerle, P. *J. Org. Chem.* **2000,** *65,* 352-359.

(11) Briehn, C. A.; Schiedel, M. S.; Bonsen, E. M.; Schuhmann, W.; Bäuerle, P. *Angew. Chem. Int. Ed.* **2001,** *40,* 4680-4683.

(12) Briehn, C. A.; Bäuerle, P. *J. Comb. Chem.* **2002,** *4,* 457-469.

(13) Sykes, P. *A Guidebook to Mechanism in Organic Chemistry;* Longman: Essex, 3rd ed.; 1986.

(14) Plante, O. J.; Palmacci, E. R.; Seeberger, P. H. *Science* **2001,** *291,* 1523-1527.

(15) Letsinger, R. L.; Mahadeva, V. *J. Am. Chem. Soc.* **1965,** *87,* 3526-3527.

(16) Swali, V.; Wells, N. J.; Langley, G. J.; Bradley, M. *J. Org. Chem.* **1997,** *62,* 4902-4903.

(17) Advanced ChemTech, Louisville, KY "Advanced ChemTech Handbook of Combinatorial, Organic & Peptide Chemistry", 2002.

(18) Fields, G. B.; Noble, R. L. *Int. J. Pept. Protein Res.* **1990,** *35,* 161-214.

(19) Kaiser, E.; Colescot, R. l.; Bossinge, C. D.; Cook, P. I. *Anal. Biochem.* **1970,** *34,* 595-598.

(20) Sarin, V. K.; Kent, S. B. H.; Tam, J. P.; Merrifield, R. B. *Anal. Biochem.* **1981,** *117,* 147-157.

(21) Atherton, E.; Sheppard, R. C. *Solid Phase Peptide Synthesis: A Practical Approach;* IRL: Oxford, 1989.

(22) Liang, C. Y.; Krimm, S. *J. Polym. Sci.* **1958,** *27,* 241-254.

(23) Wang, S. S. *J. Am. Chem. Soc.* **1973,** *95,* 1328-1333.

(24) Carpino, L. A.; Han, G. Y. *J. Am. Chem. Soc.* **1970,** *92,* 5748-5749.

(25) Carpino, L. A.; Han, G. Y. *J. Org. Chem.* **1972,** *37,* 3404-3409.

(26) Wang, S. S. *J. Org. Chem.* **1975,** *40,* 1235-1239.

(27) Arshady, R.; Atherton, E.; Clive, D. L. J.; Sheppard, R. C. *J. Chem. Soc., Perkin Trans. 1* **1981,** 529-537.

(28) Atherton, E.; Logan, C. J.; Sheppard, R. C. *J. Chem. Soc., Perkin Trans. 1* **1981,** 538-546.

(29) Story, S. C.; Aldrich, J. V. *Int. J. Pept. Protein Res.* **1992,** *39,* 87-92.

CHAPTER 3

IDENTIFICATION OF SIGNIFICANT FACTORS IN SOLID PHASE SYNTHESIS OF POLY(THIOPHENE)S USING A TWO-LEVEL FACTORIAL DESIGN

3.1 Introduction

Chapter 2 described the choice of a linker for solid phase synthesis of poly(thiophene)s (PTs). The HMBA linker was shown to be stable for five hours in the presence of ferric chloride, indicating that it is suitable for oxidative polymerization. In this chapter, conditions for copolymerization of bead-mounted 3-thienylalanine (3TA) and 3-hexylthiophene (3HT) will be determined. A general scheme for the copolymerization and cleavage is shown in figure 3.1. Eight factors predicted to have an effect on polymerization, based on either literature reports or our own observations, are identified. Systematically varying each of these factors individually, even at only two levels (for example, "high 3HT concentration and low 3HT concentration") would require 2^8=256 separate experiments. Even with the ten-unit parallel synthesizer, this would be cost- and time-prohibitive. Therefore, we will use a statistical method often employed in industry to experiment with many different factors simultaneously while reaching statistically sound conclusions. The effects of the different factors on copolymerization will be assessed by fluorescence spectroscopy of the copolymers.

3.1.1 Design of Experiments

Design of Experiments (DOE) is a statistical method which can be used to determine cause-and-effect relationships in any process that has definable inputs and

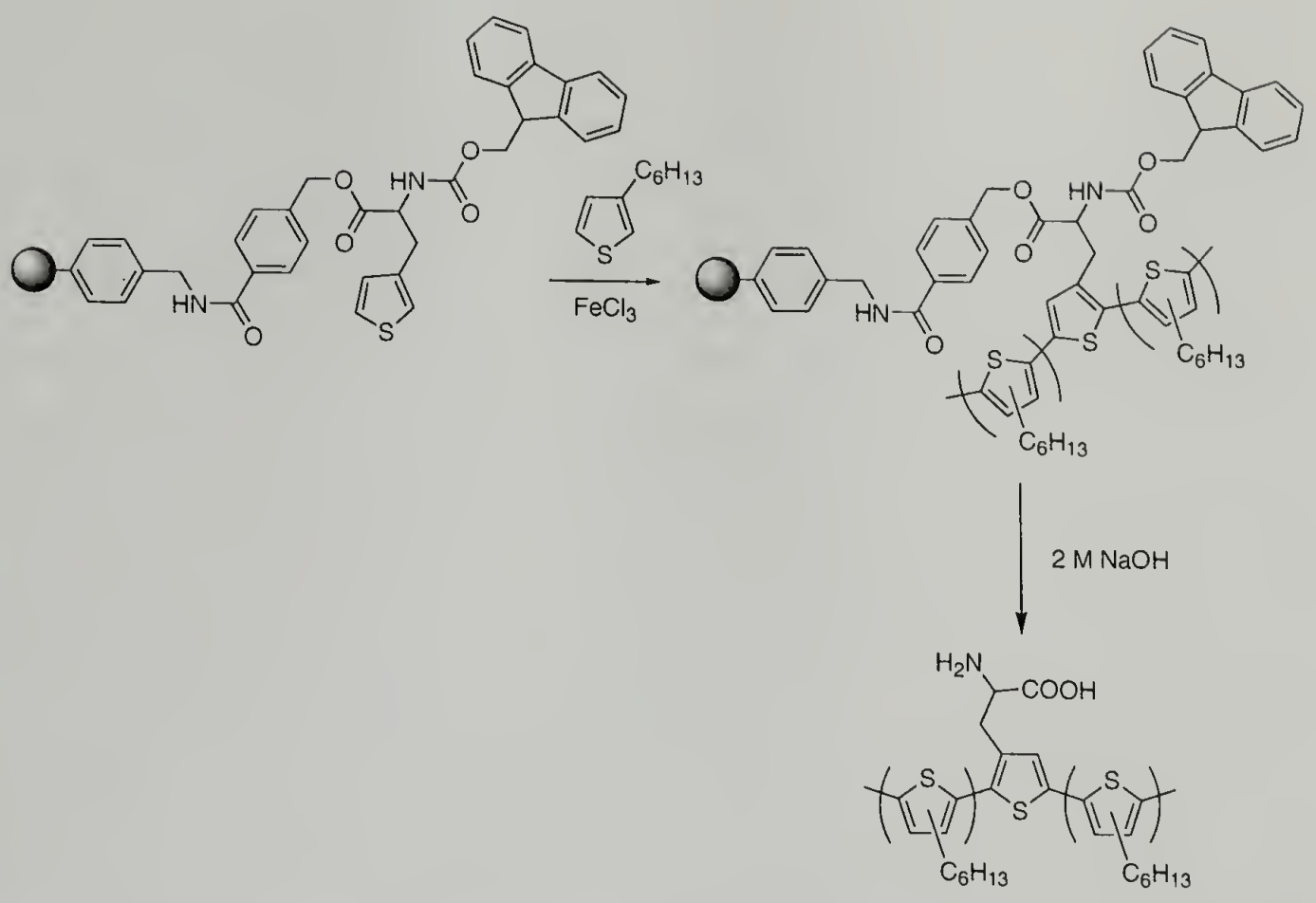

Figure 3.1. Solid-phase copolymerization of immobilized Fmoc-3TA with 3HT, followed by saponification.

outputs.[1] It has two advantages over traditional, one-factor-at-a-time (OFAT) experimentation:

1. By contrasting averages rather than contrasting individual runs, effects and errors can be estimated in fewer runs. For example, a two-level factorial experiment with two factors can provide in four runs the same precision as an OFAT experiment can provide in six replicates. This efficiency improves as more factors are added: a two-level factorial experiment with three factors and eight runs provides the same precision as an OFAT experiment with sixteen replicates.

2. Interactions of factors are revealed. OFAT methodology does not detect when the effect of a combination of two factors is greater than the individual factors.

Table 3.1. Test factors for 3-octylthiophene polymerization conditions from Laakso et al.[4]

Factor	Name	Units	Low (-)	High (+)
A	Temperature	°C	-5	10
B	Polymerization time	h	1	2
C	Addition time	min	15	45
D	$FeCl_3$:3OT	ratio	3	5

As a result, factorial design can provide more statistically reliable conclusions at a lower cost than traditional experimentation.

Examples of DOE are becoming more common in the polymer and molecular biology literature as the statistical tools become more accessible to academic researchers. For example, Shan et al. studied the effects of five factors on the copolymerization of ethylene and 1-octene using a metallocene catalyst, and identified several two-factor interactions which were not predicted by the accepted polymerization mechanism.[2] And, Hasenwinkle et al. doubled the expression of a recombinant protein in *E. coli* from 4 to 8 g/L by optimizing the inducer concentration and the induction time in shake flasks and in a high-density fermentor.[3]

3.1.1.1 Two-level factorials

Laakso and Järvinen used a two-level factorial design to study the ferric chloride oxidative polymerization of 3-octylthiophene. Their data can be used to provide an example of the basic principles of DOE.[4] As shown in table 3.1, they studied four different factors: temperature (A), polymerization time (B), addition time (C), and $FeCl_3$ to monomer ratio (D). The factors can be set at a low (-) or a high (+) level. In two-level factorial designs, it is important to set the levels as far apart as practical, so that it is more likely to see an effect, but not so far apart that the operating boundaries of the experiment are exceeded. For example, it would not be practical to have a low level of catalyst ratio of 0:1, or a polymerization time of 30 days. This decision is based upon the experience of the experimenter.

Table 3.2. Results from 3-octylthiophene polymerization experiment from Laakso et al.[4]

Standard order	A: Temp.	B: Pzn time	C: Addn. time	D: ratio	Y_1: Yield (g)	Y_2: Solubility
1	-5 (-)	1 (-)	15 (-)	3 (-)	4.5	5.0
2	10 (+)	1 (-)	15 (-)	3 (-)	5.5	5.0
3	-5 (-)	2 (+)	15 (-)	3 (-)	5.0	5.0
4	10 (+)	2 (+)	15 (-)	3 (-)	5.8	5.0
5	-5 (-)	1 (-)	45 (+)	3 (-)	4.8	4.0
6	10 (+)	1 (-)	45 (+)	3 (-)	5.4	4.5
7	-5 (-)	2 (+)	45 (+)	3 (-)	5.7	4.5
8	10 (+)	2 (+)	45 (+)	3 (-)	5.4	4.5
9	-5 (-)	1 (-)	15 (-)	5 (+)	8.6	4.5
10	10 (+)	1 (-)	15 (-)	5 (+)	8.0	4.0
11	-5 (-)	2 (+)	15 (-)	5 (+)	9.6	2.0
12	10 (+)	2 (+)	15 (-)	5 (+)	10	4.0
13	-5 (-)	1 (-)	45 (+)	5 (+)	8.0	4.5
14	10 (+)	1 (-)	45 (+)	5 (+)	7.9	4.5
15	-5 (-)	2 (+)	45 (+)	5 (+)	9.5	4.5
16	10 (+)	2 (+)	45 (+)	5 (+)	8.4	3.5
17	2.5	1.5	30	4	7.1	5.0

The results from performing all the combinations of the four factors in table 3.1 are shown in table 3.2. The two measured responses were yield (Y_1) and solubility (Y_2). The yield was measured in grams, while the solubility in chloroform was rated on a scale from one to five. The array is orthogonal, because there are no correlations between factors. For example, when factor D in table 3.2 is at a low level (results 1–8), factors A, B, and C contain an equal number of pluses and minuses. Therefore, any effect of D is not influenced by factors A, B, or C, and there is no correlation. The results are listed in "standard order", which makes the orthogonality of the array apparent. However, the experiments should be run in random order, so that the chance of an unknown time-related variable influencing the result is reduced. In other words, there is no correlation between the known factors and time.

3.1.1.2 Calculation of effects

The first step in the analysis is calculation of effects of the main factors (A, B, C, and D) on the responses (Y_1 and Y_2). An effect is calculated as

$$\text{Effect} = \frac{\sum Y_+}{n_+} - \frac{\sum Y_-}{n_-} \tag{3.1}$$

where $\sum Y_+$ is the sum of the effects when the factor is set at the high level, and n_+ is the number of runs when the factor is set at the high level. So, based on table 3.2, the effect of factor A on Y_1 can be calculated as:

$$\begin{aligned} \text{Effect}Y_1 &= \frac{5.5+5.8+5.4+5.4+8.0+10+7.9+8.4}{8} \\ &\quad - \frac{4.5+5.0+4.8+5.7+8.6+9.6+8.0+9.5}{8} \\ &= 7.05 - 6.96 \\ &= 0.09 \end{aligned} \tag{3.2}$$

The calculated effects for the factors (shown in coded form as "+" and "-") are shown in table 3.3. Since the yield varied from 4.5 to 10 grams, it appears that factor A has a minimal impact of only 0.09.

3.1.1.3 Interaction effects

In addition to effects arising from the four main factors, there may be effects caused by the interaction of factors. The ability to recognize an effect arising from, for example, the combination of temperature and polymerization time on solubility, is one of the features that distinguishes DOE from OFAT experimentation. The eleven effects resulting from interactions of the main factors are listed in table 3.4. The levels for the combinations are calculated by multiplying the levels of the parent factors. For example, when A and B are at their low levels, their two-factor

Table 3.3. Coded factor levels for main effects and results from 3-octylthiophene polymerization experiment

Std.	A	B	C	D	Y_1	Y_2
1	-	-	-	-	4.5	5.0
2	+	-	-	-	5.5	5.0
3	-	+	-	-	5.0	5.0
4	+	+	-	-	5.8	5.0
5	-	-	+	-	4.8	4.0
6	+	-	+	-	5.4	4.5
7	-	+	+	-	5.7	4.5
8	+	+	+	-	5.4	4.5
9	-	-	-	+	8.6	4.5
10	+	-	-	+	8.0	4.0
11	-	+	-	+	9.6	2.0
12	+	+	-	+	10	4.0
13	-	-	+	+	8.0	4.5
14	+	-	+	+	7.9	4.5
15	-	+	+	+	9.5	4.5
16	+	+	+	+	8.4	3.5
Effect Y_1	0.09	0.84	-0.24	3.49	7.0	
Effect Y_2	0.13	0.00	-0.31	-0.75		4.3

interaction AB is at its high level. The calculated effects on response Y_1 for each factor are shown in the last row of the table.

3.1.1.4 Normal variation

From table 3.3, it appears that factors B and D have the largest effects on the response Y_1 (0.84 and 3.49). However, it is possible that these effects are the result of normal variation in the data, due to experimental error, changes in environmental conditions, operator fatigue, etc. The normality of the data can be determined graphically by plotting the effects sorted in ascending order versus the expected values for a normal distribution. In this "normal plot", effects which lie upon a straight line vary normally, while outliers indicate which effects are most likely significant. Sensitivity can be increased by using the absolute values of the effects, in effect using only the positive half of the normal distribution curve – a

Table 3.4. Coded factor levels for interaction effects and results from 3-octylthiophene polymerization experiment

Std.	AB	AC	AD	BC	BD	CD	ABC	ABD	ACD	BCD	ABCD	Y_1
1	+	+	+	+	+	+	-	-	-	-	+	4.5
2	-	-	-	+	+	+	+	+	+	-	-	5.5
3	-	+	+	-	-	+	+	+	-	+	-	5.0
4	+	-	-	-	-	+	-	-	+	+	+	5.8
5	+	-	+	-	+	-	+	-	+	-	+	4.8
6	-	+	-	-	+	-	-	+	-	-	-	5.4
7	-	-	+	+	-	-	-	+	+	-	+	5.7
8	+	+	-	+	-	-	+	-	-	-	-	5.4
9	+	+	-	+	-	-	-	+	+	+	-	8.6
10	-	-	+	+	-	-	+	-	-	+	+	8.0
11	-	+	-	-	+	-	+	-	+	-	+	9.6
12	+	-	+	-	+	-	-	+	-	-	-	10
13	+	-	-	-	-	+	+	+	-	-	+	8.0
14	-	+	+	-	-	+	-	-	+	-	-	7.9
15	-	-	-	+	+	+	-	-	-	+	-	9.5
16	+	+	+	+	+	+	+	+	+	+	+	8.4
Effect	-0.14	-0.32	-0.44	-0.11	0.42	-0.36	-0.34	0.14	0.06	-0.14	-0.16	7.0

"half-normal" plot. The absolute values of the effects on response Y_1, sorted in ascending order, and their cumulative probabilities are shown in table 3.5.

Plotting the values of table 3.5 reveals that two effects, B and D, indeed do not fall on a straight line and vary non-normally (figure 3.2). In most systems, only 20% of the main effects and two-factor interactions will be significant ("sparsity of effects").[1] The remaining effects which fall on the straight line and vary normally can be used to provide an estimate of error.

3.1.1.5 Plotting effects

To plot the effects of B and D on Y_1, the averages of B and D at their low and high levels are calculated as shown in table 3.6. The effects of B and D on yield are shown in figure 3.3. The least significant difference (LSD) bars in the plots do not overlap, indicating that one can state with 95% confidence that there are significant differences in yield at low and high levels of polymerization time and catalyst ratio.

Table 3.5. Values for half-normal plot

Point	Effect	Absolute value of effect	Cumulative probability (%)
1	ACD	0.06	6.67
2	A	0.09	13.3
3	BC	0.11	20.0
4	AB	0.14	26.7
5	ABD	0.14	33.3
6	BCD	0.14	40.0
7	ABCD	0.16	46.7
8	C	0.24	53.3
9	AC	0.32	60.0
10	ABC	0.34	66.7
11	CD	0.36	73.3
12	BD	0.42	80.0
13	AD	0.44	86.7
14	B	0.84	93.3
15	D	3.49	100

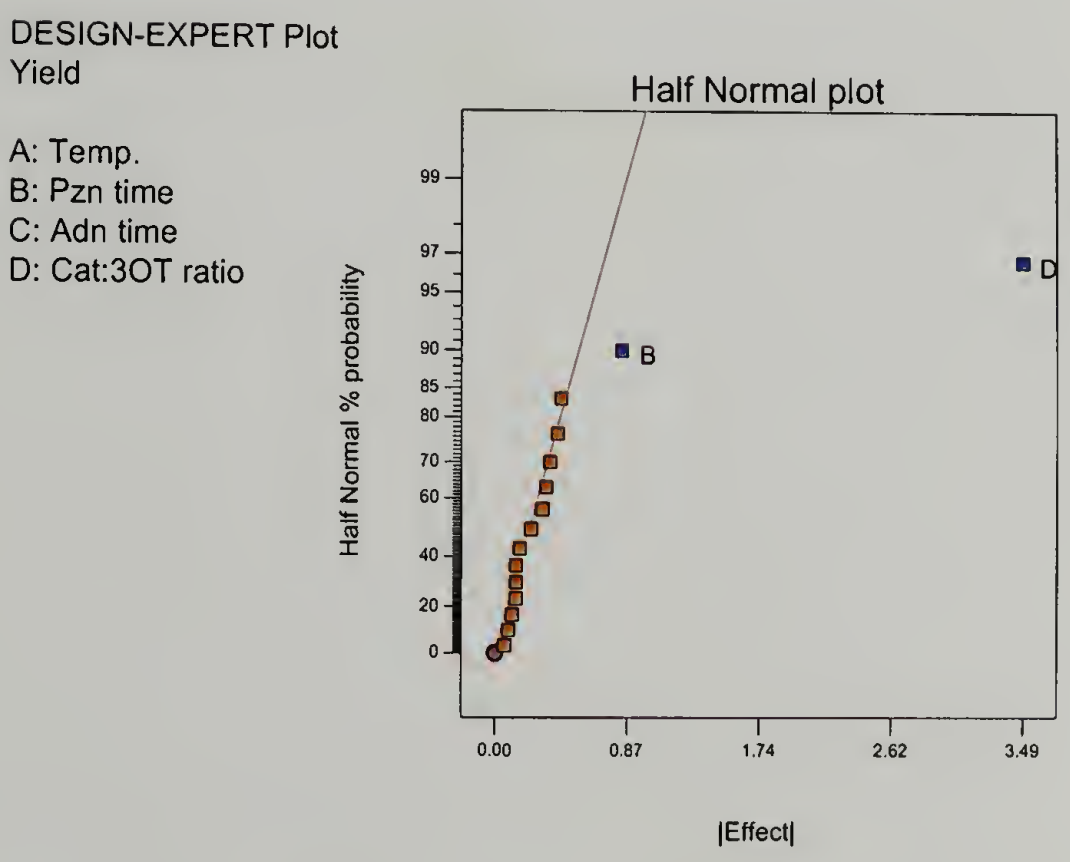

Figure 3.2. Half-normal plot of absolute values of effects on yield (Y_1)

Table 3.6. Data for plots of effects of main factors on yield (Y_1)

Factor	Standard	Level	Yield (avg. %)
B: Pzn. time	1,2,5,6,9,10,13,14	-	6.59
	3,4,7,8,11,12,15,16	+	7.43
D: Catalyst ratio	1,2,3,4,5,6,7,8	-	5.26
	9,10,11,12,13,14,15,16	+	8.75

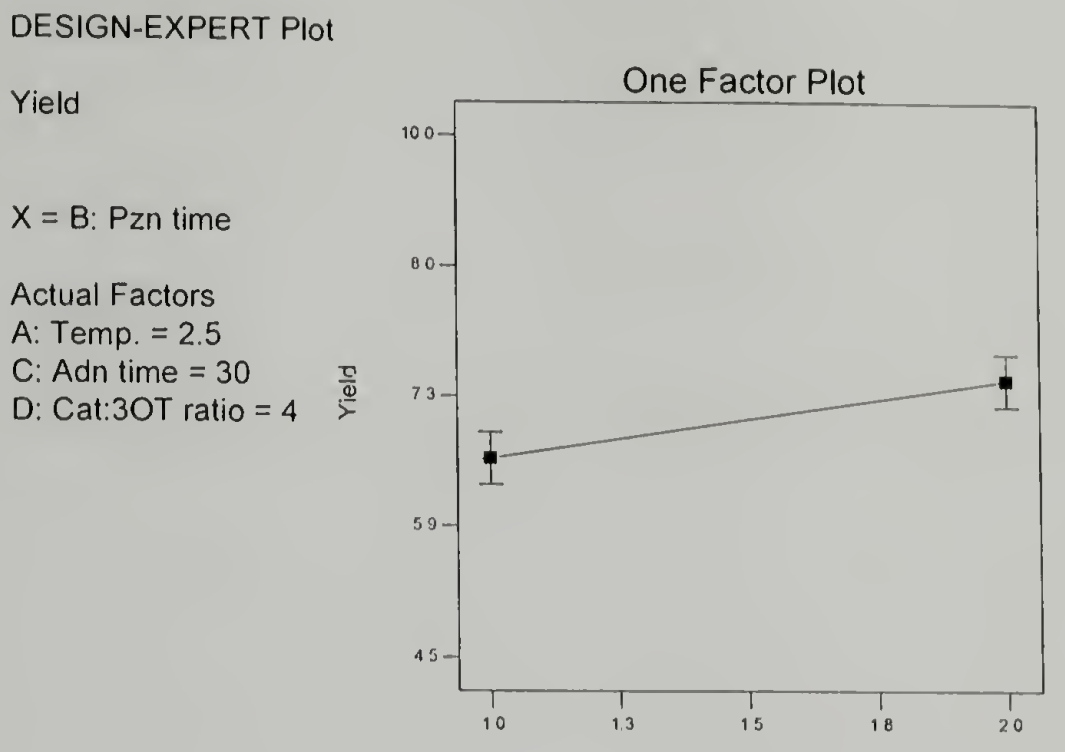

Figure 3.3. Plots of effects of main factors on yield (Y_1)

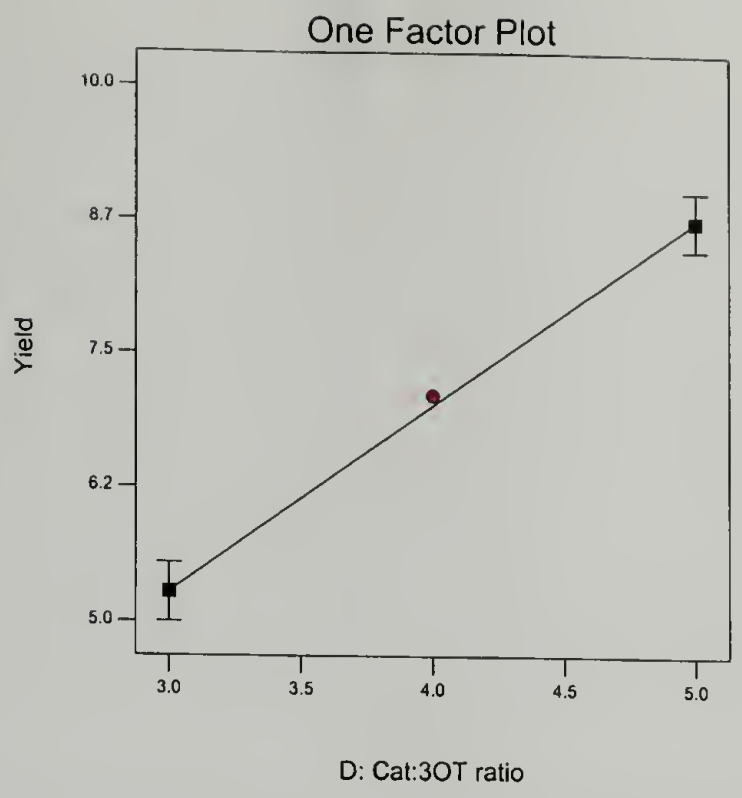

Figure 3.4. Plot of effect of catalyst to monomer ratio on yield, including center-point (red dot).

In figure 3.3, a straight line is drawn between the responses at the low and high settings for the factors. The two-level factorial design is based on the assumption that the effect is linear, so that the response could be predicted at any factor setting between low and high. However, the line could have curvature. Curvature is detected by setting all the factors at levels halfway between low and high, creating "center points" in the design. Laakso and Järvinen performed a single replicate of a center point experiment, shown in figure 3.4, which falls very close to the predicted effect. Typically, optimization of a process is achieved in two steps. First, a two-level factorial design is used to identify the factors which produce significant effects and to formulate a reasonable guess at the optimum conditions. Then, center points are added to the design to detect curvature, which can be used for further optimization.

Unfortunately, Laakso and Järvinen's own analysis of their data appears flawed. They claim that a shorter monomer addition time has a significant effect on yield and solubility, but it can be calculated that there is a 38% chance that that effect

is due to noise. They also report "a conflict between the effect of oxidant on yield together with molar mass and solubility," when it is clear that the oxidant ratio has a significant effect on yield and an insignificant effect on solubility. It is possible that Laakso and Järvinen set up a two-level factorial design, but then tried to interpret their results using a conventional OFAT approach by drawing conclusions from each individual experiment.

3.1.1.6 Response model: prediction and validity

The response Y_1 to the effects B and D can be predicted by a mathematical equation. The intercept of the response is the average of all the actual responses (7.0, the penultimate row of table 3.3). Each effect coefficient is one-half the value of the effect (the factor levels are -1 and +1, a difference of 2). The model equation for yield is

$$Y_1 = 7.0 + 0.42B + 1.75D + 0.42BD \tag{3.3}$$

The model equation is plotted in figure 3.5, with the actual responses shown for comparison. (The intercept in the plot is for the coded values, not the actual values in equation 3.3.)

The validity of the model can be confirmed graphically as well. The residuals are the differences between the actual responses and the responses predicted by equation 3.3, shown in table 3.7. They should vary normally, as can be confirmed by constructing a normal plot. In figure 3.6, (left), the residuals (mostly) fall upon a line, indicating normal variation. A second test is to plot the residuals versus the predicted values (figure 3.7, right). The residuals do not increase with the predicted level (a megaphone pattern), indicating the amount of variance is constant.

3.1.1.7 Fractional factorials and aliasing

Laakso and Järvinen used a full-factorial experimental design – all combinations of factors were covered. But, only the effects of factors B and D were sig-

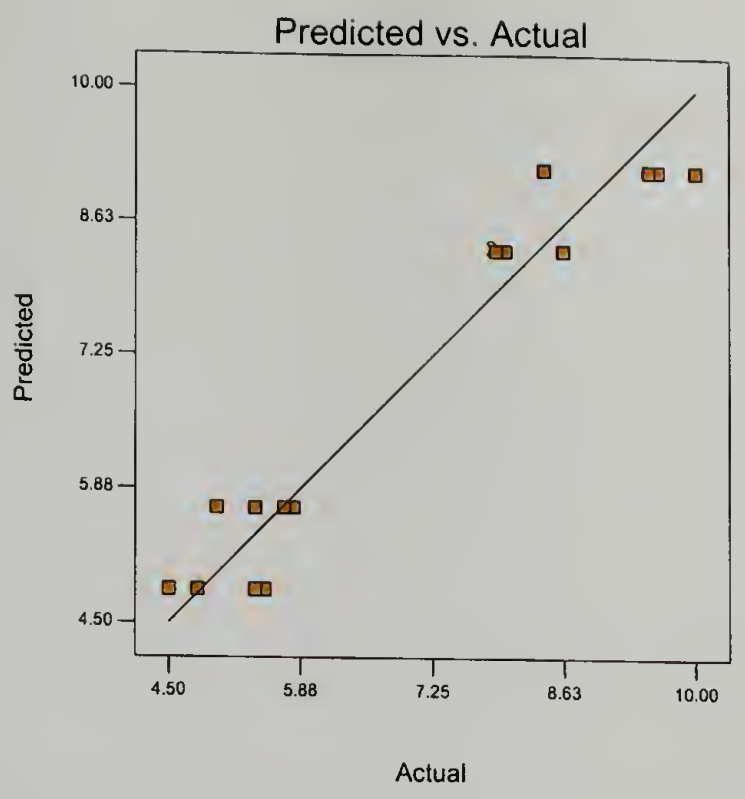

Figure 3.5. Predicted (equation 3.3) and actual responses of yield (Y_1).

Table 3.7. Residuals for yield (Y_1)

Std.	B	D	BD	Y_1 Actual	Y_1 Pred.	Residual
1	-	-	+	4.5	4.84	-0.34
2	-	-	+	5.5	4.84	0.66
3	+	-	-	5.0	5.68	-0.68
4	+	-	-	5.8	5.68	0.12
5	-	-	+	4.8	4.84	-0.04
6	-	-	+	5.4	4.84	0.56
7	+	-	-	5.7	5.68	0.02
8	+	-	-	5.4	5.68	-0.28
9	-	+	-	8.6	8.33	0.27
10	-	+	-	8.0	8.33	-0.33
11	+	+	+	9.6	9.17	0.43
12	+	+	+	10	9.17	0.83
13	-	+	-	8.0	8.33	-0.33
14	-	+	-	7.9	8.33	-0.43
15	+	+	+	9.5	9.17	0.33
16	+	+	+	8.4	9.17	-0.77

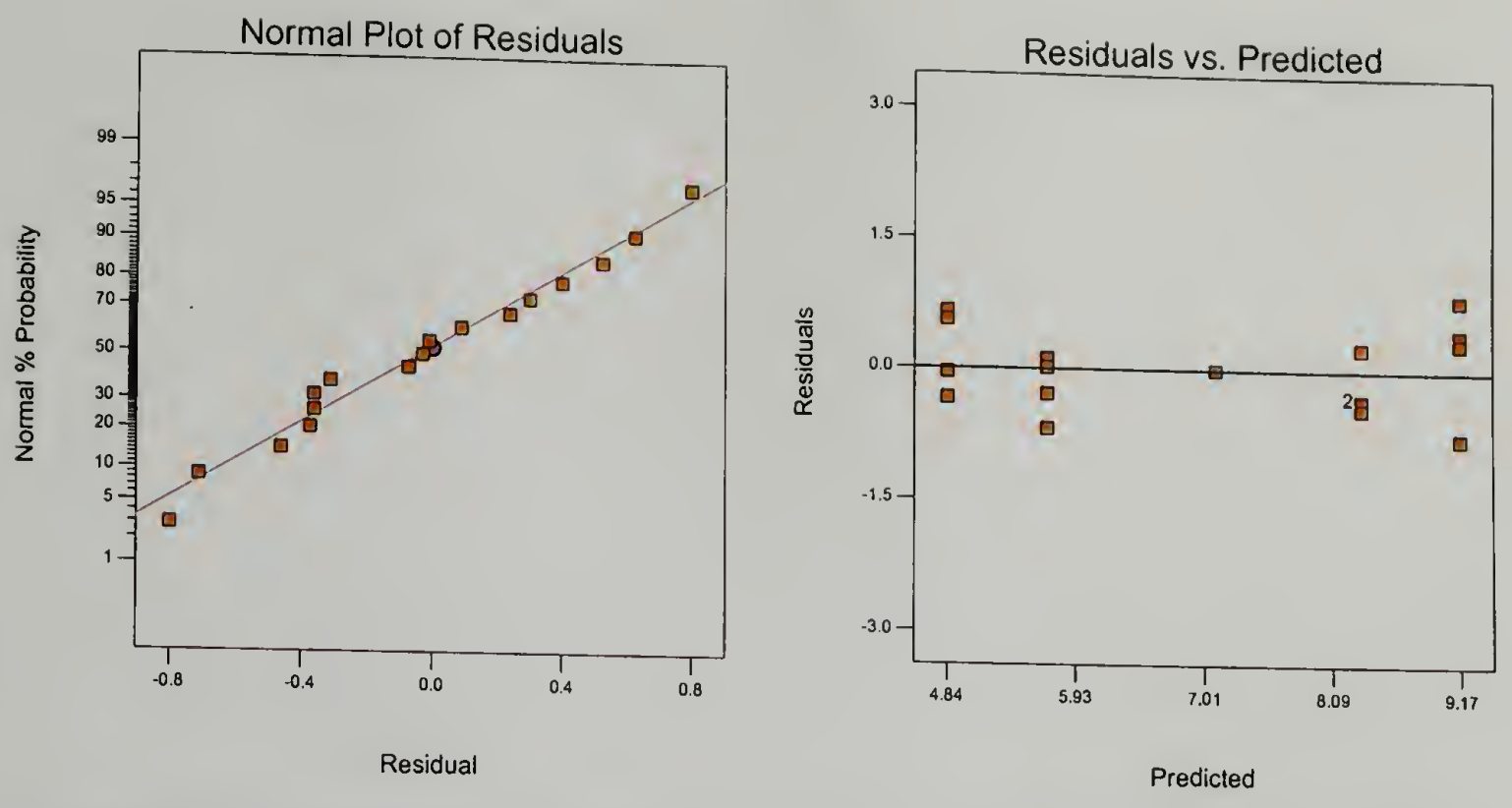

Figure 3.6. Checking model validity: Normal plot of residuals (left) and comparison of residuals versus predicted response (right).

nificant. Because of sparsity of effects, they could have predicted before the experiment that the chances that the effect of the three-factor interaction ABC being significant would be low. If they had chosen to ignore the effects of higher order interactions like ABC, they could have performed the experiment in half as many runs.

In table 3.8, eight of the runs from tables 3.3 and 3.4 have been deleted, producing a fractional factorial design. The main effects A, B, C, and D have balanced patterns of high and low levels. But, each two-factor interaction has a twin: the pattern of high and low levels for AB is identical to that of CD. Similarly, AC and BD are the same, and AD and BC are the same. The two-factor interactions AB and CD are aliased. This is a Resolution IV design: two factor interactions are aliased with each other (2+2=4), and main factors are aliased with three factor interactions (1+3=4). In comparison, the original experiment was a Resolution V design, where two factor interactions are aliased with three factor interactions (2+3=5), and main factors are aliased with four-factor interactions (1+4=5). In a fractional factorial ex-

Table 3.8. Coded factor levels for Resolution IV fractional factorial

Std.	A	B	C	D	AB	AC	AD	BC	BD	CD
1	-	-	-	-	+	+	+	+	+	+
4	+	+	-	-	+	-	-	-	-	+
6	+	-	+	-	-	+	-	-	+	-
7	-	+	+	-	-	-	+	+	-	-
10	+	-	-	+	-	-	+	+	-	-
11	-	+	-	+	-	+	-	-	+	-
13	-	-	+	+	+	-	-	-	-	+
16	+	+	+	+	+	+	+	+	+	+

periment, if an aliased factor is shown to have a significant effect on the measured response, than it is necessary to run additional experiments to determine which of the aliased factors is the actual cause.

3.1.2 Fluorescence

Fluorescence is one of two types of luminescence, the other being phosphorescence, which are distinguished by the nature of the exited state and the emission rate. In fluorescence, an electron is excited from the ground state to an excited state so that the electron in the excited state has the opposite spin of the electron in the ground state. Because relaxation to the ground state is spin-allowed, the electron can quickly return to the ground state with concomitant emission of a photon. In phosphorescence, the excited electron has the same spin as the electron in the ground state, the transition is spin-forbidden, and the emission rates are 10^5 to 10^8 s^{-1} slower.[5] These processes are illustrated by a Jabłoński diagram, shown in figure 3.7.[6]

An electron can be excited from the ground state, S_0, to an excited state, S_1. The electronic energy level S_1 consists of a number of vibrational energy levels; the electron quickly relaxes to the lowest vibrational energy level of the excited state S_1 by a process called internal conversion. Energy can also be lost by collisional quenching with a solvent, although this happens on a slightly longer time scale

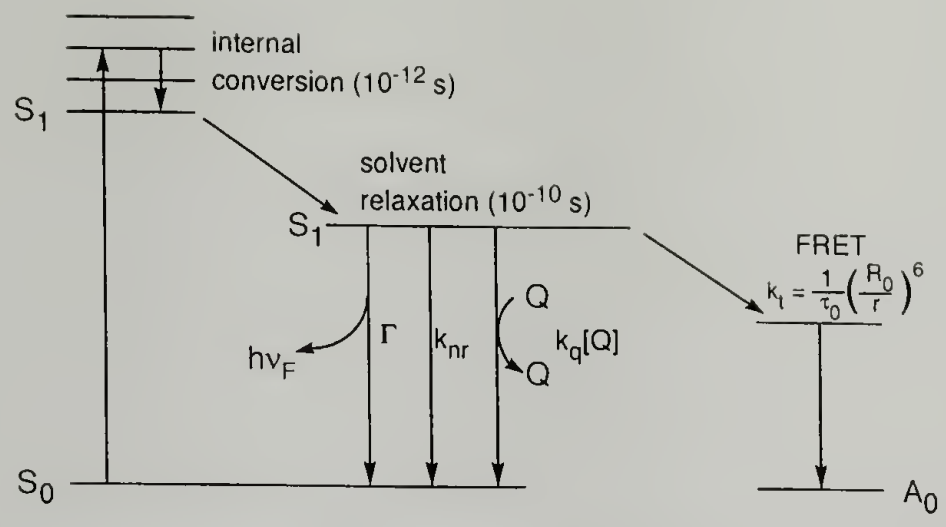

Figure 3.7. Jabłoński diagram showing the pathways for radiative and non-radiative relaxation of an excited electron to the ground state.

(10^{-10} rather than 10^{-12} seconds). The electron can now return to the ground state by radiative decay of a photon ($h\nu$), described by a rate constant Γ. Alternatively, the electron can relax by non-radiative decay, with a rate constant k_{nr}. The quantum yield Q, the number of emitted photons relative to the number of absorbed photons, is

$$Q = \frac{\Gamma}{\Gamma + k_{nr}} \tag{3.4}$$

Highly fluorescent molecules have a quantum yield close to unity. The fluorescence lifetime τ is

$$\tau = \frac{1}{\Gamma + k_{nr}} \tag{3.5}$$

The longer the lifetime of the excited state, the greater the chance the fluorophore can interact with other molecules. Thus, the quantum yield and the fluorescence lifetime are the two most important descriptors of a fluorophore.

The excited fluorophore can dissipate energy and return to the ground state by collisions with other molecules besides the solvent. Collisional quenching occurs when the excited molecule transfers energy to a quenching molecule that can occur by a variety of mechanisms, depending on the pair of molecules. The decrease in fluorescence intensity due to quenching is described by the Stern-Volmer equation,

$$\frac{F_0}{F} = 1 + K[Q] = 1 + k_q \tau_0 [Q] \tag{3.6}$$

where F_0 and F are the fluorescence intensities in the absence and presence of the quencher, K is the Stern-Volmer quenching constant, $[Q]$ is the quencher concentration, k_q is the bimolecular quenching constant, and τ_0 is the fluorescence lifetime of the unquenched fluorophore. Quenching can be dynamic, if the excited-state fluorophore collides with a quenching molecule, or static, if the ground-state fluorophore forms a non-fluorescent complex with the quenching molecule.

Finally, the excited fluorophore can return to the ground state by transferring its energy to another molecule via dipole resonance. This process, fluorescence resonance energy transfer (FRET), can occur when the emission spectrum of a fluorophore overlaps with the absorption spectrum of an acceptor. It is more appropriately named for its discoverer – thus, Förster resonance energy transfer – because it does not involve emission of a photon from the fluorophore. Rather, the dipole moment of the donor resonates with that of the acceptor, transferring energy which may or may not be emitted by the acceptor. The amount of energy transfer depends upon the extent of spectral overlap, and the distance between the donor and acceptor. The rate of energy transfer k_t is

$$k_t = \frac{1}{\tau_0} \left(\frac{R_0}{r} \right)^6 \tag{3.7}$$

where R_0 is the Förster radius, and r is the distance between the donor and acceptor. R_0 is the distance at which energy transfer is 50% efficient, and is one way of quantifying the spectral overlap. Typical values of R_0 for fluorophores and acceptors range between 30 and 60 Å.[7]

3.1.3 Biological applications of poly(thiophene) fluorescence

3.1.3.1 Amine-reactive fluorescent tags

Barbarella et al. have studied oligo(thiophene) isothiocyanates as fluorescent tags for biological applications. Oligo(thiophene)s containing a central thiophene-*S,S*-dioxide unit have high solid-state and solution photoluminescence quantum efficiencies, approaching 70% in the solid-state and 85% in solution, depending on the structure.[8] By varying the degree of electron delocalization by substituting side groups, photoluminescence emission maxima wavelengths could be tuned from 400 to 800 nm.[9] Improvement of the aqueous solubility, and functionalization with an isothiocyanate group for amine coupling, produced a flexible system for producing stable bioconjugates with high quantum efficiency.[10]

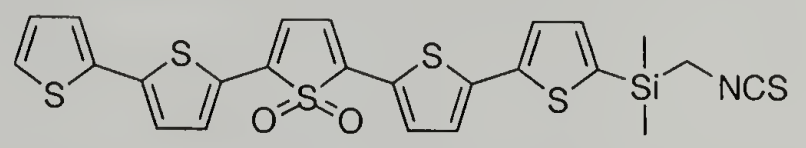

Conjugation with anti-CD3 and anti-CD8 antibodies was reported for the flexible[11] and rigid-core[12] variants of the oligomers.

3.1.3.2 DNA hybridization assays

A major focus of poly(thiophene) fluorescence research has been the development of DNA hybridization sensors. Early work attempted to detect hybridization by synthesizing conducting polymers with single-stranded DNA side chains. Complexation with the complementary DNA would perturb the conjugated polymer backbone, resulting in a change measured by electrochemistry. Using poly(pyrrole) and a 14 base oligonucleotide, Garnier et al. reported a detection limit of 10^{-11} mol, two orders of magnitude lower than the contemporary fluorescence detection techniques.[13] Lee and Shim did not report a detection limit using oligonucleotide-conjugated poly(thiophene)s (rather than poly(pyrrole)s) in 2001.[14]

In 2002, Gaylord, Heeger, and Bazan demonstrated an alternative system based on FRET between a poly(phenylene) and a fluorophore-labeled single-stranded DNA (ssDNA), based on two ideas. First, conjugated polymers can act as optical amplifiers, and have high fluorescence quenching efficiencies which result from exciton migration to low-energy sites along the backbone. Second, the electrostatic interaction between a double-stranded DNA (dsDNA) and a positively-charged conducting polymer should be stronger than the interaction between a ssDNA and the conducting polymer. As shown in figure 3.8 (left), when a labeled ssDNA hybridizes with its complementary strand, the negatively-charged dsDNA can form a strong electrostatic interaction with the positively-charged conducting polymer. The close proximity of the conducting polymer and the complex results in FRET from the polymer to the fluorophore, producing a detectable fluorescence signal. When a non-complementary ssDNA is introduced instead (figure 3.8, right), the complex is not formed, and the weak electrostatic interactions prevent the conducting polymer and the fluorophore from approaching each other. A detection limit of 10^{-11} mol ssDNA using a standard fluorimeter was achieved using this method.[15,16] Later developments using this system included RNA detection[17] and multiple DNA detection by synthesizing conducting polymers with multiple fluorescence emission maxima.[18]

The FRET technique requires a ssDNA labeled with a fluorophore, and has a detection limit comparable to the earlier results by Garnier et al. Later in 2002, Leclerc et al. described a poly(thiophene)-based system which did not require labeling of the ssDNA probe, and reached much lower detection limits. Positively-charged poly(1*H*-imidazolium, 1-methyl-3-(2-((4-methyl-3-thienyl)oxy)ethyl) chloride) forms aggregates with ssDNA, quenching the poly(thiophene) fluorescence. But, the polymer can wrap around a complementary DNA double helix, forming a fluorescent triplex (figure 3.9).[19,20] Using an LED

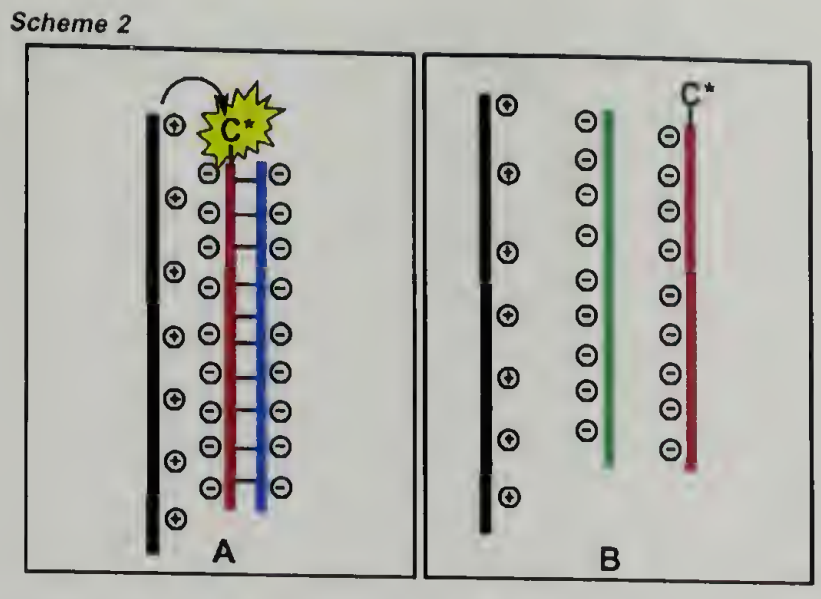

Figure 3.8. FRET-based ssDNA detection. Left: Red ssDNA labeled with a fluorophore hybridizes with its complementary blue ssDNA. Because of electrostatic interactions, the black conducting polymer is close enough for FRET, detectable as fluorescence emission. Right: The labeled red ssDNA does not hybridize with non-complementary green ssDNA, and so the conducting polymer does not form a complex. Reprinted with permission from Gaylord, B. S.; Heeger, A. J.; Bazan, G. C. *J. Am. Chem. Soc.* **2002,** *125,* 896–900. Copyright 2002 American Chemical Society.

source fluorimeter, a detection limit of 0.5×10^{-21} mol, or approximately 300 20-mer oligonucleotide molecules, was achieved. Additionally, mismatches of one base in a 20-mer oligonucleotide could be detected in that concentration range.[21]

3.2 Experimental

3.2.1 Materials

PL-HMBA resin (0.96 mmol/g) was obtained from Polymer Laboratories (Amherst, MA). Fmoc-3TA was obtained from PepTech (Cambridge, MA) and used as received. Ninhydrin (A.C.S. reagent), 1-hydroxybenzotriazole (HOBt, less than 5% water), 4-(*N*,*N*-dimethylamino)pyridine (DMAP, 99+%), 1,3-diisopropylcarbodiimide (DIC, 99%), 3-hexylthiophene (3HT, 99+%), Proton-Sponge (1,8-bis(*N*,*N*-dimethylamino)naphthalene), and 2,2′-bithiophene (BT, 97%) were obtained from Aldrich (Milwaukee, WI) and used as received. Ferric chloride (anhydrous, 99.99%,

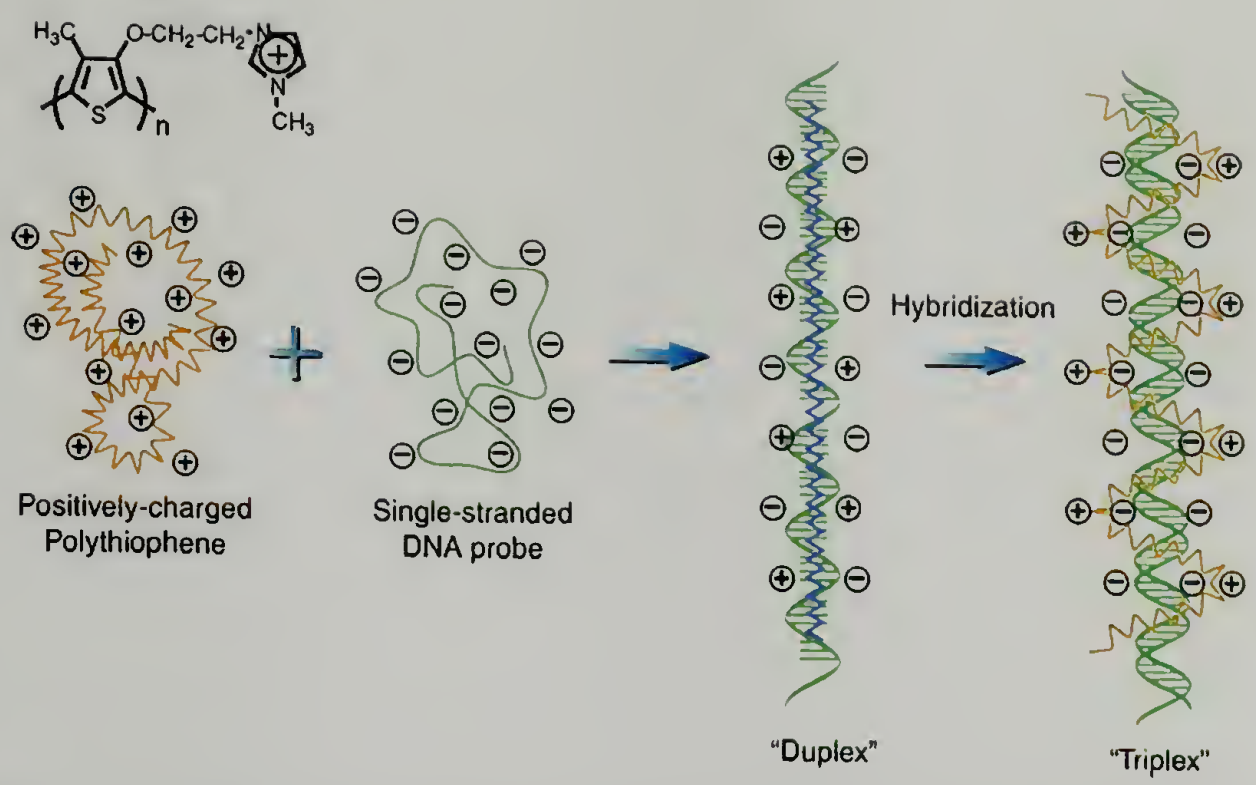

Figure 3.9. Formation of a quenched poly(thiophene)/ssDNA duplex and a fluorescent poly(thiophene)/dsDNA triplex. Reprinted with permission from Doré, K.; Dubus, S.; Ho, H. A.; Lévesque, I.; Brunette, M.; Corbeil, G.; Boissinot, M.; Boivin, G.; Bergeron, M. G.; Boudreau, D.; Leclerc, M. *J. Am. Chem. Soc.* **2004**, *126*, 4240–4244. Copyright 2004 American Chemical Society.

packaged under argon in ampules, and 97%) was obtained from Aldrich. Acetic anhydride (*puriss. p.a.*, $\geq$ 99.5%) was obtained from Fluka (Milwaukee, WI). Methanol, chloroform, tetrahydrofuran (THF), dichloromethane (DCM), *N*,*N*-dimethylformamide (DMF), and pyridine were obtained from EM Science (Gibbstown, NJ).

3.2.2 Solid-phase polymerizations

Fmoc-3TA was immobilized on HMBA resin as described in Chapter 2. Copolymerizations were run in blocks of four. A 6 dram (24 ml) vial with a Teflon-lined septum was charged with 50 mg loaded resin and a calculated amount of ferric chloride, and purged with argon. The resin and catalyst were suspended in 1 ml anhydrous chloroform. Depending on the experiment, appropriate amounts of 3HT, Proton-Sponge, and bithiophene were dissolved in anhydrous chloroform in a second vial. This monomer solution was then added at a calculated rate to the vial containing the resin using a syringe pump.

After the predetermined reaction time, the mixture was suspended in an excess of methanol. The solid phase resin was filtered into a tared coarse-frit Soxhlet micro-extraction thimble, and extracted with methanol until the filtrate was colorless. The resin was then extracted with THF until colorless, and dried overnight under vacuum over Drierite.

3.2.3 HMBA Linker cleavage

The copolymer was cleaved from the HMBA resin with NaOH/THF.[22] A 1/2 dram (2 ml) vial was charged with 5 mg resin, 1 ml THF, and a magnetic stirring bar. To this, one drop of 1 M aqueous sodium hydroxide was added, and the mixture stirred for two to five days at room temperature. The resin was removed by filtration, and the solvent removed by evaporation under an argon stream.

3.2.4 Fluorescence and UV/vis spectroscopy

UV/vis spectra were recorded on a Cary 50 Bio spectrometer (Varian, Palo Alto, CA). The dry polymer was dissolved in 4 ml chloroform and filtered through an Acrodisc 0.45 μm PTFE syringe filter (Pall Gelman Laboratory, Ann Arbor, MI) into a 1 cm quartz cuvette, and degassed by bubbling with argon for five minutes. Emission spectra were collected with a QuantaMaster Steady State Fluorimeter (Photon Technology International, Ontario, Canada) equipped with a xenon lamp, 5 nm excitation and emission slits, and an Model 814 photomultiplier tube in photon counting mode. Emission spectra were recorded by excitation at the UV/visible absorption maxima. Excitation spectra were recorded by monitoring emission at the emission spectra maxima.

3.3 Results and discussion

3.3.1 Choice of factors

Eight factors were chosen to optimize the copolymerization conditions:

Factor A: 3HT:3TA ratio

Factor B: Catalyst:monomer ratio

Factor C: Polymerization time

Factor D: Monomer concentration

Factor E: Anhydrous catalyst

Factor F: Proton-Sponge

Factor G: Monomer addition rate

Factor H: Bithiophene

3.3.1.1 Factor A: 3HT:3TA ratio

The choice of comonomer and its degree of incorporation will determine the solubility of the copolymer and will influence the conjugation length of the backbone. 3HT was chosen as comonomer because of its low oxidation potential (about 1.7 V vs. SCE[23]), its solubility in organic solvents, and its lack of branching at the α-carbon. Ready production of radical cations in the presence of $FeCl_3$ resulting from the low oxidation potential is desired, since the extent of the influence of the constrained environment inside the crosslinked resin on the rate and degree of polymerization cannot be predicted. Incorporation of a hydrophobic side chain should enable casting of water-insoluble films, which could be useful for studies such as protein binding. Finally, steric congestion introduced into the thiophene side chain has been shown to lead to weakly conjugated polymers, or to completely

inhibit electrochemical polymerization.[24] Copolymerization using 3HT, with its linear alkane side chain, should produce a backbone where the only major source of steric congestion is located at the single 3TA in the copolymer.

The ratio of 3HT to 3TA will affect the degree of polymerization and the ease of purification. Too much 3HT, and the system will be saturated with homopolymer, making extraction difficult (especially if it were to crosslink). Too little 3HT, and the degree of polymerization of chains attached to the bead will be low, producing oligomers, dimers, or no detectable reaction on the bead at all. Ratios of 3HT to 3TA of 5:1 and 20:1 were chosen: this should be a large enough range to observe an effect.

3.3.1.2 Factor B: Catalyst:monomer ratio

Sugimoto and coworkers conducted the first oxidative polymerization of a thiophene using $FeCl_3$ in 1986 using a ratio of 4 mol $FeCl_3$ to 1 mol 3HT.[25] This recipe has been used extensively, despite a lack of agreement on the mechanism of oxidative polymerization of thiophenes (section 1.2.3.2).[26,27] While stepwise cross-coupling reactions such as those developed by McCullough (using a nickel catalyst)[28] and Rieke (using a zinc catalyst)[29] produce nearly 100% head-to-tail couplings, and thus improved conjugation and enhanced conductivity,[30] they require highly pure monomer and are difficult to scale up.

Attempts to approach this degree of regioregularity using the more convenient $FeCl_3$-catalyzed polymerization have concentrated on keeping the catalyst concentration low during the polymerization. By keeping the Fe^{3+}/Fe^{2+} ratio low, the concentration of active species in the polymerization mixture remains low, resulting in a more selective polymerization with a lower risk of miscouplings between the 2- and 4-positions on the thiophene rings. Andersson et al. produced poly(3-(4-octylphenyl)thiophene) with a head-to-tail content of 94% by slowly adding $FeCl_3$

to the reaction mixture as the polymerization proceeded.[31] Subsequently, it was shown that precipitation of $FeCl_3$ from a saturated nitromethane solution added to a carbon tetrachloride solution of the monomer produced poly(3-hexylthiophene)s with higher regioregularities and conductivities.[32] Finally, Qiao and coworkers investigated the effect of different amounts of catalyst on the polymerization of 3-dodecylthiophene, using catalyst to monomer ratios of 2:1, 3:1, and 4:1. They concluded from NMR and WAXS that a ratio of 3:1 produced the highest number of head-to-tail linkages, around 82%.[33]

We chose to use catalyst to monomer (3HT and 3TA combined) ratios of 1:1 and 4:1. By setting the levels this far apart, we hoped to encompass some of the features of the low catalyst concentrations described above, as well as the higher ratio commonly used in the literature.

3.3.1.3 Factor C: Polymerization time

Polymerization times in the literature vary from 20 minutes to days. As shown in table 3.1, Laakso and Järvinen tried polymerization times of one and two hours;[4] our analysis of their data found that the longer polymerization time increased their yield significantly (figure 3.3, left). Della Casa et al. polymerized 2-(3-thienyl)ethyl hexanoate with $FeCl_3$, and found that the yield and conductivity increased as the polymerization time was increased from 1, to 5, to 24 hours.[34]

Polymerization times of 5 and 24 hours were used, calculated as the time after completion of addition of the monomer to the reaction mixture.

3.3.1.4 Factor D: Monomer concentration

A variety of concentrations of monomer have been reported in the literature. Sugimoto and coworkers used 0.1 M in their 1986 paper.[25] Others used 0.03 M[35] to 0.05 M,[31] or a higher concentration of 0.33 M.[36] Since we are working under

heterogeneous conditions, there will be a high effective concentration of Fmoc-3TA in the bead, and a lower concentration of 3HT in solution.

In an attempt to encompass the range of concentrations in the literature, while being mindful of the high local concentration of the artificial amino acid, final 3HT concentrations of 0.05 M and 0.20 M were used.

3.3.1.5 Factor E: Anhydrous catalyst

Our experience has shown that there may be an improvement in polymer quality when anhydrous rather than technical grade $FeCl_3$ is used. Gallazzi and coworkers reported an increase in soluble product when anhydrous catalyst was further dried by refluxing in $SOCl_2$, vacuum filtering, washing with anhydrous pentane, vacuum drying, and storing under argon.[37]

We chose to compare the differences between using Aldrich "anhydrous powder, 99.99+%," weighed out under argon in a glove bag, and "97%," weighed out in air on the benchtop with no precautions to exclude moisture. (In all cases, however, the reaction mixture was purged with argon before and during the polymerization, and anhydrous chloroform was used.)

3.3.1.6 Factor F: Proton-Sponge

It is also common in the literature to maintain a stream of inert gas over a $FeCl_3$-catalyzed polymerization to remove HCl generated during the reaction. Stochiometrically, the polymerization reaction can be written as:

$$\text{n thiophene} + 2\text{n } FeCl_3 \longrightarrow (\text{thiophene})_n + 2\text{n } FeCl_2 + 2\text{n HCl} \qquad (3.8)$$

It has been shown that bubbling HCl gas through the reaction mixture effectively quenches polymerization, possibly due to complexation with $FeCl_3$ to form $FeCl_4^-$.[26] Others found that the insoluble fraction of poly(3,3″-didodecyl-2,2′:5′,2″-terthio-

phene) decreased when the anhydrous $FeCl_3$ was dried even further, and attributed this to a reduction in moisture-generated HCl.[37] If generation of mislinkages, resulting in insoluble product, was due to HCl accumulating during the reaction, then addition of a "proton sponge" might reduce mislinkage formation.

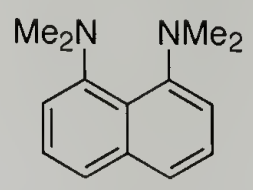

1,8-Bis(dimethylamino)naphthalene has a pK_a of 12.1, which is 10 million times more basic than *N,N*-dimethylaniline (pK_a=5.1). This is due to the formation of strong N···H···N hydrogen bonds upon monoprotonation, and the accompanying relaxation of steric strain. Additionally, there is a low rate of deprotonation due to the strong hydrogen bonds and steric shielding by the methyl groups – five orders of magnitude less than the deprotonation of ammonium ions. This combination of high thermodynamic basicity and kinetic inactivity results in a "proton sponge" – it does not nucleophilically attack other molecules, but soaks up protons when they are present.[38,39]

Proton-Sponge was added in an equimolar amount to the 3-hexylthiophene concentration, to compensate for some of the HCl formed during the reaction.

3.3.1.7 Factor G: Monomer addition rate

Our experience has shown that increasing the rate of monomer addition increases the yield of insoluble polymer, and is reflected by the language "dropwise addition of monomer" typically found in the literature.[35,40] Adding the monomer all at once instantly produces insoluble crosslinked polymer, due partially to the sudden high concentration in active radical cation species.[25] It was shown that dropwise addition of 3,3″-didodecyl-2,2′:5′,2″-terthiophene to a catalyst suspension produced much less insoluble polymer than adding the monomer all at once. Additionally, the soluble polymer produced by dropwise addition was more nearly

monodisperse than the soluble fraction produced by adding the monomer all at once.[37]

Use of a syringe pump to add the monomer solution permitted setting addition rates specified in ml/h. A slow rate of 0.5 ml/h and a fast rate of 2.5 ml/h were used, although both are "dropwise" additions. Because of the different volumes of the monomer solutions, these rates resulted in total monomer addition times ranging from less than 30 minutes to more than 30 hours.

3.3.1.8 Factor H: Bithiophene

2,2′-Bithiophene (BT) has been used as an additive in electrochemical polymerization to increase the rate of polymerization and to lower the required applied potential (E_{ox}=1.17 V vs. SCE).[41–43] BT addition also produces polymers with a lower average molecular weight.[44] We have observed that addition of BT to the oxidative polymerization of alkylthiophenes increased the $CHCl_3$-insoluble fraction of polymer, but also increased the overall yield. The insolubility may have been due to higher molecular weights, crosslinking, or a combination of both.

However, addition of a small amount of BT may relieve the steric congestion around the Fmoc-3TA site, increasing conversion and conjugation length of the polymer backbone. Therefore, we chose to include 0.05 mol BT per mol 3HT.

3.3.1.9 Excluded factors

Two other factors, temperature and solvent, may have had significant effects on the polymerization, but were not included in the experimental design.

The first polymerization of 3HT using $FeCl_3$ was performed at 30 °C,[25] and since then polymerizations of thiophenes have been performed at 0 °C,[45] room temperature,[36] and 40 °C.[37] Laakso and Järvinen compared reactions run at -5 °C and 10 °C, but our analysis (figure 3.2) concluded that temperature did not have a significant effect on either solubility or yield. Reactions run at lower temperatures

might proceed more slowly and produce more regioregular products. However, technical limitations precluded running reactions at temperatures other than ambient.

Most of the $FeCl_3$-catalyzed thiophene polymerizations described in the literature were perfomed in chloroform, possibly because the first was performed in chloroform,[25] or because some argue that the insoluble portion of the $FeCl_3$ is the active catalyst.[26] Della Casa et al. reported no difference in the regioregularity of poly(3-hexanoyloxyethylthiophene) prepared in chloroform or nitromethane.[34] However, Barbarella and coworkers demonstrated that the regioselectivity of the oligomerization of 3-(methylsulfanyl)thiophene depended on the solvent (chloroform, dichloromethane, nitromethane, or a mixture), and postulated that the stabilization of the radical cation by the solvent was the deciding factor.[40] This was supported by Andreani and coworkers, who found that polymerizations in carbon tetrachloride produced more soluble poly(3,3″- and 3′,4′-dialkyl-2,2′:5′,2″-terthiophene)s than polymerizations run in chloroform.[46] The experimental design described below was limited to eight factors, and so solvent was not included as a factor. It may have interesting effects on polymerization, however, and could be included in future designs.

3.3.2 Experimental design

A Resolution V two-level factorial design with eight factors would require 2^8, or 256, runs. However, this design resolution is probably unnecessary. The rule of thumb of sparsity of effects says that only 20% of the main effects and two-factor interactions will be significant in a system (section 3.1.1.4). So, the remainder of the main effects and two-factor interactions, as well as the higher order interactions, will vary only to the extent of the normal error, and will be lost in the noise.[1] A Resolution IV design, where main effects are aliased with three-factor interactions

and two-factor interactions are aliased with each other, requires fewer runs. A Resolution IV, eight-factor, two-level experiment requires only 16 runs, or 1/16th the runs required for a Resolution V design.

However, two-factor interactions are aliased with each other in a Resolution IV design (section 3.1.1.7). If we planned 32 instead of 16 runs (a 1/8th fractional factorial, instead of a 1/16th fractional factorial), some of the two-factor interactions would not be aliased. But, we would have to guess before performing the experiment which factors would be most likely to interact. A better strategy is to perform a "semifoldover" after performing the first 16 runs and determining if there were any aliased two-factor interactions, so that there are no wasted runs resulting from guessing which factors might be prone to interact.[47]

Also, it quickly became apparent that this experiment would be performed over multiple days, with different batches of loaded resin, catalyst, Soxhlet extraction times, etc. However, there are statistical methods for "blocking" out known sources of variation. By blocking variations which we can control, and randomizing what we can't control (or don't know), we still can produce statistically meaningful comparisons. The sixteen experiments were performed in four blocks. Within each block, the same sources of loaded resin and catalyst were used, the extractions were performed for the same amount of time, etc., but there was variation from block to block as more loaded resin was needed and different batches of catalyst was used on different days. The complete experimental design is shown in table 3.9, listed in standard order (as opposed to the randomized, blocked run order in which the experiments were actually performed).

3.3.3 Fluorescence in concentrated solution

Fluorescence was chosen to measure the response of the polymerization to different conditions for two reasons. First, the fluorescence emission is characteristic

Table 3.9. Resolution IV eight-factor, two-level experimental design for optimization of polymerization conditions. High levels are in red.

Std.	Run	Block	A: 3HT: 3TA ratio	B: Catalyst: monomer ratio	C: Pzn. time (h)	D: Monomer conc. (mM)	E: Anhyd. catalyst	F: Proton sponge	G: Addn. rate (ml/h)	H: BT
1	16	4	5	1	5	0.05	No	No	0.50	No
2	4	1	20	1	5	0.05	Yes	Yes	2.50	No
3	12	3	5	4	5	0.05	Yes	Yes	0.50	Yes
4	8	2	20	4	5	0.05	No	No	2.50	Yes
5	6	2	5	1	24	0.05	Yes	No	2.50	Yes
6	9	3	20	1	24	0.05	No	Yes	0.50	Yes
7	3	1	5	4	24	0.05	No	Yes	2.50	No
8	15	4	20	4	24	0.05	Yes	No	0.50	No
9	14	4	5	1	5	0.20	No	Yes	2.50	Yes
10	2	1	20	1	5	0.20	Yes	No	0.50	Yes
11	11	3	5	4	5	0.20	Yes	No	2.50	No
12	5	2	20	4	5	0.20	No	Yes	0.50	No
13	7	2	5	1	24	0.20	Yes	Yes	0.50	No
14	10	3	20	1	24	0.20	No	No	2.50	No
15	1	1	5	4	24	0.20	No	No	0.50	Yes
16	13	4	20	4	24	0.20	Yes	Yes	2.50	Yes

of the polymer conjugation length, which is dependent on degree of polymerization and on regioregularity.[48] Second, as fluorescence is one of the most sensitive analytical techniques, lower concentrations of sample isolated from smaller-scale polymerizations can be used (as compared with the amount of material required for solution NMR, for example).[5]

Using the experimental design given in table 3.9, sixteen samples were prepared and extracted with methanol (to remove residual catalyst) and THF (to remove unbound poly(3-hexylthiophene) homopolymer) using the multiple Soxhlet extraction apparatus shown in figure 3.10. The polymer-containing resin beads were then dried under vacuum, and 5 mg samples treated with NaOH in THF to cleave the polymer from the resin. The absorbance and fluorescence spectra of the concentrated solutions are shown in figure 3.11, with the results summarized in table 3.10. The absorbance maxima vary for the undiluted samples, and

Table 3.10. Fluorescence emission maxima of concentrated chloroform polymer solutions.

Std.	λ_F (nm)	Std.	λ_F (nm)
1	455	9	458
2	499	10	564
3	492	11	502
4	562	12	473
5	454	13	452
6	488	14	495
7	480	15	563
8	561	16	467

range between 0.5 and 1.5 absorbance units. (Results for solutions diluted to 0.05 absorbance units at their absorption maxima will be described in section 3.3.4.)

Table 3.10 shows that the emission peaks are clustered around three wavelengths: 450, 490, and 560 nm. The effect of each factor is calculated using equation 3.1. The effects are then plotted on a half-normal plot; those which do not vary normally are labeled (figure 3.12).*

Before we can continue, however, we remember that table 3.9 is a Resolution IV design. Single factors are aliased with three-factor interactions (but we ignore those as too improbable), but two-factor interactions are aliased with each other. Factor AD is aliased with three other two-factor interactions: BF, CG, and EH. Similarly, factor AF is aliased with BD, CH, and EG.

To dealias the interactions, we could perform a foldover on one of the factors. This would add another group of runs where the signs for all the factors are reversed, thereby doubling the number of runs. However, it is more efficient to perform a semifoldover, which generates only half the number of the original runs. We pick a factor that is involved in the largest two-factor interaction, and lay out the runs where all the other levels are reversed. We then guess which level of the

*Factor D is included in our model, even thought it appears to vary normally, to maintain model "hierarchy". This is because its parent two-factor interaction AD is significant. Even if D by itself is not significant, it does make a difference in conjunction with factor A.

Figure 3.10. Four simultaneous THF Soxhlet extractions of Fmoc-3TA-loaded resins after copolymerization with 3HT, under visible (top) and 254 nm UV (bottom) illumination.

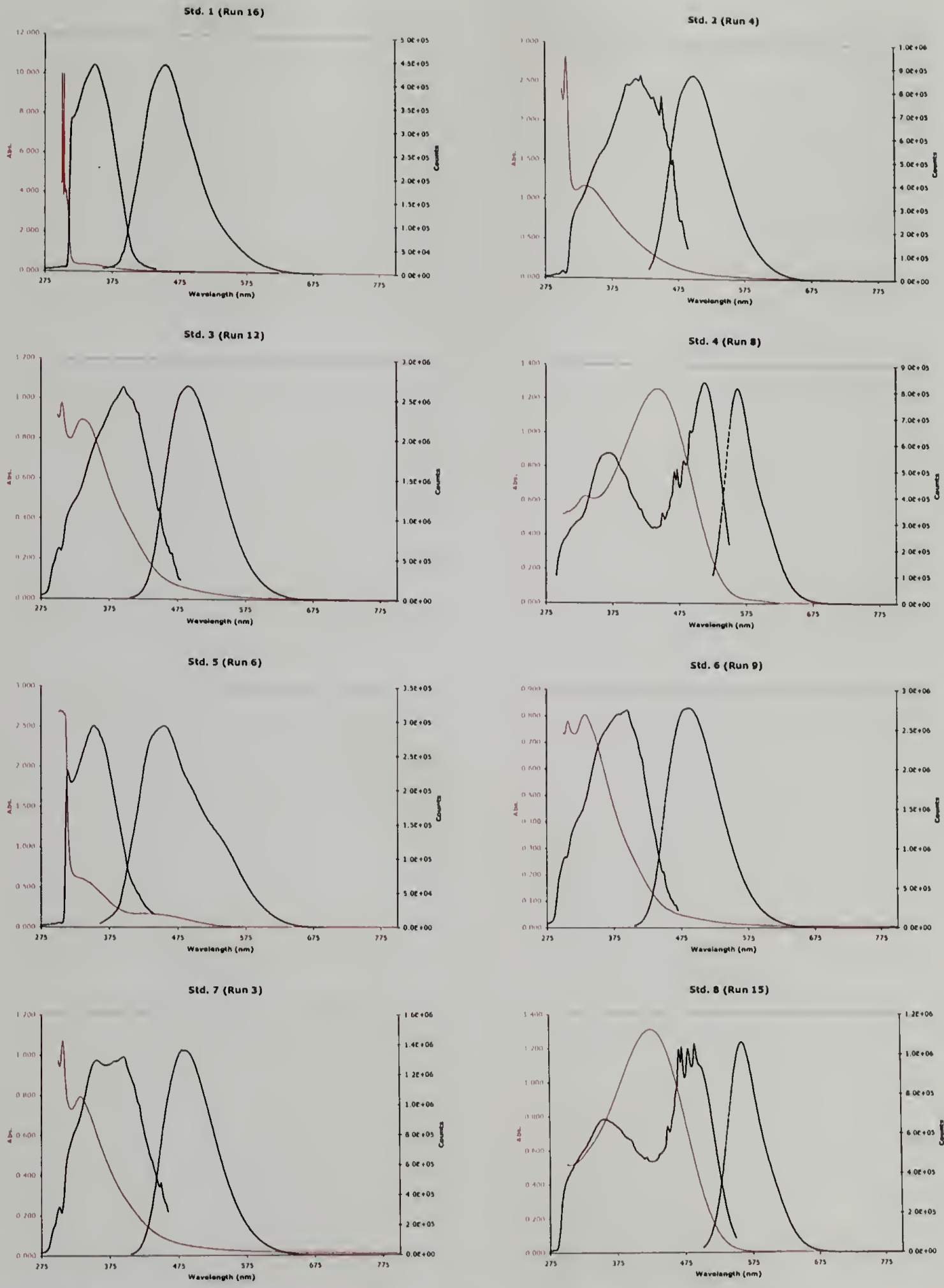

Figure 3.11. Fluorescence (—) and absorption (—) spectroscopy of concentrated polymer solutions.

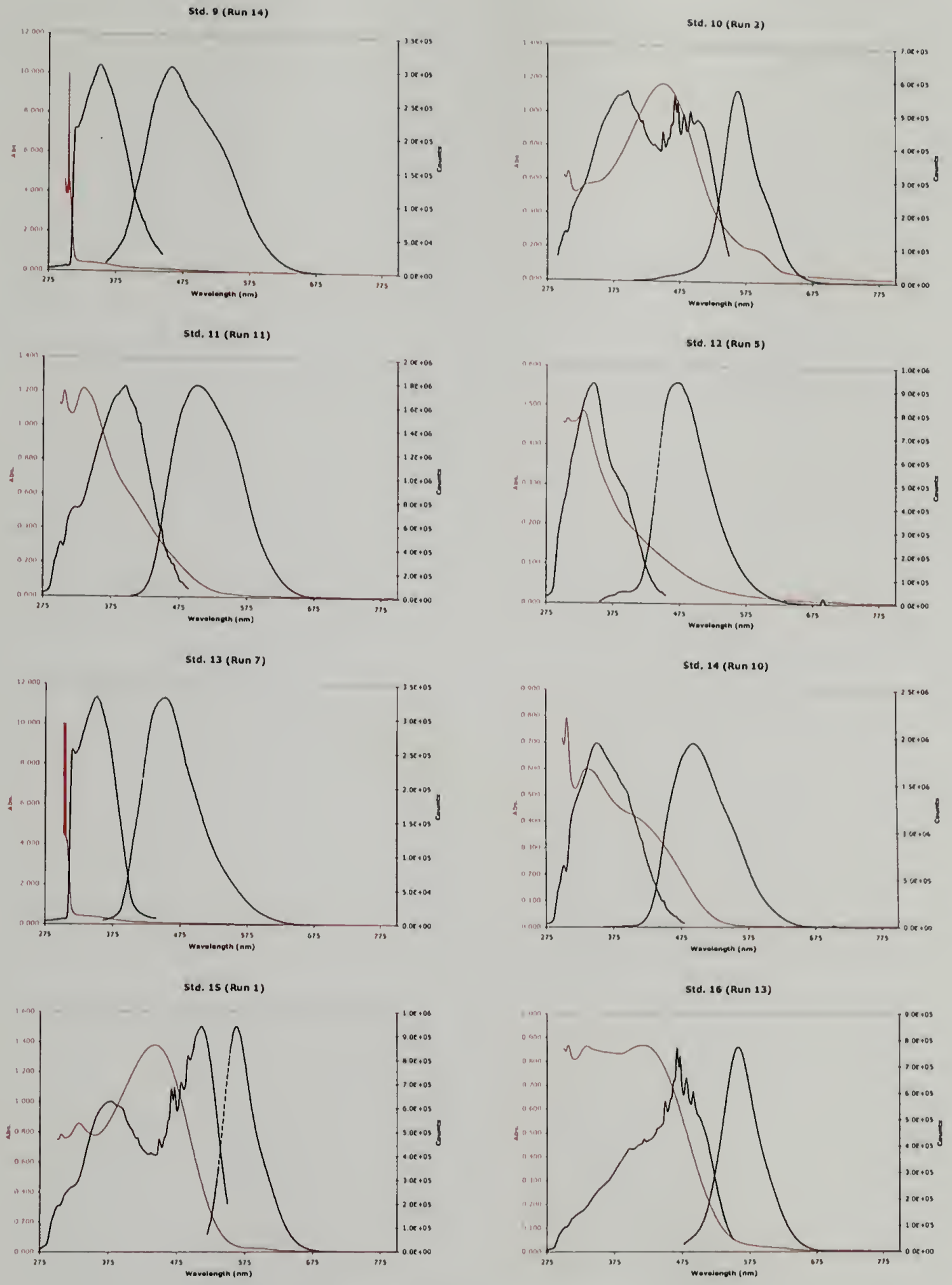

Figure 3.11 (continued).

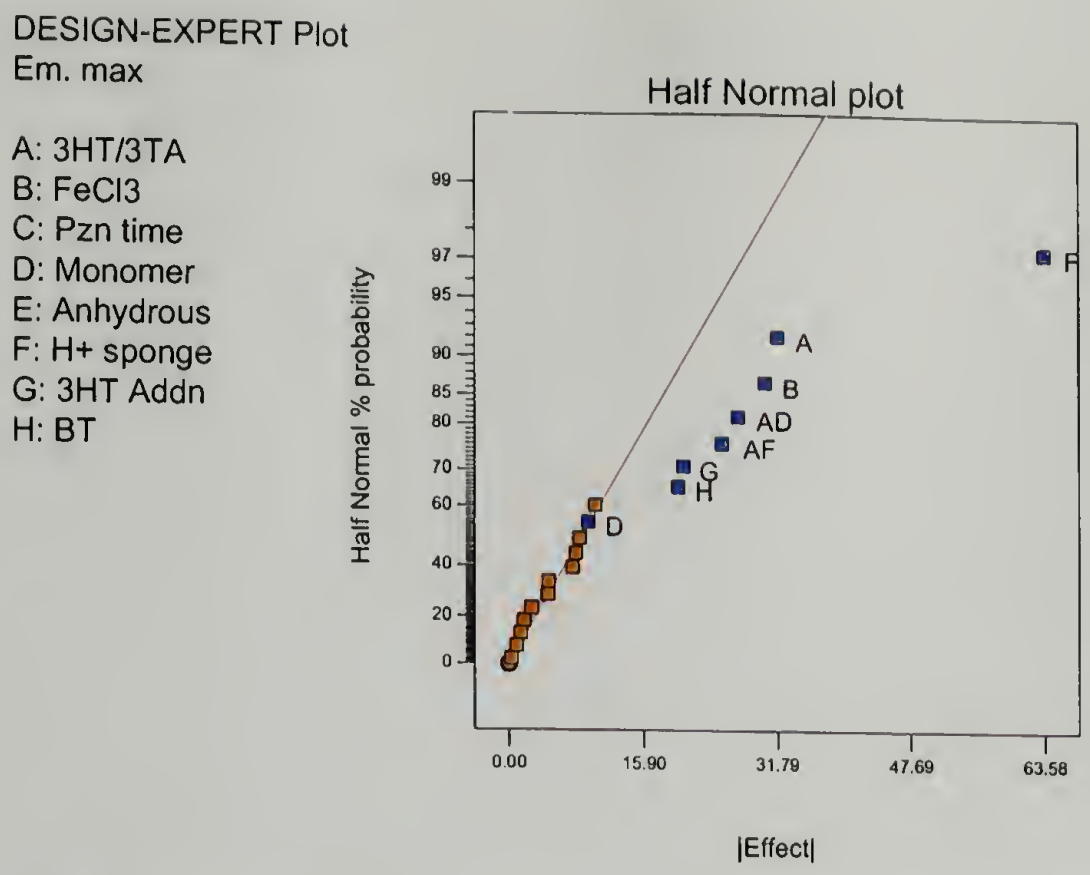

Figure 3.12. Half-normal plot of the effects of the factors in table 3.9 on the fluorescence maxima of polymers in concentrated solution.

folded-over factor will give the more desired response, and only perform the runs at that level.[47]

In our case, we are lucky, because factor A (the ratio of 3HT to 3TA) is involved in both aliased two-factor interactions. Otherwise, we would have to perform two foldovers. Factor A also has the second-largest effect according to the half-normal plot, and so should provide meaningful results. We guess that a higher ratio of 3HT to 3TA will produce higher molecular weight polymers with a longer conjugation length, and so we will use the high level of factor A. The resulting semifold is shown in table 3.11.

The additional eight polymerizations were conducted. The spectra are shown in figure 3.13, and the results summarized in table 3.12. We guessed correctly, because the half-normal plot after the additional eight runs (not shown) was identical to the one shown in figure 3.12: factors AD and AF were significant. (If we had guessed incorrectly, and one or both of the two-factor interactions had re-

Table 3.11. Semifold on polymerization optimization on factor A set at 20. All runs are in Block 5.

Std.	Run	A: 3HT: 3TA ratio	B: Catalyst: monomer ratio	C: Pzn. time (h)	D: Monomer conc. (mM)	E: Anhyd. catalyst	F: Proton sponge	G: Addn. rate (ml/h)	H: BT
17	24	20	1	5	0.05	No	No	0.50	No
18	22	20	4	5	0.05	Yes	Yes	0.50	Yes
19	20	20	1	24	0.05	Yes	No	2.50	Yes
20	18	20	4	24	0.05	No	Yes	2.50	No
21	21	20	1	5	0.20	No	Yes	2.50	Yes
22	17	20	4	5	0.20	Yes	No	2.50	No
23	19	20	1	24	0.20	Yes	Yes	0.50	No
24	23	20	4	24	0.20	No	No	0.50	Yes

Table 3.12. Fluorescence emission maxima of concentrated chloroform polymer solutions resulting from semifold on factor A.

Std.	λ_F (nm)
17	564
18	541
19	564
20	479
21	475
22	558
23	478
24	563

mained aliased, a second semifoldover on one of the remaining factors could be performed.)

To determine if our model is valid before we draw conclusions from it, we perform analysis of variance (ANOVA). By comparing the signal (the significant effects) to the noise (the effects which we didn't include in the model), we can calculate that there is a 99.99% chance that the fluorescence is significantly affected by one or more of the chosen effects. We also can test each chosen effect for significance, and find that only factor D (which we included to maintain hierarchy) is not significant. The equation for the response predicted by the model (in coded terms) is

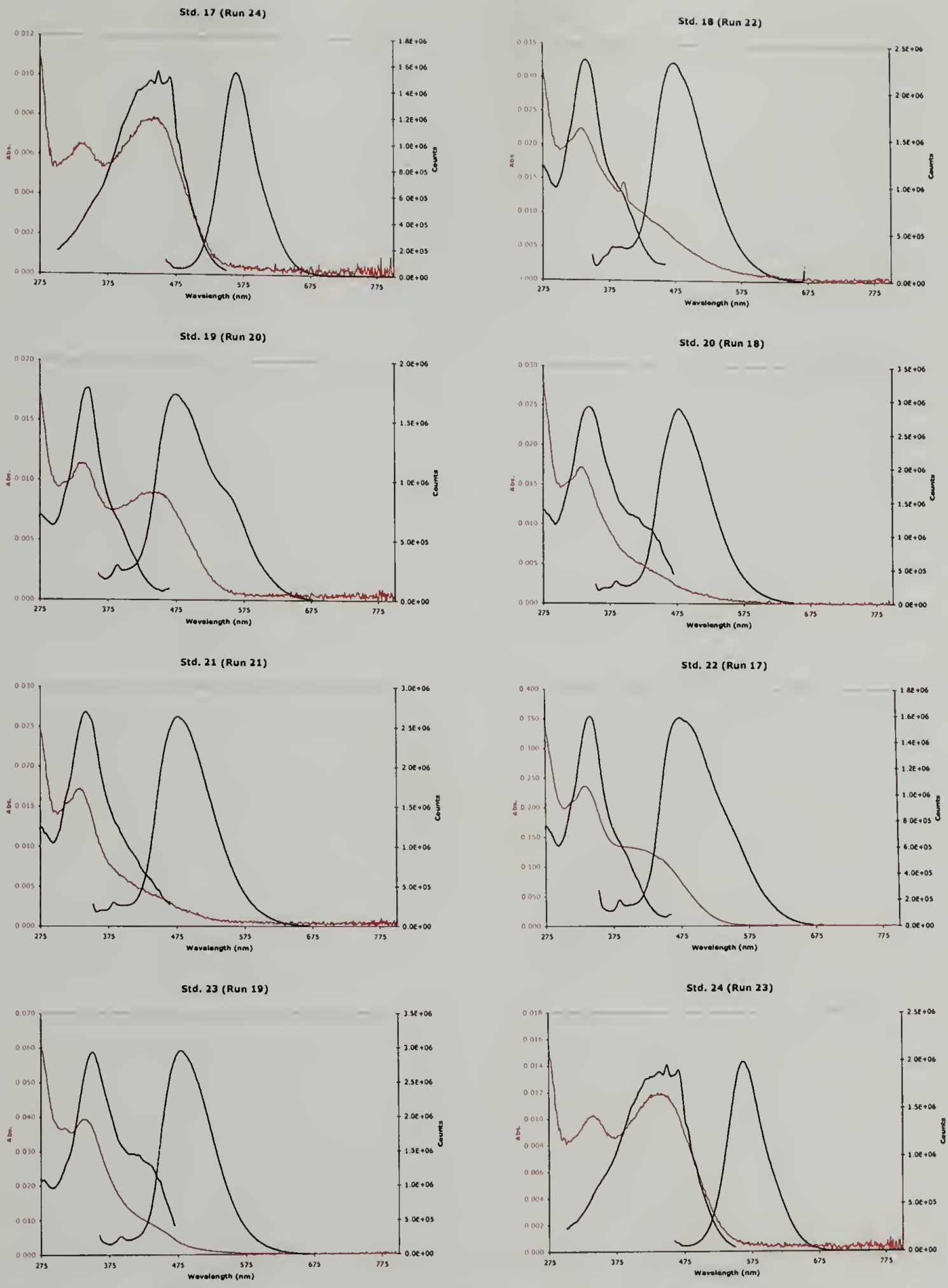

Figure 3.13. Fluorescence (—) and absorption (—) spectroscopy of concentrated polymer solutions resulting from semifold on factor A.

$$\begin{aligned}\lambda_F =& 500.64 + (15.81 \times A) + (12.29 \times B) + (0.094 \times D) - (22.34 \times F) \\ & - (8.38 \times G) + (8.12 \times H) - (11.66 \times AD) - (10.84 \times AF)\end{aligned} \tag{3.9}$$

Finally, we examine the assumptions which underlie the ANOVA. The difference between the response predicted by the model and the actual measured response is called the "residual". A plot of the predicted response vs. the actual measurements is shown in figure 3.14 (top left). By plotting the residuals on a full-normal plot (top right), we see that the residuals are basically distributed normally (they fall along the straight line). Plotting the residuals vs. run (bottom left) shows a random pattern, indicating that there were no variables that influenced the response during the experiment (reagent deterioration, fatigue, etc.). The Outlier T plot (bottom right) measures how each data point fits in with the rest of the points of the model. The outlier t statistic is the number of standard deviations between an actual data point and the predicted value at that point using a model based on all of the data *except* this point. Run 18 is outside the limits of 3.5 standard deviations, but there were no special causes to analyze the data without that point (contaminated the solution, forgot to add catalyst, etc.), so it was included in the model.

With the validity of the statistics verified, we can plot the effects of the significant factors. The effects of the three main factors on the fluorescence emission maxima are shown in figure 3.15. The confidence intervals on the points correspond to the least significant difference (LSD). If the bars do not overlap, then we can state with 95% confidence that the results are significantly different. In all three cases in figure 3.15, the results are significantly different. The values of the other factors not involved in the comparison are set to either their low level (if a categorical factor) or the average value (if a numerical factor). Since center points were

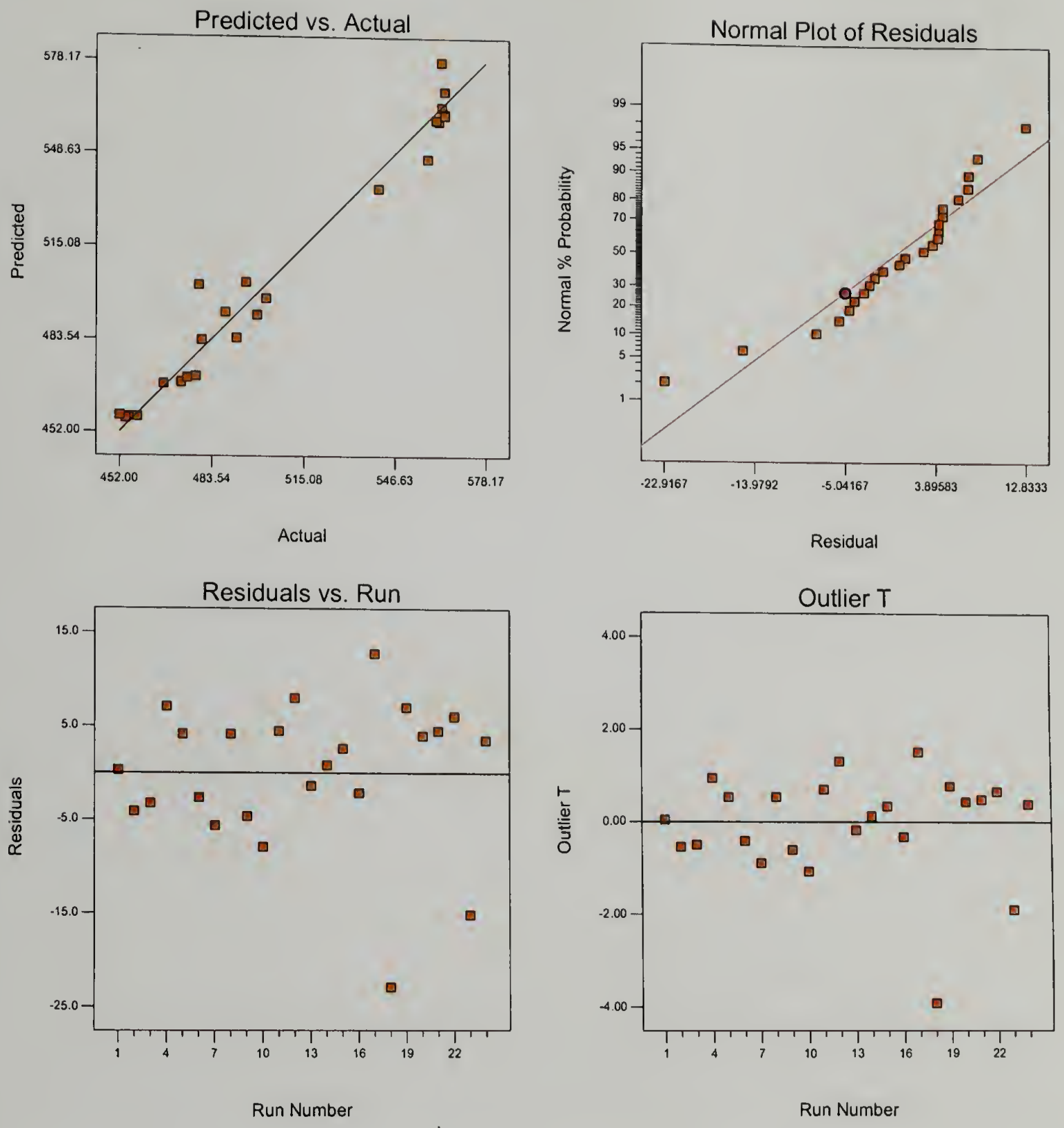

Figure 3.14. Model diagnostic plots for effects on fluorescence in concentrated solution.

Em. max

X = B: FeCl3

Actual Factors
A: 3HT/3TA = 13
C: Pzn time = 15
D: Monomer = 0.13
E: Anhydrous = No
F: H+ sponge = No
G: 3HT Addn = 1.50
H: BT = No

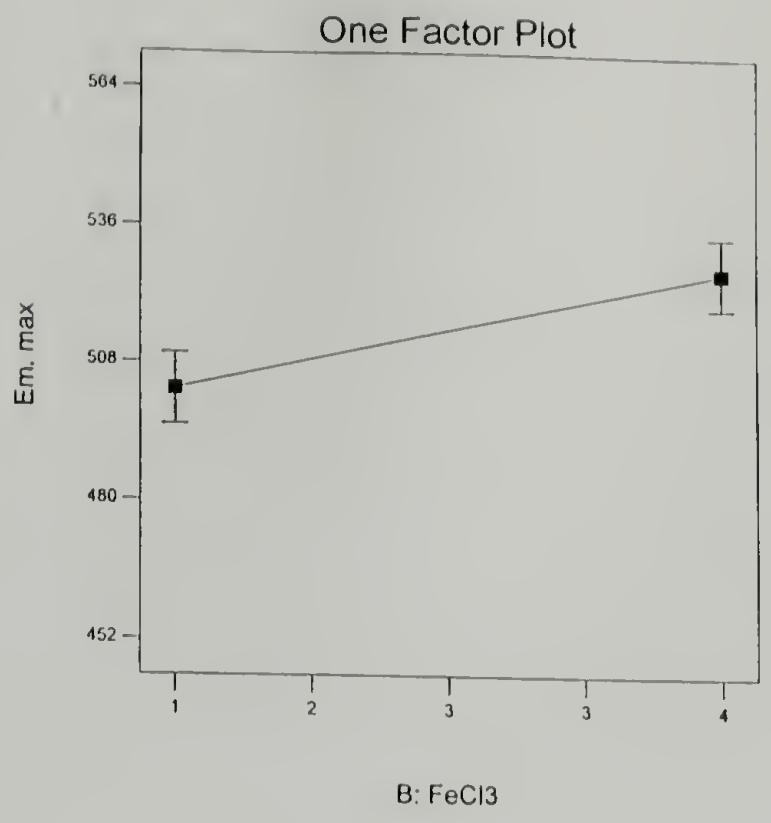

Em. max

X = G: 3HT Addn

Actual Factors
A: 3HT/3TA = 13
B: FeCl3 = 3
C: Pzn time = 15
D: Monomer = 0.13
E: Anhydrous = No
F: H+ sponge = No
H: BT = No

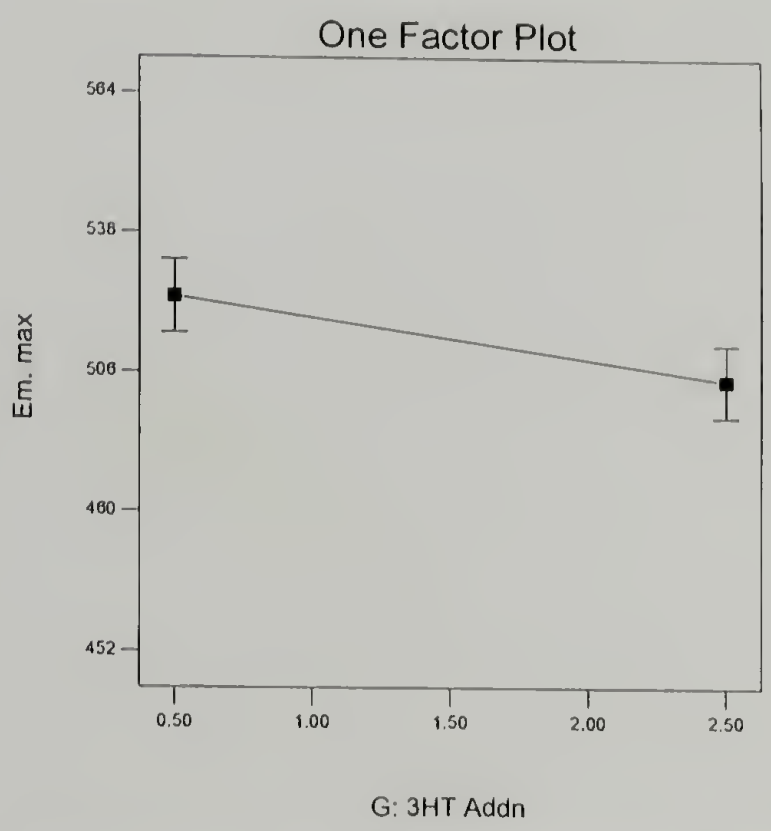

Figure 3.15. Main effects on polymerization detected in concentrated solution.

not included in our screening design, we assume the lines connecting the low and high factors to be straight, but there may be curvature.

The plots show that the emission maxima in concentrated solutions are higher when a 4:1 ratio of catalyst to monomer is used, when the monomer solution is

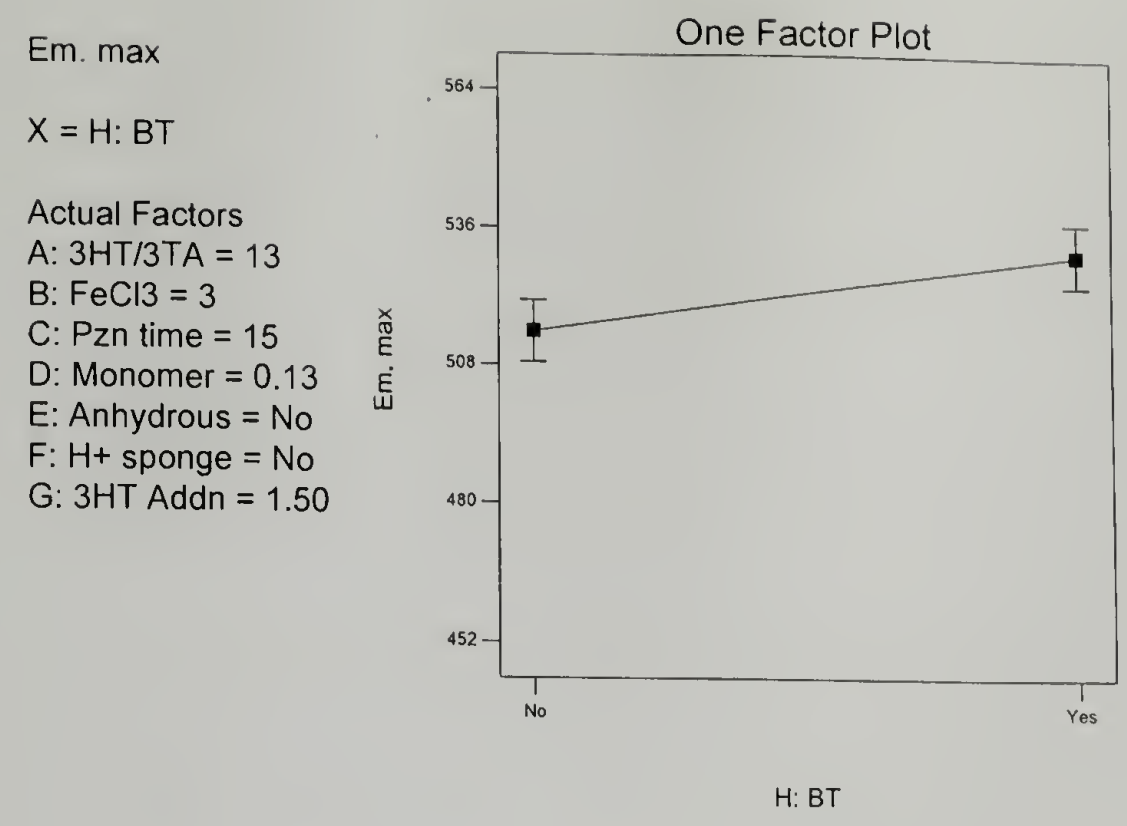

Figure 3.15 (continued).

added at a slower rate of 0.50 ml/h, and in the presence of a small percentage of bithiophene.

Plots of the two significant and dealiased two-factor interactions are shown in figure 3.16. These relationships, which would not be detectable by an OFAT experiment, show some interesting features. Figure 3.16 (left) shows the interaction between the monomer ratio and monomer concentration. The monomer ratio is plotted on the X axis. Two lines for the monomer concentration are plotted on the graph, at low (D-, 0.05 mM) and high (D+, 0.20 mM) levels. At a low monomer ratio, the higher monomer concentration produces significantly higher emission maxima. The emission maxima are significantly higher in both cases at the higher monomer ratio. But, the lower monomer concentration produces the higher maxima at the higher ratio. The interaction between the monomer ratio and addition of Proton-Sponge (figure 3.16, right) shows that there is no significant increase in emission maxima at the higher monomer ratio in the presence of the Proton-

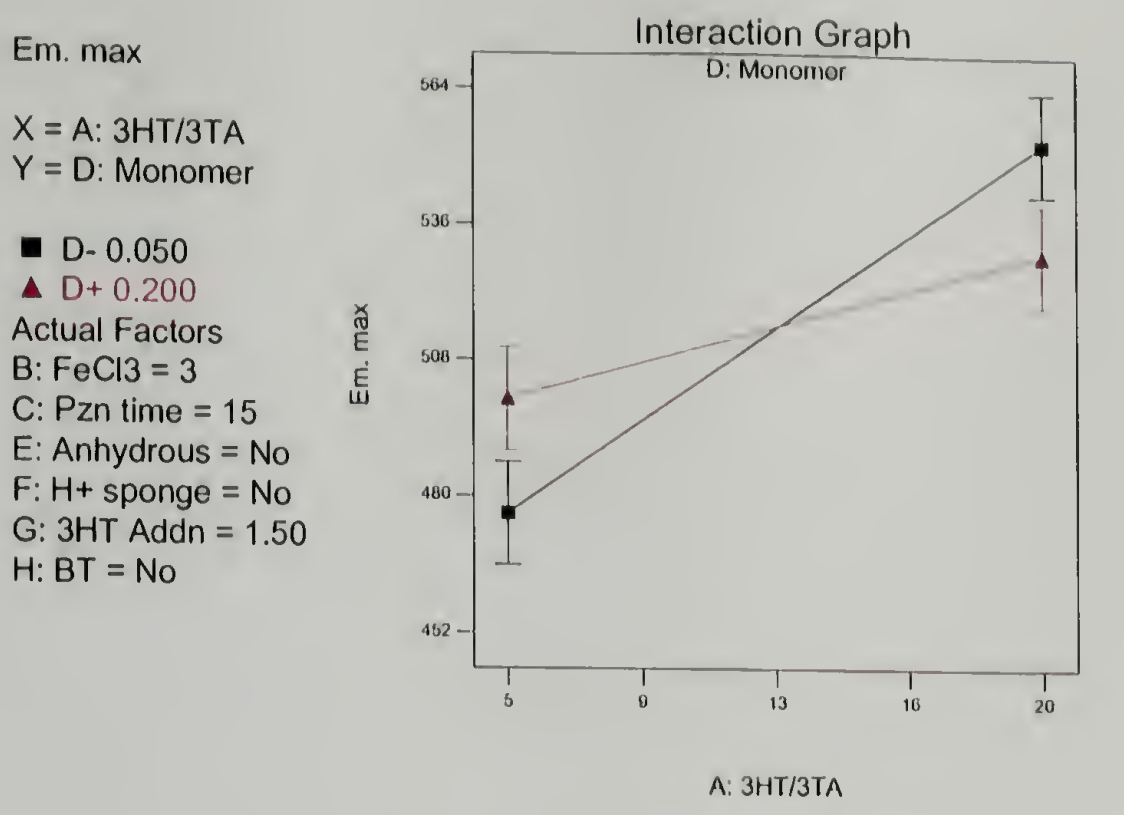

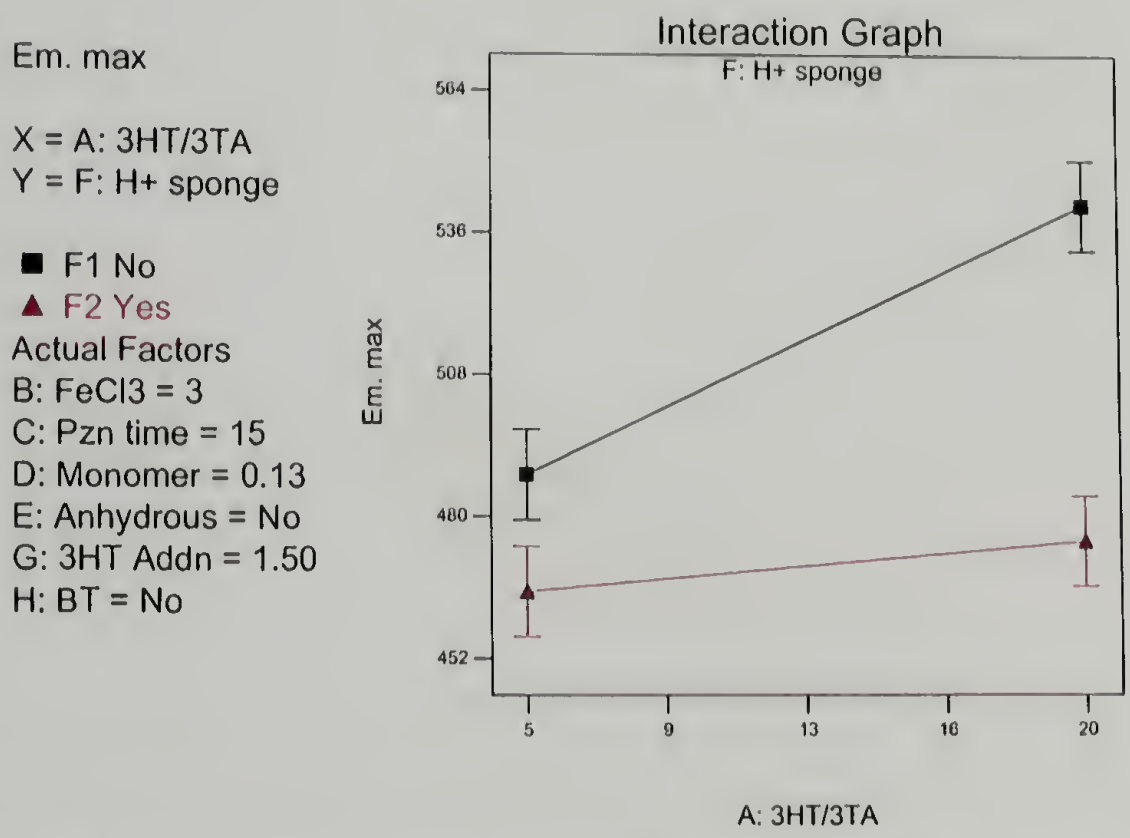

Figure 3.16. Two factor interactions on polymerization detected in concentrated solution.

Sponge (F2, Yes). However, leaving the Proton-Sponge out (F1, No) produces a significantly higher emission. And, in the absence of Proton-Sponge, the higher monomer ratio produces a higher emission.

3.3.4 Fluorescence in dilute solution

Meijer and coworkers demonstrated aggregation of oligo(thiophene)s in non-polar solvents and formation of twisted planar structures. This behavior was induced by introduction of chiral end-groups[49] or side-groups;[50] CD spectroscopy resolved the optical rotation in emission resulting from aggregation.[51] Fluorescence measurements of the π-π^* transition are very sensitive to the aggregation state of the oligo(thiophene).

Therefore, absorption and fluorescence spectroscopy was performed on very dilute solutions of our polymers. This would identify factors which may affect aggregation more than conjugation length. The concentrated samples were diluted to a maximum optical absorbance less than 0.05 units, filtered, and purged with argon. The spectroscopy results of all 24 runs are shown in figure 3.17. The spectra broadly fall into three categories, with emission maxima around 460 nm, 480 nm, and 560 nm. The measured absorbance and emission maxima and other data are summarized in table 3.13.

Many of the samples with the lowest values of λ_{max} in table 3.13 have absorption spectra with well-defined structure. These discrete absorption peaks may correspond to populations of oligomers of defined length. Bäuerle et al. synthesized a series of regioregular oligo(3-dodecylthiophene)s, and determined the λ_{max} for each oligomer (table 3.14).[52] The absorption wavelength increases dramatically at first in the series, but the increase with size levels off after the dodecamer. The series of peaks in the absorption spectra of experiments 1, 5, 9, and 13 may correspond to dimer, trimer, etc., of the 3HT/3TA copolymer. The absorption maxima of the samples with the longest fluorescence emission wavelengths range between 425 and 448 nm; based on table 3.14, these samples may have a degree of polymerization greater than 10 ($M_w \geq 1850$).

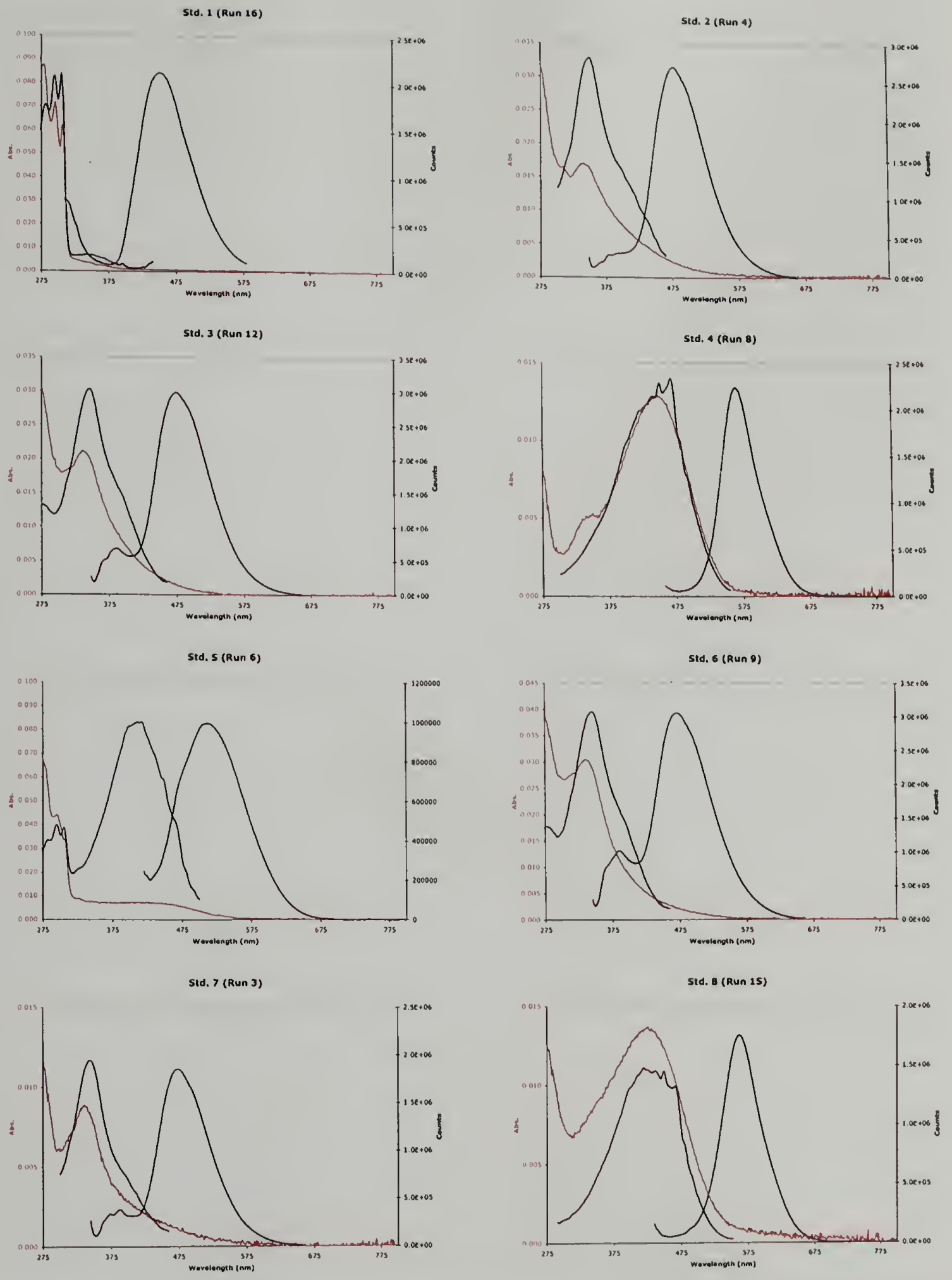

Figure 3.17. Fluorescence (—) and absorption (—) spectroscopy of dilute polymer solutions.

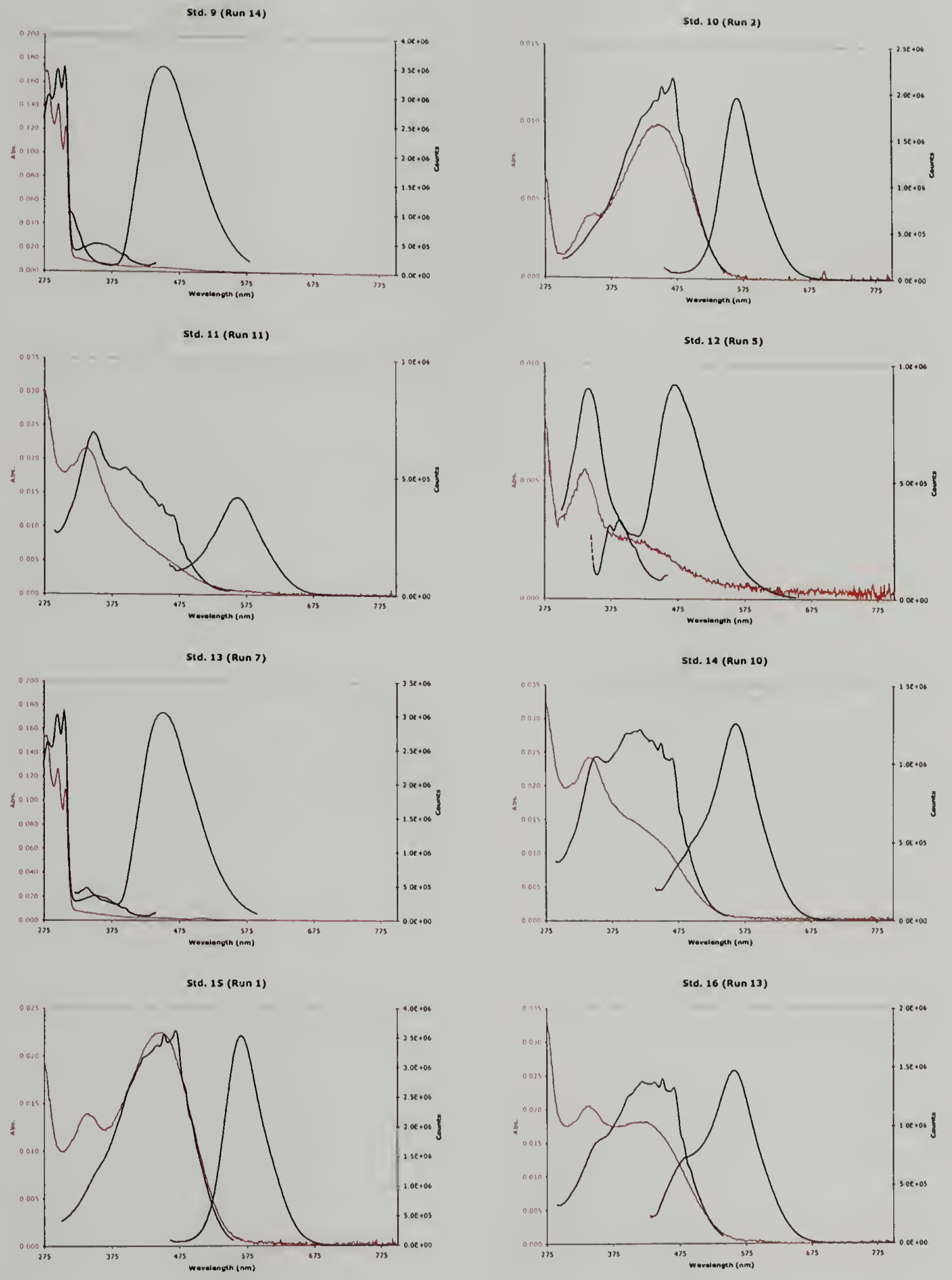

Figure 3.17 (continued).

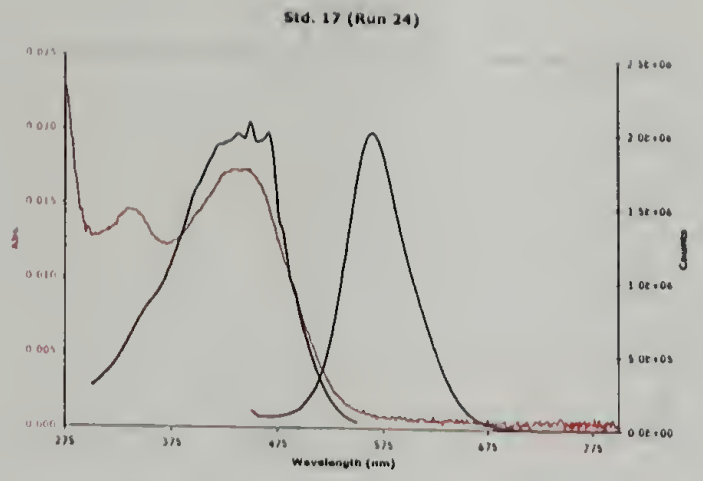

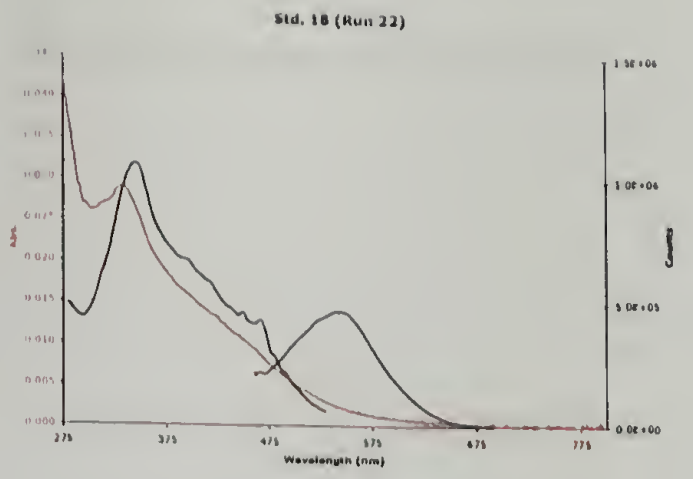

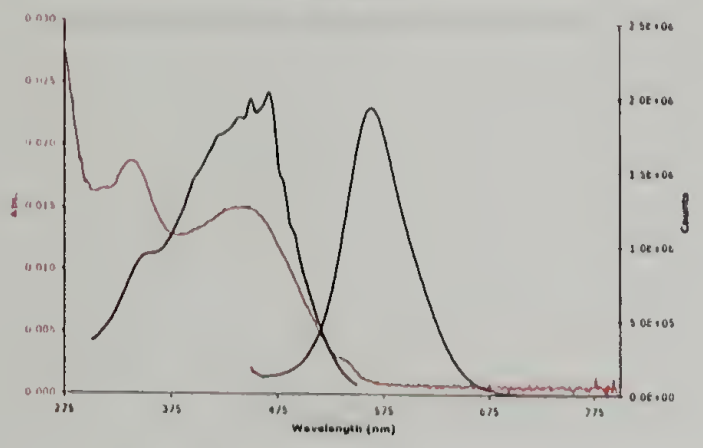

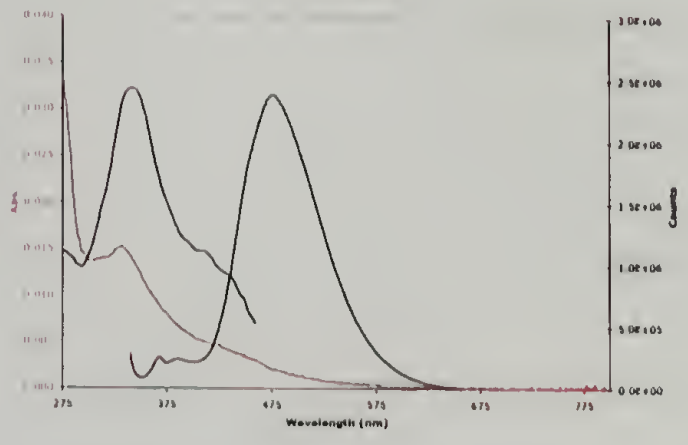

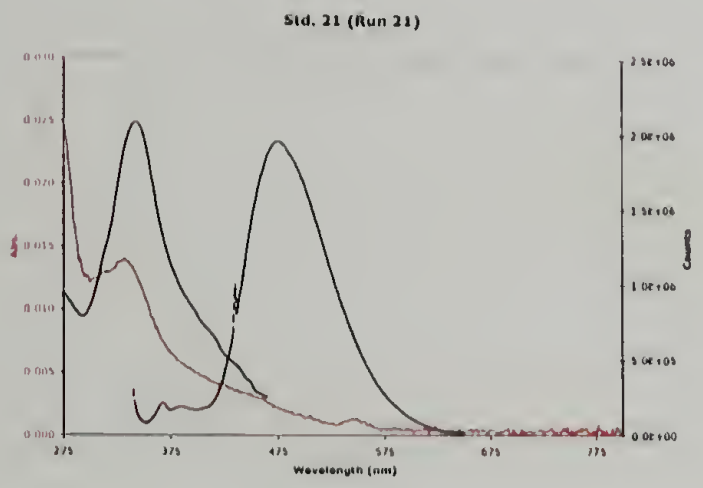

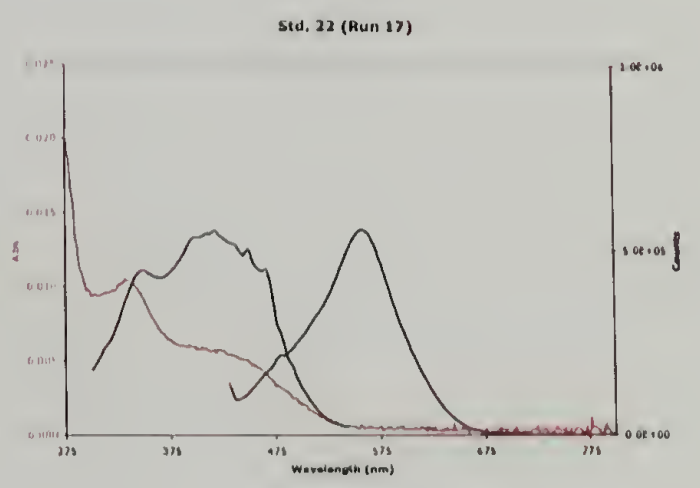

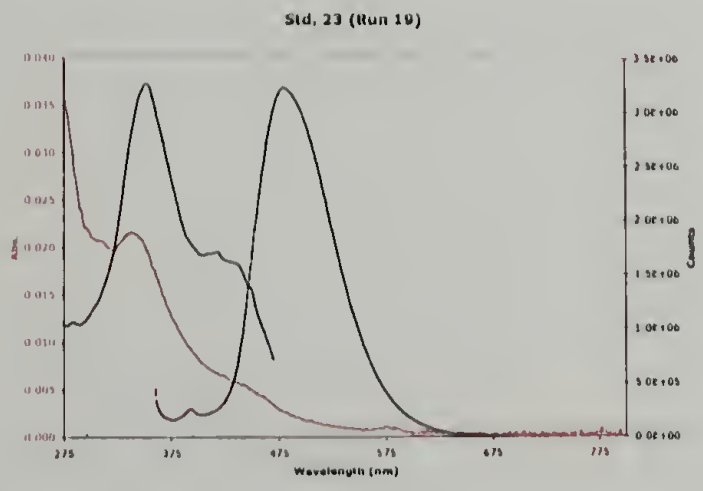

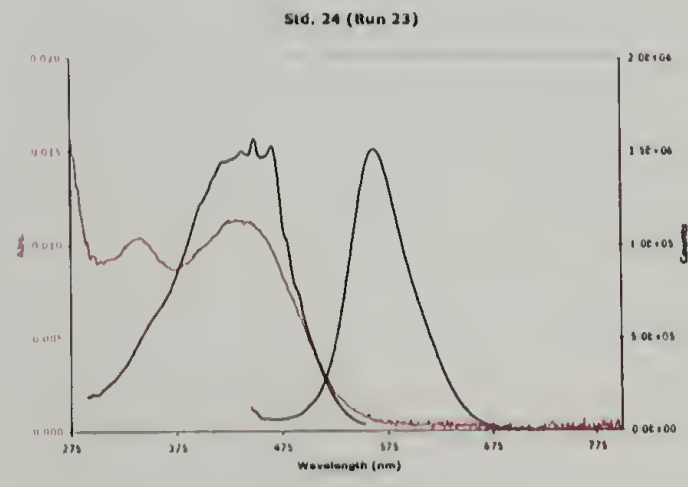

Figure 3.17 (continued).

Table 3.13. Spectral properties of dilute (Abs < 0.05) polymer solutions.

Std.	Run	λ_{max} (nm)	λ_F (nm)	FWHM (nm)[a]	Δ (eV)
1	16	307	461	91	1.35
2	4	338	487	91	1.12
3	12	338	484	94	1.11
4	8	448	572	65	0.60
5	6	307	516	115	1.64
6	9	335	480	96	1.12
7	3	335	482	88	1.13
8	15	425	566	68	0.73
9	14	306	462	95	1.37
10	2	445	571	63	0.61
11	11	337	558	88	1.46
12	5	335	479	91	1.11
13	7	306	462	96	1.37
14	10	430	554	91	0.65
15	1	447	571	68	0.60
16	13	420	549	122	0.69
17	24	441	569	69	0.63
18	22	333	534	113	1.40
19	20	442	567	70	0.62
20	18	414	486	90	0.44
21	21	332	486	93	1.18
22	17	419	551	97	0.71
23	19	426	491	85	0.39
24	23	439	569	69	0.65

[a]Full-width, half-maximum of the fluorescence band.

The half-normal plot of effects on emission in dilute solution (figure 3.18) is dramatically different from the half-normal plot for concentrated solution (figure 3.12). Addition of the Proton-Sponge (factor F) still has the greatest effect on the emission wavelength, but there are only two other significant effects, not eight – only the 3HT to 3TA ratio (A) and the catalyst ratio (B). Half-normal plots of the FWHM and Stokes shift (not shown) did not reveal any measurable effects on those two responses. The model equation for fluorescence emission maximum (in coded terms) is

$$\lambda_F = 515.75 + (16.37 \times A) + (12.29 \times B) - (30.96 \times F) \qquad (3.10)$$

Table 3.14. Absorption maxima for a series of regioregular oligo(dodecylthiophene)s synthesized by successive iodination/Suzuki-coupling reaction sequences.[52]

λ_{max} (nm)	oligo(3-dodecylthiophene)s
331	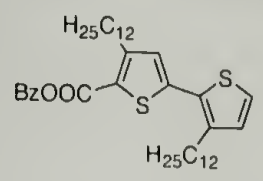
391	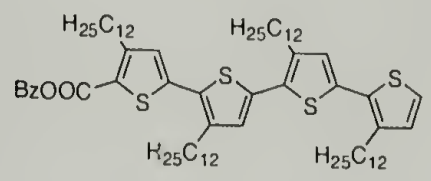
414	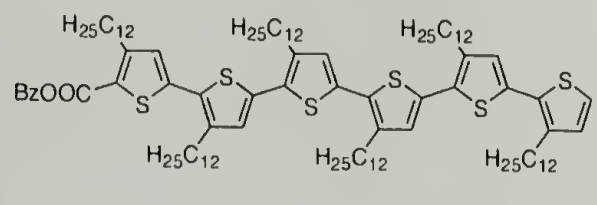
427	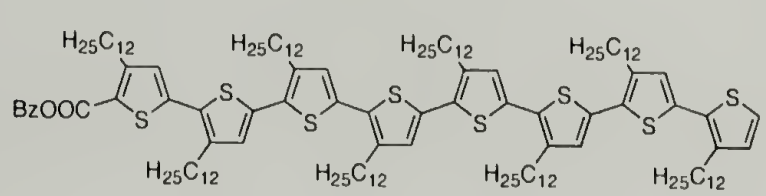
433	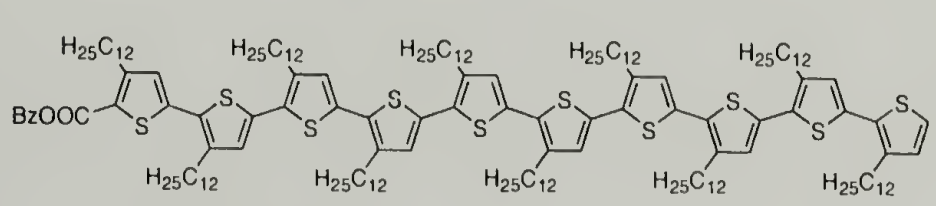

Again, there is a 99.99% chance that the fluorescence is significantly affected by one or more of the factors.

The effects of the three significant factors are plotted in figure 3.19. When measured in dilute solution, the emission maximum increases significantly when the 3HT to 3TA ratio is increased from 5 to 20, and decreases significantly when Proton-Sponge is added. The effect of the catalyst to monomer ratio was insignificant (the LSD bars overlap), confirmed by the F-test of term B in the ANOVA of the model. More replicates might show that there is a significant difference between the low and high catalyst levels on the fluorescence emission maxima in dilute solution, but it cannot be concluded from these data.

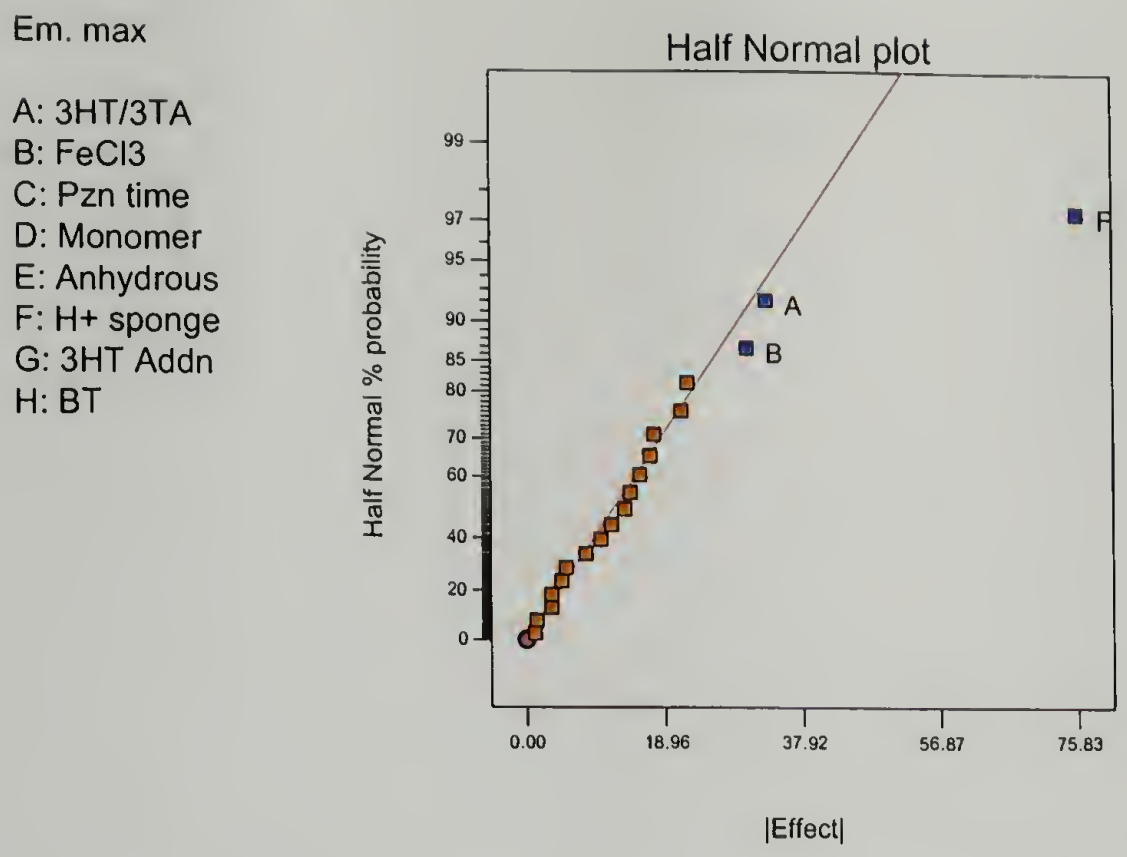

Figure 3.18. Half-normal plot of the effects of the factors in table 3.9 on the fluorescence maxima of polymers in dilute solution.

The diagnostic plots shown in figure 3.20 are similar to those for the measurements in high concentration shown in figure 3.14. Once again, there is an outlier (Run 16), but there was no extenuating circumstance to justify exclusion from the model.

3.4 Conclusions

Fluorescence measurements performed in both concentrated and dilute solution agree that a higher ratio of 3HT to 3TA increases the fluorescence emission maximum, an indicator of conjugation length. Similarly, addition of Proton-Sponge decreases the emission maximum. Increasing the catalyst to monomer ratio, using a slower monomer addition rate and a lower monomer concentration, and adding bithiophene increases the emission maximum in concentrated solution. These factors may cause the polymer to aggregate in concentrated solution.

Em. max

X = A: 3HT/3TA

Actual Factors
B: FeCl3 = 3
C: Pzn time = 15
D: Monomer = 0.13
E: Anhydrous = No
F: H+ sponge = No
G: 3HT Addn = 1.50
H: BT = No

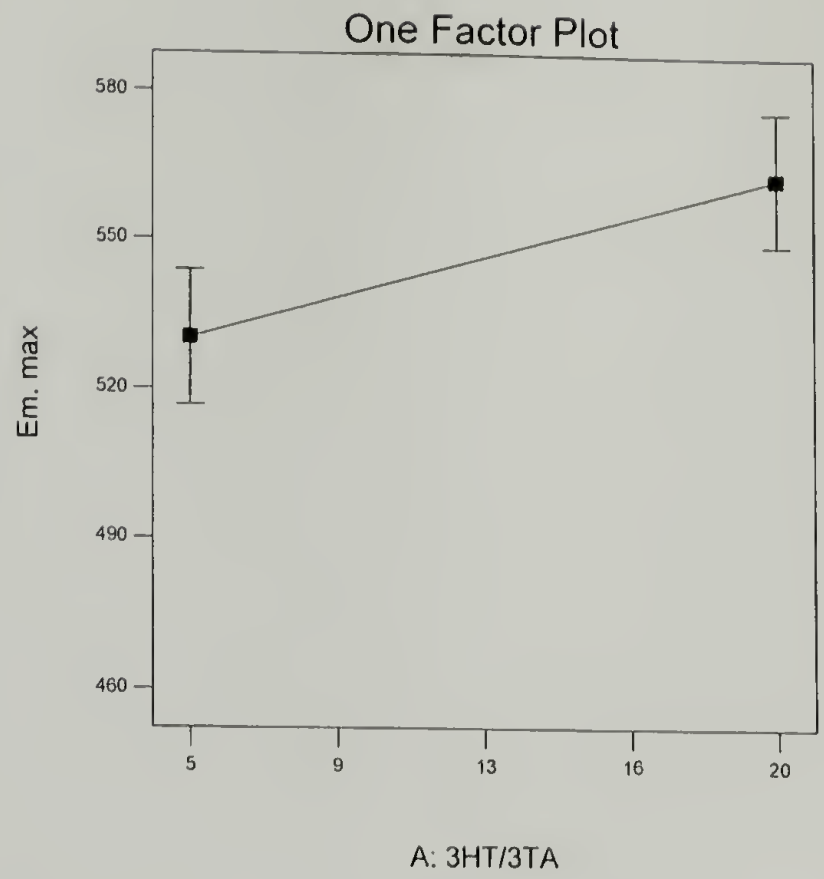

Em. max

X = B: FeCl3

Actual Factors
A: 3HT/3TA = 13
C: Pzn time = 15
D: Monomer = 0.13
E: Anhydrous = No
F: H+ sponge = No
G: 3HT Addn = 1.50
H: BT = No

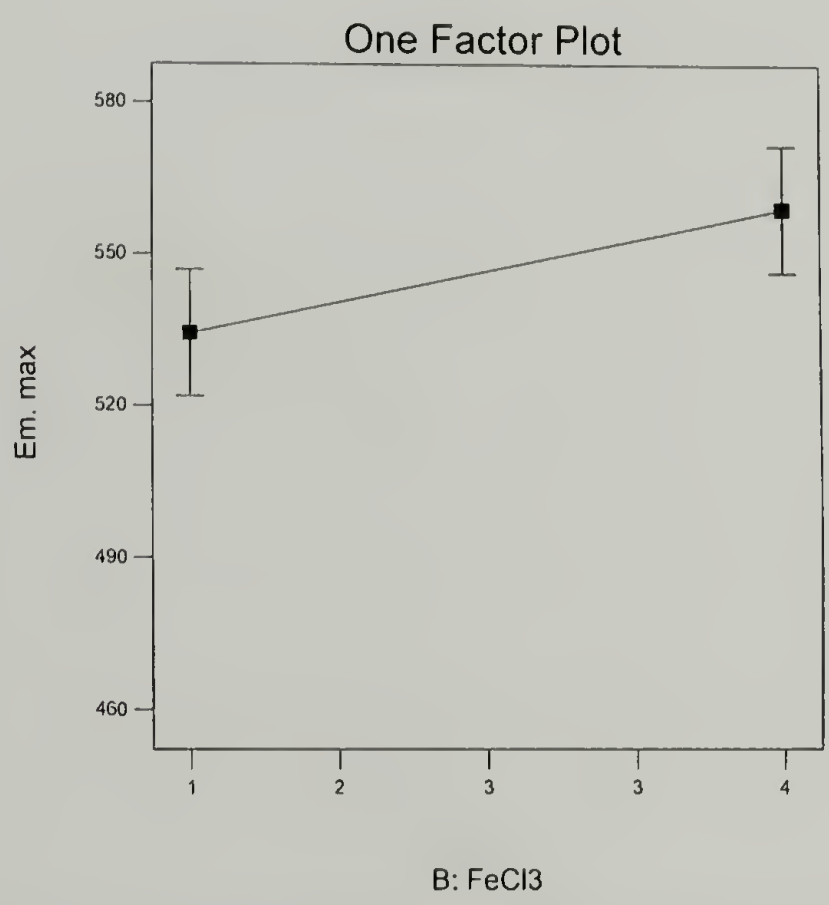

Figure 3.19. Main effects on polymerization detected in dilute solution.

Continued, next page.

Figure 3.19, continued.

Em. max

X = F: H+ sponge

Actual Factors
A: 3HT/3TA = 13
B: FeCl3 = 3
C: Pzn time = 15
D: Monomer = 0.13
E: Anhydrous = No
G: 3HT Addn = 1.50
H: BT = No

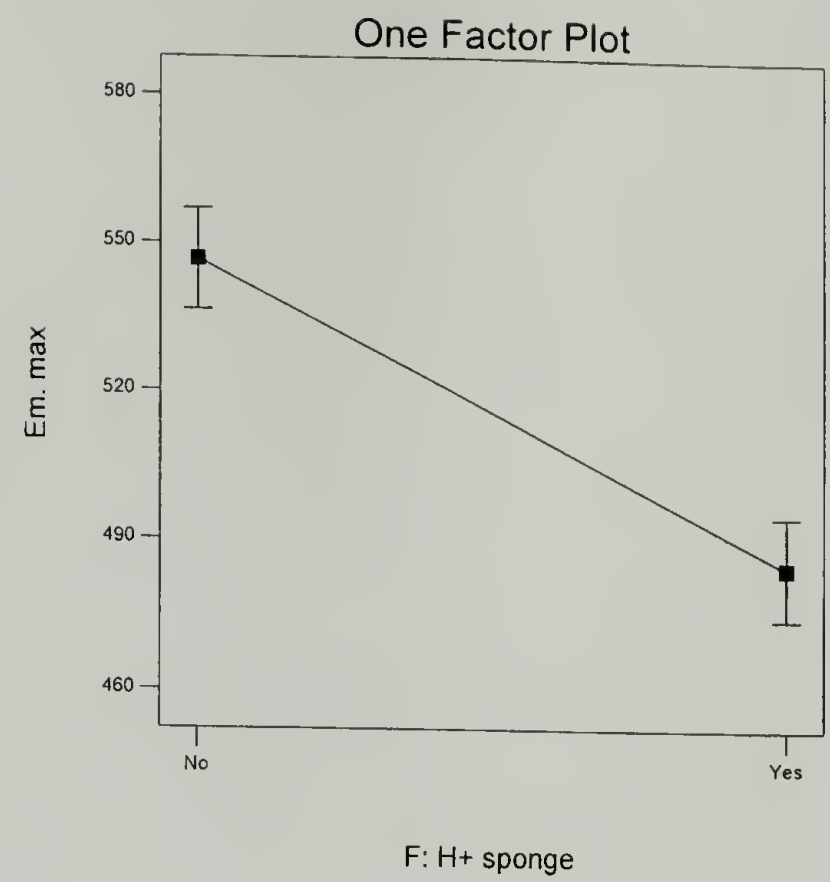

In the next chapter, polypeptides containing 3-thienylalanine will be copolymerized with 3-hexylthiophene with consideration of the factors that were shown to have a statistically significant effect on polymerization. The polypeptide will incorporate 3TA, a spacer, and biotin for binding experiments with streptavidin.

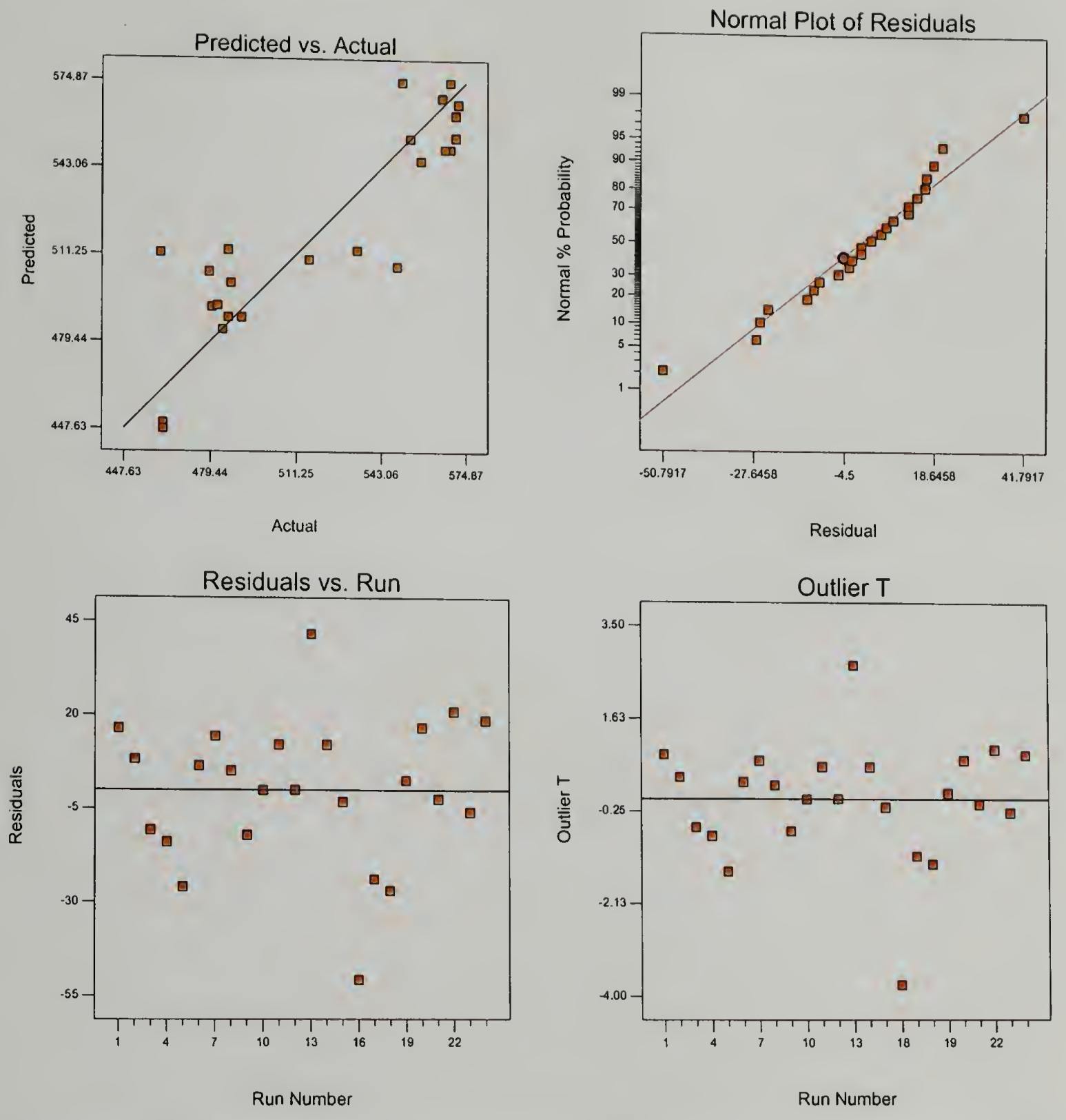

Figure 3.20. Model diagnostic plots for effects on fluorescence in dilute solution.

3.5 References

(1) Anderson, M. J.; Whitcomb, P. J. *DoE Simplified: Practical Tools for Effective Experimentation;* Productivity: Portland, OR, 2000.

(2) Shan, C. L. P.; Soares, J. B. P.; Penlidis, A. *J. Polym. Sci. Pol. Chem.* **2002,** *40,* 4426-4451.

(3) Hasenwinkle, D.; Jervis, E.; Kops, O.; Liu, C.; Lesnicki, G.; Haynes, C. A.; Kilburn, D. G. *Biotechnol. Bioeng.* **1997,** *55,* 854-863.

(4) Laakso, J.; Järvinen, H.; Skagerberg, B. *Synth. Met.* **1993,** *55,* 1204-1208.

(5) Lakowicz, J. *Principles of Fluorescence Spectroscopy;* Kluwer Academic/Plenum: New York, 2nd ed.; 1999.

(6) Jabłoński, A. *Z. Phys.* **1935,** *94,* 38-46.

(7) Haugland, R. P. *Handbook of Fluorescent Probes and Research Products;* Molecular Probes: Eugene, OR, 9th ed.; 2002.

(8) Barbarella, G.; Favaretto, L.; Sotgiu, G.; Antolini, L.; Gigli, G.; Cingolani, R.; Bongini, A. *Chem. Mat.* **2001,** *13,* 4112-4122.

(9) Barbarella, G.; Favaretto, L.; Sotgiu, G.; Zambianchi, M.; Bongini, A.; Arbizzani, C.; Mastragostino, M.; Anni, M.; Gigli, G.; Cingolani, R. *J. Am. Chem. Soc.* **2000,** *122,* 11971-11978.

(10) Barbarella, G. *Chem. Eur. J.* **2002,** *8,* 5072-5077.

(11) Barbarella, G.; Zambianchi, M.; Pudova, O.; Paladini, V.; Ventola, A.; Cipriani, F.; Gigli, G.; Cingolani, R.; Citro, G. *J. Am. Chem. Soc.* **2001,** *123,* 11600-11607.

(12) Sotgiu, G.; Zambianchi, M.; Barbarella, G.; Aruffo, F.; Cipriani, F.; Ventola, A. *J. Org. Chem.* **2003,** *68,* 1512-1520.

(13) Korri-Youssoufi, H.; Garnier, F.; Srivastava, P.; Godillot, P.; Yassar, A. *J. Am. Chem. Soc.* **1997,** *119,* 7388-7389.

(14) Lee, T. Y.; Shim, Y. B. *Anal. Chem.* **2001,** *73,* 5629-5632.

(15) Gaylord, B. S.; Heeger, A. J.; Bazan, G. C. *Proc. Natl. Acad. Sci. U.S.A.* **2002,** *99,* 10954-10957.

(16) Gaylord, B. S.; Heeger, A. J.; Bazan, G. C. *J. Am. Chem. Soc.* **2003,** *125,* 896-900.

(17) Liu, B.; Baudrey, S.; Jaeger, L.; Bazan, G. C. *J. Am. Chem. Soc.* **2004,** *126,* 4076-4077.

(18) Liu, B.; Bazan, G. C. *J. Am. Chem. Soc.* **2004,** *126,* 1942-1943.

(19) Ho, H. A.; Boissinot, M.; Bergeron, M. G.; Corbeil, G.; Doré, K.; Boudreau, D.; Leclerc, M. *Angew. Chem. Int. Ed.* **2002,** *41,* 1548-1551.

(20) Leclerc, M.; Ho, H. A.; Boissinot, M. Canadian Patent Application 2 442 860, 2002.

(21) Doré, K.; Dubus, S.; Ho, H. A.; Lévesque, I.; Brunette, M.; Corbeil, G.; Boissinot, M.; Boivin, G.; Bergeron, M. G.; Boudreau, D.; Leclerc, M. *J. Am. Chem. Soc.* **2004,** *126,* 4240-4244.

(22) Atherton, E.; Sheppard, R. C. *Solid Phase Peptide Synthesis: A Practical Approach;* IRL: Oxford, 1989.

(23) Schopf, G.; Koßmehl, G. *Adv. Polym. Sci.* **1997,** *129,* 1-166.

(24) Roncali, J.; Garreau, R.; Yassar, A.; Marque, P.; Garnier, F.; Lemaire, M. *J. Phys. Chem.* **1987,** *91,* 6706-6714.

(25) Sugimoto, R.; Taketa, S.; Gu, H. B.; Yoshino, K. *Chem. Express* **1986,** *1,* 635-638.

(26) Niemi, V. M.; Knuuttila, P.; Österholm, J. E.; Korvola, J. *Polymer* **1992,** *33,* 1559-1562.

(27) Olinga, T.; François, B. *Synth. Met.* **1995,** *69,* 297-298.

(28) McCullough, R. D.; Tristramnagle, S.; Williams, S. P.; Lowe, R. D.; Jayaraman, M. *J. Am. Chem. Soc.* **1993,** *115,* 4910-4911.

(29) Chen, T. A.; Rieke, R. D. *J. Am. Chem. Soc.* **1992,** *114,* 10087-10088.

(30) McCullough, R. D. *Adv. Mater.* **1998,** *10,* 93-116.

(31) Andersson, M. R.; Selse, D.; Berggren, M.; Järvinen, H.; Hjertberg, T.; Inganäs, O.; Wennerström, O.; Österholm, J. E. *Macromolecules* **1994,** *27,* 6503-6506.

(32) Bizzarri, P. C.; Andreani, F.; Della Casa, C.; Lanzi, M.; Salatelli, E. *Synth. Met.* **1995,** *75,* 141-147.

(33) Qiao, X. Y.; Wang, X. H.; Zhao, X. J.; Liu, J.; Mo, Z. S. *Synth. Met.* **2000,** *114,* 261-265.

(34) Della Casa, C.; Andreani, F.; Bizzarri, P. C.; Salatelli, E. *J. Mater. Chem.* **1994,** *4,* 1035-1039.

(35) Maior, R. M. S.; Hinkelmann, K.; Eckert, H.; Wudl, F. *Macromolecules* **1990,** *23,* 1268-1279.

(36) Della Casa, C.; Salatelli, E.; Andreani, F.; Bizzarri, P. C. *Makromol. Chem., Macromol. Symp.* **1992,** *59,* 233-246.

(37) Gallazzi, M. C.; Bertarelli, C.; Montoneri, E. *Synth. Met.* **2002,** *128,* 91-95.

(38) Staab, H. A.; Saupe, T. *Angew. Chem. Int. Ed.* **1988,** *27,* 865-879.

(39) Brzeziński, B.; Grech, E.; Malarski, Z.; Sobczyk, L. *J. Chem. Soc., Perkin Trans. 2* **1991,** 857-859.

(40) Barbarella, G.; Zambianchi, M.; DiToro, R.; Colonna, M.; Iarossi, D.; Goldoni, F.; Bongini, A. *J. Org. Chem.* **1996,** *61,* 8285-8292.

(41) Yen, W.; Chan, C.-C.; Jing, T.; Jang, G.-W.; Hsueh, K. F. *Chem. Mat.* **1991,** *3,* 888-897.

(42) Welzel, H. P.; Koßmehl, G.; Engelmann, G.; Hunnius, W. D.; Plieth, W. *Electrochim. Acta* **1999,** *44,* 1827-1832.

(43) Waltman, R. J.; Bargon, J.; Diaz, A. F. *J. Phys. Chem.* **1983,** *87,* 1459-1463.

(44) Yen, W.; Jing, T. *Macromolecules* **1993,** *26,* 457-463.

(45) Ng, S. C.; Ma, Y. F.; Chan, H. S. O.; Dou, Z. L. *Synth. Met.* **1999,** *100,* 269-277.

(46) Andreani, F.; Salatelli, E.; Lanzi, M. *Polymer* **1996,** *37,* 661-665.

(47) Anderson, M. J.; Whitcomb, P. J. "How to save runs, yet reveal breakthrough interactions, by doing only a semifoldover on medium-resolution screening designs", Technical Report, Stat-Ease, Inc.,.

(48) Izumi, T.; Kobashi, S.; Takimiya, K.; Aso, Y.; Otsubo, T. *J. Am. Chem. Soc.* **2003,** *125,* 5286-5287.

(49) Kilbinger, A. F. M.; Schenning, A.; Goldoni, F.; Feast, W. J.; Meijer, E. W. *J. Am. Chem. Soc.* **2000,** *122,* 1820-1821.

(50) Langeveld-Voss, B. M. W.; Janssen, R. A. J.; Christiaans, M. P. T.; Meskers, S. C. J.; Dekkers, H.; Meijer, E. W. *J. Am. Chem. Soc.* **1996,** *118,* 4908-4909.

(51) Langeveld-Voss, B. M. W.; Janssen, R. A. J.; Meijer, E. W. *J. Mol. Struct.* **2000,** *521,* 285-301.

(52) Kirschbaum, T.; Azumi, R.; Mena-Osteritz, E.; Bäuerle, P. *New J. Chem.* **1999,** *23,* 241-250.

CHAPTER 4

RESIN-MOUNTED COPOLYMERIZATION AND PURIFICATION OF POLYPEPTIDE/POLY(3-HEXYLTHIOPHENE) GRAFTS

4.1 Introduction

Using the HMBA solid phase linker chosen for its stability under oxidative polymerization conditions (Chapter 2), and the reaction conditions which result in poly(3-hexylthiophene)s with high fluorescence emissions (Chapter 3), copolymerization of 3-hexylthiophene (3HT) and polypeptides was performed next, as described in this chapter. This required consideration of the design of the polypeptide, and the design of the purification scheme. The reagents used in the solid phase peptide synthesis, and the means of monitoring of the progress of the couplings, needed to be selected as well.

4.1.1 Polypeptide design, copolymerization, and purification

A polypeptide for copolymerization experiments needed to meet three criteria. First, it should contain an amino acid, or amino acid sequence, that could be easily detected, in order to confirm that the amide backbone of the peptide was stable under the polymerization conditions. Fluorescence or radiolabeling are commonly used for sensitive detection. Second, the polypeptide should not hinder copolymerization by steric constraints imposed by bulky amino acids close to the thiophene moiety. Practically, this could be accomplished by introducing a spacer between the 3-thienylalanine (3TA) residue and the detectable amino acid.

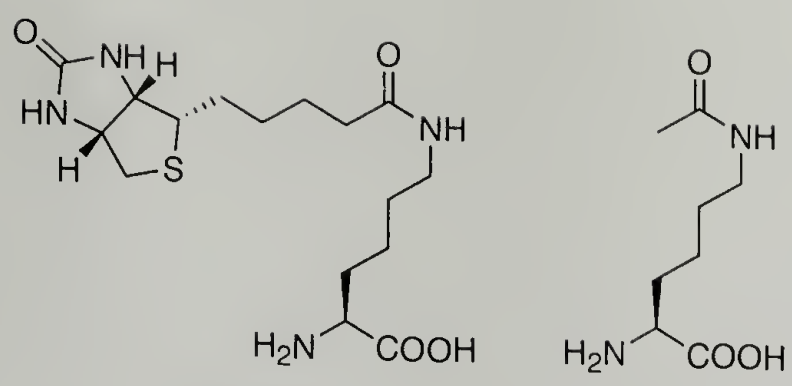

Figure 4.1. *N*-ε-(*d*-biotinyl)-L-lysine (Biocytin) and *N*-ε-acetyl-L-lysine (LysAc) residues used for polypeptide detection.

Finally, the polypeptide should be relatively short and incorporate inexpensive amino acids to reduce the time and cost of synthesis.

These three criteria are met by the six-residue polypeptide

3TAGlyGlyGlyXxxGly

where Xxx corresponds to either *N*-ε-(*d*-biotinyl)-L-lysine (Biocytin) or *N*-ε-acetyl-L-lysine (LysAc) (figure 4.1). Biocytin provides an extremely sensitive means of secondary detection via formation of biotin-streptavidin binding complexes.[1] The flexibility of this system results from the variety of fluorophores which can be attached to streptavidin,[2] while the high binding constant provides sensitivity at low concentrations (see section 4.1.3). LysAc was chosen as a control to determine the degree of non-specific binding of the copolymer to streptavidin. Finally, a triglycine spacer is used to separate the thiophene-containing 3TA residue from the detectable biocytin or nonbinding LysAc residue. Four of the six residues in the sequence are glycine, which is inexpensive relative to other amino acids.

As described in section 2.1, a solid phase resin should simplify purification by providing a means of separating the fraction of peptide-containing copolymer from the much larger fraction of poly(3-hexylthiophene) homopolymer. The resin-based synthesis and purification scheme is shown in figure 4.2. The HMBA resin

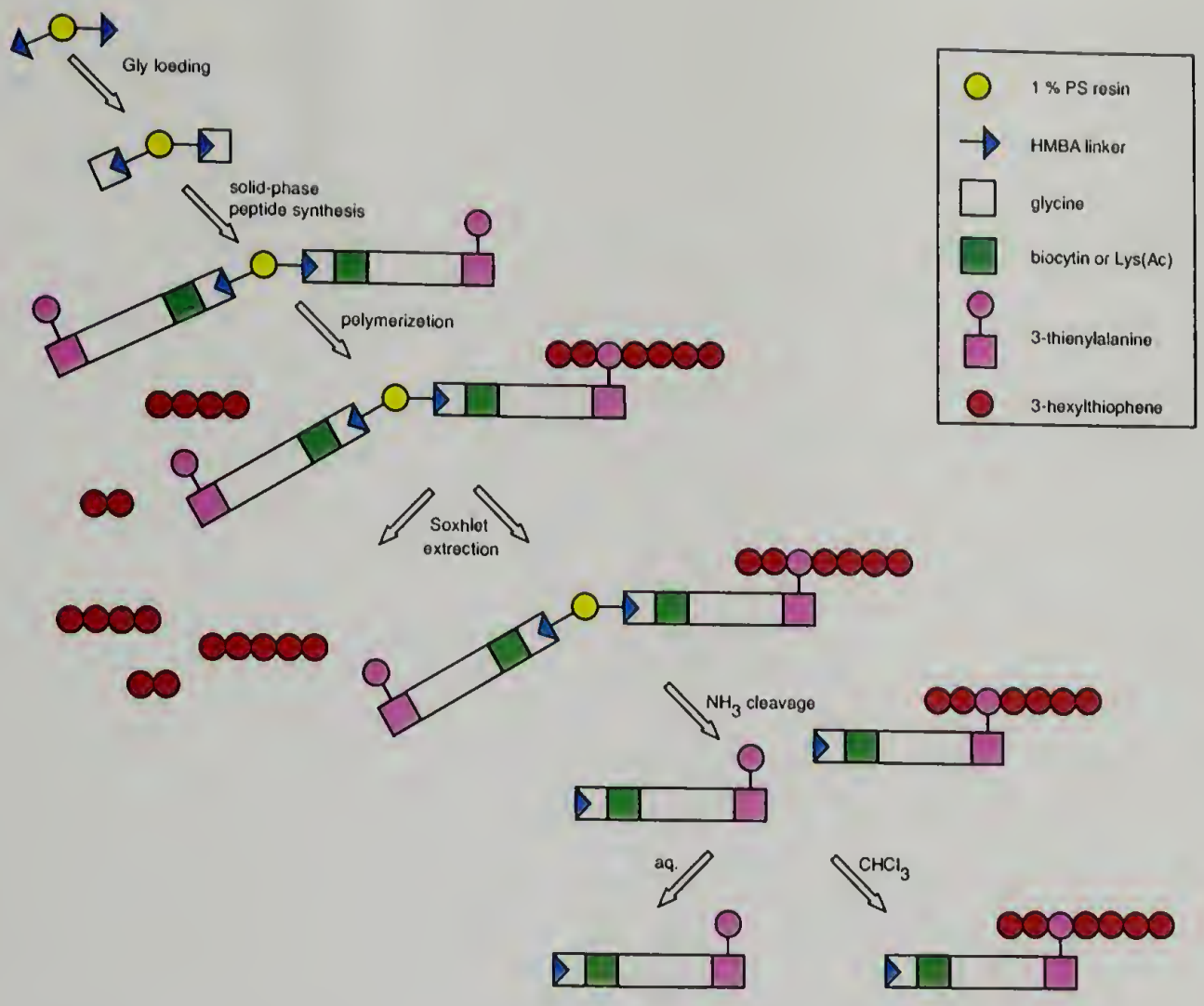

Figure 4.2. Strategy for synthesizing and purifying a graft copolymer of a peptide and 3-hexylthiophene.

is loaded with glycine, followed by solid phase synthesis of the rest of the peptide. After 3HT polymerization, the beads are exhaustively Soxhlet extracted with THF and chloroform, removing any poly(3-hexylthiophene) not covalently linked to the resin via the peptide. Following cleavage from the resin, the mixture can be extracted into aqueous and organic fractions to separate unreacted peptide from the peptide/poly(3-hexylthiophene) copolymer.

4.1.2 Solid phase peptide synthesis

As described in Chapter 2, HMBA resin was selected because of the linker stability under oxidative polymerization conditions. The other major components in

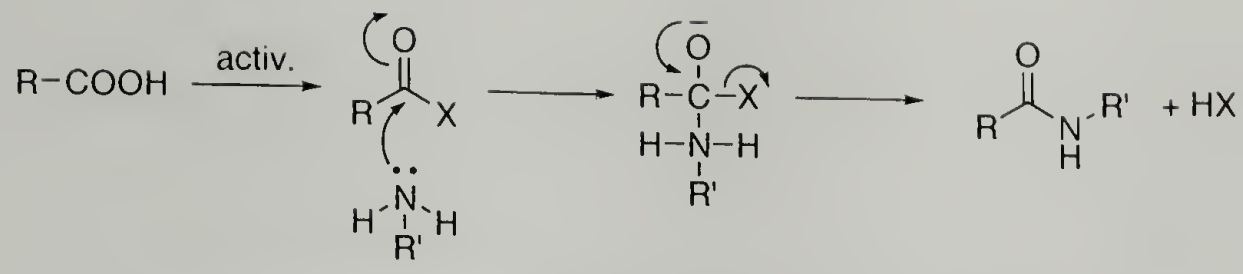

Figure 4.3. Activation and coupling of amino acids.

solid phase peptide synthesis are the coupling reagents and the amino acid protecting groups.

4.1.2.1 Coupling reagents

Carboxylic acids are insufficiently electrophilic to acylate the amino acid. But, by replacing the hydroxyl group with an electron-withdrawing group, nucleophilic attack of the carbonyl carbon by the amino group is possible (figure 4.3).[3]

The use of *N,N'*-dicyclohexylcarbodiimide (DCC) as a method for forming peptide bonds was first proposed by Sheehan and Hess in 1955,[4,5] and is one of the most popular coupling agents used today. Silverstein and coworkers elucidated the mechanism of DCC coupling in a trio of papers published in 1966.[6–8] As shown in figure 4.4, an *O*-acylisourea is formed upon addition of the reagent to the N-protected amino acid. A second amino compound can then react to make an amide bond, or a symmetrical anhydride can be formed. The symmetrical anhydride can then acylate the amine. In both cases, dicyclohexylurea is produced. An unreactive side product, the *N*-acylisourea, can result from *O*- to *N*-acyl migration. In solid-phase synthesis, the similarly reactive *N,N'*-diisopropylcarbodiimide (DIC) is preferred over DCC, because of the improved solubility of diisopropylurea.[3]

In solution, carbodiimide couplings typically are performed by adding one equivalent of coupling reagent to a solution containing one equivalent each of the two components to be linked by a peptide bond. In this "coupling reagent

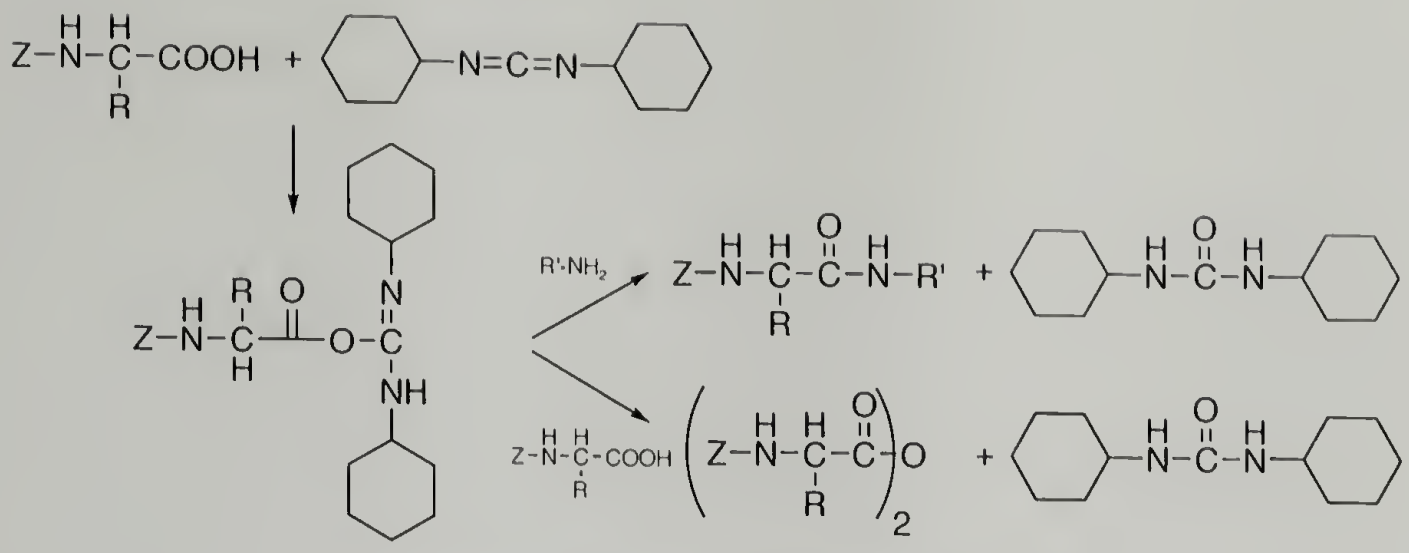

Figure 4.4. Peptide coupling using DCC.

mode," the *O*-acylisourea reacts with unreacted amino acid, forming symmetrical anhydrides, more rapidly than it reacts with amines, forming amide bonds. When predominantly symmetrical anhydrides are made, nearly half of the coupling reagent is left unreacted. Then, as the symmetrical anhydride reacts with the amines, one half of the anhydride is freed and reacts with the remaining coupling reagent. Therefore, the DCC and the *O*-acylisourea is consumed completely, but only gradually. The reaction rate is slower in solid phase synthesis than in solution, because of the limited accessibility of the amines on the resin. As a result, the *O*-acylisourea has a longer lifetime, and more time to rearrange to form the unreactive *N*-acylisourea.[3]

Alternatively, couplings can be performed in "symmetrical anhydride mode." By adding one equivalent of coupling reagent to two equivalents of amino acid, the coupling agent is completely consumed to form the symmetrical anhydride. The anhydride reacts rapidly, shortening the lifetime of the *O*-acylisourea, reducing the amount of *N*-acylisourea formed. The disadvantage of this method is the need for twice as much protected amino acid, which may be costly.[3]

Formation of the unreactive *N*-acylurea can also be suppressed by addition of a second nucleophile. König and Geiger reported that 1-hydroxybenzotriazole

(HOBt) reacts with an *O*-acylisourea to form an *O*-acyl-1-hydroxybenzotriazole, which is an even stronger acylating agent than the symmetric anhydride.[9]

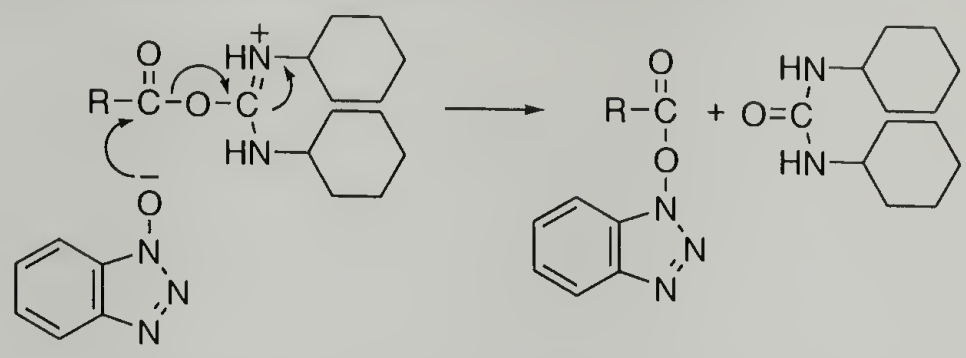

The HOBt is regenerated when it reacts with the free amine, so only a catalytic amount is needed. Additionally, since HOBt is a weak acid, it reduces deprotonation of the chiral carbon proton, suppressing racemization during the coupling. The reaction of HOBt with the *O*-acylisourea is faster in the presence of a tertiary amine, probably due to base-catalyzed transesterification. Using a sterically hindered tertiary base, such as *N,N*-diisopropylethylamine (DIPEA), rather than triethylamine, results in lower degrees of racemization at the amino acid chiral center.[3]

Since the introduction of DIC in peptide synthesis, newer coupling reagents that also avoid racemization and side reactions have been developed. These reagents incorporate either phosphonium or aminium groups. In 1975, Castro et al. described generation of an oxybenzotriazole (OBt) in situ using (benzotriazol-1-yloxy)-tris(dimethylamino)phosphonium hexafluorophosphate (BOP).[10]

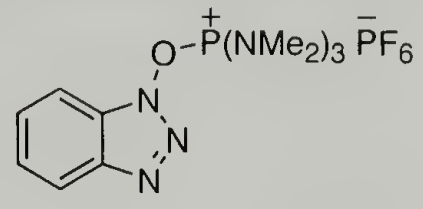

Couplings performed with BOP are fast with low levels of racemization. However, the byproduct of the reaction, hexamethylphosphoramide, is highly carcinogenic. A second generation coupling agent, PyBOP, where the dimethylamino groups of

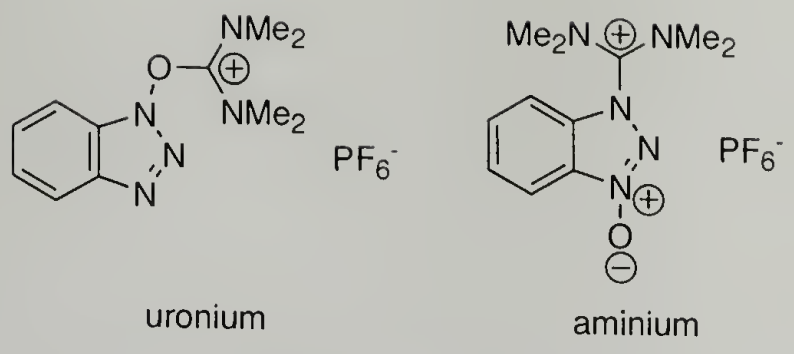

Figure 4.5. Two isomers of "HBTU".

BOP are replaced by pyrrolidino groups, is safer and yields coupling rates even faster than BOP while maintaining low levels of racemization.[11,12]

Aminium-based coupling reagents[13] such as *O*-(benzotriazol-1-yl)-*N*,*N*,*N*′,*N*′-tetramethyluronium hexafluorophosphate (HBTU) are very reactive, requiring as little as six minutes for completion of coupling. HBTU was first synthesized by Dourtoglou et al. in 1978, who assigned the uronium structure shown in figure 4.5 (left).[14,15] Later, Carpino synthesized the similar compound 1-hydroxy-7-azabenzotriazole (HATU), assigning the same uronium structure despite noting inconsistencies in the NMR spectroscopic data.[16] However, X-ray crystallography and solid-state NMR spectroscopy results reported the next year indicated that the true structures were the aminium isomers, not the uronium isomers – but the popularity of HBTU as a coupling reagent meant the name stuck. More recently, Carpino et al. did synthesize the uronium isomer of "HBTU" under different reaction conditions, and found increased reactivity of the uronium isomer compared with the aminium isomer.[17]

4.1.2.2 Fmoc protecting group

A solid phase peptide synthesis protecting group should be stable under coupling conditions, but also readily removed under orthogonal deprotecting conditions. In 1932, Bergmann and Zervas introduced the carbobenzoxy group (Cbz, or simply Z), which undergoes simultaneous fission and decarboxylation during

catalytic hydrogenation.[18]

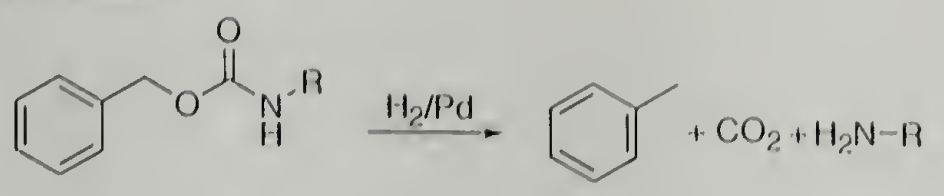

The synthesis of more complex peptides, often with a variety of blocked side chain functionalities, resulted in the development of more sophisticated protecting groups that required less rigorous cleavage conditions while maintaining orthogonality to the coupling conditions and the side chain protecting groups. The 9-fluoromethoxycarbonyl (Fmoc) amino protecting group, developed by Carpino and Han, combines acid resistance with sensitivity to weak bases.[19,20]

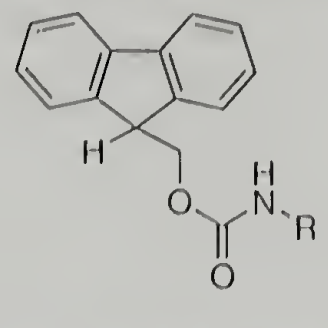

Fmoc was shown to be stable in the presence of trifluoroacetic acid, HBr/acetic acid, and HBr/nitromethane for two days, and refluxing 0.9 N HCl/acetic acid for ten hours.[21] Therefore, Fmoc was chosen for protection of the peptides which would be copolymerized with 3-hexylthiophene in the presence of ferric chloride.

4.1.3 Biotin and avidin

Two molecules, biotin and avidin, have made an incalculable impact on molecular biology by providing a nearly-universal solution to labeling biomolecules, while minimally affecting their structure and function. The biotin-avidin binding system is characterized by its strength: the dissociation constant for the biotin-avidin complex is on the order of 10^{-15} M, or about 21 kcal/mol. This is comparable to metal chelate bond strengths, and is extraordinarily high for a non-covalent interaction between a protein and a ligand.[1]

The toxicity of raw egg-white was first reported in 1916, although the toxic compound itself was not identified.[22] Vitamin H, later identified as biotin, was isolated in the 1930s,[23] and implicated avidin as the molecule responsible for raw egg-white toxicity.[24] Two decades later, the coenzyme function of covalently bound biotin in the biosynthesis of fatty acids was discovered simultaneously by Lynen et al.* and by Wakil and Gibson.[25,26] This discovery led to renewed interest in avidin, as well as the analogous protein isolated from *Streptomyces avidinii*, streptavidin.[27] A 1975 review included dissociation constants for a number of biotin derivatives and evidence for the tetrameric structure of avidin.[28] One of the first examples of an application of the biotin-avidin system to a biomolecular problem was work performed by Davidson et al. By attaching biotin to tRNA, hybridizing the tRNA with the complementary double-stranded DNA, and then labeling the tRNA with an electron-dense ferritin-avidin complex, the locations at which the tRNA hybridizes with its complementary DNA could be visualized by electron microscopy.[29] By 1990, hundreds of applications of the biotin-avidin complex were described in the literature.[1]

The utility of the biotin-avidin system in the context of a conducting polymer biosensor was recognized in the early 1990s. Biotinylation of electropolymerized poly(thiophene) films with pendant hydroxyl groups, followed by addition of streptavidin, produced a generic surface to which biotinylated biomolecules could be attached.[30] Streptavidin conjugated alkaline phosphatase was immobilized on such a poly(thiophene) surface while retaining its activity, catalyzing the conversion of an organophosphorus substrate to a chemiluminescent product. However, in this example, the poly(thiophene) component acted only as an anchoring sub-

---

*Feodor Lynen would share the 1964 Nobel Prize in Physiology or Medicine with Konrad Bloch "for their discoveries concerning the mechanism and regulation of the cholesterol and fatty acid metabolism."

strate; its electrochemical properties were not exploited.[31] Spectroscopic detection of avidin binding to biotinylated poly(thiophene)s in solution was reported by Faïd and Leclerc in 1996, where avidin binding resulted in a hypsochromic shift of 150 nm, reflecting a deviation from coplanarity caused by binding of the 68 000 Dalton protein.[32] Later work demonstrated an electrochemical oxidation peak shift of +200 mV resulting from avidin binding.[33] Similar results have been shown for *N*-substituted poly(pyrrole)s,[34,35] and used to construct DNA arrays.[36]

4.2 Experimental

4.2.1 Materials and methods

N,*N*-Diisopropylcarbodiimide (DIC, 99%), Fmoc-glycine (Fmoc-Gly), *t*-amyl alcohol (99%), *N*,*N*-diisopropylethylamine (DIPEA, 99.5%), *N*-ε-(+)-biotinyl-L-lysine (biocytin, 99%), ferric chloride (anhydrous, 99.99+%), and ammonia (*ca.* 7 N in methyl alcohol) were obtained from Aldrich (Milwaukee, WI) and used as received. Sodium citrate dihydrate (99%, A.C.S. reagent) and sodium chloride (99%, A.C.S. reagent) were obtained from Mallinckrodt Baker (Phillipsburg, NJ) and used as received. Benzotriazolyloxy-tris(pyrrolidino)-phosphonium hexafluorophosphate (PyBOP, >97%, *purum.*) and 2-(*1H*-benzotriazol-1-yl)-1,1,3,3-tetramethyluronium hexafluorophosphate (HBTU, *purum.*, 97%), were obtained from Fluka (Buchs, Switzerland) and used as received. 1-Hydroxybenzotriazole (HOBt, <5% water) was obtained from Aldrich and dried *in vacuo* over phosphorous pentoxide before use. *N*-α-Fmoc-3-thienyl-L-alanine (Fmoc-3TA, 98%) was obtained from PepTech Corp. (Burlington, MA) and used as received. *N*-α-Fmoc-*N*-ε-acetyl-L-lysine (Fmoc-LysAc, ≥98%) and *N*-α-Fmoc-*N*-ε-(*d*-biotinyl)-L-lysine (Fmoc-Bio, >95%) were obtained from Anaspec (San Jose, CA) and used without further purification. Avidin and streptavidin were purchased from Molecular Probes (Eugene, OR).

Phosphate buffered saline (PBS) buffer was prepared by dissolving 2.6 g (1.9 mmol) potassium phosphate (monobasic), 1.15 g (8.1 mmol) sodium phosphate (anhydrous), and 8.75 g (150 mmol) sodium chloride in 800 ml deionized water, adjusting the pH to 7.2 with sodium hydroxide, and adjusting the final volume to 1000 ml. Standard saline citrate (SSC) buffer was prepared by dissolving 8.75 g (0.15 mol) sodium chloride and 4.4 g (0.015 mol) sodium citrate dihydrate in 800 ml deionized water, adjusting the pH to 7.2 with sodium hydroxide, and adjusting the final volume to 1000 ml.

LC-MS/MS data was obtained at the Caltech Mass Spectroscopy facility using a LCQ Classic ion trap mass spectrometer and a Surveyor HPLC (ThermoFinnigan, San Jose). Separation was achieved using a Michrom Magic C18 5 μm 200 Å column (Michrom BioResources, Auburn, CA). The mobile phase was a gradient increasing from 2% acetonitrile/ 98% water/ 0.1 M acetic acid to 90% acetonitrile/10% water/ 0.1 M acetic acid over 30 minutes. NMR spectra were recorded on a 300 MHz Varian Mercury spectrometer in chloroform-d, dimethyl sulfoxide-d_6, or methanol-d_4. Fluorescence emission spectra were collected with a QuantaMaster Steady State Fluorimeter (Photon Technology International, Ontario, Canada) equipped with a xenon lamp, 5 nm excitation and emission slits, and an Model 814 photomultiplier tube in photon counting mode. Solutions were filtered through a Pall Life Sciences (East Hills, NY) 0.2 μm membrane Acrodisc syringe filter prior to measurements.

4.2.2 Solid phase peptide synthesis

Peptide coupling reactions using PyBOP were performed according to standard procedures[37] using the following sequence:

0. Prewash

    (a) Wash with DMF (1 min, 5×).

1. Deprotection

    (a) Add 20% piperidine in DMF (3 min, 1×).

    (b) Drain and repeat (7 min, 1×).

    (c) Wash with DMF (1 min, 10×).

2. Reference

    (a) Remove resin sample for Step 4.

3. Acylation

    (a) Dissolve 1.1 equivalents of Fmoc-aa in DMF (5 ml/g amino acid) and add to resin.

    (b) Add 1.1 equivalents of 1 M PyBOP solution, 2.2 equivalents of DIPEA, and 1.1 equivalents of 0.5 M HOBt solution to the resin.

    (c) Agitate with bubbling argon (30 min).

4. Test

    (a) Remove resin sample for Kaiser test.

    (b) Continue agitation (30 min).

5. Wash

    (a) Wash with DMF (1 min, 10×).

6. Proceed to Step 1, or store overnight and proceed to Step 0.

4.2.3 Copolymerization and purification

Copolymerization and workup typically proceeded as follows:

1. Polymerization in a 8-dram vial under argon:

reagent	mmol	mass (mg)
resin	varies	100
3HT	0.20	33.7
$FeCl_3$	0.80	129.8

(a) Charge vial with:

(b) Dissolve monomer in 4 ml $CHCl_3$, addition rate 0.5 ml/hr.

(c) Total reaction time: eight hours.

2. Precipitate into methanol, transfer into tared Soxhlet thimble.

3. Soxhlet extraction with:

   (a) methanol

   (b) acetone

   (c) THF

   (d) acetone

   (e) methanol

4. Dry over P_2O_5.

5. Deprotect in 20% piperidine/DMF (3+7 minutes).

6. Wash resin (1 minute each):

   (a) 10× DMF

   (b) 3× *t*-amyl alcohol

   (c) 3× acetic acid

   (d) 3× *t*-amyl alcohol

   (e) 3× ether

7. Dry over P_2O_5.

8. Reswell in a minimum of DMF and transfer to a roundbottom flask equipped with a stirbar.

9. Stir overnight over cold NH_3/MeOH.

10. Cool, filter, wash with MeOH, combine fractions.

11. Concentrate, redissolve in chloroform, wash with water, dry with magnesium sulfate.

12. Concentrate and dry over P_2O_5.

4.3 Results and Discussion

4.3.1 Solid phase synthesis

4.3.1.1 Choice of coupling reagent

The acetylated lysine and biotinylated lysine side chains had a dramatic effect on the coupling reaction rate. Coupling either Fmoc-LysAc or Fmoc-Bio to glycine-loaded HMBA resin using DIC was complete within an hour. However, after deprotection, adding the next Fmoc-glycine was much slower. The couplings were not complete after reacting overnight, and required a second addition of the reagents and another overnight reaction before coupling was complete. A more reactive coupling reagent, PyBOP, was tried, but this still required two additions of reagents. However, by using HBTU, the coupling was complete after running overnight with a single addition of reagents. As the three remaining amino acids were coupled – two glycines and 3-thienylalanine – the reaction rates seemed to increase, but were still run overnight to ensure complete coupling. This apparent increase in reaction rates as the reaction took place further from the bulky LysAc or Bio supports the conclusion that steric constraints were hindering access to the site of amide bond formation.

4.3.1.2 Purity and sequence using LC-MS/MS

Electrospray ionization (ESI) mass spectroscopy was first described by John B. Fenn in 1988, for which he received the 2002 Nobel Prize in Chemistry.[1] ESI is a gentle ionization technique which minimizes fragmentation of the sample molecule. As a result, it is possible to observe the ions corresponding to components in a mixture. In a tandem (MS/MS) spectrometer, ions of a particular mass can then be selected and fragmented in a second analyzer. In the case of peptides, these fragments can be used to deduce the structure and sequence of the peptide.[38] Introducing a separation method, such as gas or liquid chromatography, before the mass spectroscopy analysis results in a so-called "hyphenated" technique, enhancing the analysis.

Peptide structural determination is based upon the fragmentation of the polyamide backbone. As shown in figure 4.6, peptides can fragment at three different places in the backbone, resulting in ions which retain the amino-terminal (a, b, c) or the carboxylic acid-terminal (x, y, z). The double primes on the c and y ions correspond to the two additional hydrogen atoms on those fragments. The a, b, and y ions are most commonly observed in peptide mass spectroscopy.[38]

The LC-MS/MS data for the LysAc peptide is shown in figure 4.7. Liquid chromatography (figure 4.7, top) detected two peaks at retention times of 4.50 minutes and 11.66 minutes. The ratio of the area of the larger peak to the area of the smaller peak is 8.4:1, indicating that approximately 89% of the sample eluted at 4.50 minutes. The 4.50 minute peak (figure 4.7, middle) produced a molecular ion of 569.2 Daltons; the calculated molecular weight of the LysAc peptide is 568.7 Daltons. The 569.2 Dalton ion was then fragmented, producing the pattern shown in figure

[1] Awarded one-half jointly to John B. Fenn and Koichi Tanaka "for their development of soft desorption ionisation methods for mass spectrometric analyses of biological macromolecules."

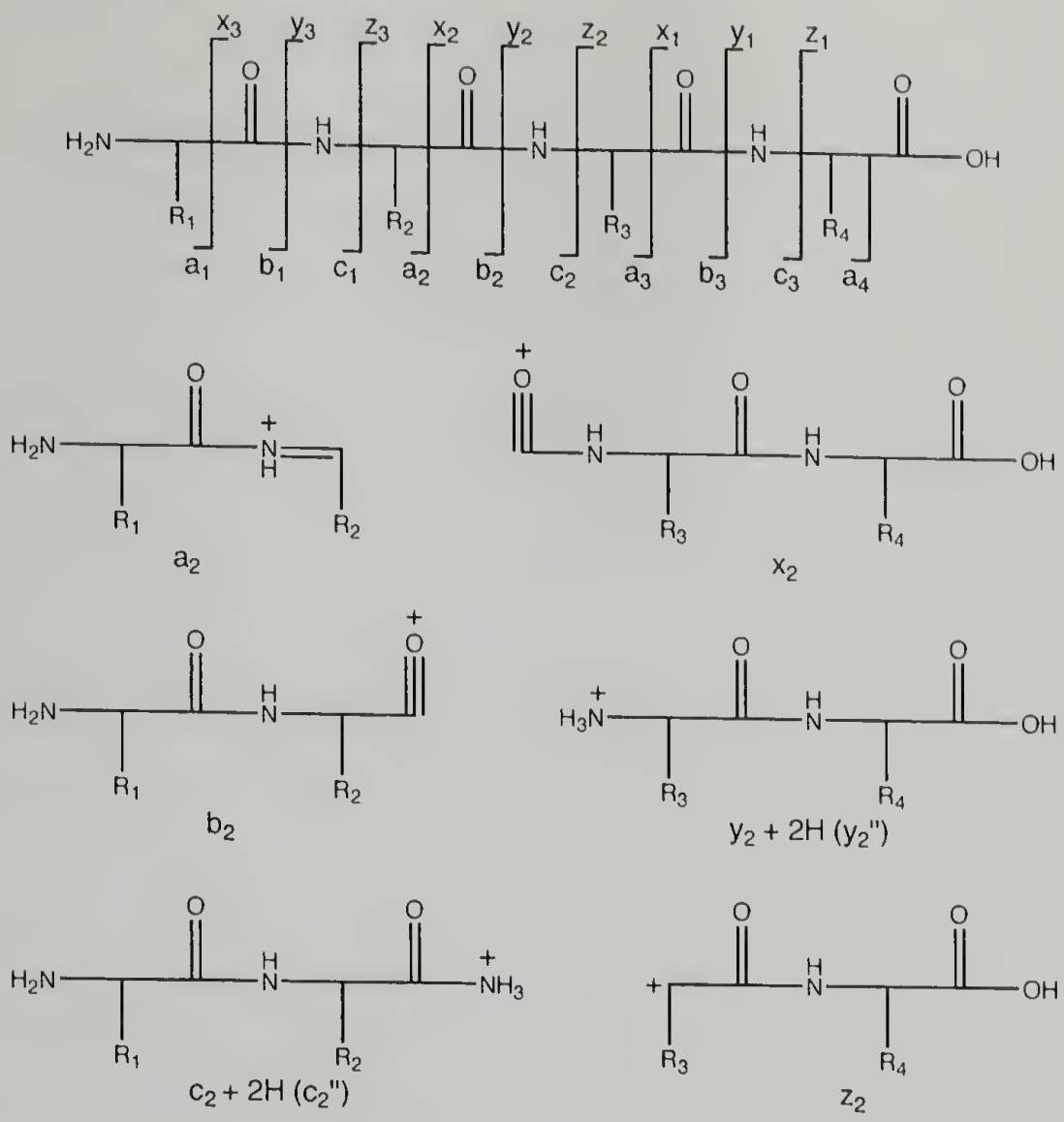

Figure 4.6. Fragmentation of a peptide into complementary ions.[38]

4.7 (bottom). Many of the MS/MS peaks can be identified as specific fragments of the peptide (within ± 1 Dalton), as summarized in table 4.1.

The identity of the 609.2 Dalton ion observed at retention times between 11.38 and 11.72 minutes (figure 4.8) was not determined. The difference between the observed and the calculated masses is 40.5 Daltons. Acetylation of the terminal amine would increase the calculated mass by 42 Daltons, but recalculation of the fragmentation pattern using this scenario did not agree with the observed MS/MS 609.2 ion fragmentation. Neither insertion of another glycine residue into the backbone or addition of glycine to a deprotected lysine side chain produces the ob-

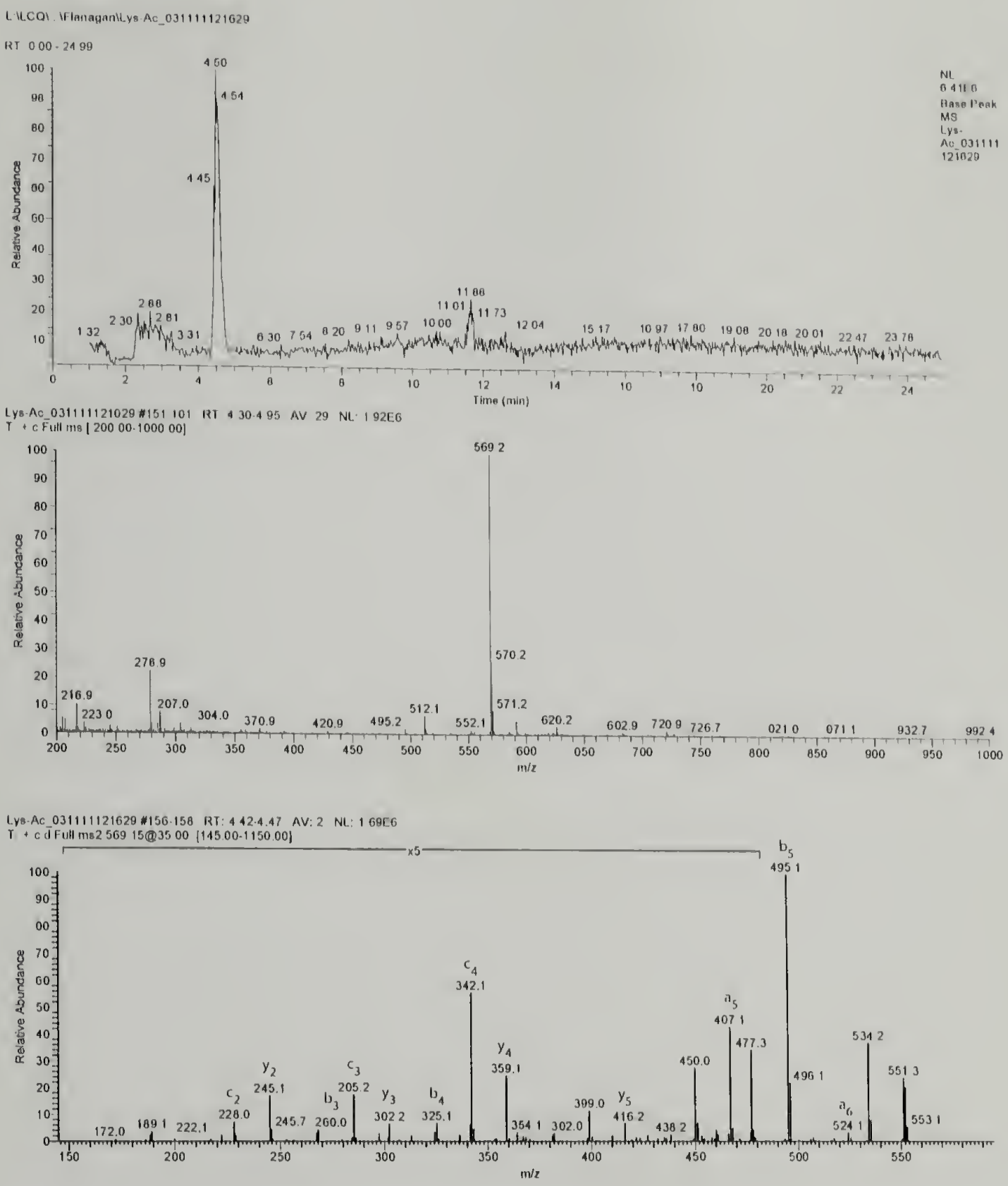

Figure 4.7. LC-MS/MS of LysAc peptide (product). Top: LC of sample. Middle: MS of LC peak at retention time (RT) 4.30–4.95. Bottom: MS/MS of 569.2 ion from RT 4.30–4.95. Labels indicate fragments as designated in table 4.1.

Table 4.1. Calculated and observed fragmentation ions from MS/MS of 569.2 ion of LysAc peptide (figure 4.7).

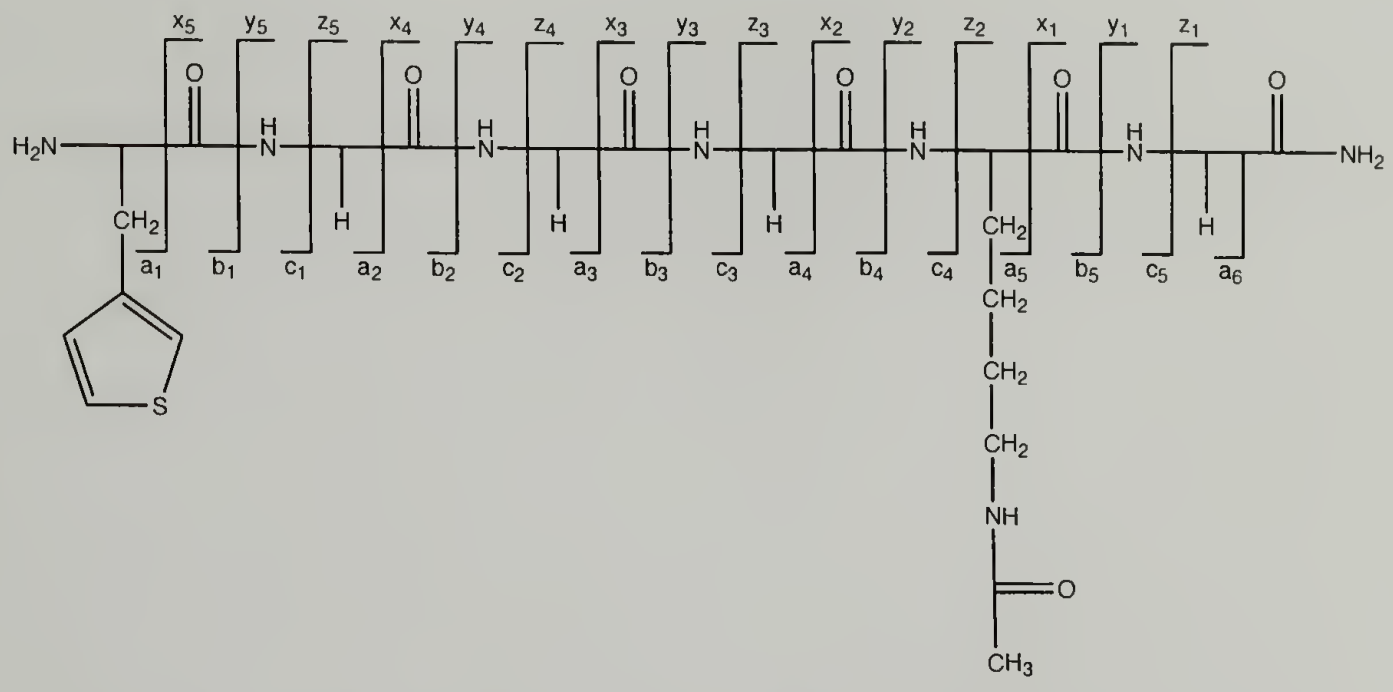

Fragment	Calculated	Observed	Fragment	Calculated	Observed
a_1	—	—	x_1	101.0	—
b_1	—	—	y_1	75.1	—
c_1	—	—	z_1	59.0	—
a_2	183.1	—	x_2	271.1	—
b_2	211.1	—	y_2	245.2	245.1
c_2	228.1	228.0	z_2	229.1	—
a_3	240.1	—	x_3	328.2	—
b_3	268.1	268.0	y_3	302.2	302.2
c_3	285.1	285.2	z_3	286.2	—
a_4	297.1	—	x_4	385.2	—
b_4	325.1	325.1	y_4	359.2	359.1
c_4	342.1	342.1	z_4	343.2	—
a_5	467.2	467.1	x_5	442.2	—
b_5	495.2	495.1	y_5	416.2	416.2
c_5	512.2	—	z_5	400.2	—
a_6	523.5	524.1			

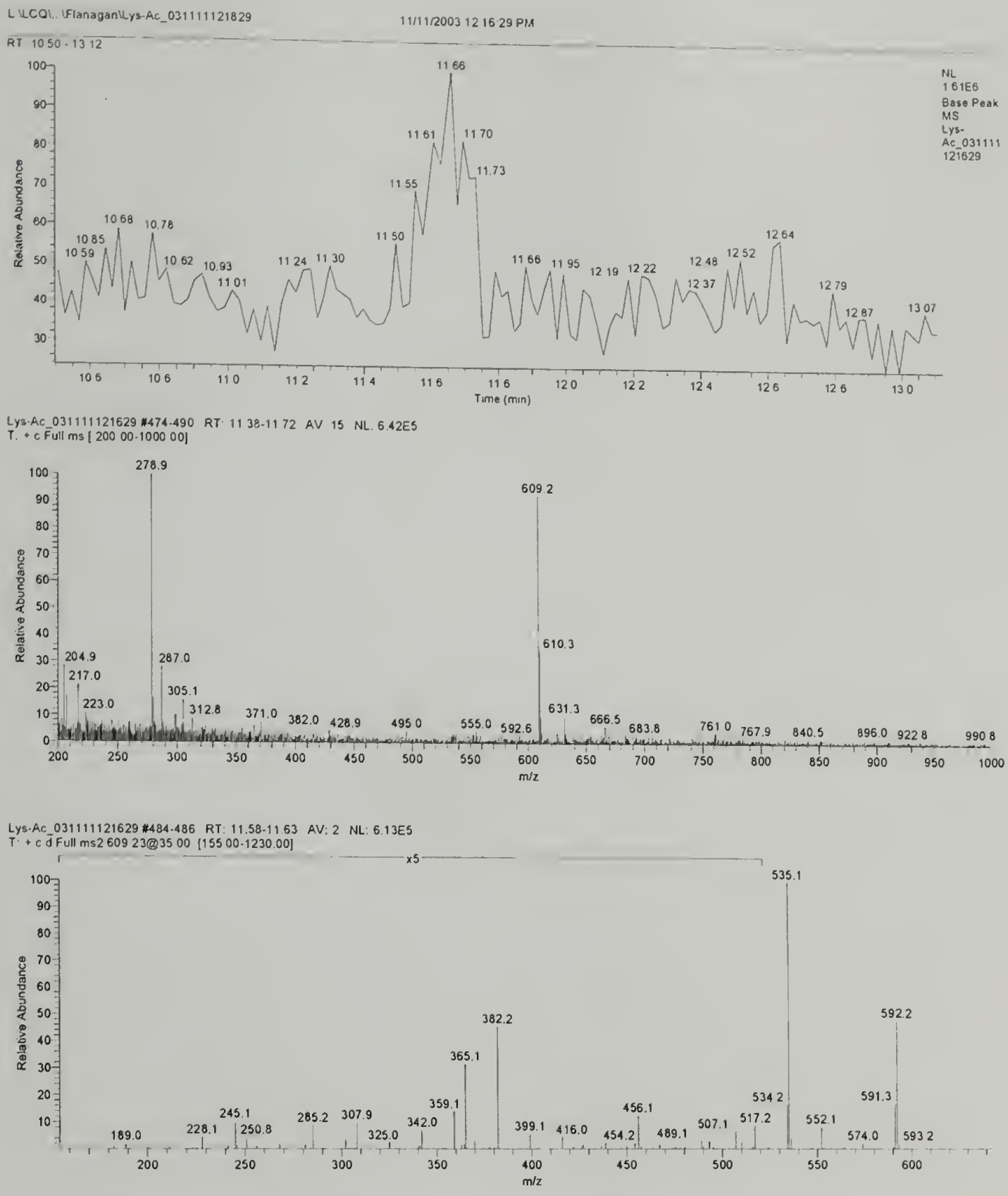

Figure 4.8. LC-MS/MS of LysAc peptide (contaminant). Top: LC of sample. Middle: MS of LC peak at RT 11.38–11.72. Bottom: MS/MS of 609.2 ion from RT 11.38–11.72.

Table 4.2. Calculated and observed fragmentation ions from MS/MS of 611.3 ion of LysAc peptide (contaminant). Observed ions with discrepancies from the calculated value are highlighted.

Fragment	Calculated	Observed	Fragment	Calculated	Observed
a_1	—	—	x_1	101.0	—
b_1	—	—	y_1	75.1	—
c_1	—	—	z_1	59.0	—
a_2	225.1	—	x_2	271.1	—
b_2	253.1	250.8	y_2	245.2	245.1
c_2	270.1	—	z_2	229.1	228.1
a_3	282.1	285.2	x_3	328.2	—
b_3	310.1	307.9	y_3	302.2	486.2
c_3	327.1	325.0	z_3	286.2	469.2
a_4	339.1	—	x_4	385.2	—
b_4	367.1	365.1	y_4	359.2	359.1
c_4	384.1	382.2	z_4	343.2	342.0
a_5	509.2	507.1	x_5	442.2	—
b_5	537.2	535.1	y_5	416.2	416.0
c_5	554.2	552.1	z_5	400.2	399.1

served mass. While the contaminant has not been identified, it could be easily removed by liquid chromatography.

Similar LC-MS/MS analysis can be performed on the Biocytin peptide. As shown in figures 4.9 and 4.10, two peaks are identified by LC at retention times of 14.22 and 18.20 minutes. The ratio of the area of the larger peak to the area of the smaller peak is 5.3:1, indicating that approximately 84% of the sample elutes at 14.22 minutes. The molecular ion observed at 14.22 minutes is 753.2 Daltons; the calculated molecular mass is 752.9 Daltons. Many of the peaks resulting from the fragmentation of the 752.9 ion (figure 4.9, bottom) can be identified, as summarized in table 4.3. Additionally, a peak observed at 525.6 Daltons may correspond to fragmentation of the biocytin side-chain amide bond between the amine and the carboxyl, where charge is retained on the amine (calculated: 527.6 Daltons, observed: 525.6 Daltons).

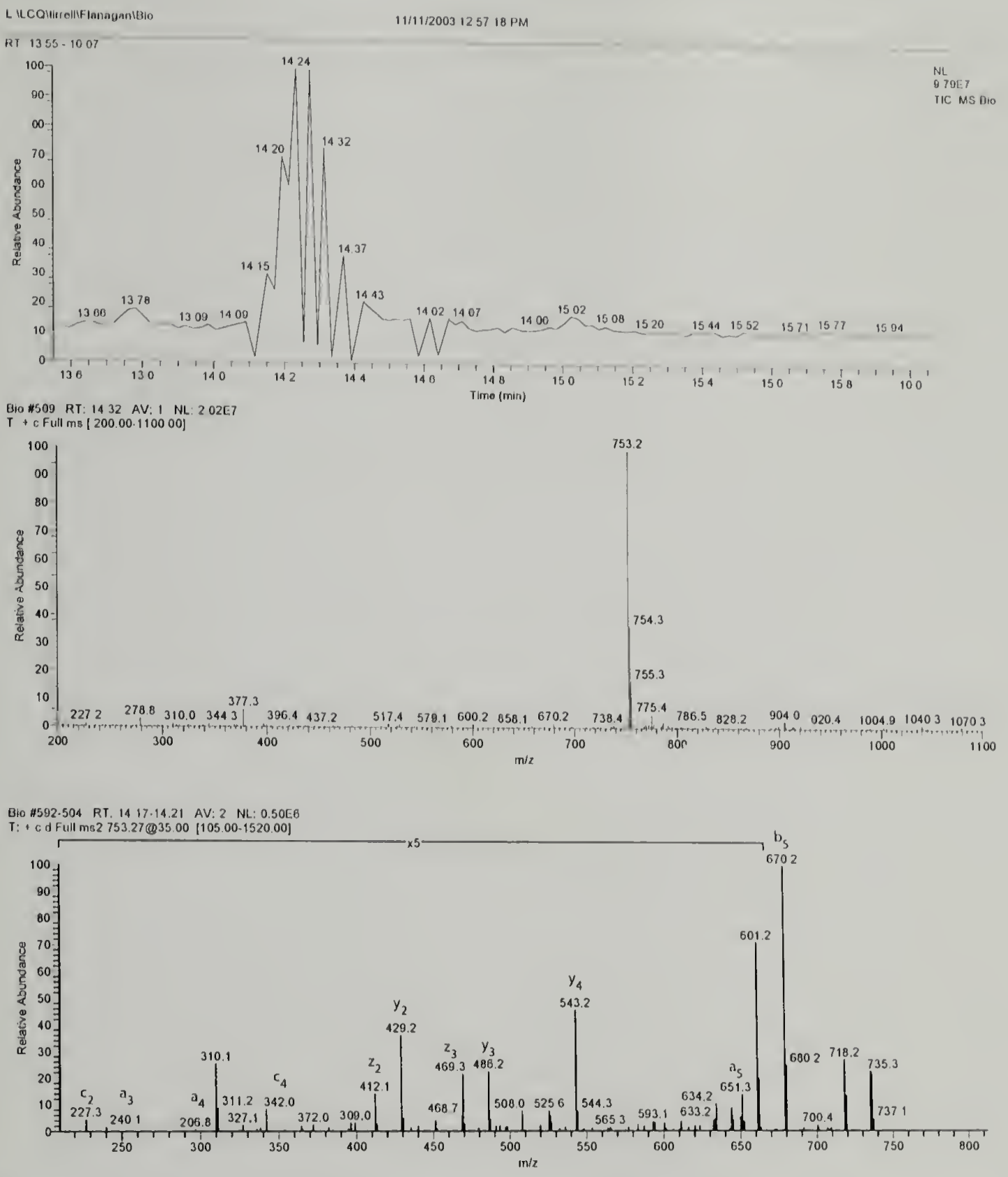

Figure 4.9. LC-MS/MS of Biocytin peptide (product). Top: LC of sample. Middle: MS of LC peak at RT 14.32. Bottom: MS/MS of 753.3 ion from RT 14.17–14.21.

Table 4.3. Calculated and observed fragmentation ions from MS/MS of 753.3 ion of Biocytin peptide (figure 4.9).

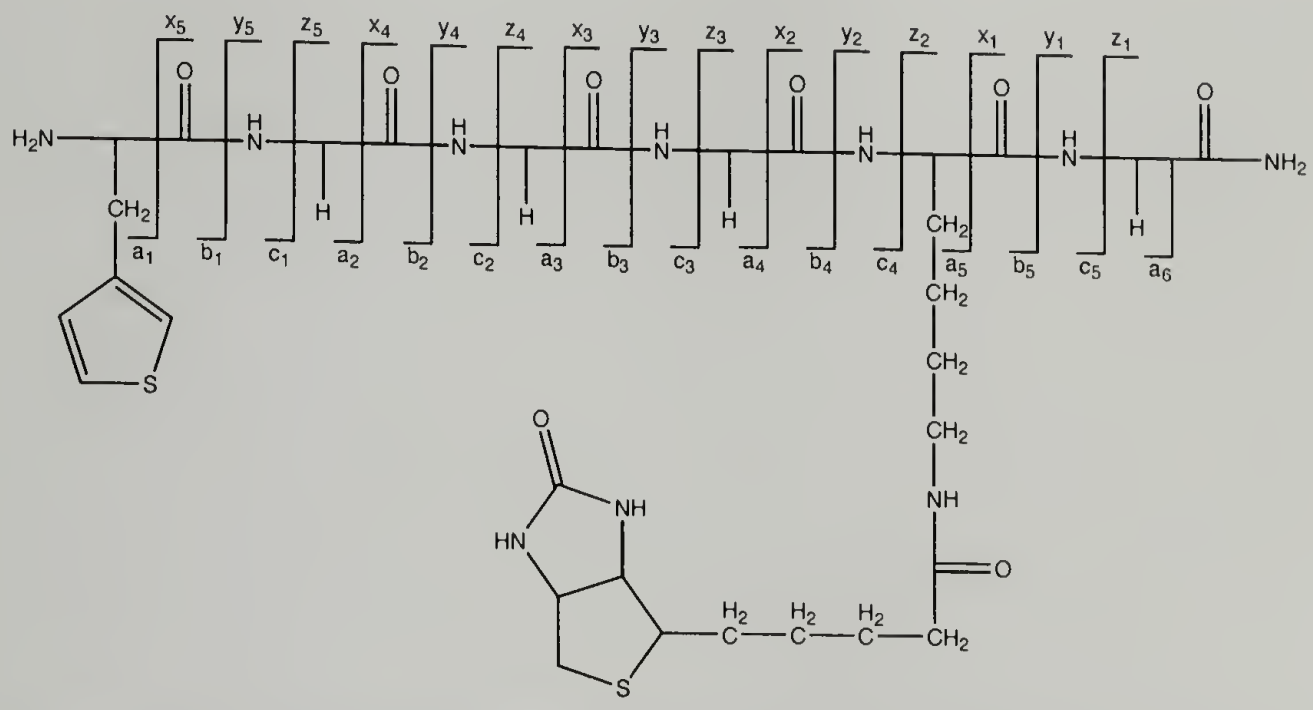

Fragment	Calculated	Observed	Fragment	Calculated	Observed
a_1	—	—	x_1	101.0	—
b_1	—	—	y_1	75.1	—
c_1	—	—	z_1	59.0	—
a_2	183.1	—	x_2	455.2	—
b_2	211.1	—	y_2	429.2	429.2
c_2	228.1	—	z_2	413.2	412.1
a_3	240.1	240.1	x_3	512.2	—
b_3	268.1	—	y_3	486.3	486.2
c_3	285.1	—	z_3	470.2	469.3
a_4	297.1	296.8	x_4	569.3	—
b_4	325.1	—	y_4	543.3	543.2
c_4	342.1	342.0	z_4	527.3	—
a_5	651.3	651.3	x_5	626.3	—
b_5	679.3	679.2	y_5	600.3	—
c_5	696.3	—	z_5	584.3	—
a_6	707.9	—			

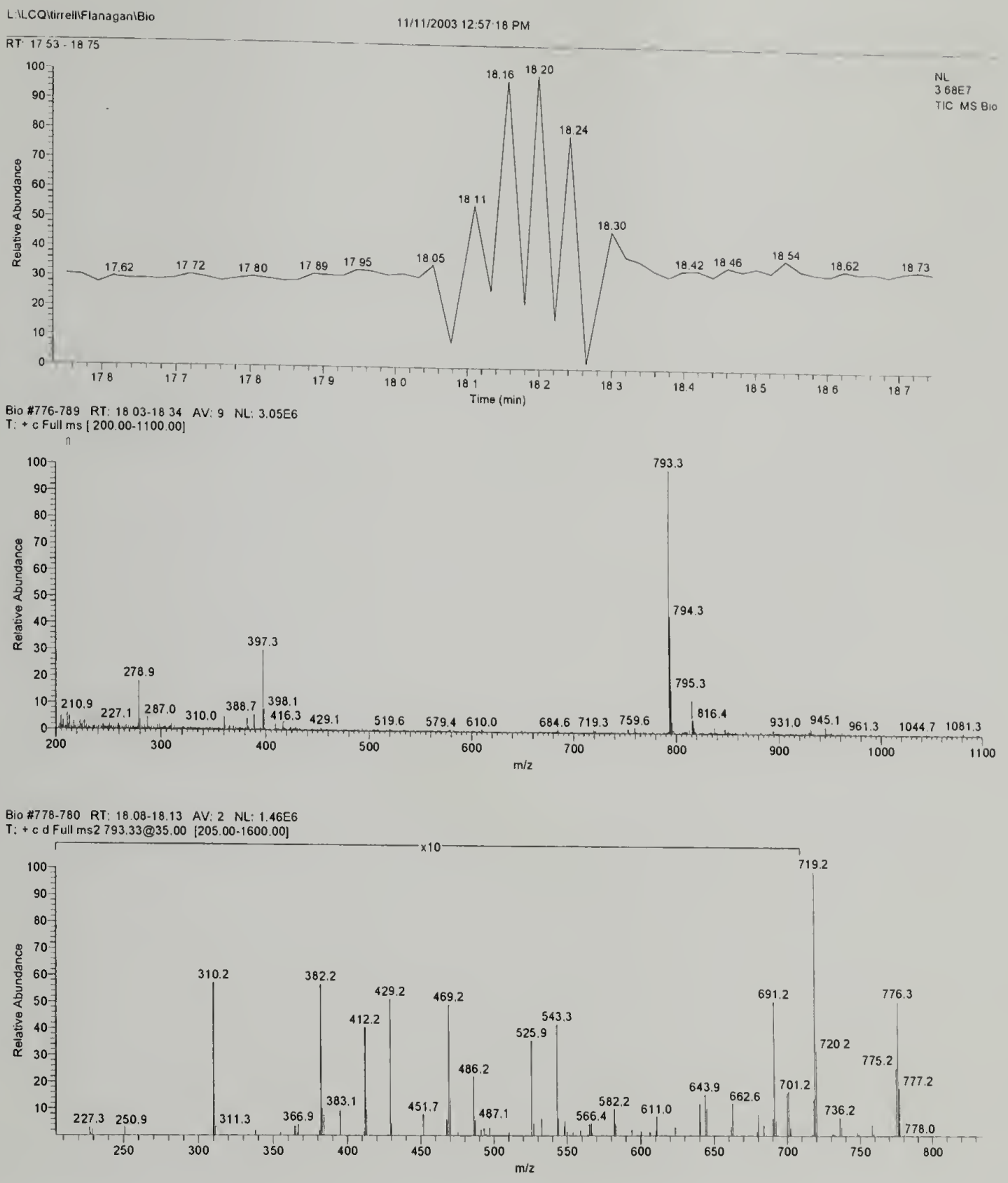

Figure 4.10. LC-MS/MS of Biocytin peptide (contaminant). Top: LC of sample. Middle: MS of LC peak at RT 18.03–18.34. Bottom: MS/MS of 793.33 ion from RT 18.08-18.13.

As in the case of the LysAc peptide, a contaminating peak was detected by LC (figure 4.10) with a retention time of approximately 18 minutes and a molecular ion peak 40 Daltons higher than the calculated mass (calculated: 752.9 Daltons, observed: 793.3 Daltons). Again, if one assumes that the terminal amine was acetylated at some point either during the workup or analysis, it would account for the discrepancy in the observed mass. However, the ions observed from the fragmentation of the 793.3 ion (figure 4.10, bottom) do not wholly agree with the predicted fragmentation ions. The x, y, and z ions should be identical to those of the unmodified peptide, while the a, b, and c ions will increase by 40 Daltons. But, as shown in table 4.4, there are differences of exactly 1 or 2 Daltons in both cases (when the charge remains on the N-terminal fragment or the C-terminal fragment). Causes for these differences have not been determined.

Typically in solid phase peptide synthesis, peptides are subject to further purification after cleavage from the resin. Ion-exchange chromatography or preparative reverse-phase high-performance liquid chromatography (HPLC) are often employed.[37] However, as shown in figure 4.2 copolymerization with 3-hexylthiophene is designed to occur while the peptide is immobilized on the solid phase resin. Therefore, the samples were used despite the presence of the unknown contaminant, without any additional purification.

4.3.1.3 Structural assignment using multidimensional NMR

Structural assignment of the ^{1}H NMR signals of the two peptides could be accomplished using modest field strengths (300 MHz) by spreading the spectrum out into two dimensions. While totally correlated spectroscopy (TOCSY) is often used for peptide structural determination because it isolates the spin systems of individual amino acid residues,[39] correlated spectroscopy (COSY) experiments identifying through-bond couplings were sufficient for our simple peptides. Interpretation of

Table 4.4. Calculated and observed fragmentation ions from MS/MS of 793.3 ion of Biocytin peptide (figure 4.10). Observed ions with discrepancies from the calculated value are highlighted.

Fragment	Calculated	Observed	Fragment	Calculated	Observed
a_1	—	—	x_1	101.0	—
b_1	—	—	y_1	75.1	—
c_1	—	—	z_1	59.0	—
a_2	225.1	227.3	x_2	455.2	—
b_2	253.1	250.9	y_2	429.2	429.2
c_2	270.1	—	z_2	413.2	412.1
a_3	282.1	—	x_3	512.2	—
b_3	310.1	310.2	y_3	486.3	486.2
c_3	327.1	—	z_3	470.2	469.2
a_4	339.1	—	x_4	569.3	—
b_4	367.1	366.9	y_4	543.3	543.3
c_4	384.1	382.2	z_4	527.3	525.9
a_5	693.3	691.2	x_5	626.3	—
b_5	721.3	719.2	y_5	600.3	—
c_5	738.3	736.2	z_5	584.3	582.2

the NMR spectra is most easily accomplished by beginning with the simplest component, biotin, and working through to the more complex spectra of the peptides (and in section 4.3.2.2, the copolymers).

The 1D ^{1}H NMR spectrum of biotin is shown in figure 4.11. While a complete assignment can probably be made using figure 4.11, the couplings and coupling strengths are made apparent by the COSY shown in figure 4.12. Beginning with the urea proton at a, the assignments can be walked through the molecule by connecting a to c, c to b, b to e, and e to f. The protons in the alkyl acid side chain can be determined in a similar fashion. The e and f protons strongly couple, but are non-equivalent, because they experience different environments despite attachment to the same carbon. The three pairs of h protons are not readily distinguishable, because both the 1D signals and the 2D coupling peaks overlap. The 1D ^{1}H NMR spectrum of biocytin (figure 4.13) can be assigned analogously, with the additional side chain protons (e, i, and d). The multiplet at approximately 3.2 ppm results

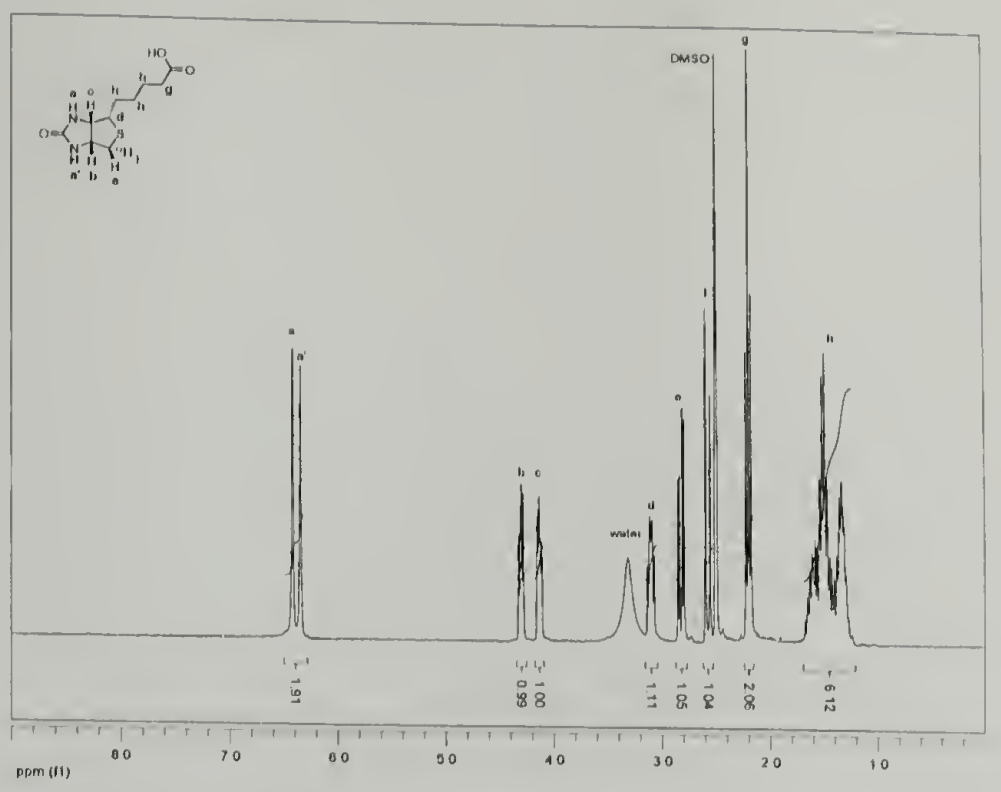

Figure 4.11. Proton NMR spectrum of biotin (300 MHz, DMSO-d_6).

from an overlap of the two protons labeled "e" in the figure. (The exchangeable protons a and a′ do not appear in figure 4.13 because the spectrum was collected in deuterated methanol rather than deuterated DMSO.)

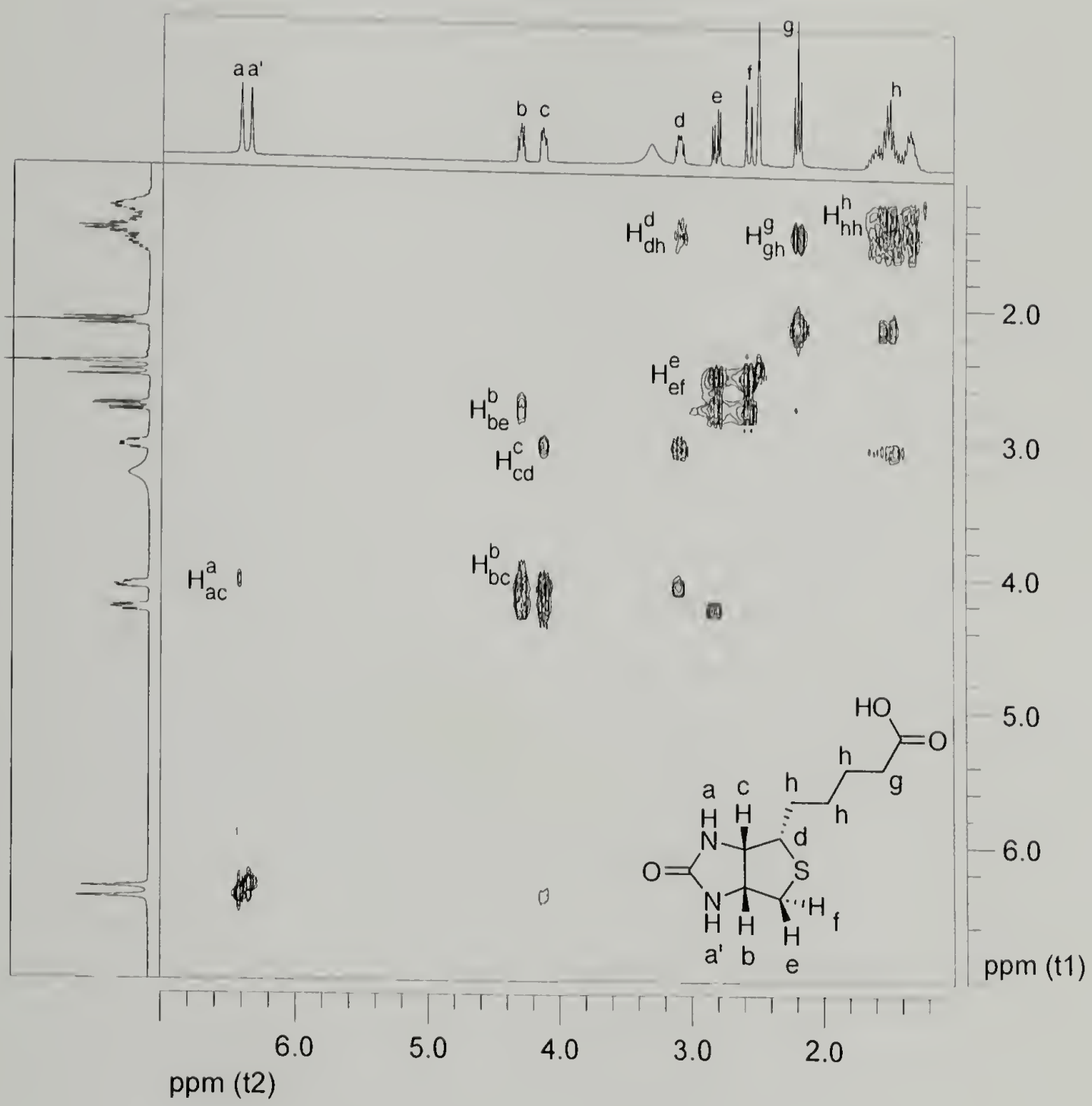

Figure 4.12. COSY spectrum of biotin. (300 MHz, DMSO-d_6)

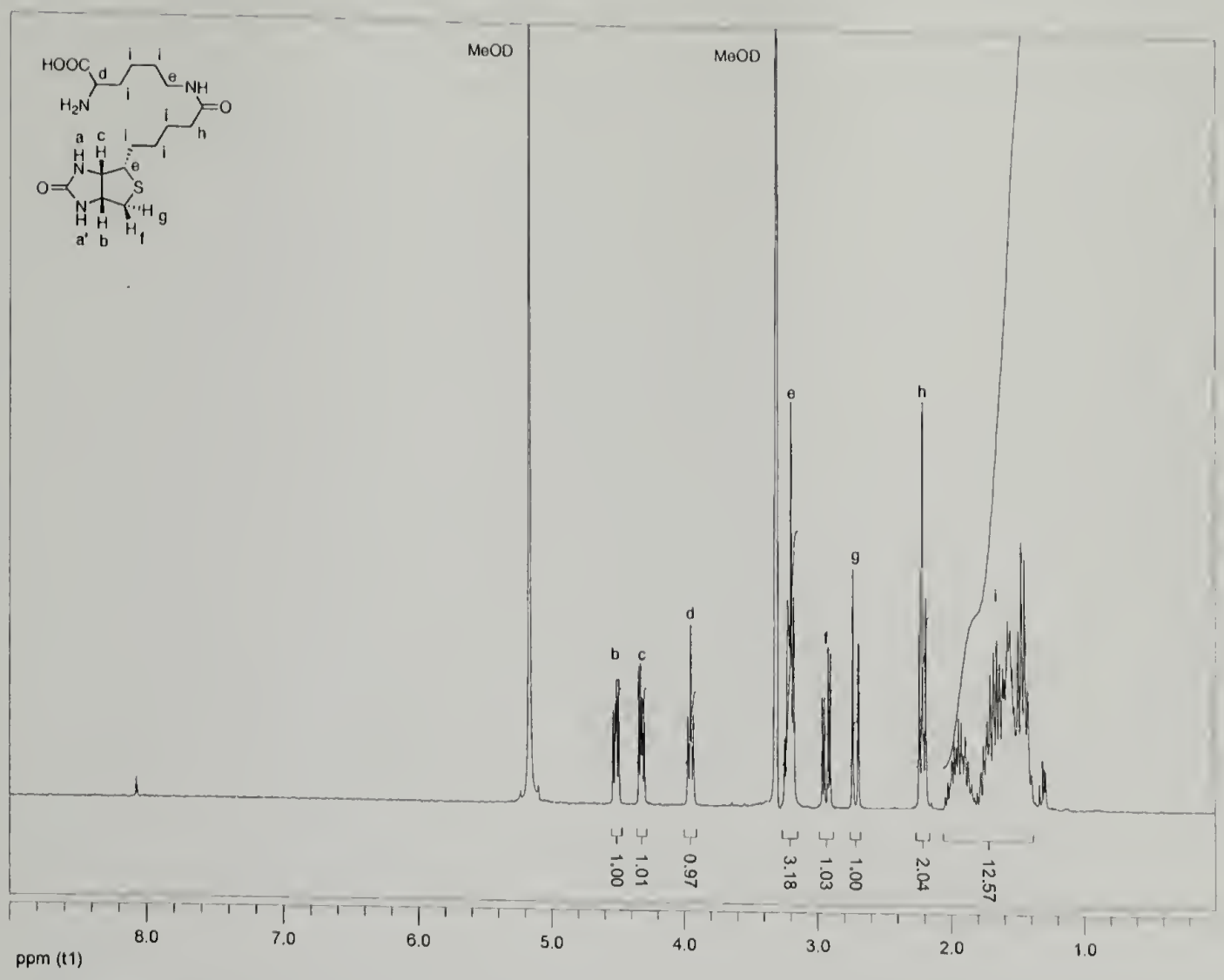

Figure 4.13. Proton NMR spectrum of biocytin (300 MHz, methanol-d_4).

The 1D ^{1}H NMR spectrum of the biocytin peptide (figure 4.14) is more complicated than figure 4.13, but can be worked out by spreading the signals into two dimensions (figure 4.15). After identifying the characteristic signals from the biocytin urea protons at e and e′, connections can be made between the biocytin protons: e′ to e, e to g, g to f, f to m, and m to o (figure 4.16). Couplings between the thiophene ring protons are clearly seen in figure 4.16: b to c, b to d, and c to d. The other protons in the 3-thienylalanine residue are also apparent on page 143: i to k and n, and k and n to each other. The k and n protons are nonequivalent; this is also observed in the 1D NMR spectrum of enantiopure 3-thienylalanine. Glycine residue and amide protons are distinguished by strong couplings between signals above 7 ppm and below 4 ppm. Finally, by identifying the side chain amide pro-

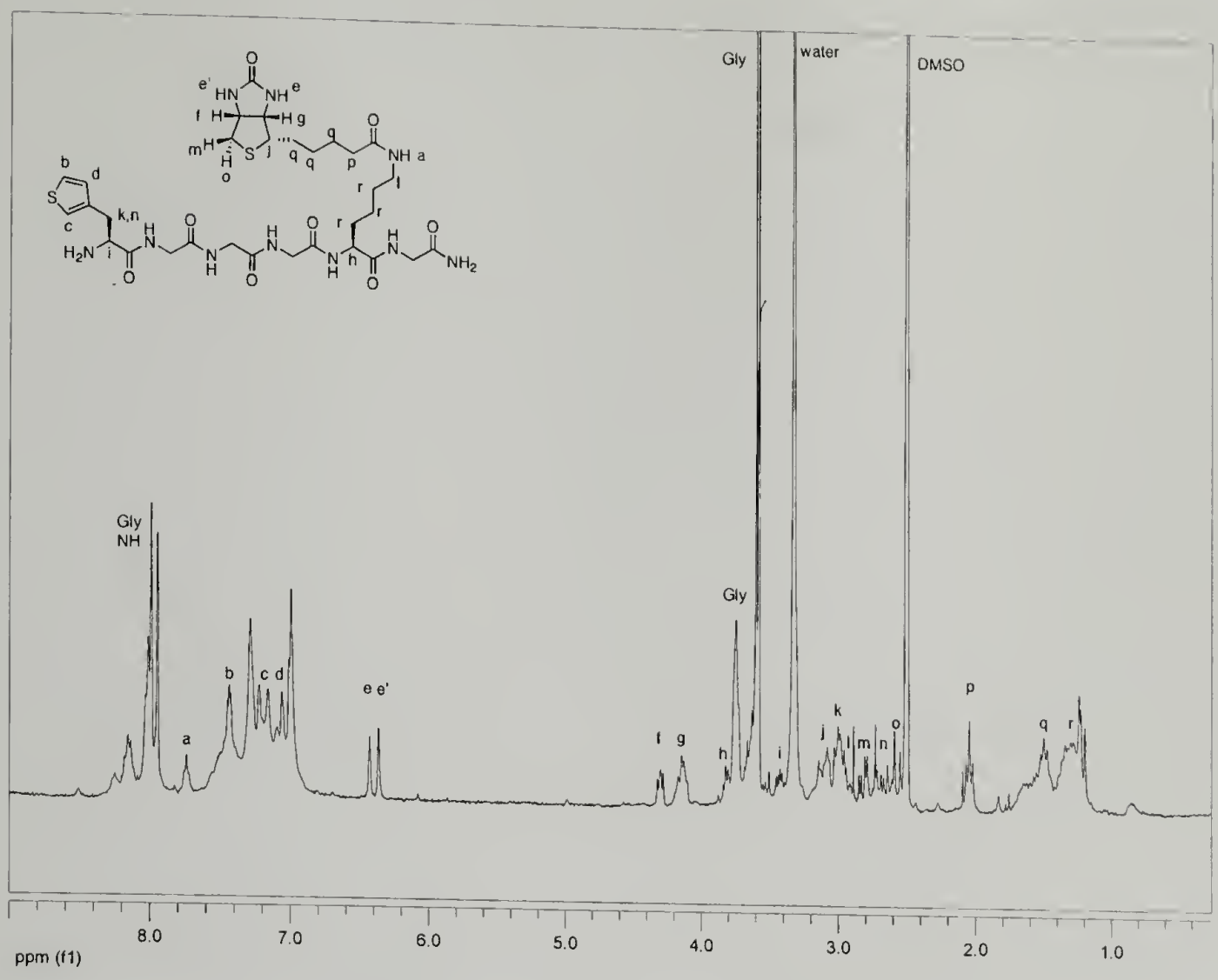

Figure 4.14. Proton NMR spectrum of biocytin peptide (300 MHz, DMSO-d_6).

ton at a, the side chain protons a, l, r, and p and q can be identified, completing the assignment.

The 1D spectrum of the LysAc peptide is simpler (figure 4.17) than that of the biocytin peptide. Without the complicating biotin signals, the splitting of the thiophene ring protons c, d, and e is apparent (figure 4.17, inset), as well as the splitting of the two nonequivalent protons arising from the chiral center of the LysAc residue (l). Conclusive assignments are made using the COSY spectrum (figure 4.18). The lysine side chain and peptide chain amide protons are identified by couplings between b and i and a and f, respectively. The signal at i can then be linked with m, and f with l, completing the side chain (figure 4.19). Finally, the thiophene ring proton assignments are confirmed (figure 4.19): c to d, c to e, and d to e.

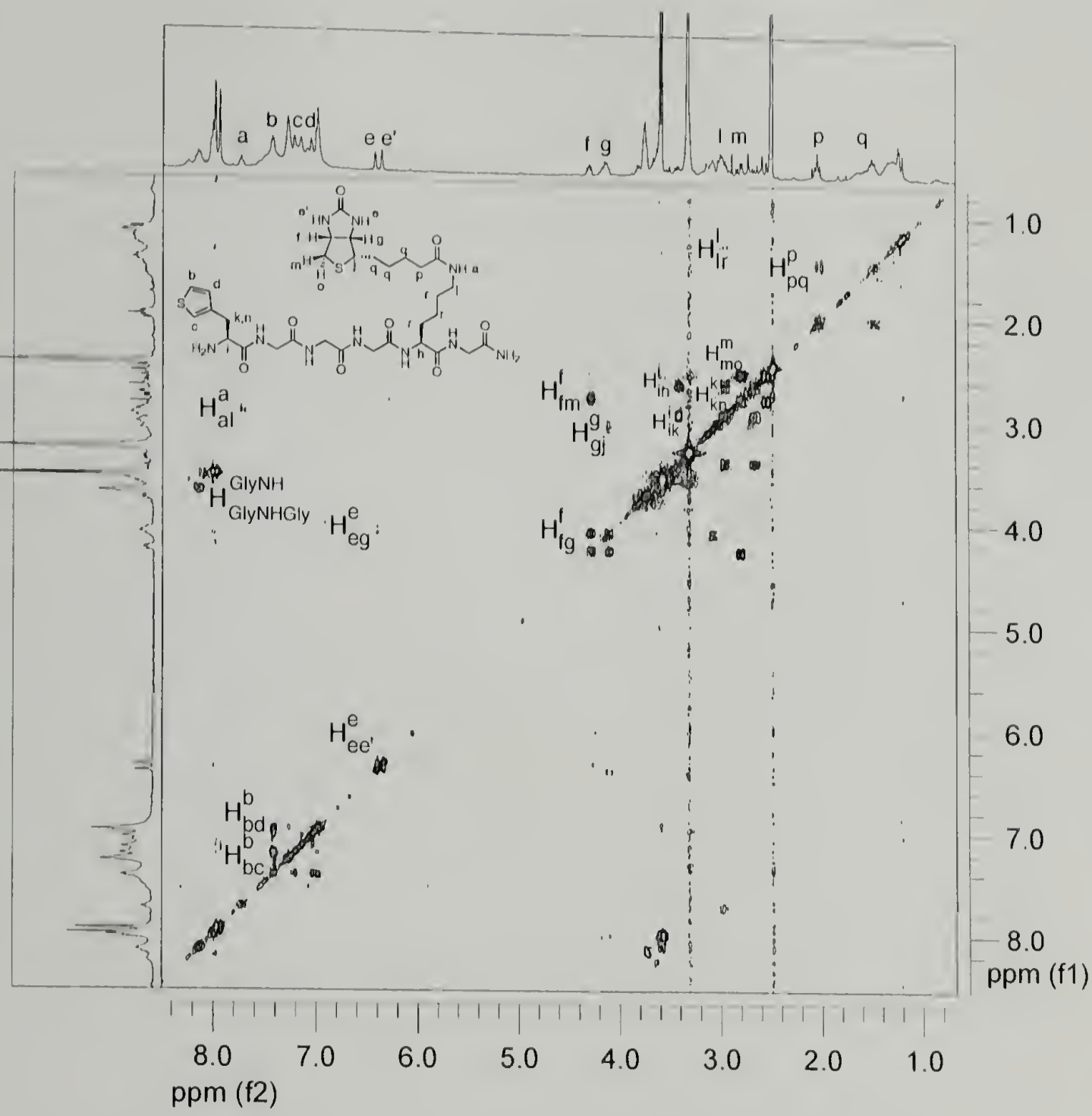

Figure 4.15. COSY spectrum of biocytin peptide (300 MHz, DMSO-d_6).

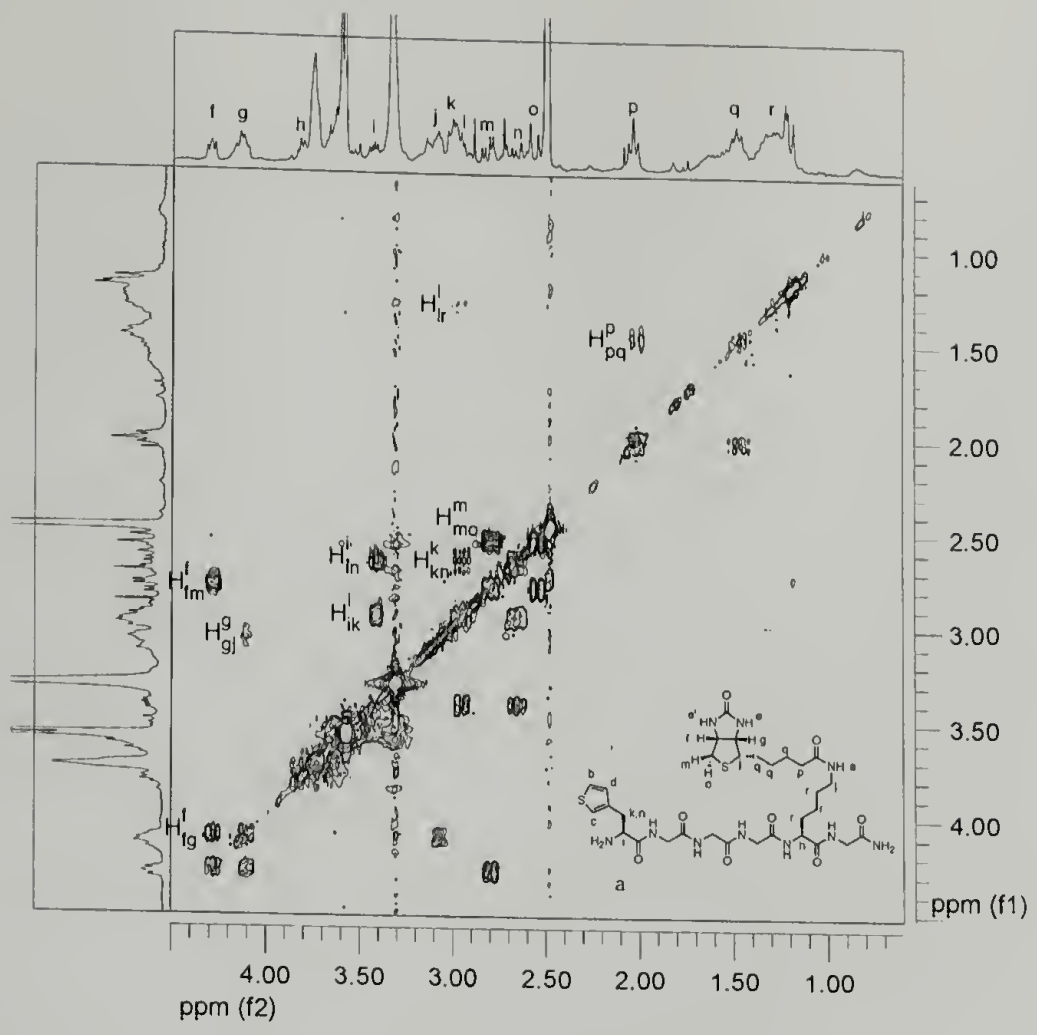

Figure 4.16. Biocytin peptide: expansions of figure 4.15.

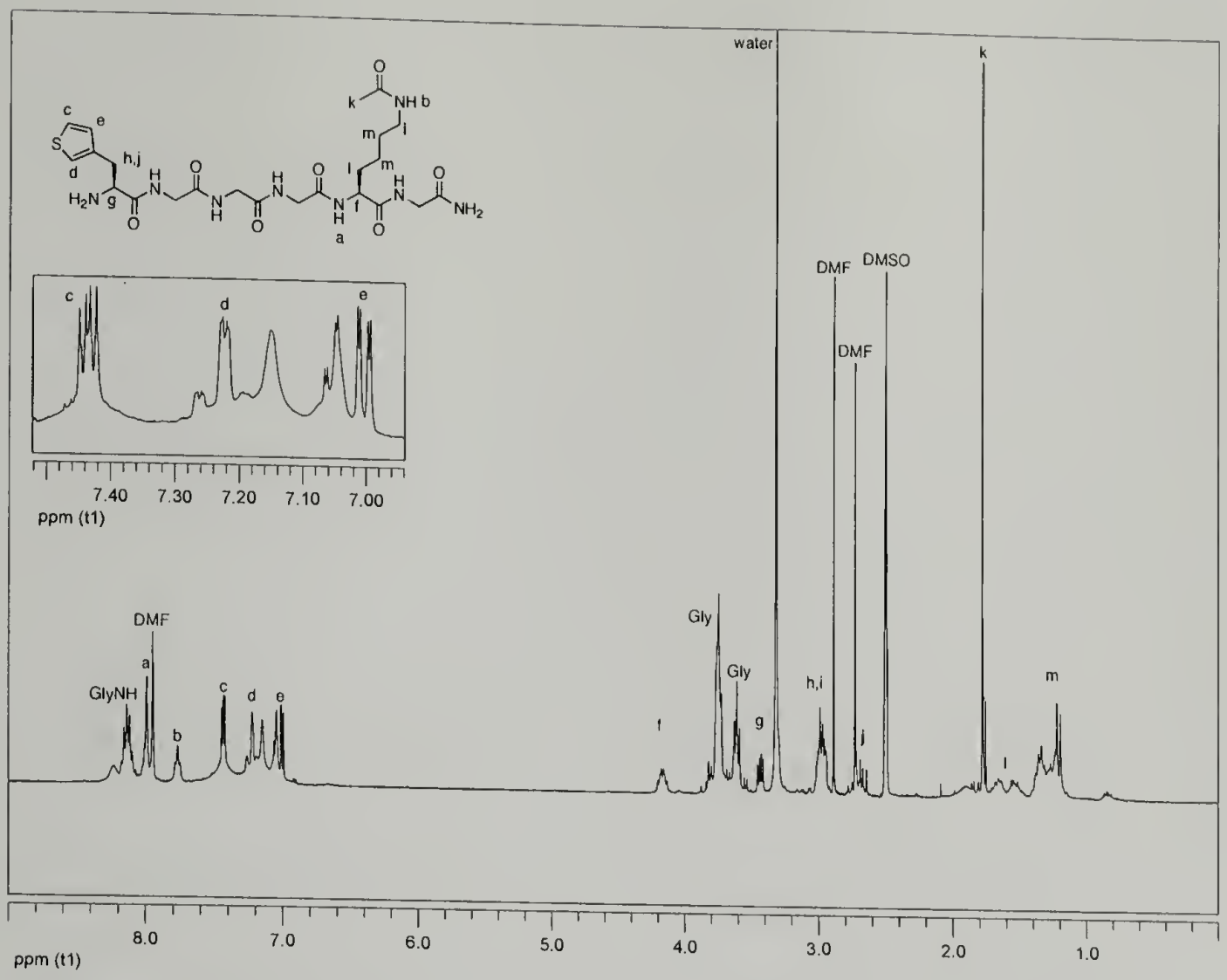

Figure 4.17. Proton NMR spectrum of LysAc peptide (300 MHz, DMSO-d_6).

In addition to supporting the mass spectroscopy evidence, confirming the synthesis of the peptides, these NMR spectra will be used as a basis for determining the changes in structure after graft copolymerization with 3-hexylthiophene.

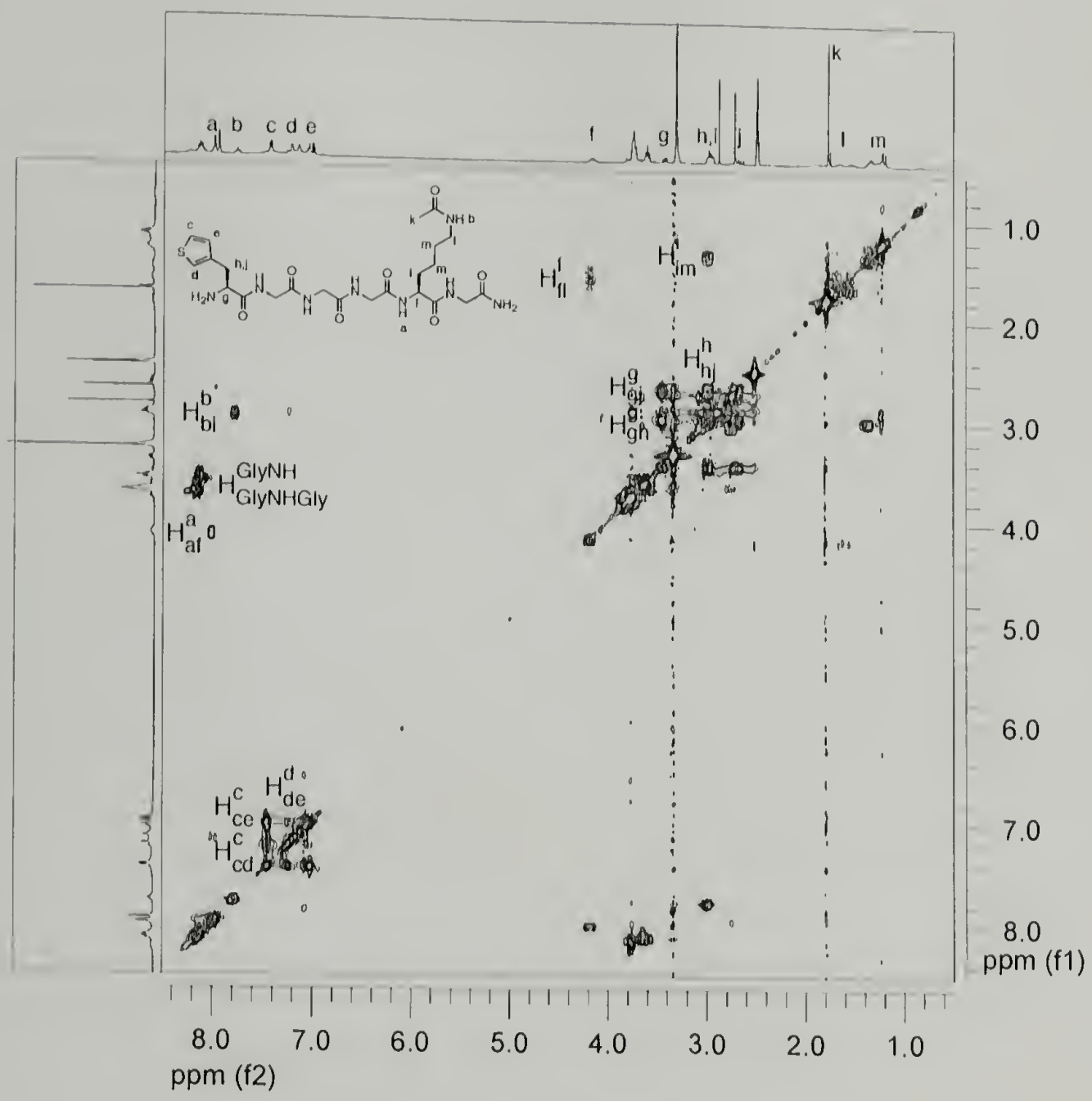

Figure 4.18. COSY spectrum of LysAc peptide (300 MHz, DMSO-d_6).

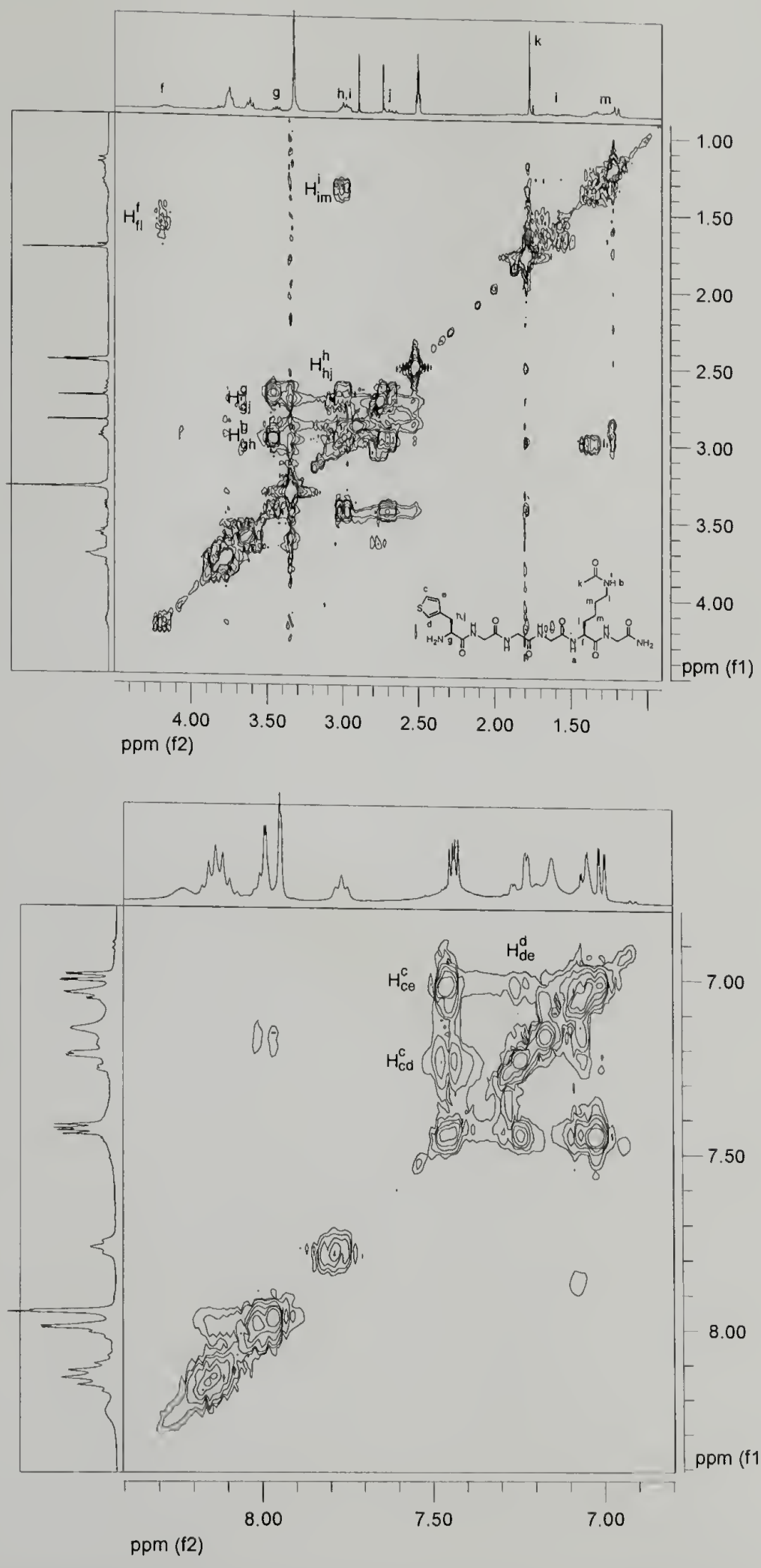

Figure 4.19. Lys(ac) peptide: expansions of figure 4.18.

4.3.2 Copolymerization

4.3.2.1 Oxidative polymerization and cleavage

In Chapter 3, factors which had significant effects on the fluorescence emission maxima of 3HT/3TA copolymers were identified (figures 3.15 and 3.16). Lower molecular weight polymers should be easier to characterize by NMR spectroscopy than higher molecular weight polymers, so reaction conditions which should provide intermediate molecular weights were used for oxidative copolymerization. These conditions are:

A: 3HT:3TA ratio: 20:1

B: $FeCl_3$:monomer ratio: 1:1

C: polymerization time: 5 h

D: monomer concentration: 0.05 mmol/mL

E: anhydrous catalyst: no

F: Proton-Sponge: no

G: monomer addition rate: 0.5 ml/hour

H: bithiophene: no

After copolymerization and exhaustive Soxhlet extraction, the red resin beads were fluorescent in good solvents for poly(3-hexylthiophene), such as THF or chloroform. The mass of the beads did not significantly increase after polymerization, which could be due to low yield, or to cleavage of the copolymer from the bead during the polymerization or extraction.

Cleavage of the copolymers from the resin was first attempted using 7 *N* ammonia in methanol, producing the peptide amide. The poor swelling of the microporous resin beads in methanol resulted in incomplete cleavage from the resin,

even after shaking for two days. Alternatively, cleavage with a dilute solution of sodium hydroxide in THF rapidly cleaved the copolymer from the resin, resulting in the carboxylic acid (presumably as the salt).

4.3.2.2 NMR spectroscopy of peptide copolymers

The one dimensional proton NMR spectrum of the poly(Bio-co-3HT) graft copolymer is shown in figure 4.20. As in the case of the peptides, the assignments were made based on identification of through-bond couplings shown in the COSY spectrum in figure 4.21. The most prominent features of the COSY spectra are the peaks corresponding to coupling of protons in the 3-hexylthiophene side chain, demonstrating successful copolymerization to a moderate molecular weight. In the first expansion shown in figure 4.22, the proton assignments can be made through the side chain from z to y, y to x, x to w, and w to v. The 4-position thiophene proton c at 7.3 ppm does not couple with the side chain protons.

A major concern before this experiment was the stability of the peptide backbone after exposure to oxidative polymerization conditions. The peptide does appear to have remained intact, with strong coupling signals from the glycine protons to the amide bond protons. Additionally, connections can be made for the biocytin residue side chain, confirming its presence in the copolymer. Biocytin proton assignments can be made coupling g to j, j to q, and q to p, as well as f to m and l to r. Finally, coupling signals between b and d are observed for the 3-thienylalanine thiophene ring. Two pairs of coupled b and d protons are observed, which may result from formation of a head-to-head or a head-to-tail link from 3-thienylalanine to the first 3-hexylthiophene monomer.

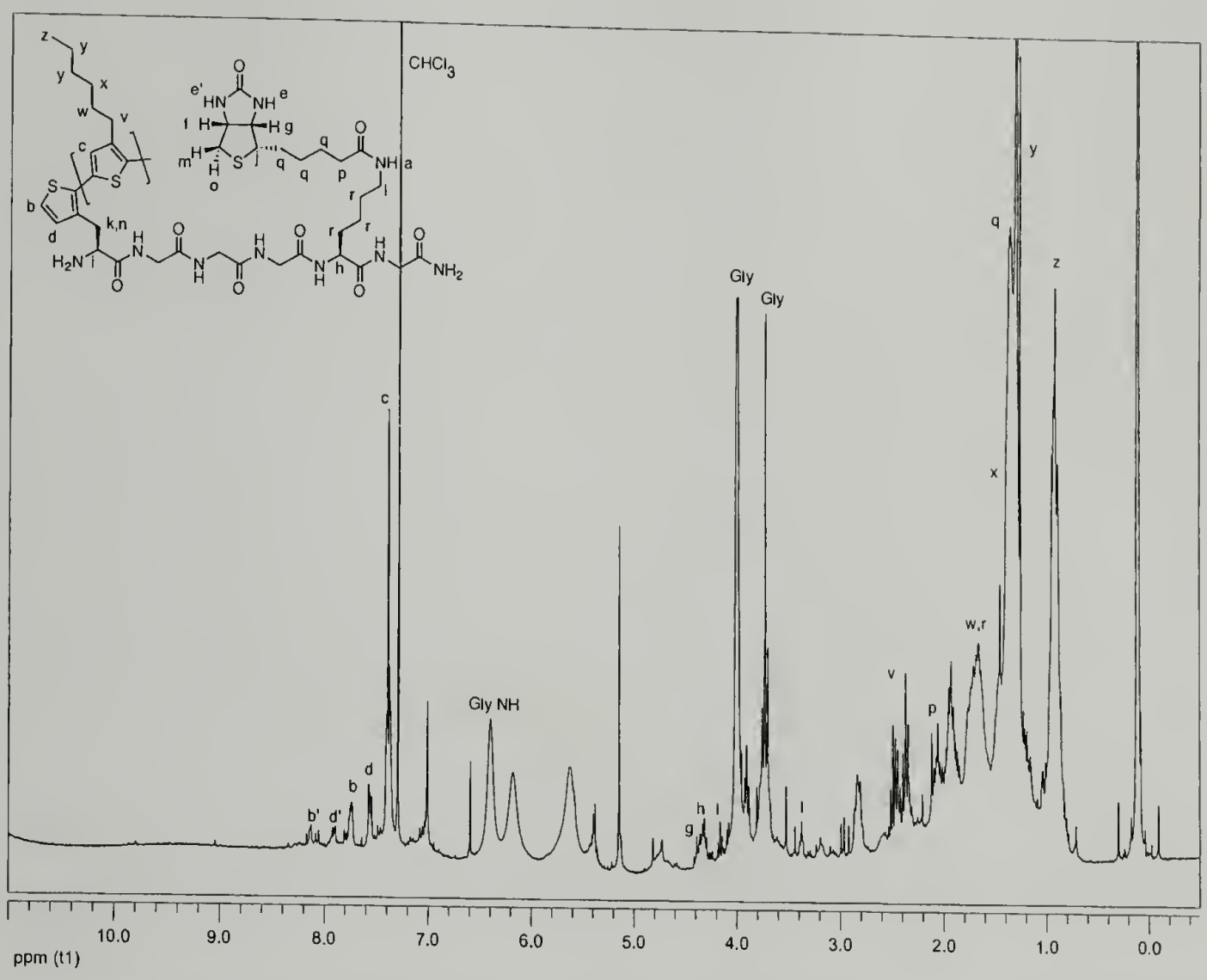

Figure 4.20. Proton NMR spectrum of poly(3-hexylthiophene)/biocytin peptide copolymer (300 MHz, chloroform-*d*).

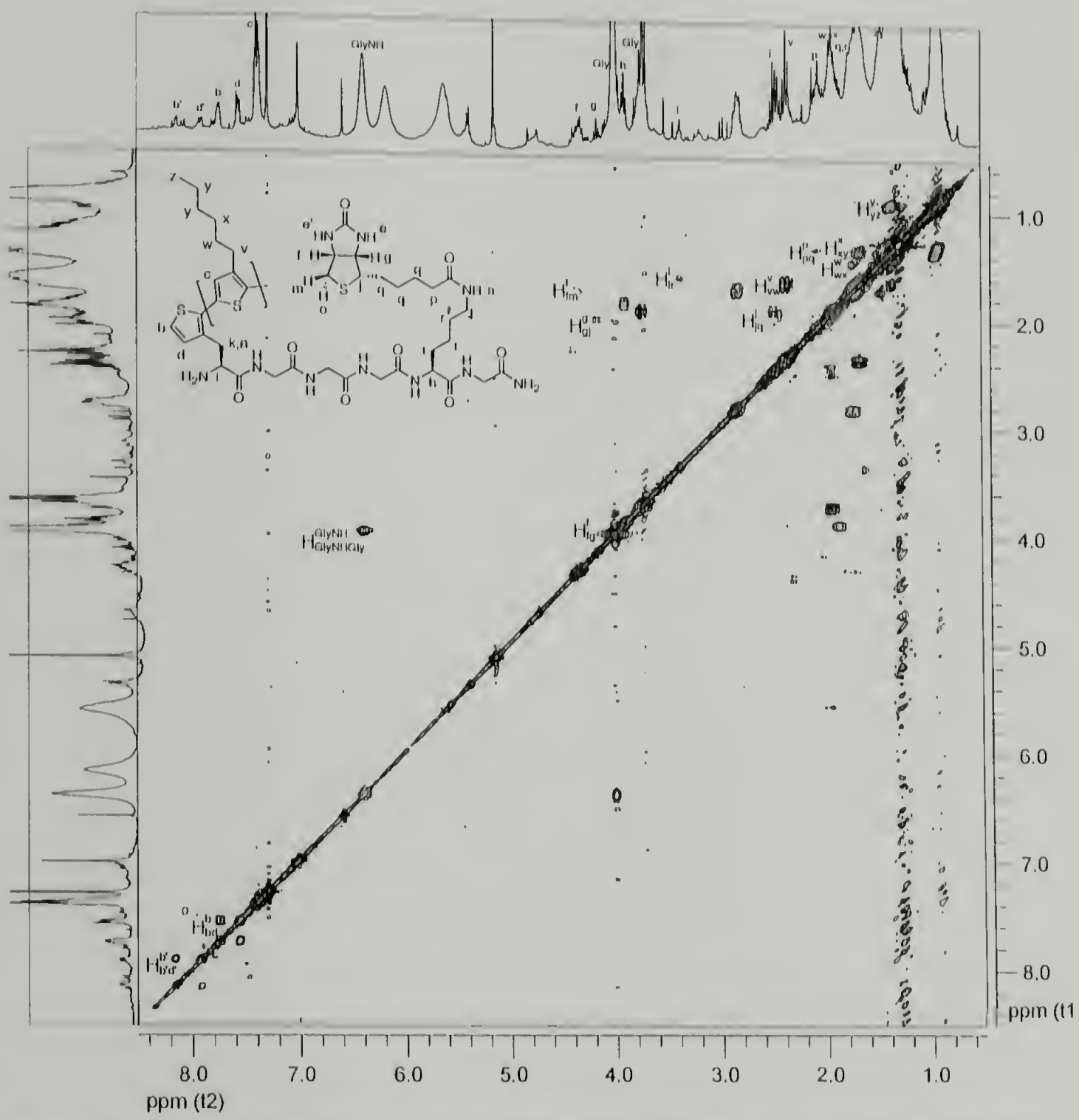

Figure 4.21. COSY spectrum of poly(3-hexylthiophene)/biocytin peptide copolymer (300 MHz, chloroform-*d*).

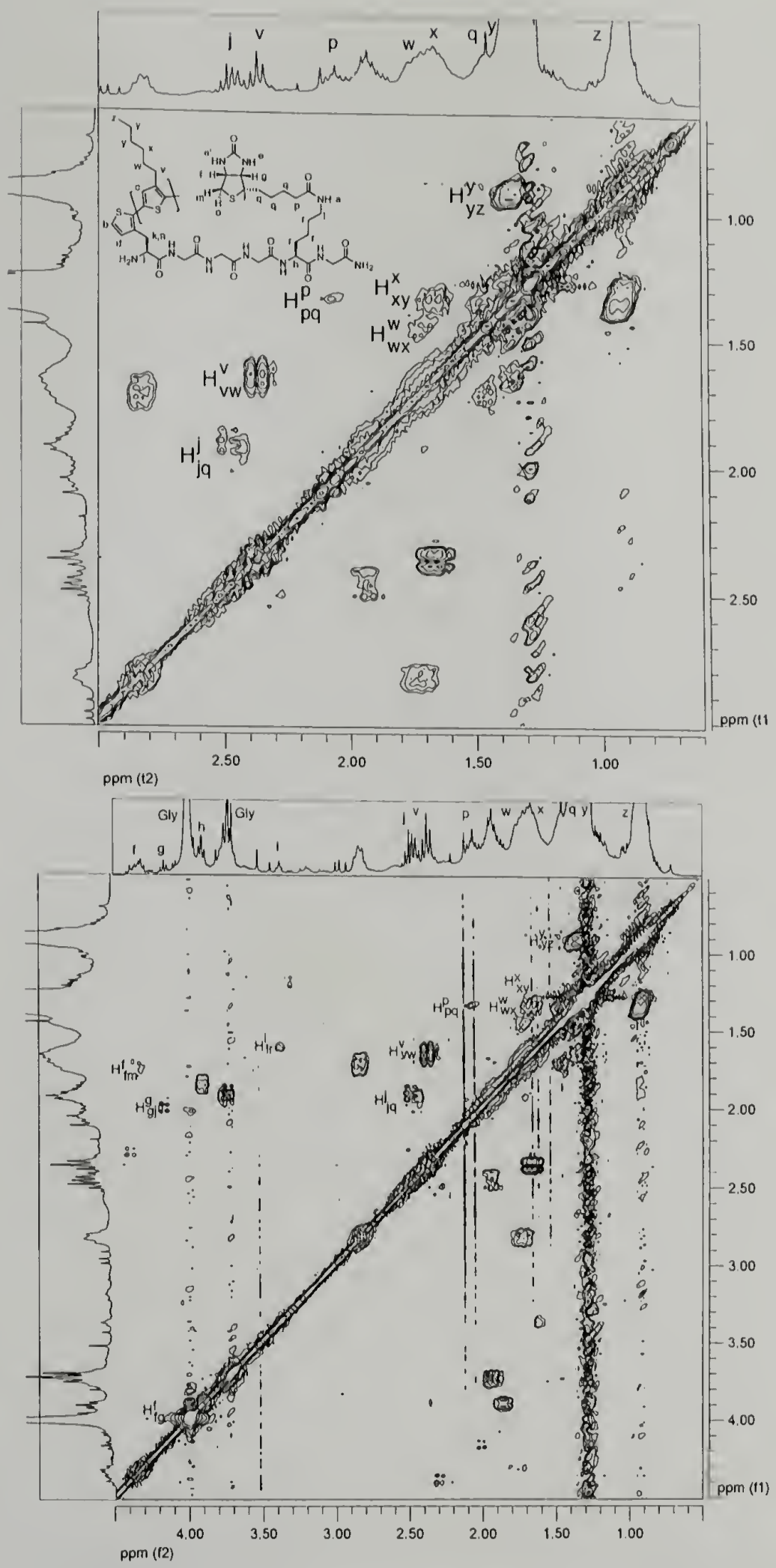

Figure 4.22. Poly(3-hexylthiophene)/biocytin peptide copolymer: expansions of figure 4.21.

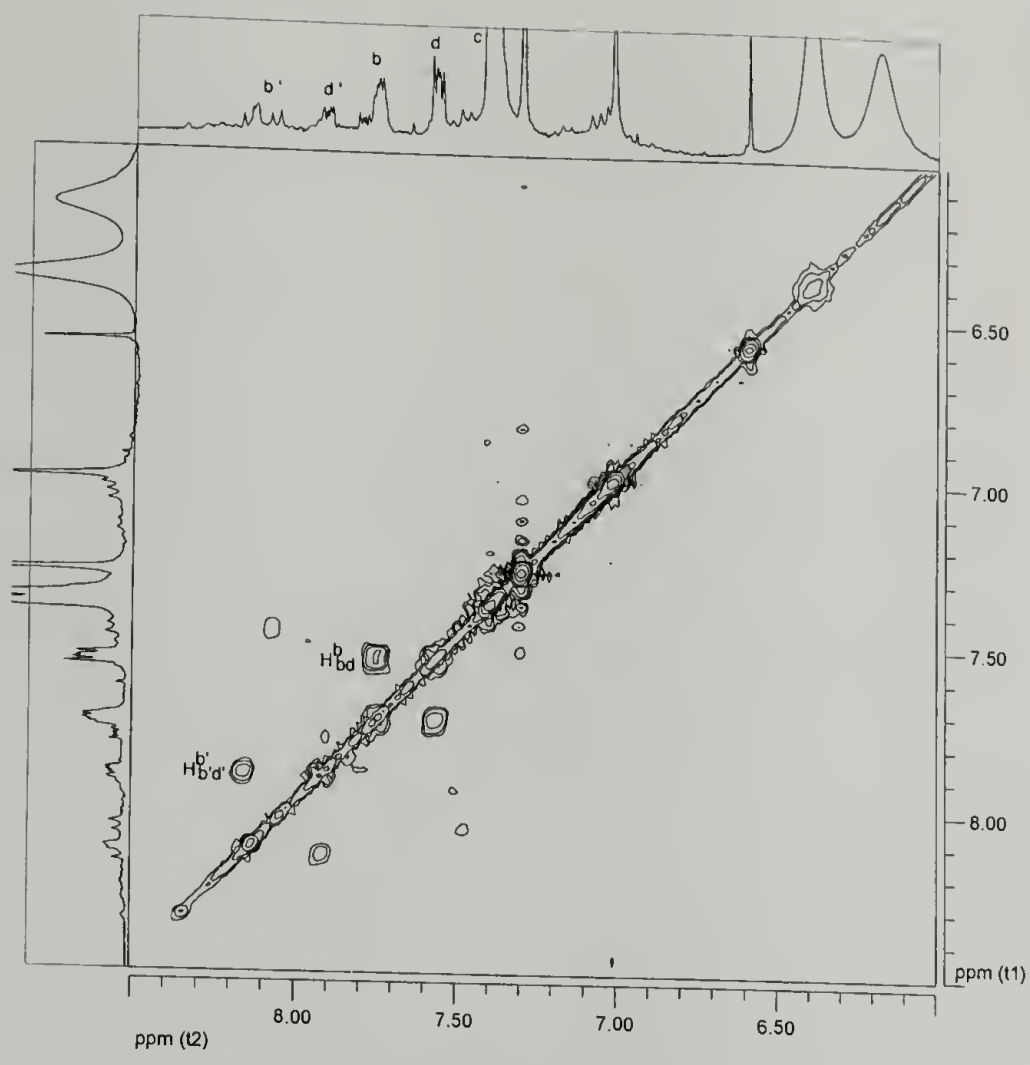

Figure 4.22 (continued).

The stability of the peptide bond under oxidative polymerization conditions is confirmed by the proton NMR spectrum of the poly(LysAc-co-3HT) copolymer, shown in figure 4.23. The spectrum is simpler than that for the biocytin copolymer, but correlation spectroscopy again aids in assignment of proton signals (figure 4.24). In addition to the strong signals corresponding to couplings between the 3-hexylthiophene side chain protons (z to y, y to x, x to w, and w to v), and the coupling between the glycine protons and the adjacent amide protons, the integrity of the protected lysine side chain is confirmed by couplings i to m and f to l. The relatively low intensity of proton c on the 3-hexylthiophene thiophene ring may be due to the long relaxation time of the proton, despite recording the spectrum with a 5 second recycle delay.

The one-dimensional NMR spectra of the copolymers also permit estimation of molecular weight. As shown in figure 4.25 (top), integration of the z protons of

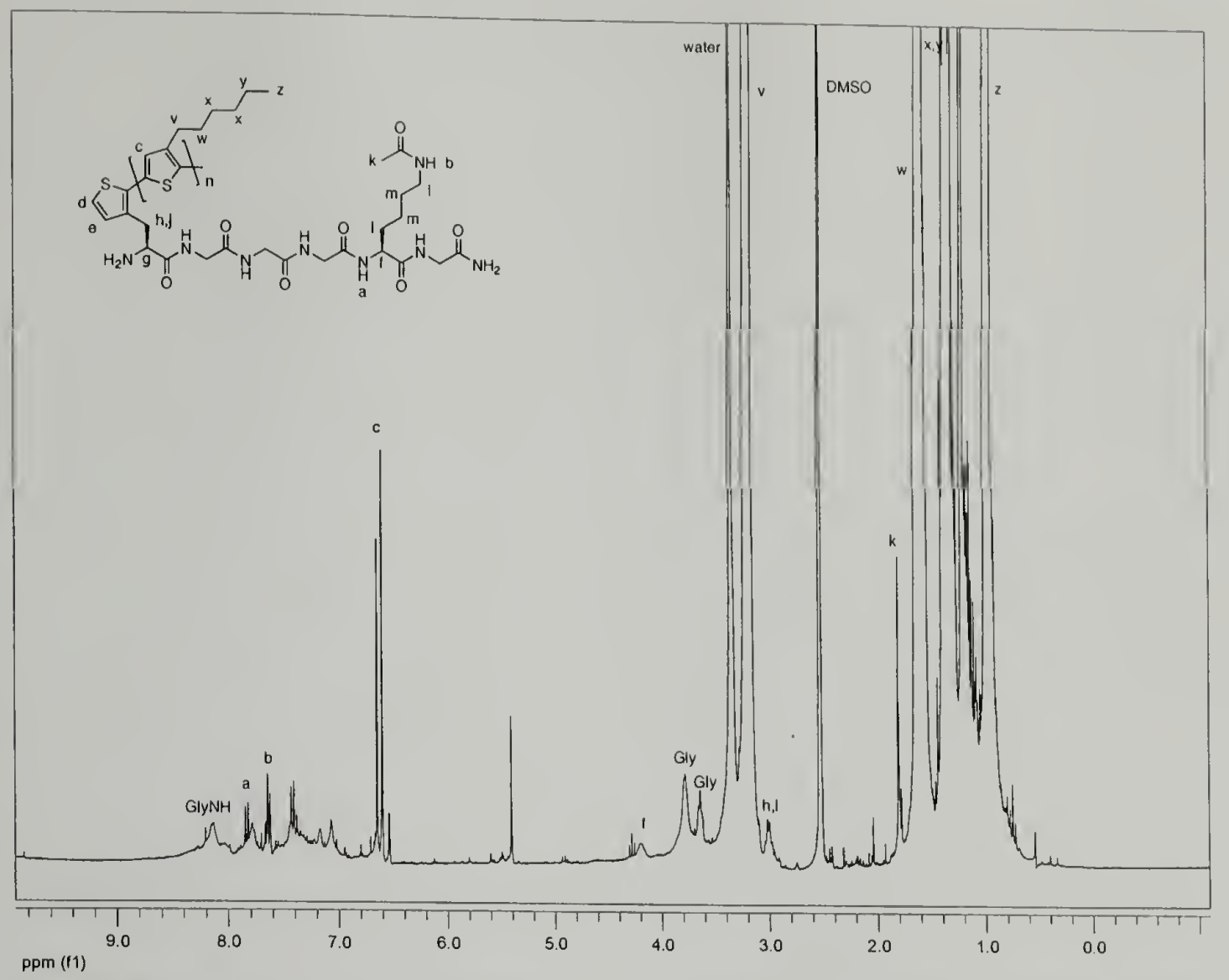

Figure 4.23. Proton NMR spectrum of poly(3-hexylthiophene)/Lys(Ac) peptide copolymer (300 MHz, DMSO-d_6).

3-hexylthiophene and the l protons of the biocytin residue results in a ratio of 89:1. Assuming that only one peptide is incorporated into each copolymer, this results in an average degree of polymerization of 60. Based on the molecular weight of 3-hexylthiophene (168.3 Daltons) and the peptide (753.3 Daltons), a number average molecular weight of 10 850 g/mol can be estimated. Similarly, integration of the 3-hexylthiophene v protons, and protons f and k of the protected lysine residue, results in a ratio of 80:1:3 (figure 4.25, bottom). With a degree of polymerization of 40 and a peptide molecular weight of 568.7 Daltons, a number average molecular weight of 7300 g/mol can be estimated for the Lys(Ac) copolymer. These estimated molecular weights are consistent with the fluorescence emission maxima observed for both copolymers, described in the next section.

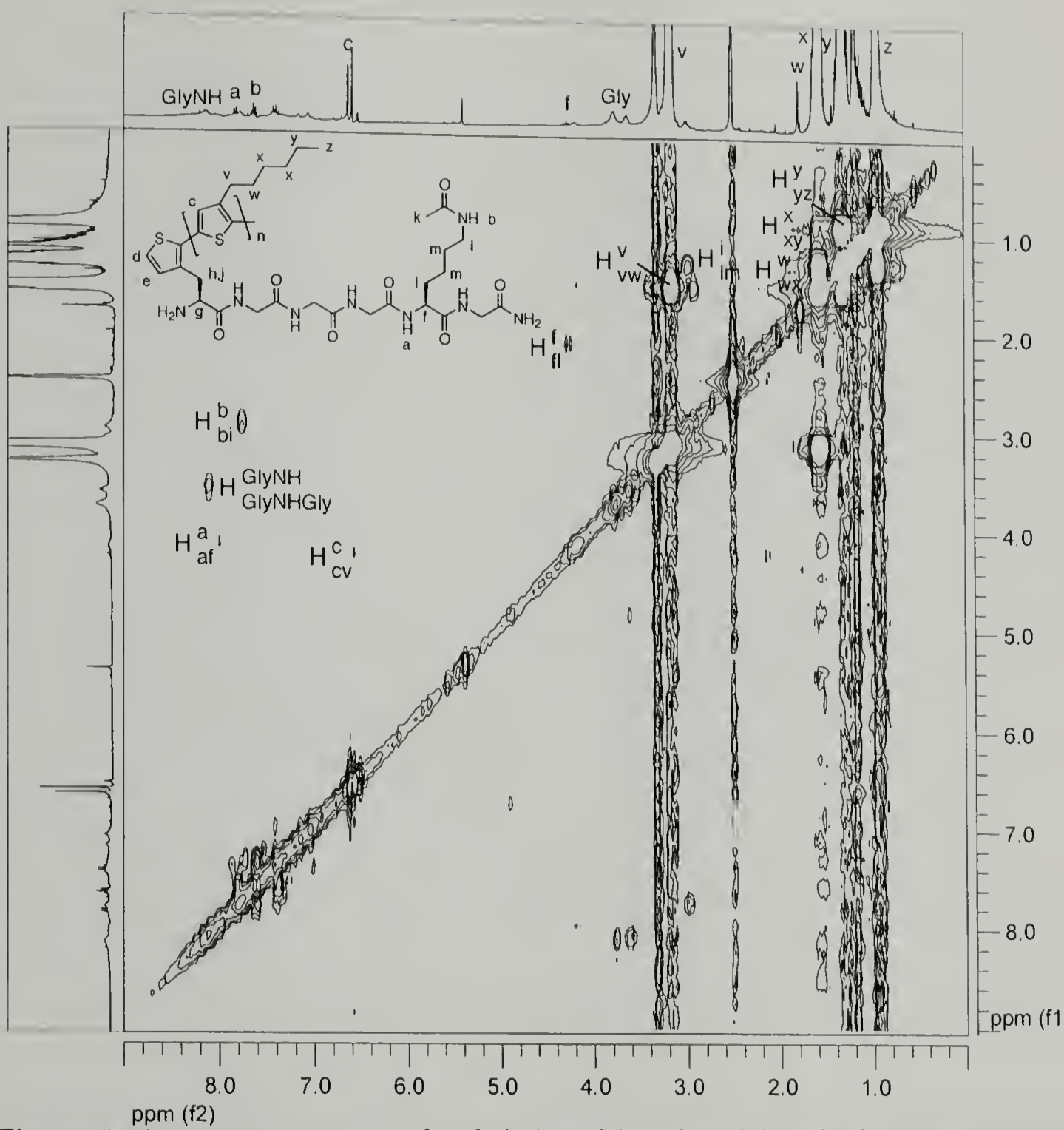

Figure 4.24. COSY spectrum of poly(3-hexylthiophene)/Lys(Ac) peptide copolymer (300 MHz, DMSO-d_6).

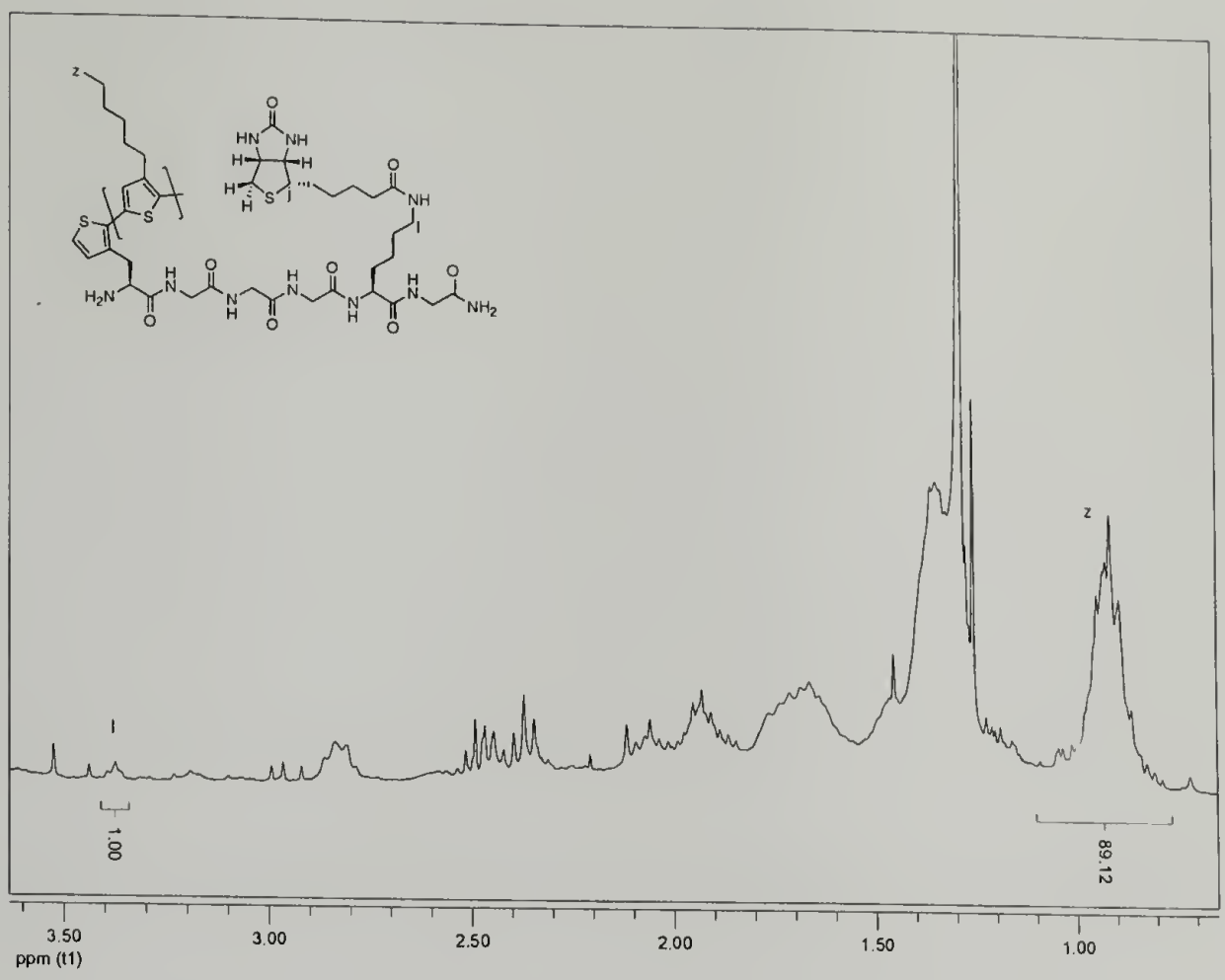

Figure 4.25. Expansions of figures 4.20 (top) and 4.23 (bottom) to estimate number average molecular weight of poly(3-hexylthiophene)/Biocytin and poly(3-hexylthiophene)/Lys(Ac) peptide copolymers, respectively.

4.3.2.3 Fluorescence spectroscopy

The peptide copolymers demonstrated intense fluorescence after cleavage from the solid phase resin, at wavelengths comparable to the copolymers containing only 3-thienylalanine shown in the previous chapter. Fluorescence was observed in aqueous and organic solvents, and in the solid-state as spots on glass slides. Representative spectra of the copolymers in PBS buffer are shown in figure 4.26. It was anticipated that binding of streptavidin to the biotin functionality would cause the poly(3-hexylthiophene) backbone to deviate from coplanarity, resulting in a fluorescence emission shift to lower wavelengths. However, as shown in figure 4.26, only quenching is observed.

There are at least two possible explanations for this observation. First, the NMR spectra of the copolymers indicate high degrees of polymerization (40 to 60 3-hexylthiophene units). If the peptide was grafted to the conjugated polymer in the middle of the conjugated polymer chain, binding could halve the effective conjugation length to 20 to 30 3-hexylthiophene units. But, the NMR data indicate that the conjugated polymer chain grows from only one side of the 3-thienylalanine thiophene ring – there are strong signals for the protons at the 4 and 5 positions. Therefore, binding of streptavidin might cause a deviation from coplanarity for only the first few 3-hexylthiophene units. For conjugated chains with these high degrees of polymerization, this would result in a shift of only a few nanometers. A second possible explanation is the proximity of the biotin moiety to the conjugated polymer backbone. A triglycine spacer was included in the peptide design to ensure the biotin moiety would not be sterically blocked by the conjugated polymer so that it could not bind streptavidin. However, if this distance is too great, then the conjugated polymer backbone might not feel the influence of streptavidin complex formation. One way to check this possibility is to study the fluorescence quenching observed in figure 4.26.

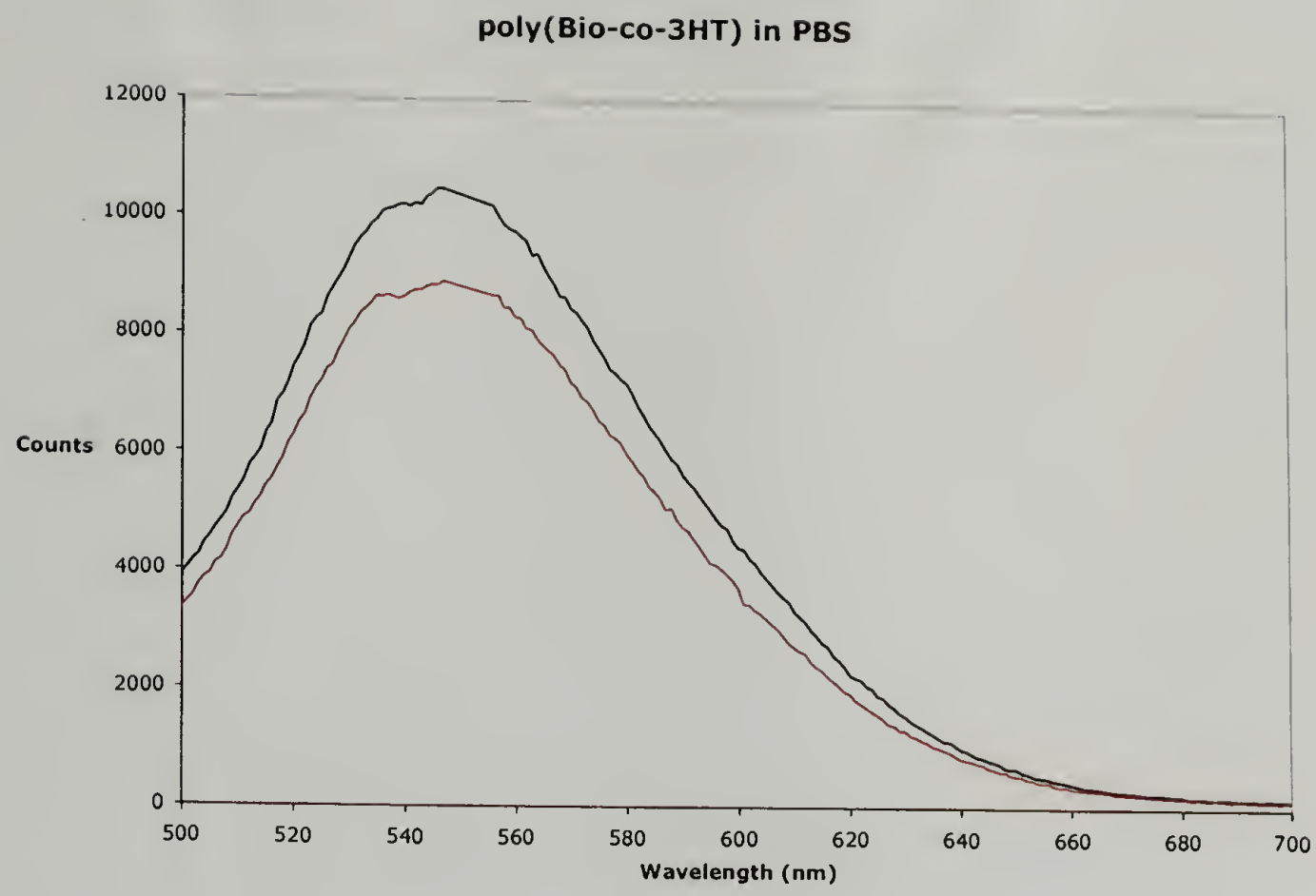

Figure 4.26. Fluorescence emission spectra of poly(Bio-co-3HT) (top) and poly(Lys-co-3HT) (bottom) in PBS buffer with excitation at 450 nm, **before** and after 1 hr incubation with 150 nM streptavidin.

Biotin-fluorophore conjugates with short spacers (about 14 atoms) are effectively quenched when bound to avidin or streptavidin.[40] As a result, biotin-fluorophore conjugates are more often used to measure avidin or streptavidin concentration by fluorescence quenching rather than to directly fluorescently label (strept)avidin. Gruber et al. synthesized biotin-poly(ethylene glycol) conjugates, and found that conjugates with 18 or 43 ethylene glycol repeat units preserved fluorescence even after (strept)avidin binding.[41,42] There are 19 atoms between the poly(thiophene) component and the biotin component in poly(Bio-co-3HT), an intermediate distance which could result in partial quenching of fluorescence. Fluorescence quenching of poly(Bio-co-3HT) can be compared with poly(LysAc-co-3HT), which should have nearly identical fluorescence properties but not bind to (strept)avidin.

The copolymer solutions were diluted in THF to an absorption of 0.05 units at 450 nm, and 10 μL dissolved in 3000 μL of SSC buffer. The fluorescence emission spectra were then measured with excitation at 450 nm as 2 μL aliquots of 1 μg/μL unlabeled avidin in SSC were added. The integrals of the emission spectra can be plotted using the Stern-Volmer equation (equation 3.6), as shown in figure 4.27. The slope of the line provides the Stern-Volmer constant K, which in turn is dependent on the bimolecular quenching constant and the fluorophore lifetime in the absence of quencher. The Stern-Volmer constants are 1.26×10^{6} M^{-1} and 1.71×10^{6} M^{-1} for poly(LysAc-co-3HT) and poly(Bio-co-3HT), respectively.

The fluorescence lifetimes τ_0 of poly(3-hexylthiophene)s in chloroform and THF are around 0.6 ns,[43,44] and can be used to estimate the bimolecular quenching constant k_q from equation 3.6. For poly(LysAc-co-3HT) and poly(Bio-co-3HT), these values are 2.1×10^{15} $M^{-1}s^{-1}$ and 2.9×10^{15} $M^{-1}s^{-1}$, respectively. These values are higher than what would be expected for diffusion-controlled quenching (about 1×10^{10} $M^{-1}s^{-1}$), indicating that there is some type of binding interaction between the fluorophore and the quencher.[45] The hydrophobic poly(3-hexylthiophene) block

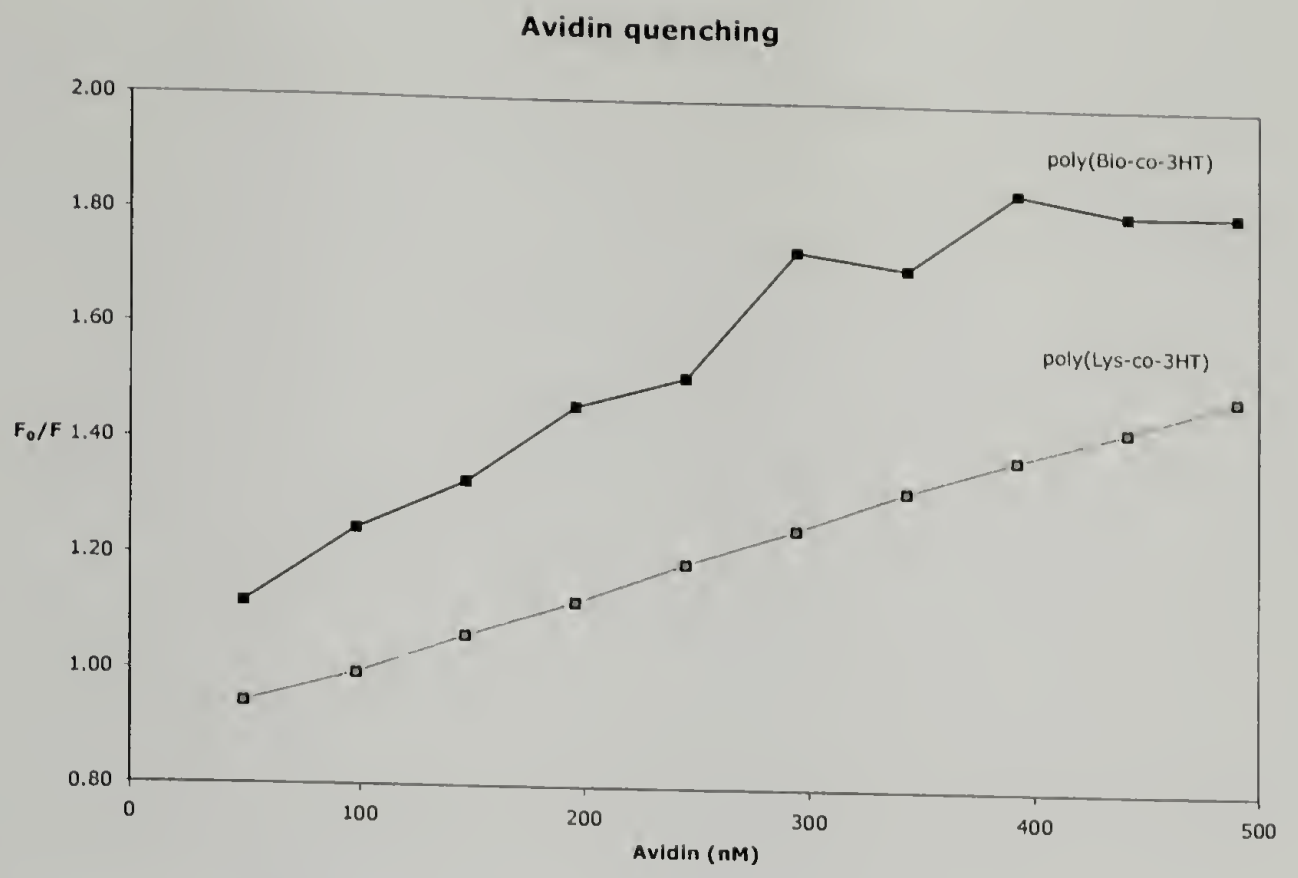

Figure 4.27. Stern-Volmer plots of quenching of poly(Bio-co-3HT) and poly(LysAc-co-3HT) with avidin in SSC buffer.

would be expected to be barely soluble in buffer without the peptide block, and so interactions with the avidin surface could be more favorable. Non-specific interactions with avidin appear to be comparable for both copolymers; however, they could be reduced by using a water-soluble poly(thiophene) rather than poly(3-hexylthiophene).

4.4 Conclusions

In summary, the two peptides "LysAc" and "Bio" were synthesized on HMBA solid-phase resin, as demonstrated by LC-MS/MS and by multidimensional NMR spectroscopy. The contaminants detected by liquid chromatography probably result from acetylation of the peptide terminal amine groups, based on partial agreement of the observed ions with the values calculated for such a modification. Assignment of the 1D proton NMR spectra of the peptides before copolymerization

was accomplished by examining through-bond connections detected by 2D correlation spectroscopy. After copolymerization, the largest signals in the proton NMR spectra correspond to the 3-hexylthiophene side chains, indicating successful polymerization. The peptides remain intact after oxidative polymerizations, with many of the cross peaks observed before polymerization preserved. Number average molecular weights of 7300 and 10 850 g/mol were estimated for the poly(LysAc-co-3HT) and poly(Bio-co-3HT) copolymers, based on integration of resolvable proton signals in the one-dimensional spectrum. These high molecular weights were confirmed by fluorescence emission maxima around 550 nm in buffered aqueous solutions, organic solvents, and in the solid phase. A shift in fluorescence emission was not observed after incubation with streptavidin, which may be due to the high degrees of polymerization or to the length of the peptide linker.

4.5 References

(1) Wilchek, M.; Bayer, E. A. Introduction to Avidin-Biotin Technology. In *Methods in Enzymology*, Vol. 184; Wilchek, M.; Bayer, E. A., Eds.; Academic: San Diego, 1990.

(2) Haugland, R. P. *Handbook of Fluorescent Probes and Research Products;* Molecular Probes: Eugene, OR, 9th ed.; 2002.

(3) Bodanszky, M. *Peptide Chemistry;* Springer-Verlag: Heidelberg, 1988.

(4) Sheehan, J. C.; Hess, G. P. *J. Am. Chem. Soc.* **1955,** *77,* 1067-1068.

(5) Sheehan, J. C.; Goodman, M.; Hess, G. P. *J. Am. Chem. Soc.* **1956,** *78,* 1367-1369.

(6) DeTar, D. F.; R., S. *J. Am. Chem. Soc.* **1966,** *88,* 1013-1019.

(7) DeTar, D. F.; Silverstein, R. *J. Am. Chem. Soc.* **1966,** *88,* 1020-1023.

(8) DeTar, D. F.; Silverstein, R.; Rogers, F. F. *J. Am. Chem. Soc.* **1966,** *88,* 1024-1030.

(9) König, W.; Geiger, R. *Chem. Ber. Recl.* **1970,** *103,* 788-798.

(10) Castro, B.; Dormoy, J. R.; Evin, G.; Selve, C. *Tetrahedron Lett.* **1975,** 1219-1222.

(11) Coste, J.; Le-Nguyen, D.; Castro, B. *Tetrahedron Lett.* **1990,** *31,* 205-208.

(12) Coste, J.; Frérot, E.; Jouin, P.; Castro, B. *Tetrahedron Lett.* **1991,** *32,* 1967-1970.

(13) Knorr, R.; Trzeciak, A.; Bannwarth, W.; Gillessen, D. *Tetrahedron Lett.* **1989,** *30,* 1927-1930.

(14) Dourtoglou, V.; Ziegler, J. C.; Gross, B. *Tetrahedron Lett.* **1978,** 1269-1272.

(15) Dourtoglou, V.; Gross, B.; Lambropoulou, V.; Zioudrou, C. *Synthesis-Stuttgart* **1984,** 572-574.

(16) Carpino, L. A. *J. Am. Chem. Soc.* **1993,** *115,* 4397-4398.

(17) Carpino, L. A.; Imazumi, H.; El-Faham, A.; Ferrer, F. J.; Zhang, C. W.; Lee, Y. S.; Foxman, B. M.; Henklein, P.; Hanay, C.; Mügge, C.; Wenschuh, H.; Klose, K.; Beyermann, M.; Bienert, M. *Angew. Chem. Int. Ed.* **2002,** *41,* 442-445.

(18) Bergmann, M.; Zervas, L. *Ber. Dtsch. Chem. Ges.* **1932,** *65,* 1192-1201.

(19) Carpino, L. A.; Han, G. Y. *J. Am. Chem. Soc.* **1970,** *92,* 5748-5749.

(20) Carpino, L. A.; Han, G. Y. *J. Org. Chem.* **1972,** *37,* 3404-3409.

(21) Story, S. C.; Aldrich, J. V. *Int. J. Pept. Protein Res.* **1992,** *39,* 87-92.

(22) Bateman, W. G. *J. Biol. Chem.* **1916,** *26,* 263-291.

(23) Kögl, F.; Tönnis, B. *Z. Physiol. Chem.* **1936,** *242,* 43-78.

(24) György, P. Biotin. In *The Vitamins: Chemistry, physiology, pathology,* Vol. 1; Sebrell, W. H.; Harris, R. S., Eds.; Academic: New York, 1954.

(25) Lynen, F.; Knappe, J.; Lorch, E.; Jütting, G.; Ringelmann, E. *Angew. Chem.* **1959,** *71,* 481-486.

(26) Wakil, S. J.; Gibson, D. M. *Biochim. Biophys. Acta* **1960,** *41,* 122-129.

(27) Chaiet, L.; Wolf, F. J. *Arch. Biochem. Biophys.* **1964,** *106,* 1-5.

(28) Green, N. M. *Adv. Protein Chem.* **1975,** *29,* 85-133.

(29) Broker, T. R.; Angerer, L. M.; Yen, P. H.; Hershey, N. D.; Davidson, N. *Nucleic Acids Res.* **1978,** *5,* 363-384.

(30) Samuelson, L. A.; Kaplan, D. L.; Lim, J. O.; Kamath, M.; Marx, K. A.; Tripathy, S. K. *Thin Solid Films* **1994,** *242,* 50-55.

(31) Pande, R.; Kamtekar, S.; Ayyagari, M. S.; Kamath, M.; Marx, K. A.; Kumar, J.; Tripathy, S. K.; Kaplan, D. L. *Bioconjugate Chem.* **1996,** *7,* 159-164.

(32) Faïd, K.; Leclerc, M. *Chem. Commun.* **1996,** 2761-2762.

(33) Faïd, K.; Leclerc, M. *J. Am. Chem. Soc.* **1998,** *120,* 5274-5278.

(34) Torres-Rodriguez, L. M.; Roget, A.; Billon, M.; Bidan, G. *Chem. Commun.* **1998,** 1993-1994.

(35) Torres-Rodriguez, L. M.; Billon, M.; Roget, A.; Bidan, G. *J. Electroanal. Chem.* **2002,** *523,* 70-78.

(36) Bidan, G.; Billon, M.; Galasso, K.; Livache, T.; Mathis, C.; Roget, A.; Torres-Rodriguez, L. M.; Vieil, E. *Appl. Biochem. Biotechnol.* **2000,** *89,* 183-193.

(37) Atherton, E.; Sheppard, R. C. *Solid Phase Peptide Synthesis: A Practical Approach;* IRL: Oxford, 1989.

(38) Snyder, A. P. *Interpreting Protein Mass Spectra: A Comprehensive Resource;* Oxford University: New York, 2000.

(39) Sanders, J. K. M.; Hunter, B. K. *Modern NMR spectroscopy: A guide for chemists;* Oxford University: Oxford, 2nd ed.; 1993.

(40) Gruber, H. J.; Marek, M.; Schindler, H.; Kaiser, K. *Bioconjugate Chem.* **1997,** *8,* 552-559.

(41) Kaiser, K.; Marek, M.; Haselgrübler, T.; Schindler, H.; Gruber, H. J. *Bioconjugate Chem.* **1997,** *8,* 545-551.

(42) Marek, M.; Kaiser, K.; Gruber, H. J. *Bioconjugate Chem.* **1997,** *8,* 560-566.

(43) Linton, J. R.; Frank, C. W.; Rughooputh, S. *Synth. Met.* **1989,** *28,* C393-C398.

(44) Belletête, M.; Mazerolle, L.; Desrosiers, N.; Leclerc, M.; Durocher, G. *Macromolecules* **1995,** *28,* 8587-8597.

(45) Lakowicz, J. *Principles of Fluorescence Spectroscopy;* Kluwer Academic/Plenum: New York, 2nd ed.; 1999.

CHAPTER 5

CONCLUSIONS AND FUTURE DIRECTIONS

5.1 Conclusions

This thesis has described the synthesis of graft copolymers of peptides and conjugated polymers linked by the artificial amino acid 3-thienylalanine. This was accomplished using solid phase synthesis, enabling the separation of poly(3-hexylthiophene) homopolymer from the desired copolymer by exhaustive Soxhlet extraction. A solid phase resin linker stable under oxidative polymerization conditions was selected based on measurement of amino acid protecting groups and elemental analysis. Conditions which significantly affected the copolymerization, as measured by fluorescence spectroscopy, were identified using a two-level factorial design with eight factors.

Peptides with glycine spacers between 3-thienylalanine and a biotin-containing residue were synthesized and characterized by LC-MS/MS and two dimensional NMR spectroscopy. The factors found to be statistically significant were used to determine copolymerization conditions. Degrees of polymerization between 40 and 60 3-hexylthiophene units were estimated from the NMR spectra, and confirmed by the long fluorescence emission wavelengths. A shift in fluorescence emission was not observed upon incubation of the biotin-containing copolymer with streptavidin, which may be due to the length of the conjugated polymer backbone, or to the distance between the biotin moiety and the conjugated polymer backbone.

5.2 Future directions

While this work has described the graft copolymerization using peptides immobilized on a solid support, the technique could be generally applicable for any system where one component is assembled step-wise on a resin, and where purification would be difficult without immobilization of the desired copolymer. The polymerization catalyst need not be limited to ferric chloride, but to any coupling reaction with orthogonal chemistry (i.e., the immobilized component is not degraded during the second polymerization reaction). Some opportunities for future experimentation are described below, ordered approximately by increasing departure from the current work.

5.2.1 Comonomers

The most obvious experiment to propose is changing the comonomer to another substituted thiophene. Two kinds of monomers in particular warrant exploration. The first is a water-soluble thiophene, such as 3-thiophene acetic acid (3TAA). Osada et al. have noted abrupt changes in both viscosity and UV/vis absorbance spectra of poly(3TAA) over a relatively narrow pH range (pH 5–6).[1] After crosslinking with a diamine, the swelling and conductivity of poly(3TAA) gels showed similar sensitivity to pH.[2] An electroresponsive gel incorporating specific peptide sequences might be useful in biomaterials applications.[3]

A second interesting comonomer would be 3,4-ethylenedioxythiophene (EDOT). As described in section 1.2.4, PEDOT's stability, conductivity, and transparency have made it the material of choice in numerous applications. By blocking the 3- and 4-positions of the heterocyclic ring, mislinkages during polymerization are avoided.[4] And, if the ethylene bridge is substituted so that two chiral centers are created, then the regioregularity of the resulting polymer is preordained.[5] (This strategy is similar to the poly(3,4-bis((*S*)-2-methylbutoxy)thiophene) reported ear-

lier by Meijer et al.[6])

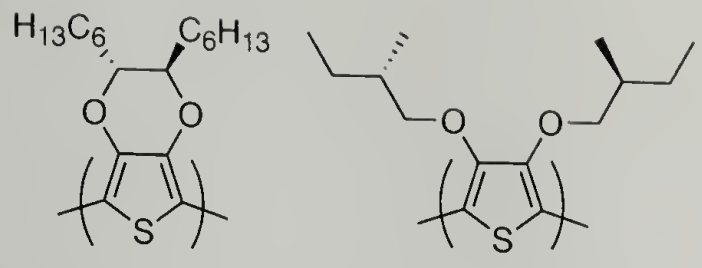

Finally, EDOT is oxidized at a relatively low potential (1.2 V vs. Ag/Ag^+). Therefore, it may be possible to synthesize graft copolymers of peptides and PEDOT, with perfect regioregularity – even with chiral centers – by electrochemical rather than chemical means. Because of the lack of mislinkages, there would not be insoluble, crosslinked material to contaminate the resin-immobilized copolymer, so the ratio of homopolymer to copolymer could be much higher and still permit purification. Electrochemical copolymerization, gentler and without the by-products of oxidative copolymerization, might then be used to synthesize copolymers under less harsh conditions. This might permit the use of longer peptide sequences, or other defined-sequence biopolymers.

5.2.2 Peptide sequences

Given the ability to cast conducting graft copolymers into films, an exciting extension of this work would be the formation of conducting films with cell adhesion peptide sequences. For example, incorporation of the fibronectin-derived RGD and CS5 cell-binding domains into artificial elastin-like peptides has been shown to significantly increase the adhesion of endothelial cells to the elastin-like films.[7,8] Peptide sequences which promote specific adhesion to a variety of cell types have been identified.[9]

Given the conductive properties of our graft copolymers, incorporation of a sequence that binds neurons would be especially interesting. Patel and Poo first noted enhanced growth of *Xenopus laevis* neurons when cultured in the presence of an external electric field.[10] More recently, Langer et al. noted enhancement of

neurite outgrowth of rat PC-12 nerve cells grown on poly(pyrrole) films subjected to electrical stimulation.[11] Sephel et al. identified a 19-amino acid sequence within the A chain of laminin which promoted neuronal cell adhesion, spreading, migration, and neurite outgrowth. Moreover, by testing smaller sequences within the 19-amino acid sequence, they found that the pentapeptide IKVAV (Ile-Lys-Val-Ala-Val) was the active site for cell adhesion and neurite outgrowth.[12] Therefore, this IKVAV sequence would be an excellent target for synthesis of a neuron-binding conducting graft copolymer. The copolymer could be designed as part of a device where the neuron binds to a specific location on an electrical circuit, such as part of a field-effect transistor.[13,14]

5.2.3 Other sequence-defined biopolymers

By synthesizing the appropriate thiophene-functionalized monomer, any biopolymer which can be assembled by solid phase synthesis can have a conducting polymer graft. For many years, the only other biopolymers synthesized on a solid support were oligonucleotides.[15] In 1997, Garnier et al. electrochemically synthesized a poly(pyrrole) grafted with a 14-nucleoside pendant group. When incubated with the complementary nucleoside, the oxidation potential of the shifted to higher voltages and the current intensity decreased. This was attributed to conformational changes in the backbone caused by the bulky hybridized oligonucleotide.[16] A similar strategy was later extended to nucleoside-functionalized poly(thiophene)s.[17] In both these cases, the graft copolymer was prepared by coupling an amino-functionalized oligonucleoside to a carboxylic acid-functionalized, electrochemically-prepared polymer film. In our system, where the oligonucleoside is immobilized on a solid support, excess oligonucleoside would not be required to reach high degrees of attachment.

Recently, Seeberger et al. have designed protection and coupling chemistries for the solid phase synthesis of oligosaccharides.[18] The problem was difficult to solve, because four hydroxyl groups on each monosaccharide need to be protected and deprotected, compared with one amino group on an amino acid, or one hydroxyl group on a nucelobase.[19] Synthesis of an thiophene-functionalized monosaccharide could lead to conjugated polymer/polysaccharide grafts, which might be useful for studying the interactions of oligosaccharides and glycoconjugates in nature, using the sensitive electrochemical and spectroscopic detection techniques made possible by the poly(thiophene) graft.

5.3 References

(1) Kim, B. S.; Chen, L.; Gong, J. P.; Osada, Y. *Macromolecules* **1999,** *32,* 3964-3969.

(2) Chen, L.; Kim, B.; Nishino, M.; Gong, J. P.; Osada, Y. *Macromolecules* **2000,** *33,* 1232-1236.

(3) Petka, W. A.; Harden, J. L.; McGrath, K. P.; Wirtz, D.; Tirrell, D. A. *Science* **1998,** *281,* 389-392.

(4) Groenendaal, L.; Zotti, G.; Aubert, P. H.; Waybright, S. M.; Reynolds, J. R. *Adv. Mater.* **2003,** *15,* 855-879.

(5) Caras-Quintero, D.; Bäuerle, P. *Chem. Commun.* **2004,** 926-927.

(6) Langeveld-Voss, B. M. W.; Janssen, R. A. J.; Meijer, E. W. *J. Mol. Struct.* **2000,** *521,* 285-301.

(7) Heilshorn, S. C.; DiZio, K. A.; Welsh, E. R.; Tirrell, D. A. *Biomaterials* **2003,** *24,* 4245-4252.

(8) Liu, J. C.; Heilshorn, S. C.; Tirrell, D. A. *Biomacromolecules* **2004,** *5,* 497-504.

(9) Hersel, U.; Dahmen, C.; Kessler, H. *Biomaterials* **2003,** *24,* 4385-4415.

(10) Patel, N.; Poo, M. M. *J. Neurosci.* **1982,** *2,* 483-496.

(11) Schmidt, C. E.; Shastri, V. R.; Vacanti, J. P.; Langer, R. *Proc. Natl. Acad. Sci. U.S.A.* **1997,** *94,* 8948-8953.

(12) Tashiro, K.; Sephel, G. C.; Weeks, B.; Sasaki, M.; Martin, G. R.; Kleinman, H. K.; Yamada, Y. *J. Biol. Chem.* **1989,** *264,* 16174-16182.

(13) Fromherz, P.; Offenhäusser, A.; Vetter, T.; Weis, J. *Science* **1991,** *252,* 1290-1293.

(14) Kaul, R. A.; Syed, N. I.; Fromherz, P. *Phys. Rev. Lett.* **2004,** *92,* 038102.

(15) Letsinger, R. L.; Mahadeva, V. *J. Am. Chem. Soc.* **1965**, *87*, 3526-3527.

(16) Korri-Youssoufi, H.; Garnier, F.; Srivastava, P.; Godillot, P.; Yassar, A. *J. Am. Chem. Soc.* **1997**, *119*, 7388-7389.

(17) Lee, T. Y.; Shim, Y. B. *Anal. Chem.* **2001**, *73*, 5629-5632.

(18) Plante, O. J.; Palmacci, E. R.; Seeberger, P. H. *Science* **2001**, *291*, 1523-1527.

(19) Dörwald, F. Z. *Organic Synthesis on Solid Phase;* Wiley-VCH: Weinheim, 2000.

APPENDIX

SYNTHESIS AND CHARACTERIZATION OF 3-THIENYLALANINE

A.1 Introduction

During the course of this work, the commercial availability of the monomer β-3-thienyl-DL-alanine (3TA) has been inconsistent, requiring the synthesis of moderate quantities of 3TA at various stages. Two syntheses of 3TA were reported in 1949, one by Dittmer et al. via a 2-bromo-3-bromomethylthiophene intermediate,[1,2] and a second by Campaigne et al. using a more convenient 3-bromomethyl intermediate.[3-5] More recent work using rhodium catalysts[6] or biotransformations in *E. coli*[7] have also been reported. An adaptation of the synthesis reported by Campaigne et al. is described below (figure A.1), with additional clarifications based on numerous executions of this synthesis at various scales.

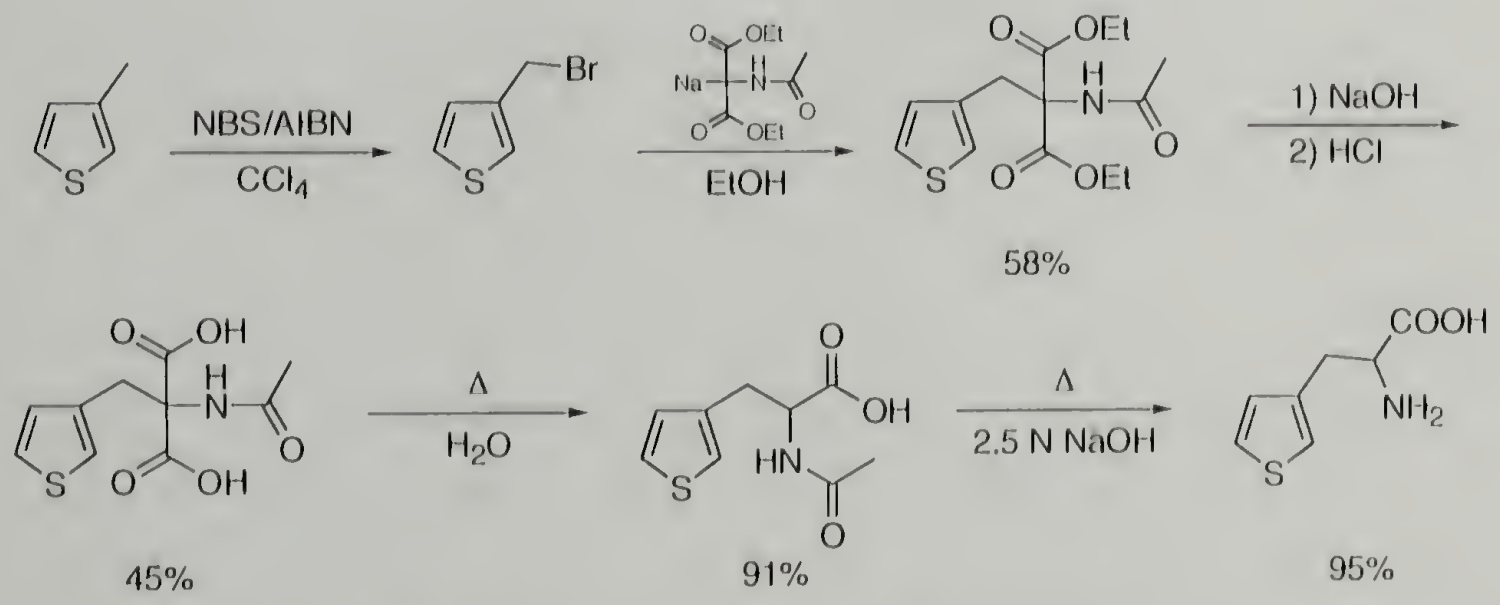

Figure A.1. Synthesis of 3-thienylalanine.

A.2 Experimental

A.2.1 Materials

3-Methylthiophene (98%) obtained from Aldrich (Milwaukee, WI) was dried with sodium sulfate and distilled under reduced pressure (bp 114 °C/ 738 mm) from sodium metal. *N*-Bromosuccinimide (NBS, 99%) from Aldrich was recrystallized from boiling water and dried *in vacuo* over phosphorous pentoxide. Diethyl acetamidomalonate (98%) from Aldrich was recrystallized from benzene and petroleum ether. Azobis(isobutyronitrile) (AIBN, 98%) from Aldrich was recrystallized from methanol. Potassium bromide (99+%, FT-IR grade) from Aldrich was recrystallized from water and heated *in vacuo* at 130 °C for four hours. Carbon tetrachloride and sodium from Aldrich, and ethanol from EMD Chemicals (Gibbstown, NJ) were used as received.

A.2.2 Characterization

^{1}H NMR spectra were obtained on a 300 MHz General Electric QE-300 Plus, using deuterated methanol, acetic acid, or water (Aldrich). IR spectra were run on a Perkin-Elmer 1600 FT-IR using potassium bromide pellets (sample 1% w/w) in transmission mode.

A.2.3 Diethyl 3-thienylacetamidomalonate

3-Methylthiophene (19 ml, 0.20 mol) dissolved in 100 ml CCl_4 is brought to reflux, followed by addition of 35.6 g (0.20 mol) NBS and 0.1 g AIBN with direct illumination by a 300 W halogen lamp. When addition of subsequent 0.1 g portions of AIBN causes no further reaction, the reaction mixture is cooled to room temperature, and the precipitated succinimide is filtered. This 3-thienylmethylbromide solution is added to a 0.5 M ethanolic solution of sodiodiethylacetamidomalonate. This sodioester is previously prepared by adding 43.4 g (0.2 mol) diethylacetamidomalonate to a solution of 5.1 g (0.22 mol) sodium in 400 ml absolute ethanol.

The mixture is heated at 60 °C for two hours, followed by filtration of the precipitated sodium bromide. After the filtrate is concentrated to less than 100 ml by rotary evaporation, the residue is triturated using an overhead paddle mixer with an equal volume of petroleum ether, forming a yellow powder of diethyl 3-thienylacetamidomalonate which is filtered and dried. This crude product can be recrystallized from ethanol and water (50% v/v). Yield: 38 g (58%). ^{1}H NMR ($CDCl_3$) δ: 1.29 (t, 6H, CH_2CH_3), 2.04 (s, 3H, C=OCH_3), 3.70 (s, 2H, CCH_2), 4.26 (q, 4H, CH_2CH_3), 6.62 (dd, 1H, SCHC*H*C), 6.76 (d, 1H, SC*H*CCH), 6.91 (dd, SC*H*CHC) ppm. FT-IR ν: 1747.1 (C=OOCH_2 stretch), 1644.3 (C=O*N*H stretch), 1515.0 (C=O*NH* bend), 1193.3 (C=OOCH_2 stretch) cm^{-1}.

A.2.4 3-Thienylacetamidomalonic acid

In a covered beaker, 6.3 g (0.02 mol) diethyl 3-thienylacetamidomalonate and 20 ml 10% w/v NaOH in H_2O are mixed to a paste and allowed to stand, with occasional mixing, until dissolution is complete (around 36 hours). The resulting solution is then filtered, cooled in ice, and neutralized with 4.74 ml concentrated HCl. The mixture is allowed to stand at room temperature for an hour to permit growth of white crystals, which can be filtered, washed with ice water, and air-dried. Yield: 2.01 g (45%). ^{1}H NMR (MeOD) δ: 2.00 (s, 3H, C=OCH_3), 3.63 (s, 2H, CCH_2), 6.83 (dd, 1H, SCHC*H*C), 7.02 (d, 1H, SC*H*CCH), 7.29 (dd, SC*H*CHC) ppm. FT-IR ν: 2919.2 (C=O*OH* stretch), 1738.3 (C=O*O*H stretch), 1617.9 (C=O*N*H stretch), 1525.3 (C=O*NH* bend) cm^{-1}.

A.2.5 *N*-Acetyl-β-3-thienylalanine

1.35 g (0.006 mol) 3-thienylacetamidomalonic acid is suspended in 15 ml H_2O, refluxed for two hours, and then rotary evaporated to near dryness. After cooling, the white precipitate is collected, washed with cold water, and air-dried. Yield: 0.988 g (91%). ^{1}H NMR (MeOD) δ: 1.90 (s, 3H, C=OCH_3), 3.01 (dd, 1H, CCH_2),

3.20 (dd, 1H, CCH_2), 4.63 (t, 1H, CH_2CHNH), 6.98 (dd, 1H, SCHC*H*C), 7.12 (d, SC*H*CCH), 7.32 (dd, SC*H*CHC) ppm. FT-IR ν: 2907.5 (C=O*OH* stretch), 1700.2 (*C*=OOH stretch), 1618.2 (*C*=ONH stretch), 1557.0 (C=O*NH* bend) cm^{-1}.

A.2.6 β-3-Thienylalanine

N-Acetyl-β-3-thienylalanine (0.544 g, 0.003 mol)and 5 ml 2.5 N NaOH are refluxed for five hours. The condenser is removed for the last half-hour to permit concentration of the reaction mixture to about half of its original volume. The solution is cooled on ice, and then titrated with concentrated HCl to a pH between 5 and 7. The solution is held at 4 °C for 8 hours, the resulting crystals collected, and washed with ethanol and ether. Yield: 0.40 g (95%). ^{1}H NMR: (DMSO/TFAA) δ: 3.13 (dd, 2H, CHCH_2), 4.21 (t, 1H, CH_2CH), 7.01 (dd, 1H, SCHC*H*C), 7.31 (d, 1H, SC*H*CCH), 7.52 (dd, 1H, SC*H*CHC) ppm. FT-IR ν: 3095.5 (broad CHNH_3^+ stretch), 2351.1 (asymmetric CHNH_3^+ bend overtone), 1625.2 (asymmetric CHNH_3^+ bend), 1584.1 (asymmetric CHCOO^- stretch), 1501.8 (symmetric CHNH_3^+ bend), 1413.7 (symmetric CHCOO^- stretch) cm^{-1}.

A.3 References

(1) Dittmer, K. *J. Am. Chem. Soc.* **1949,** *71,* 1205-1207.

(2) Dunn, F. W.; Dittmer, K. *J. Biol. Chem.* **1951,** *188,* 263-273.

(3) Campaigne, E.; LeSuer, W. M. *J. Am. Chem. Soc.* **1948,** *70,* 1555-1558.

(4) Campaigne, E.; Bourgeois, R. C.; Garst, R.; McCarthy, W. C.; Patrick, R. L.; Day, H. G. *J. Am. Chem. Soc.* **1948,** *70,* 2611.

(5) Garst, R. G.; Campaigne, E.; Day, H. G. *J. Biol. Chem.* **1949,** *180,* 1013-1020.

(6) Döbler, C.; Kreuzfeld, H. J.; Krause, H. W.; Michalik, M. *Tetrahedron: Asymmetry* **1993,** *4,* 1833-1842.

(7) Meiwes, J.; Schudok, M.; Kretzschmar, G. *Tetrahedron: Asymmetry* **1997,** *8,* 527-536.

BIBLIOGRAPHY

Abdou, M. S. A., and Holdcroft, S. Oxidation of π-conjugated polymers with gold trichloride – Enhanced stability of the electronically conducting state and electroless deposition of Au(0). *Synth. Met. 60*, 2 (1993), 93–96.

Advanced ChemTech. *Advanced ChemTech Handbook of Combinatorial, Organic & Peptide Chemistry*. Louisville, KY, 2002.

Anderson, M. J., and Whitcomb, P. J. How to save runs, yet reveal breakthrough interactions, by doing only a semifoldover on medium-resolution screening designs. Tech. rep., Stat-Ease, Inc.

Anderson, M. J., and Whitcomb, P. J. *DoE Simplified: Practical Tools for Effective Experimentation*. Productivity, Portland, OR, 2000.

Andersson, M., Ekeblad, P. O., Hjertberg, T., Wennerström, O., and Inganäs, O. Polythiophene with a free amino-acid side-chain. *Polym. Commun. 32*, 18 (1991), 546–548.

Andersson, M. R., Selse, D., Berggren, M., Järvinen, H., Hjertberg, T., Inganäs, O., Wennerström, O., and Österholm, J. E. Regioselective polymerization of 3-(4-octylphenyl)thiophene with $FeCl_3$. *Macromolecules 27*, 22 (1994), 6503–6506.

Andreani, F., Salatelli, E., and Lanzi, M. Novel poly(3,3″- and 3′,4′-dialkyl-2.2′:5′,2″-terthiophene)s by chemical oxidative synthesis: Evidence for a new step towards the optimization of this process. *Polymer 37*, 4 (1996), 661–665.

Arshady, R., Atherton, E., Clive, D. L. J., and Sheppard, R. C. Peptide-synthesis. 1. Preparation and use of polar supports based on poly(dimethylacrylamide). *J. Chem. Soc., Perkin Trans. 1*, 2 (1981), 529–537.

Atherton, E., Logan, C. J., and Sheppard, R. C. Peptide-synthesis. 2. Procedures for solid-phase synthesis using *N*-α-fluorenylmethoxycarbonylamino acids on polyamide supports – Synthesis of substance-p and of acyl carrier protein 65–74 decapeptide. *J. Chem. Soc., Perkin Trans. 1*, 2 (1981), 538–546.

Atherton, E., and Sheppard, R. C. *Solid Phase Peptide Synthesis: A Practical Approach*. IRL, Oxford, 1989.

Barbarella, G. Oligothiophene isothiocyanates as fluorescent markers. *Chem. Eur. J. 8*, 22 (2002), 5072–5077.

Barbarella, G., Bongini, A., and Zambianchi, M. Regiochemistry and conformation of poly(3-hexylthiophene) via the synthesis and the spectroscopic characterization of the model configurational triads. *Macromolecules 27*, 11 (1994), 3039–3045.

Barbarella, G., Favaretto, L., Sotgiu, G., Antolini, L., Gigli, G., Cingolani, R., and Bongini, A. Rigid-core oligothiophene-S,S-dioxides with high photoluminescence efficiencies both in solution and in the solid state. *Chem. Mat. 13*, 11 (2001), 4112–4122.

Barbarella, G., Favaretto, L., Sotgiu, G., Zambianchi, M., Bongini, A., Arbizzani, C., Mastragostino, M., Anni, M., Gigli, G., and Cingolani, R. Tuning solid-state photoluminescence frequencies and efficiencies of oligomers containing one central thiophene-S,S-dioxide unit. *J. Am. Chem. Soc. 122*, 48 (2000), 11971–11978.

Barbarella, G., Zambianchi, M., DiToro, R., Colonna, M., Iarossi, D., Goldoni, F., and Bongini, A. Regioselective oligomerization of 3-(alkylsulfanyl)thiophenes with ferric chloride. *J. Org. Chem. 61*, 23 (1996), 8285–8292.

Barbarella, G., Zambianchi, M., Pudova, O., Paladini, V., Ventola, A., Cipriani, F., Gigli, G., Cingolani, R., and Citro, G. Oligothiophene isothiocyanates as a new class of fluorescent markers for biopolymers. *J. Am. Chem. Soc. 123*, 47 (2001), 11600–11607.

Bartus, J. Electrically conducting thiophene polymers. *J. Macromol. Sci., Chem. A28*, 9 (1991), 917–924.

Bässler, H. Electronic excitation. In *Electronic Materials: The Oligomer Approach*, K. Müllen and G. Wegner, Eds. Wiley-VCH, Weinheim, 1998.

Bateman, W. G. The digestibility and utilization of egg proteins. *J. Biol. Chem. 26*, 1 (1916), 263–291.

Bäuerle, P., and Scheib, S. Molecular recognition of alkali ions by crown-ether-functionalized poly(alkylthiophenes). *Adv. Mater. 5*, 11 (1993), 848–853.

Belletête, M., Mazerolle, L., Desrosiers, N., Leclerc, M., and Durocher, G. Spectroscopy and photophysics of some oligomers and polymers derived from thiophenes. *Macromolecules 28*, 25 (1995), 8587–8597.

Bergmann, M., and Zervas, L. Über ein allgemeines Verfahren der Peptid-Synthese. *Ber. Dtsch. Chem. Ges. 65* (1932), 1192–1201.

Bidan, G., Billon, M., Galasso, K., Livache, T., Mathis, C., Roget, A., Torres-Rodriguez, L. M., and Vieil, E. Electropolymerization as a versatile route for immobilizing biological species onto surfaces - Application to DNA biochips. *Appl. Biochem. Biotechnol. 89*, 2-3 (2000), 183–193.

Bizzarri, P. C., Andreani, F., Della Casa, C., Lanzi, M., and Salatelli, E. Ester-functionalized poly(3-alkylthienylene)s: Substituent effects on the polymerization with $FeCl_3$. *Synth. Met. 75*, 2 (1995), 141–147.

Bodanszky, M. *Peptide Chemistry*. Springer-Verlag, Heidelberg, 1988.

Briehn, C. A., and Bäuerle, P. Design and synthesis of a 256-membered, π-conjugated oligomer library of regioregular head-to-tail coupled quater(3-arylthiophene)s. *J. Comb. Chem. 4*, 5 (2002), 457–469.

Briehn, C. A., Kirschbaum, T., and Bäuerle, P. Polymer-supported synthesis of regioregular head-to-tail-coupled oligo(3-arylthiophene)s utilizing a traceless silyl linker. *J. Org. Chem. 65*, 2 (2000), 352–359.

Briehn, C. A., Schiedel, M. S., Bonsen, E. M., Schuhmann, W., and Bäuerle, P. Single-compound libraries of organic materials: From the combinatorial synthesis of conjugated oligomers to structure-property relationships. *Angew. Chem. Int. Ed. 40*, 24 (2001), 4680–4683.

Broker, T. R., Angerer, L. M., Yen, P. H., Hershey, N. D., and Davidson, N. Electron microscopic visualization of trna genes with ferretin-avidin:biotin labels. *Nucleic Acids Res. 5*, 2 (1978), 363–384.

Brzeziński, B., Grech, E., Malarski, Z., and Sobczyk, L. Protonation of 1,8-bis(dimethylamino)naphthalene by various acids in acetonitrile. *J. Chem. Soc., Perkin Trans. 2*, 6 (1991), 857–859.

Campaigne, E., Bourgeois, R. C., Garst, R., McCarthy, W. C., Patrick, R. L., and Day, H. G. The synthesis of β-3-thienylalanine. *J. Am. Chem. Soc. 70*, 7 (1948), 2611.

Campaigne, E., and LeSuer, W. M. 3-substituted thiophenes. I. *J. Am. Chem. Soc. 70*, 4 (1948), 1555–1558.

Caras-Quintero, D., and Bäuerle, P. Synthesis of the first enantiomerically pure and chiral, disubstituted 3,4-ethylenedioxythiophenes (EDOTs) and corresponding stereo- and regioregular PEDOTs. *Chem. Commun.*, 8 (2004), 926–927.

Carpino, L. A. 1-Hydroxy-7-azabenzotriazole – An efficient peptide coupling additive. *J. Am. Chem. Soc. 115*, 10 (1993), 4397–4398.

Carpino, L. A., and Han, G. Y. 9-Fluorenylmethoxycarbonyl function, a new base-sensitive amino-protecting group. *J. Am. Chem. Soc. 92*, 19 (1970), 5748–5749.

Carpino, L. A., and Han, G. Y. 9-Fluorenylmethoxycarbonyl amino-protecting group. *J. Org. Chem. 37*, 22 (1972), 3404–3409.

Carpino, L. A., Imazumi, H., El-Faham, A., Ferrer, F. J., Zhang, C. W., Lee, Y. S., Foxman, B. M., Henklein, P., Hanay, C., Mügge, C., Wenschuh, H., Klose, K., Beyermann, M., and Bienert, M. The uronium/guanidinium peptide coupling reagents: Finally the true uronium salts. *Angew. Chem. Int. Ed. 41*, 3 (2002), 442–445.

Castro, B., Dormoy, J. R., Evin, G., and Selve, C. Reactions of peptide bond. 4. Benzotriazonyl-*N*-oxytridimelthylamino phosphonium hexafluorophosphate (BOP). *Tetrahedron Lett.*, 14 (1975), 1219–1222.

Chaiet, L., and Wolf, F. J. The properties of streptavidin, a biotin-binding protein produced by Streptomycetes. *Arch. Biochem. Biophys. 106* (1964), 1–5.

Chen, L., Kim, B., Nishino, M., Gong, J. P., and Osada, Y. Environmental responses of polythiophene hydrogels. *Macromolecules 33*, 4 (2000), 1232–1236.

Chen, T. A., O'Brien, R. A., and Rieke, R. D. Use of highly reactive zinc leads to a new, facile synthesis for polyarylenes. *Macromolecules 26*, 13 (1993), 3462–3463.

Chen, T. A., and Rieke, R. D. The first regioregular head-to-tail poly(3-hexylthiophene-2,5-diyl) and a regiorandom isopolymer – Ni vs. Pd catalysis of 2(5)-bromo-5(2)-(bromozincio)-3-hexylthiophene polymerization. *J. Am. Chem. Soc. 114*, 25 (1992), 10087–10088.

Chen, T. A., Wu, X., and Rieke, R. D. Regiocontrolled synthesis of poly(3-alkylthiophenes) mediated by Rieke Zinc – Their characterization and solid-state properties. *J. Am. Chem. Soc. 117*, 1 (1995), 233–244.

Coste, J., Frérot, E., Jouin, P., and Castro, B. Oxybenzotriazole free peptide coupling reagents for *N*-methylated amino-acids. *Tetrahedron Lett. 32*, 17 (1991), 1967–1970.

Coste, J., Le-Nguyen, D., and Castro, B. PyBOP – A new peptide coupling reagent devoid of toxic by-product. *Tetrahedron Lett. 31*, 2 (1990), 205–208.

Datta, D., Wang, P., Carrico, I. S., Mayo, S. L., and Tirrell, D. A. A designed phenylalanyl-tRNA synthetase variant allows efficient in vivo incorporation of aryl ketone functionality into proteins. *J. Am. Chem. Soc. 124*, 20 (2002), 5652–5653.

de Souza, J. M., and Pereira, E. C. Luminescence of poly(3-thiopheneacetic acid) in alcohols and aqueous solutions of poly(vinyl alcohol). *Synth. Met. 118*, 1-3 (2001), 167–170.

Della Casa, C., Andreani, F., Bizzarri, P. C., and Salatelli, E. Characterization of poly(3-hexanoyloxyethyl-2,5-thienylene) synthesized under different conditions – A comparative study. *J. Mater. Chem. 4*, 7 (1994), 1035–1039.

Della Casa, C., Salatelli, E., Andreani, F., and Bizzarri, P. C. Synthesis of new conducting poly(2,5-thienylene)s containing alkylhydroxy and alkylester side-chains. *Makromol. Chem., Macromol. Symp. 59* (1992), 233–246.

DeSimone, J. M., Guan, Z., and Elsbernd, C. S. Synthesis of fluoropolymers in supercritical carbon dioxide. *Science 257*, 5072 (1992), 945–947.

DeTar, D. F., and R., Silverstein. Reactions of carbodiimides. 1. Mechanisms of reactions of acetic acid with dicyclohexylcarbodiimide. *J. Am. Chem. Soc. 88*, 5 (1966), 1013–1019.

DeTar, D. F., and Silverstein, R. Reactions of carbodiimides. 2. Reactions of dicyclohexylcarbodiimide with carboxylic acids in presence of amines and phenols. *J. Am. Chem. Soc. 88*, 5 (1966), 1020–1023.

DeTar, D. F., Silverstein, R., and Rogers, F. F. Reactions of carbodiimides. 3. Reactions of carbodiimides with peptide acids. *J. Am. Chem. Soc. 88*, 5 (1966), 1024–1030.

Diaz-Quijada, G. A., Pinto, B. M., and Holdcroft, S. Regiochemical analysis of water soluble conductive polymers: Sodium poly(ω-(3-thienyl)alkanesulfonates). *Macromolecules 29*, 16 (1996), 5416–5421.

Dittmer, K. The synthesis and microbiological properties of β-3-thienylalanine, a new anti-phenylalanine. *J. Am. Chem. Soc. 71*, 4 (1949), 1205–1207.

Döbler, C., Kreuzfeld, H. J., Krause, H. W., and Michalik, M. Unusual amino-acids. 4. Asymmetric synthesis of thienylalanines. *Tetrahedron: Asymmetry 4*, 8 (1993), 1833–1842.

Doré, K., Dubus, S., Ho, H. A., Lévesque, I., Brunette, M., Corbeil, G., Boissinot, M., Boivin, G., Bergeron, M. G., Boudreau, D., and Leclerc, M. Fluorescent polymeric transducer for the rapid, simple, and specific detection of nucleic acids at the zeptomole level. *J. Am. Chem. Soc. 126*, 13 (2004), 4240–4244.

Dörwald, F. Z. *Organic Synthesis on Solid Phase*. Wiley-VCH, Weinheim, 2000.

Dougherty, M. J., Kothakota, S., Mason, T. L., Tirrell, D. A., and Fournier, M. J. Synthesis of a genetically engineered repetitive polypeptide containing periodic selenomethionine residues. *Macromolecules 26*, 7 (1993), 1779–1781.

Dourtoglou, V., Gross, B., Lambropoulou, V., and Zioudrou, C. *O*-Benzotriazolyl-*N*,*N*,*N*′,*N*′-tetramethyluronium hexafluorophosphate as coupling reagent for the synthesis of peptides of biological interest. *Synthesis-Stuttgart*, 7 (1984), 572–574.

Dourtoglou, V., Ziegler, J. C., and Gross, B. L'Hexafluorophosphate de *O*-benzotriazolyl-*N*,*N*-tetramethyluronium: Un reactif de couplage peptidique nouveau et efficace. *Tetrahedron Lett.*, 15 (1978), 1269–1272.

Dunn, F. W., and Dittmer, K. The synthesis and microbiological properties of some peptide analogues. *J. Biol. Chem. 188*, 1 (1951), 263–273.

Elsenbaumer, R. L., Jen, K.-Y., Miller, G. G., Eckhardt, H., Shacklette, L. W., and Jow, R. Poly(alkyl thiophenes) and poly(substituted heteroaromatic vinylenes): Versatile, highly conductive, processible polymers with tunable properties. In *Electronic Properties of Conjugated Polymers*, H. Kuzmany, M. Mehring, and S. Roth, Eds. Springer, Berlin, 1987.

Elsenbaumer, R. L., Jen, K. Y., and Oboodi, R. Processible and environmentally stable conducting polymers. *Synth. Met. 15*, 2-3 (1986), 169–174.

Englebienne, P., and Weiland, M. Synthesis of water-soluble carboxylic and acetic acid- substituted poly(thiophenes) and the application of their photochemical properties in homogeneous competitive immunoassays. *Chem. Commun.*, 14 (1996), 1651–1652.

Faïd, K., Fréchette, M., Ranger, M., Mazerolle, L., Lévesque, I., Leclerc, M., Chen, T. A., and Rieke, R. D. Chromic phenomena in regioregular and nonregioregular polythiophene derivatives. *Chem. Mat. 7*, 7 (1995), 1390–1396.

Faïd, K., and Leclerc, M. Functionalized regioregular polythiophenes: Towards the development of biochromic sensors. *Chem. Commun.*, 24 (1996), 2761–2762.

Faïd, K., and Leclerc, M. Responsive supramolecular polythiophene assemblies. *J. Am. Chem. Soc. 120*, 21 (1998), 5274–5278.

Fields, G. B., and Noble, R. L. Solid-phase peptide-synthesis utilizing 9-fluorenylmethoxycarbonyl amino acids. *Int. J. Pept. Protein Res. 35*, 3 (1990), 161–214.

Flory, P. J. Phase equilibria in solutions of rod-like particles. *Proc. R. Soc. London, Ser. A 234*, 1196 (1956), 73–89.

Fraleoni-Morgera, A., Della Casa, C., Lanzi, M., and Bizzarri, P. C. Investigation on different procedures in the oxidative copolymerization of a dye-functionalized thiophene with 3-hexylthiophene. *Macromolecules 36*, 23 (2003), 8617–8620.

Fromherz, P., Offenhäusser, A., Vetter, T., and Weis, J. A neuron-silicon junction: A Retzius cell of the leech on an insulated-gate field-effect transistor. *Science 252*, 5010 (1991), 1290–1293.

Frommer, J. E. Conducting polymer solutions. *Acc. Chem. Res. 19*, 1 (1986), 2–9.

Früchtel, J. S., and Jung, G. Organic chemistry on solid supports. *Angew. Chem. Int. Ed. 35*, 1 (1996), 17–42.

Furter, R. Expansion of the genetic code: Site-directed *p*-fluoro-phenylalanine incorporation in *Escherichia coli*. *Protein Sci. 7*, 2 (1998), 419–426.

Gallazzi, M. C., Bertarelli, C., and Montoneri, E. Critical parameters for product quality and yield in the polymerisation of 3,3''-didodecyl-2,2':5',2''-terthiophene. *Synth. Met. 128*, 1 (2002), 91–95.

Garnier, F. Field-effect transistors based on conjugated materials. In *Electronic Materials: The Oligomer Approach*, K. Müllen and G. Wegner, Eds. Wiley-VCH, Weinheim, 1998.

Garst, R. G., Campaigne, E., and Day, H. G. 3-substituted thiophenes. IV. Synthesis of β-3-thienylalanine and its antagonism to phenylalanine in the rat. *J. Biol. Chem. 180*, 3 (1949), 1013–1020.

Gaylord, B. S., Heeger, A. J., and Bazan, G. C. DNA detection using water-soluble conjugated polymers and peptide nucleic acid probes. *Proc. Natl. Acad. Sci. U.S.A. 99*, 17 (2002), 10954–10957.

Gaylord, B. S., Heeger, A. J., and Bazan, G. C. DNA hybridization detection with water-soluble conjugated polymers and chromophore-labeled single-stranded DNA. *J. Am. Chem. Soc. 125*, 4 (2003), 896–900.

Goto, H., Okamoto, Y., and Yashima, E. Metal-induced supramolecular chirality in an optically active polythiophene aggregate. *Chem. Eur. J. 8*, 17 (2002), 4027–4036.

Goto, H., Okamoto, Y., and Yashima, E. Solvent-induced chiroptical changes in supramolecular assemblies of an optically active, regioregular polythiophene. *Macromolecules 35*, 12 (2002), 4590–4601.

Goto, H., and Yashima, E. Electron-induced switching of the supramolecular chirality of optically active polythiophene aggregates. *J. Am. Chem. Soc. 124*, 27 (2002), 7943–7949.

Goto, H., Yashima, E., and Okamoto, Y. Unusual solvent effects on chiroptical properties of an optically active regioregular polythiophene in solution. *Chirality 12*, 5-6 (2000), 396–399.

Green, N. M. Avidin. *Adv. Protein Chem. 29* (1975), 85–133.

Groenendaal, L., Zotti, G., Aubert, P. H., Waybright, S. M., and Reynolds, J. R. Electrochemistry of poly(3,4-alkylenedioxythiophene) derivatives. *Adv. Mater. 15*, 11 (2003), 855–879.

Gruber, H. J., Marek, M., Schindler, H., and Kaiser, K. Biotin-fluorophore conjugates with poly(ethylene glycol) spacers retain intense fluorescence after binding to avidin and streptavidin. *Bioconjugate Chem. 8*, 4 (1997), 552–559.

György, P. Biotin. In *The Vitamins: Chemistry, physiology, pathology*, W. H. Sebrell and R. S. Harris, Eds., vol. 1. Academic, New York, 1954, pp. 525–618.

Harrison, M. G., and Friend, R. H. Optical applications. In *Electronic Materials: The Oligomer Approach*, K. Müllen and G. Wegner, Eds. Wiley-VCH, Weinheim, 1998.

Hasenwinkle, D., Jervis, E., Kops, O., Liu, C., Lesnicki, G., Haynes, C. A., and Kilburn, D. G. Very high-level production and export in *escherichia coli* of a cellulose binding domain for use in a generic secretion- affinity fusion system. *Biotechnol. Bioeng. 55*, 6 (1997), 854–863.

Haugland, R. P. *Handbook of Fluorescent Probes and Research Products*, 9th ed. Molecular Probes, Eugene, OR, 2002.

Heffner, G. W., and Pearson, D. S. Solution processing of a doped conducting polymer. *Synth. Met. 44*, 3 (1991), 341–347.

Heilshorn, S. C., DiZio, K. A., Welsh, E. R., and Tirrell, D. A. Endothelial cell adhesion to the fibronectin CS5 domain in artificial extracellular matrix proteins. *Biomaterials 24*, 23 (2003), 4245–4252.

Hersel, U., Dahmen, C., and Kessler, H. RGD modified polymers: Biomaterials for stimulated cell adhesion and beyond. *Biomaterials 24*, 24 (2003), 4385–4415.

Heuer, H. W., Wehrmann, R., and Kirchmeyer, S. Electrochromic window based on conducting poly(3,4-ethylenedioxythiophene)poly(styrene sulfonate). *Adv. Funct. Mater. 12*, 2 (2002), 89–94.

Ho, H. A., Boissinot, M., Bergeron, M. G., Corbeil, G., Doré, K., Boudreau, D., and Leclerc, M. Colorimetric and fluorometric detection of nucleic acids using cationic polythiophene derivatives. *Angew. Chem. Int. Ed. 41*, 9 (2002), 1548–1551.

Hotta, S. Electrochemical synthesis and spectroscopic study of poly(3-alkylthienylenes). *Synth. Met. 22*, 2 (1987), 103–113.

Hotta, S., Rughooputh, S. D. D. V., and Heeger, A. J. Conducting polymer composites of soluble polythiophenes in polystyrene. *Synth. Met. 22*, 1 (1987), 79–87.

Hotta, S., Rughooputh, S. D. D. V., Heeger, A. J., and Wudl, F. Spectroscopic studies of soluble poly(3-alkylthienylenes). *Macromolecules 20*, 1 (1987), 212–215.

Hotta, S., Soga, M., and Sonoda, N. Novel organosynthetic routes to polythiophene and its derivatives. *Synth. Met. 26*, 3 (1988), 267–279.

Izumi, T., Kobashi, S., Takimiya, K., Aso, Y., and Otsubo, T. Synthesis and spectroscopic properties of a series of beta-blocked long oligothiophenes up to the 96-mer: Revaluation of effective conjugation length. *J. Am. Chem. Soc. 125*, 18 (2003), 5286–5287.

Jabłoński, A. Über den Mechanismus des Photolumineszenz von Farbstoffphosphoren. *Z. Phys. 94* (1935), 38–46.

Jonas, F., Heywang, G., Schmidtberg, W., Heinze, J., and Dietrich, M. US Patent 5 035 926, 1991.

Jung, S. D., Hwang, D. H., Zyung, T., Kim, W. H., Chittibabu, K. G., and Tripathy, S. K. Temperature dependent photoluminescence and electroluminescence properties of polythiophene with hydrogen bonding side chain. *Synth. Met. 98*, 2 (1998), 107–111.

Kaiser, E., Colescot, R. l., Bossinge, C. D., and Cook, P. I. Color test for detection of free terminal amino groups in solid phase synthesis of peptides. *Anal. Biochem. 34*, 2 (1970), 595–598.

Kaiser, K., Marek, M., Haselgrübler, T., Schindler, H., and Gruber, H. J. Basic studies on heterobifunctional biotin-peg conjugates with a 3-(4-pyridyldithio)propionyl marker on the second terminus. *Bioconjugate Chem. 8*, 4 (1997), 545–551.

Kaul, R. A., Syed, N. I., and Fromherz, P. Neuron-semiconductor chip with chemical synapse between identified neurons. *Phys. Rev. Lett. 92*, 3 (2004), 038102.

Kilbinger, A. F. M., Schenning, Aphj, Goldoni, F., Feast, W. J., and Meijer, E. W. Chiral aggregates of α,ω-disubstituted sexithiophenes in protic and aqueous media. *J. Am. Chem. Soc. 122*, 8 (2000), 1820–1821.

Kim, B. S., Chen, L., Gong, J. P., and Osada, Y. Titration behavior and spectral transitions of water-soluble polythiophene carboxylic acids. *Macromolecules 32*, 12 (1999), 3964–3969.

Kirschbaum, T., Azumi, R., Mena-Osteritz, E., and Bäuerle, P. Synthesis and characterization of structurally defined head-to-tail coupled oligo(3-alkylthiophenes). *New J. Chem. 23*, 2 (1999), 241–250.

Kirschbaum, T., and Bäuerle, P. Polymer-supported synthesis of regioregular head-to-tail coupled oligo(3-alkylthiophene)s. *Synth. Met. 119*, 1-3 (2001), 127–128.

Kirschbaum, T., Briehn, C. A., and Bäuerle, P. Efficient solid-phase synthesis of regioregular head-to-tail-coupled oligo(3-alkylthiophene)s up to a dodecamer. *J. Chem. Soc., Perkin Trans. 1 8* (2000), 1211–1216.

Kirshenbaum, K., Carrico, I. S., and Tirrell, D. A. Biosynthesis of proteins incorporating a versatile set of phenylalanine analogues. *ChemBioChem 3*, 2-3 (2002), 235–237.

Knorr, R., Trzeciak, A., Bannwarth, W., and Gillessen, D. New coupling reagents in peptide chemistry. *Tetrahedron Lett. 30*, 15 (1989), 1927–1930.

Kögl, F., and Tönnis, B. Über das Bios-Problem. Darstellung von krystallisertem Biotin aus Eigelb. 20. Mitteilung über pflanzliche Wachstumsstoffe. *Z. Physiol. Chem.* 242 (1936), 43–78.

König, W., and Geiger, R. A new method for synthesis of peptides – Activation of carboxyl group with dicyclohexylcarbodiimide using 1-hydroxybenzotriazoles as additives. *Chem. Ber. Recl. 103*, 3 (1970), 788–798.

Korri-Youssoufi, H., Garnier, F., Srivastava, P., Godillot, P., and Yassar, A. Toward bioelectronics: Specific DNA recognition based on an oligonucleotide-functionalized polypyrrole. *J. Am. Chem. Soc. 119*, 31 (1997), 7388–7389.

Kothakota, S., Mason, T. L., Tirrell, D. A., and Fournier, M. J. Biosynthesis of a periodic protein containing 3-thienylalanine – A step toward genetically-engineered conducting polymers. *J. Am. Chem. Soc. 117*, 1 (1995), 536–537.

Krejchi, M. T., Atkins, E. D. T., Waddon, A. J., Fournier, M. J., Mason, T. L., and Tirrell, D. A. Chemical sequence control of beta-sheet assembly in macromolecular crystals of periodic polypeptides. *Science 265*, 5177 (1994), 1427–1432.

Krische, B., and Zagorska, M. The polythiophene paradox. *Synth. Met. 28*, 1-2 (1989), C263–C268.

Kwon, I., Kirshenbaum, K., and Tirrell, D. A. Breaking the degeneracy of the genetic code. *J. Am. Chem. Soc. 125*, 25 (2003), 7512–7513.

Laakso, J., Järvinen, H., and Skagerberg, B. Recent developments in the polymerization of 3-alkylthiophenes. *Synth. Met. 55*, 2-3 (1993), 1204–1208.

Lakowicz, J.R. *Principles of Fluorescence Spectroscopy*, 2nd ed. Kluwer Academic/Plenum, New York, 1999.

Langeveld-Voss, B. M. W., Janssen, R. A. J., Christiaans, M. P. T., Meskers, S. C. J., Dekkers, Hpjm, and Meijer, E. W. Circular dichroism and circular polarization of photoluminescence of highly ordered poly(3,4-di(S)-2-methylbutoxythiophene). *J. Am. Chem. Soc. 118*, 20 (1996), 4908–4909.

Langeveld-Voss, B. M. W., Janssen, R. A. J., and Meijer, E. W. On the origin of optical activity in polythiophenes. *J. Mol. Struct. 521* (2000), 285–301.

Leclerc, M., Ho, H. A., and Boissinot, M. Canadian Patent Application 2 442 860, 2002.

Lee, T. Y., and Shim, Y. B. Direct DNA hybridization detection based on the oligonucleotide-functionalized conductive polymer. *Anal. Chem. 73*, 22 (2001), 5629–5632.

Lemaire, M., Delabouglise, D., Garreau, R., Guy, A., and Roncali, J. Enantioselective chiral poly(thiophenes). *J. Chem. Soc., Chem. Commun.*, 10 (1988), 658–661.

Letsinger, R. L., and Mahadeva, V. Oligonucleotide synthesis on a polymer support. *J. Am. Chem. Soc. 87*, 15 (1965), 3526–3527.

Li, L., Counts, K. E., Kurosawa, S., Teja, A. S., and Collard, D. M. Tuning the electronic structure and solubility of conjugated polymers with perfluoroalkyl substituents: Poly(3-perfluorooctylthiophene), the first supercritical-CO_2-soluble conjugated polymer. *Adv. Mater. 16*, 2 (2004), 180–183.

Liang, C. Y., and Krimm, S. Infrared spectra of high polymers. 6. Polystyrene. *J. Polym. Sci. 27*, 115 (1958), 241–254.

Lin, J. W. P., and Dudek, L. P. Synthesis and properties of poly(2,5-thienylene). *J. Polym. Sci., Polym. Chem. Ed. 18*, 9 (1980), 2869–2873.

Linton, J. R., Frank, C. W., and Rughooputh, Sddv. Fluorescence studies of poly(3-hexylthiophene) solutions. *Synth. Met. 28*, 1-2 (1989), C393–C398.

Liu, B., Baudrey, S., Jaeger, L., and Bazan, G. C. Characterization of tectoRNA assembly with cationic conjugated polymers. *J. Am. Chem. Soc. 126*, 13 (2004), 4076–4077.

Liu, B., and Bazan, G. C. Interpolyelectrolyte complexes of conjugated copolymers and DNA: Platforms for multicolor biosensors. *J. Am. Chem. Soc. 126*, 7 (2004), 1942–1943.

Liu, J. C., Heilshorn, S. C., and Tirrell, D. A. Comparative cell response to artificial extracellular matrix proteins containing the RGD and CS5 cell-binding domains. *Biomacromolecules 5*, 2 (2004), 497–504.

Loponen, M. T., Taka, T., Laakso, J., Väkiparta, K., Suuronen, K., Valkeinen, P., and Österholm, J. E. Doping and dedoping processes in poly(3-alkylthiophenes). *Synth. Met. 41*, 1-2 (1991), 479–484.

Lukkari, J., Alanko, M., Pitkänen, V., Kleemola, K., and Kankare, J. Photocurrent spectroscopic study of the initiation and growth of poly(3-methylthiophene) films on electrode surfaces with different adsorption properties. *J. Phys. Chem. 98*, 34 (1994), 8525–8535.

Lukkari, J., Kankare, J., and Visy, C. Cyclic spectrovoltammetry – A new method to study the redox processes in conductive polymers. *Synth. Met. 48*, 2 (1992), 181–192.

Lukkari, J., Tuomala, R., Ristimaki, S., and Kankare, J. In situ video recording of the nucleation enhancement in the electropolymerization of 3-methylthiophene. *Synth. Met. 47*, 2 (1992), 217–231.

Lynen, F., Knappe, J., Lorch, E., Jütting, G., and Ringelmann, E. Die biochemische Funktion des Biotins. *Angew. Chem. 71*, 15/16 (1959), 481–486.

Maior, R. M. S., Hinkelmann, K., Eckert, H., and Wudl, F. Synthesis and characterization of two regiochemically defined poly(dialkylbithiophenes) – A comparative study. *Macromolecules 23*, 5 (1990), 1268–1279.

Malenfant, P. R. L., and Fréchet, J. M. J. The first solid-phase synthesis of oligothiophenes. *Chem. Commun.*, 23 (1998), 2657–2658.

Marek, M., Kaiser, K., and Gruber, H. J. Biotin-pyrene conjugates with poly(ethylene glycol) spacers are convenient fluorescent probes for avidin and streptavidin. *Bioconjugate Chem. 8*, 4 (1997), 560–566.

Marsella, M. J., and Swager, T. M. Designing conducting polymer-based sensors – Selective ionochromic response in crown-ether containing polythiophenes. *J. Am. Chem. Soc. 115*, 25 (1993), 12214–12215.

Mastragostino, M., and Soddu, L. Electrochemical characterization of n-doped polyheterocyclic conducting polymers.1. polybithiophene. *Electrochim. Acta 35*, 2 (1990), 463–466.

McCarley, T. D., Noble, C. O., DuBois, C. J., and McCarley, R. L. MALDI-MS evaluation of poly(3-hexylthiophene) synthesized by chemical oxidation with $FeCl_3$. *Macromolecules 34*, 23 (2001), 7999–8004.

McCullough, R. D. The chemistry of conducting polythiophenes. *Adv. Mater. 10*, 2 (1998), 93–116.

McCullough, R. D., and Lowe, R. D. Enhanced electrical-conductivity in regioselectively synthesized poly(3-alkylthiophenes). *J. Chem. Soc., Chem. Commun.*, 1 (1992), 70–72.

McCullough, R. D., Tristramnagle, S., Williams, S. P., Lowe, R. D., and Jayaraman, M. Self-orienting head-to-tail poly(3-alkylthiophenes) – New insights on structure-property relationships in conducting polymers. *J. Am. Chem. Soc. 115*, 11 (1993), 4910–4911.

McQuade, D. T., Pullen, A. E., and Swager, T. M. Conjugated polymer-based chemical sensors. *Chem. Rev. 100*, 7 (2000), 2537–2574.

Meier, H., Stalmach, U., and Kolshorn, H. Effective conjugation length and UV/vis spectra of oligomers. *Acta Polym. 48*, 9 (1997), 379–384.

Meiwes, J., Schudok, M., and Kretzschmar, G. Asymmetric synthesis of L-thienylalanines. *Tetrahedron: Asymmetry 8*, 4 (1997), 527–536.

Merrifield, R. B. Solid phase peptide synthesis. 1. Synthesis of a tetrapeptide. *J. Am. Chem. Soc. 85*, 14 (1963), 2149–2154.

Meyer, V. Über den Begleiter des Benzols im Steinkohlentheer. *Ber. Deutsch. Chem. Ges. 16* (1883), 1465–1478.

Murphy, A. R., Fréchet, J. M. J., Chang, P., Lee, J., and Subramanian, V. Organic thin film transistors from a soluble oligothiophene derivative containing thermally removable solubilizing groups. *J. Am. Chem. Soc. 126*, 6 (2004), 1596–1597.

Nakanishi, H., Sumi, N., Aso, Y., and Otsubo, T. Synthesis and properties of the longest oligothiophenes: The icosamer and heptacosamer. *J. Org. Chem. 63*, 24 (1998), 8632–8633.

Ng, S. C., Ma, Y. F., Chan, H. S. O., and Dou, Z. L. Syntheses and characterisation of electrically conductive and fluorescent poly[3-(ω-bromoalkyl)thiophenes]. *Synth. Met. 100*, 3 (1999), 269–277.

Niemi, V. M., Knuuttila, P., Österholm, J. E., and Korvola, J. Polymerization of 3-alkylthiophenes with $FeCl_3$. *Polymer 33*, 7 (1992), 1559–1562.

Nilsson, K. P. R., Andersson, M. R., and Inganäs, O. Conformational transitions of a free amino-acid-functionalized polythiophene induced by different buffer systems. *J. Phys.: Condes. Matter 14*, 42 (2002), 10011–10020.

Olinga, T., and François, B. Kinetics of polymerization of thiophene by $FeCl_3$ in chloroform and acetonitrile. *Synth. Met. 69*, 1-3 (1995), 297–298.

Pande, R., Kamtekar, S., Ayyagari, M. S., Kamath, M., Marx, K. A., Kumar, J., Tripathy, S. K., and Kaplan, D. L. A biotinylated undecylthiophene copolymer bioconjugate for surface immobilization: Creating an alkaline phosphatase chemiluminescence-based biosensor. *Bioconjugate Chem. 7*, 1 (1996), 159–164.

Patel, N., and Poo, M. M. Orientation of neurite growth by extracellular electric fields. *J. Neurosci. 2*, 4 (1982), 483–496.

Patil, A. O., Ikenoue, Y., Wudl, F., and Heeger, A. J. Water-soluble conducting polymers. *J. Am. Chem. Soc. 109*, 6 (1987), 1858–1859.

Petka, W. A., Harden, J. L., McGrath, K. P., Wirtz, D., and Tirrell, D. A. Reversible hydrogels from self-assembling artificial proteins. *Science 281*, 5375 (1998), 389–392.

Pina-Luis, G., Badía, R., Díaz-García, M. E., and Rivero, I. A. Fluometric monitoring of organic reactions on solid phase. *J. Comb. Chem. 6*, 3 (2004), 391–397.

Plante, O. J., Palmacci, E. R., and Seeberger, P. H. Automated solid-phase synthesis of oligosaccharides. *Science 291*, 5508 (2001), 1523–1527.

Pomerantz, M., Tseng, J. J., Zhu, H., Sproull, S. J., Reynolds, J. R., Uitz, R., Arnott, H. J., and Haider, M. I. Processable polymers and copolymers of 3-alkylthiophenes and their blends. *Synth. Met. 41*, 3 (1991), 825–830.

Qiao, X. Y., Wang, X. H., and Mo, Z. S. The $FeCl_3$-doped poly(3-alkylthiophenes) in solid state. *Synth. Met. 122*, 2 (2001), 449–454.

Qiao, X. Y., Wang, X. H., Zhao, X. J., Liu, J., and Mo, Z. S. Poly(3-dodecylthiophenes) polymerized with different amounts of catalyst. *Synth. Met. 114*, 3 (2000), 261–265.

Reddinger, J. L., and Reynolds, J. R. Molecular engineering of π-conjugated polymers. *Adv. Polym. Sci. 145* (1999), 57–122.

Richmond, M. H. The effect of amino acid analogues on growth and protein synthesis in microorganisms. *Bacteriological Rev. 26* (1962), 398–420.

Roncali, J. Conjugated poly(thiophenes) – Synthesis, functionalization, and applications. *Chem. Rev. 92*, 4 (1992), 711–738.

Roncali, J. Synthetic principles for bandgap control in linear π-conjugated systems. *Chem. Rev. 97*, 1 (1997), 173–205.

Roncali, J., Garreau, R., Yassar, A., Marque, P., Garnier, F., and Lemaire, M. Effects of steric factors on the electrosynthesis and properties of conducting poly(3-alkylthiophenes). *J. Phys. Chem. 91*, 27 (1987), 6706–6714.

Rosseinsky, D. R., and Mortimer, R. J. Electrochromic systems and the prospects for devices. *Adv. Mater. 13*, 11 (2001), 783–793.

Roux, C., and Leclerc, M. Rod-to-coil transition in alkoxy-substituted polythiophenes. *Macromolecules 25*, 8 (1992), 2141–2144.

Ruckenstein, E., and Park, J. S. Polythiophene and polythiophene-based conducting composites. *Synth. Met. 44*, 3 (1991), 293–306.

Rudge, A., Raistrick, I., Gottesfeld, S., and Ferraris, J. P. A study of the electrochemical properties of conducting polymers for application in electrochemical capacitors. *Electrochim. Acta 39*, 2 (1994), 273–287.

Rughooputh, S. D. D. V., Hotta, S., Heeger, A. J., and Wudl, F. Chromism of soluble polythienylenes. *J. Polym. Sci., Polym. Phys. Ed. 25*, 5 (1987), 1071–1078.

Sakurai, S., Goto, H., and Yashima, E. Synthesis and chiroptical properties of optically active, regioregular oligothiophenes. *Org. Lett. 3*, 15 (2001), 2379–2382.

Samuelson, L. A., Kaplan, D. L., Lim, J. O., Kamath, M., Marx, K. A., and Tripathy, S. K. Molecular recognition between a biotinylated polythiophene copolymer and phycoerythrin utilizing the biotin streptavidin interaction. *Thin Solid Films 242*, 1-2 (1994), 50–55.

Sanders, J. K. M., and Hunter, B. K. *Modern NMR spectroscopy: A guide for chemists*, 2nd ed. Oxford University, Oxford, 1993.

Sarin, V. K., Kent, S. B. H., Tam, J. P., and Merrifield, R. B. Quantitative monitoring of solid-phase peptide synthesis by the ninhydrin reaction. *Anal. Biochem. 117*, 1 (1981), 147–157.

Schmidt, C. E., Shastri, V. R., Vacanti, J. P., and Langer, R. Stimulation of neurite outgrowth using an electrically conducting polymer. *Proc. Natl. Acad. Sci. U.S.A. 94*, 17 (1997), 8948–8953.

Schopf, G., and Koßmehl, G. Polythiophenes – Electrically conductive polymers. *Adv. Polym. Sci. 129* (1997), 1–166.

Shan, C. L. P., Soares, J. B. P., and Penlidis, A. Ethylene/1-octene copolymerization studies with in situ supported metallocene catalysts: Effect of polymerization parameters on the catalyst activity and polymer microstructure. *J. Polym. Sci. Pol. Chem. 40*, 24 (2002), 4426–4451.

Sheehan, J. C., Goodman, M., and Hess, G. P. Peptide derivatives containing hydroxyamino acids. *J. Am. Chem. Soc. 78*, 7 (1956), 1367–1369.

Sheehan, J. C., and Hess, G. P. A new method of forming peptide bonds. *J. Am. Chem. Soc. 77*, 4 (1955), 1067–1068.

Snyder, A. P. *Interpreting Protein Mass Spectra: A Comprehensive Resource*. Oxford University, New York, 2000.

Sotgiu, G., Zambianchi, M., Barbarella, G., Aruffo, F., Cipriani, F., and Ventola, A. Rigid-core fluorescent oligothiophene-S,S-dioxide isothiocyanates. Synthesisdou, optical characterization, and conjugation to monoclonal antibodies. *J. Org. Chem. 68*, 4 (2003), 1512–1520.

Staab, H. A., and Saupe, T. Proton sponges and the geometry of hydrogen-bonds – Aromatic nitrogen bases with exceptional basicities. *Angew. Chem. Int. Ed. 27*, 7 (1988), 865–879.

Story, S. C., and Aldrich, J. V. Preparation of protected peptide amides using the Fmoc chemical protocol – Comparison of resins for solid-phase synthesis. *Int. J. Pept. Protein Res. 39*, 1 (1992), 87–92.

Street, G. B., and Clarke, T. C. Conducting polymers – A review of recent work. *IBM J. Res. Dev. 25*, 1 (1981), 51–57.

Sugimoto, R., Taketa, S., Gu, H. B., and Yoshino, K. Preparation of soluble polythiophene derivatives utilizing transition metal halides as catalysts and their property. *Chem. Express 1*, 11 (1986), 635–638.

Swali, V., Wells, N. J., Langley, G. J., and Bradley, M. Solid-phase dendrimer synthesis and the generation of super-high-loading resin beads for combinatorial chemistry. *J. Org. Chem. 62*, 15 (1997), 4902–4903.

Sykes, P. *A Guidebook to Mechanism in Organic Chemistry*, 3rd ed. Longman, Essex, 1986.

Tashiro, K., Sephel, G. C., Weeks, B., Sasaki, M., Martin, G. R., Kleinman, H. K., and Yamada, Y. A synthetic peptide containing the IKVAV sequence from the A chain of laminin mediates cell attachment, migration, and neurite outgrowth. *J. Biol. Chem. 264*, 27 (1989), 16174–16182.

ten Hoeve, W., Wynberg, H., Havinga, E. E., and Meijer, E. W. Substituted 2,2′-5′, 2″-5″, 2‴-5‴, 2⁗-5⁗, 2⁗′-5⁗′, 2⁗″-5⁗″, 2⁗‴-5⁗‴,2⁗⁗-5⁗⁗, 2⁗⁗′-5⁗⁗′, 2⁗⁗″-5⁗⁗″- Undecithiophenes – The longest characterized oligothiophenes. *J. Am. Chem. Soc. 113*, 15 (1991), 5887–5889.

Torres-Rodriguez, L. M., Billon, M., Roget, A., and Bidan, G. Electrosynthesis of a biotinylated polypyrrole film and study of the avidin recognition by qcm. *J. Electroanal. Chem. 523*, 1-2 (2002), 70–78.

Torres-Rodriguez, L. M., Roget, A., Billon, M., and Bidan, G. Synthesis of a biotin functionalized pyrrole and its electropolymerization: Toward a versatile avidin biosensor. *Chem. Commun.*, 18 (1998), 1993–1994.

Tour, J. M. Conjugated macromolecules of precise length and constitution. Organic synthesis for the construction of nanoarchitectures. *Chem. Rev. 96*, 1 (1996), 537–553.

Tourillon, G., and Garnier, F. New electrochemically generated organic conducting polymers. *J. Electroanal. Chem. 135*, 1 (1982), 173–178.

van Hest, J. C. M., Kiick, K. L., and Tirrell, D. A. Efficient incorporation of unsaturated methionine analogues into proteins in vivo. *J. Am. Chem. Soc. 122*, 7 (2000), 1282–1288.

van Hest, J. C. M., and Tirrell, D. A. Protein-based materials, toward a new level of structural control. *Chem. Commun.*, 19 (2001), 1897–1904.

Visy, C., Lukkari, J., and Kankare, J. Change from a bulk to a surface coupling mechanism in the electrochemical polymerization of thiophene. *Synth. Met. 87*, 1 (1997), 81–87.

Wakil, S. J., and Gibson, D. M. Studies on the mechanism of fatty acid synthesis. VIII. The participation of protein-bound biotin in the biosynthesis of fatty acids. *Biochim. Biophys. Acta 41* (1960), 122–129.

Waltman, R. J., Bargon, J., and Diaz, A. F. Electrochemical studies of some conducting polythiophene films. *J. Phys. Chem. 87*, 8 (1983), 1459–1463.

Wang, S. S. *para*-Alkoxybenzyl alcohol resin and *para*-alkoxybenzyloxycarbonylhydrazide resin for solid-phase synthesis of protected peptide fragments. *J. Am. Chem. Soc. 95*, 4 (1973), 1328–1333.

Wang, S. S. Solid-phase synthesis of protected peptide hydrazides – Preparation and application of hydroxymethyl resin and 3-(*p*-benzyloxyphenyl)-1,1-dimethylpropyloxycarbonylhydrazide resin. *J. Org. Chem. 40*, 9 (1975), 1235–1239.

Welzel, H. P., Koßmehl, G., Engelmann, G., Hunnius, W. D., and Plieth, W. Reactive groups on polymer covered electrodes. 6. Copolymerization of 2,2′-bithiophene with methyl thiophene-3-acetate and 3-methylthiophene. *Electrochim. Acta 44*, 11 (1999), 1827–1832.

Wilchek, M., and Bayer, E. A. Introduction to avidin-biotin technology. In *Methods in Enzymology*, M. Wilchek and E. A. Bayer, Eds., vol. 184. Academic, San Diego, 1990, pp. 5–13.

Xu, B., and Holdcroft, S. Molecular control of luminescence from poly(3-hexylthiophenes). *Macromolecules 26*, 17 (1993), 4457–4460.

Yamamoto, T., Sanechika, K., and Yamamoto, A. Preparation of thermostable and electric-conducting poly(2,5- thienylene). *J. Polym. Sci., Polym. Lett. Ed. 18*, 1 (1980), 9–12.

Yang, C., Orfino, F. P., and Holdcroft, S. A phenomenological model for predicting thermochromism of regioregular and nonregioregular poly(3-alkylthiophenes). *Macromolecules 29*, 20 (1996), 6510–6517.

Yashima, E., Goto, H., and Okamoto, Y. Metal-induced chirality induction and chiral recognition of optically active, regioregular polythiophenes. *Macromolecules 32*, 23 (1999), 7942–7945.

Yen, W., Chan, C.-C., Jing, T., Jang, G.-W., and Hsueh, K. F. Electrochemical polymerization of thiophenes in the presence of bithiophene or terthiophene – Kinetics and mechanism of the polymerization. *Chem. Mat. 3*, 5 (1991), 888–897.

Yen, W., and Jing, T. Effect of oligomeric additives and applied potential on the molecular-weight and structure of electrochemically synthesized poly(3-alkylthiophenes). *Macromolecules 26*, 3 (1993), 457–463.

Yoshikawa, E., Fournier, M. J., Mason, T. L., and Tirrell, D. A. Genetically-engineered fluoropolymers – Synthesis of repetitive polypeptides containing *p*-fluorophenylalalanine residues. *Macromolecules 27*, 19 (1994), 5471–5475.

Yu, S. J. M., Conticello, V. P., Zhang, G. H., Kayser, C., Fournier, M. J., Mason, T. L., and Tirrell, D. A. Smectic ordering in solutions and films of a rod-like polymer owing to monodispersity of chain length. *Nature 389*, 6647 (1997), 167–170.

Zhu, L., Wehmeyer, R. M., and Rieke, R. D. The direct formation of functionalized alkyl(aryl)zinc halides by oxidative addition of highly reactive zinc with organic halides and their reactions with acid chlorides, α,β-unsaturated ketones, and allylic, aryl, and vinyl halides. *J. Org. Chem. 56*, 4 (1991), 1445–1453.